

LINEAR OPTIMIZATION
WITH THE
SHADOW-VERTEX-ALGORITHM
IN THE CONTEXT
OF PROBABILISTIC INVESTIGATIONS

A study of the transition from Phase 1 to Phase 2 in the
average-case-analysis and in the smoothed analysis of the
Simplex Method

Dissertation
zur
Erlangung des Doktorgrades
der Mathematisch-Naturwissenschaftlichen Fakultät
der Universität Augsburg

vorgelegt von
Emanuel Schnalzger, M.Sc.

Augsburg 2014

Free Translation by Karl Heinz Borgwardt

Erstgutachter: Prof. Dr. Karl Heinz Borgwardt
Zweitgutachter: Prof. Dr. Dieter Jungnickel
Drittgutachter: Prof. Dr. Heiko Rögl

Tag der mündlichen Prüfung: 2. Juli 2014

Danksagung

Zunächst möchte ich mich bei all denjenigen herzlich bedanken, die auf die verschiedensten Weisen zum Gelingen dieser Arbeit beigetragen haben.

Zuallererst gilt dabei mein ganz besonderer Dank Herrn Prof. Dr. Karl Heinz Borgwardt, der mich nicht nur während der Entstehung dieser Arbeit begleitet und mir wichtige Impulse gegeben hat, sondern mir mein ganzes TopMath-Studium über als Mentor zur Seite stand und mich sowohl fachlich als auch organisatorisch über die letzten Jahre hinweg unterstützt hat.

Darüber hinaus sei Herrn Prof. Dr. Dieter Jungnickel für die Übernahme des Zweitgutachtens gedankt. Weiterhin danke ich Dr. Markus Göhl, Dr. Matthias Tinkl und Dr. Thomas Wörle für zahlreiche interessante und anregende Diskussionen sowie allen weiteren Mitgliedern des Lehrstuhls für Diskrete Mathematik, Optimierung und Operations Research für die interessante und angenehme Zusammenarbeit.

Durch seine offene und gastfreundliche Art hat mir Prof. Roman Vershynin einen Forschungsaufenthalt an der University of Michigan ermöglicht, der in vielerlei Hinsicht gewinnbringend war. Hierfür noch einmal ein herzliches Dankeschön.

An dieser Stelle möchte ich ebenfalls meinen Dank dem Cusanuswerk aussprechen, das mir durch ein Promotionsstipendium die Möglichkeit gegeben hat, die Entstehung dieser Arbeit konzentriert verfolgen zu können.

Den TopMath-Koordinatoren danke ich für die Unterstützung bei den zahlreichen organisatorischen Fragen, die im Verlauf des TopMath-Programms aufgekommen sind.

Nicht zuletzt danke ich meiner Familie, ohne deren großartige Unterstützung ich all dies gar nicht erst erreicht hätte.

Contents

1	Introduction	7
1.1	The Subject Of This Thesis	7
1.2	Structure And Content	12
2	Fundamentals	17
2.1	Notation	17
2.2	Probability Theory	20
2.2.1	Transformation Of Density Functions	20
2.2.2	The Gaussian or Normal Distribution	20
2.2.3	Chi-Quadrat-Distribution	23
2.3	The Simplex Method	25
2.3.1	The Essential Functionality	25
2.3.2	The Tableau Method	27
2.3.3	Fundamental Considerations On The Computation Time	30
2.4	The Shadow Vertex Algorithm	30
2.4.1	The Primal Shadow Vertex Algorithm	31
2.4.2	The Dual Shadow Vertex Algorithm	34
2.4.3	Numerical Realization Of The Shadow Vertex Algorithm	36
3	Hitherto Existing Smoothed Analysis Approaches For The Simplex Method	39
3.1	The Work Of Spielman And Teng	39
3.1.1	The Geometrical Fundamental Result	39
3.1.2	The Algorithmic Realization	46
3.2	The Contribution Of Vershynin	54
3.2.1	Improvement Of The Geometrical Fundamental Result	54
3.2.2	New Algorithmic Proposals	62
4	Smoothed Analysis Of Polyhedra In Dimension 2	71
4.1	Formulation Of The Problem	71
4.2	The Transformation Of Coordinates Under Use	74
4.3	An Estimation Of The Probability For Short Edges	79
4.4	The Three-Viepoints-Argument	124
4.5	An Upper Bound For The Number Of Vertices	129
5	Smoothed Analysis Of Complete Linear Optimization	141
5.1	Introduction And Main Results	141
5.2	Fundamental Geometric Results	143

5.3	An Algorithm For Solving Linear Unit Problems	143
5.4	Transformation Rules For Linear Optimization Problems	146
5.5	A Solution Procedure For Arbitrary Linear Optimization Problems	148
5.5.1	Preliminary Considerations	148
5.5.2	Algorithmic Realization	151
5.6	Smoothed Analysis Of The Algorithm	152
5.6.1	The Number Of Pivot Steps In Phase 1	153
5.6.2	The Number Of Pivot Steps In Phase 2	155
5.6.3	Combination Of Results	159
5.7	Summary And Comments	160
6	Computation Time Of Phase 2 In The Case Of Stochastic Dependency	163
6.1	Introduction And Motivation	163
6.2	Rotational-Symmetric Distributions	164
6.3	The Algorithmic Principle Of The Investigation	167
6.3.1	The Phase 1 And Its Geometrical Interpretation	167
6.3.2	The Variants Of Phase 2 Under Investigation	174
6.4	Empirical Results For The Number Of Pivot Steps	181
6.5	Consequences Of The Calculated Results	194
6.6	Complimentary Considerations On The Computation Time Of Phase 2	194
6.7	Summary	206
7	Final Remarks	209
List of Figures		211
List of Tableaus		215
Bibliography		217

1 Introduction

1.1 The Subject Of This Thesis

The issue of this work lies in the intersection of Linear Optimization and in the investigation of the running time of algorithms. Before starting, we give some bibliographical hints.: The historical statements and quotations about the origin and development of linear optimization stem from [Dan02], [Sch98], [Bor87] as well as from [Tod02]. The interpretation and formulation of different complexity measures is based on the description in [ST04]. The development of linear optimization is due to many different scientists. With their contributions to transportation problems during the fourties Dantzig, Kantorovich, Koopmans und von Neumann have build the theoretical fundamentum for linear optimization. The invention of the Simplex Method by [Dan51] for the solution of linear optimization problems has lead to a great success for the role of optimization in practice. The fifties and sixties were a time of large and significant improvements, generalizations and progress in applicability. One of the reasons for this success was the empirical observation that the computation time for the Simplex Method was rather low when practical problems had to be treated. But in their paper [KM72] Klee und Minty managed the construction of a class of linear programs, where the application of the Simplex Method using all standard pivot rules leads to a huge number of pivot steps, which turned out to be exponential in the dimensions of the problem instances. From the viewpoint of complexity theory this proved an extremely poor Worst-Case Behaviour. Formally the worst-case-complexity is defined as follows: Consider in general an algorithm \mathcal{A} , a corresponding complexity measure $\mathcal{C}_{\mathcal{A}}$, and the set Ξ_n of all possible input systems for the algorithm $\mathcal{C}_{\mathcal{A}}$ of size n . In addition let a function $f : \mathbb{N} \rightarrow \mathbb{R}_{\geq 0}$ be given. Then we say that \mathcal{A} has worst-case-complexity $f(n)$ with respect to $\mathcal{C}_{\mathcal{A}}$, if for all n :

$$\sup_{\mathbf{x} \in \Xi_n} \{\mathcal{C}_{\mathcal{A}}(\mathbf{x})\} = f(n). \quad (1.1)$$

A graphical illustration of worst-case-complexity is given in 1.1.¹ For each possible input from a two-dimensional input space the figure shows the $\mathcal{C}_{\mathcal{A}}$ -running time of algorithm \mathcal{A} . This produces such a collection of mountains as seen.

¹Figures 1.1 und 1.3 have been drawn by the author in the style of the figures on the website of Daniel Spielman for Smoothed Analysis: <http://www.cs.yale.edu/homes/spielman/SmoothedAnalysis/framework.html>.

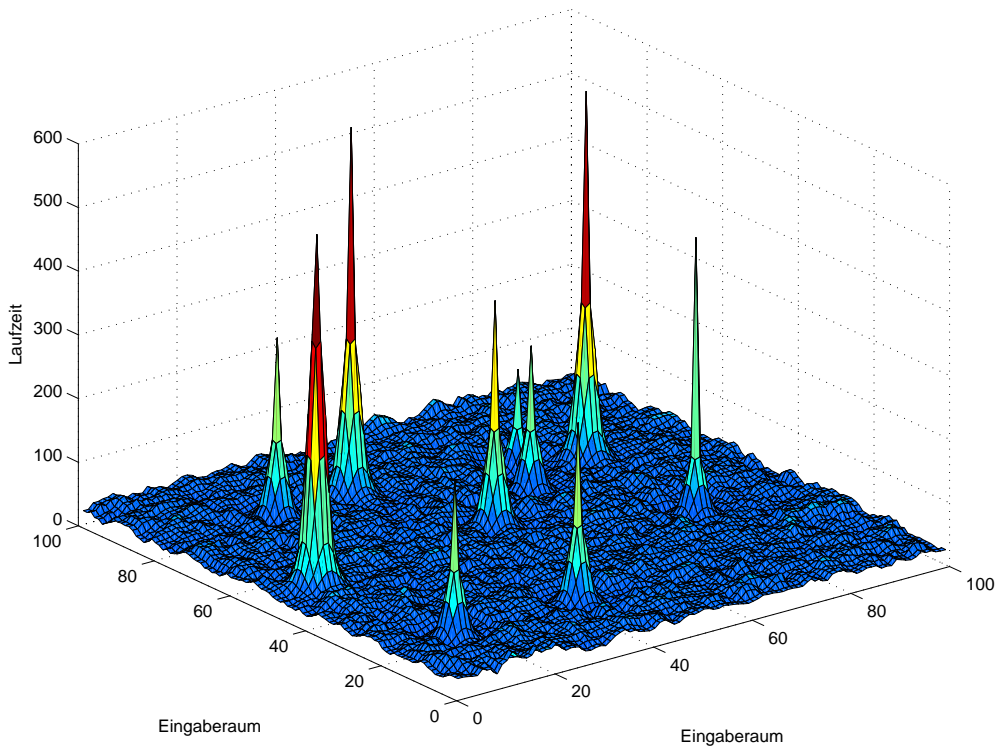


Figure 1.1: Graphical illustration of the actual computation time

The worst-case-complexity of the algorithm can be seen by finding the highest point in those running-time mountains. In the graphical interpretation the message of Klee and Minty is that there are extreme high points in the mountains of the Simplex Method.

This observation stood in dramatic contrast to the experiences made until then. It gave the motivation to a lot of investigations in form of an Average-Case-Analysis from the end of the seventies to the end of the nineties. We refer to the work of Borgwardt [Bor87], Adler, Karp und Shamir [AKS87], Haimovich [Hai83], Megiddo [Meg84], Smale [Sma83] and Todd [Tod86]. In Average-Case-Analysis one tries to calculate (theoretically) the expected value of the running time when it is assumed that the input data are somehow distributed over the input space. Therefore it is necessary to agree on a stochastic model for the input data. A formal definition for that is as follows: For a family μ of distributions μ_n auf Ξ_n we state that \mathcal{A} has average-case-complexity $g(n)$ under μ with respect to $\mathcal{C}_{\mathcal{A}}$, if

$$\mathbb{E}_{\substack{\mathbf{x} \leftarrow \Xi_n \\ \mu_n}} [\mathcal{C}_{\mathcal{A}}(\mathbf{x})] = g(n) \quad (1.2)$$

holds for all n . Here $g(n)$ is a function from \mathbb{N} to $\mathbb{R}_{\geq 0}$. In our graphical illustration this leads to a so-called running-time plane as shown in figure 1.2. The average running time is just the height of the plane which is shown.

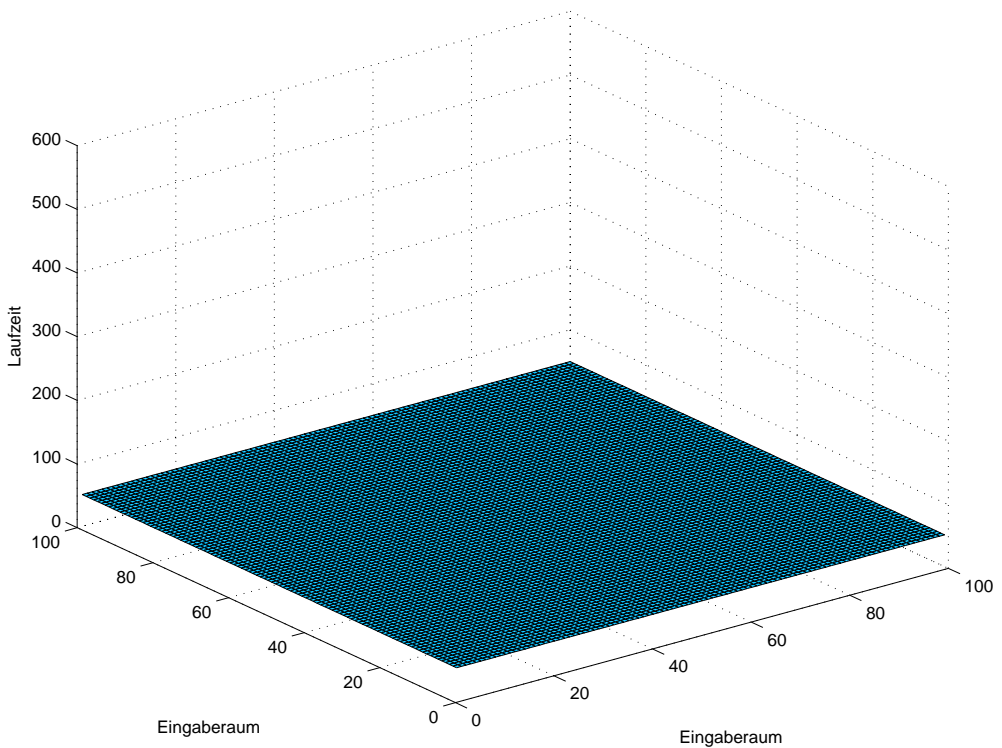


Figure 1.2: Graphical illustration of the average computation time

We should mention that the choice of the distribution family μ and the choice of specific realization of the Simplex Method (the “variant” or “pivot rule”) have a tremendous impact on the result. But in all investigated cases the average running time turned out to be polynomial in the input dimensions. So these results were extremely lower and “better” than the worst-case observations of Klee and Minty. Hence we learn that those problem instances , which had caused the great difficulties, possess a rather small weight in the average-case distribution of problems. This confirmed the practical observations made so far.

The two scientists did nor accept this as a final, satisfying confirmation of the good behaviour in practice. So they developed a third concept for judging the quality of the algorithm. They introduced the Smoothed Analysis and carried out such a calculation for the Simplex Method 2001 in [ST01]. In essence this can be interpreted as a hybrid between Average-Case and Worst-Case Anaysis. Its principle is as follows: First fix an arbitrary input problem for the algorithm (the original problem). Then the data of that problem will be slightly disturbed (or modified) according to a normal distribution. So one has a so-called perturbation set of problems. After that one imagines that all these perturbed problems are solved. And now one calculates the average running time according to that imagination. This leads to the following formal definition:

An algorithm \mathcal{A} has smoothed complexity $h(n, \sigma)$ with respect to $\mathcal{C}_{\mathcal{A}}$, if

$$\sup_{\mathbf{x} \in \Xi_n} \{\mathbb{E}_{\mathbf{g}} [\mathcal{C}_{\mathcal{A}}(\mathbf{x} + \sigma \mathbf{g})]\} = h(n, \sigma) \quad (1.3)$$

for all n and $\sigma > 0$. Here $h(n, \sigma)$ is a function from $\mathbb{N} \times \mathbb{R}_{>0}$ to $\mathbb{R}_{\geq 0}$ and $\sigma \mathbf{g}$ is a vector consisting of normally distributed random variables with mean value 0 and standard deviation σ . An illustration of that principle is given in figure 1.3.

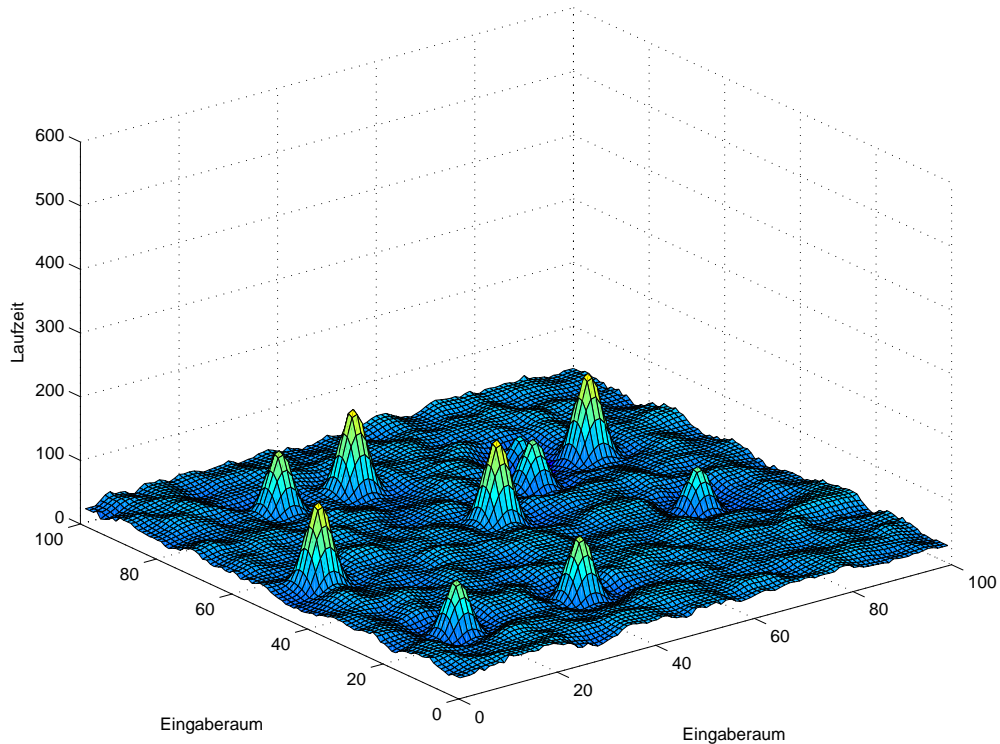


Figure 1.3: Graphical illustration of the smoothed computation time

The mountains of smoothed running times result from the data in 1.1 by calculating the average runtime on the corresponding perturbation set. These values are then plotted. In total we define the smoothed running time of the algorithm as the height of the highest point in those mountains. In their paper of 2004 [ST04] Spielman und Teng have shown that the investigated variant of the Simplex Method features a polynomial smoothed running time. Since here the running time does not depend on the input dimensions, but also on the parameter σ , polynomial is interpreted in a new way. In Worst-Case and in Average Case we speak of polynomial behaviour of algorithm \mathcal{A} , if the functions $f(n)$ resp. $g(n)$ from the formal definitions in (1.1) und (1.2) are bounded from above by polynomials $\tilde{f}(n)$ resp. $\tilde{g}(n)$. In extension of that principle the algorithm \mathcal{A} is said to possess polynomial smoothed running time, if $h(n, \sigma)$ is bounded from above by a function $\tilde{h}(n, \sigma)$, which is for its own polynomial in n and in $\frac{1}{\sigma}$ as well. For simplification we call that complexity resp. running time the $\mathcal{C}_{\mathcal{A}}$ -complexity.

As already mentioned, Spielman und Teng proposed to use the Smoothed Analysis for judgements about algorithms in augmentation to the measures used so far. We should think about those aspects, which could be explained by that new approach. Let us for the moment concentrate on one significant point, which is highlighted by Spielman and

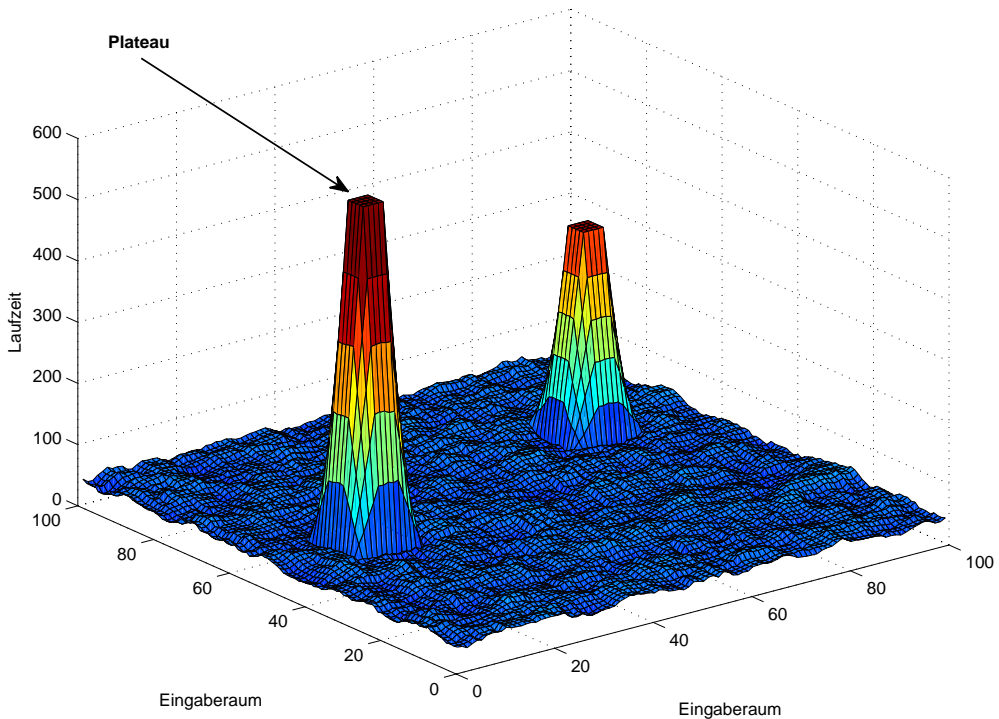


Figure 1.4: Graphical illustration of an alternative actual computation time distribution

Teng in [ST04]. For further details have a look at [ST09].

For an algorithm \mathcal{A} featuring polynomial smoothed running time, we can conclude that the critical problem instances leading to a high (exponential) running time are isolated points. Then the mountains look like in figure 1.1. In particular the form of 1.4 will become impossible. Assuming that there is a plateau with extremal height, and choosing an input in the center of that tableau, then small disturbances will lead to problems with similar running time. All these difficult problems then have a large weight in the perturbation set. As a consequence, the smoothed running time cannot be significantly smaller than the mentioned height. If we observe polynomial smoothed running time, then such plateaus cannot appear. In addition the real computation will show numerical modifications and variations (e.g. as a result of computational accuracy). So it is rather unlikely to hit some of those extremal problems. So we can expect moderate running times.

Overall the smoothed running time is a measure for the real expected running time, when we take little modifications into regard. In contrast, Average Case results are based on averaging “all over the world”.

The invention of Smoothed Analysis has lead to the investigation of further algorithms from mathematics and computer science. For instance one has investigated the numerical stability of the Gaussian elimination procedure [SST06]. One has calculated the smoothed running time of the k -Means-Algorithm [AMR11] and several properties of

integer linear programs [RV07]. In addition one has investigated binary search trees [MR07] as well as condition numbers of matrices (vgl. [BA12] und [DST11]), which occur in connection with linear programming.

The proof of exponential running time of the Simplex Method by Klee and Minty has also lead to new algorithmic approaches for the solution of linear programming problems. The first spectacular progress was the invention of the Ellipsoid Method [Kha79], which is a (weakly) polynomial solution method. Weakly means that the number of bits affects not only the effort of each single arithmetical operation, but also the number of required arithmetical operations. Because of numerical instability this algorithm was not useful for practice. But in 1984 Karmarkar [Kar84] invented another weakly polynomial solution method, (as an initial point for Inner-Point-Methods). This method was very successful and is today as competitive as the Simplex Method when large problems shall be solved.

In addition to the invention of efficient algorithms for linear programming the theoretical analysis of already known methods has great importance and interest. So it can be mentioned that Borgwardt was rewarded the Lanchester Price 1982 for his papers [Bor82b] and [Bor82a]. In these papers he had shown (strong) polynomiality of the expected running time of the Simplex Method by means of an Average-Case Analysis. As already mentioned, Spielman and Teng have published in 2004 the paper [ST04] introducing the Smoothed Analysis and showing that their Simplex-like solution method has polynomial smoothed analysis complexity. So they were rewarded the Gödel-Preis for outstanding improvements in theoretical computer science. In addition they got the Fulkerson-Price in 2009 in the field of Discrete Mathematics and D. Spielman was finally rewarded the Nevanlinna-Preis for his contributions to smoothed analysis and several other topics.

1.2 Structure And Content

In the last section we have got many interesting insights about the Simplex Method and about its probabilistic analysis. Nevertheless there are a lot of unsettled questions and of unexplained aspects, Some of those form the starting point for this thesis. After this introduction five chapters will be presented .

In chapter 2 we list the fundamentals, which will be exploited in the course of our paper. In addition to notation conventions we have summarized insights and basic formulas of probability theory and further we explain in general how the Simplex Method works. Here we focus on the shadow vertex algorithm, which is a special variant, specified by a fixed special pivot rule. This variant has got many advantageous features, which were very helpful for carrying out a probabilistic analysis. It is symptomatic that this is so far the only variant for which a probabilistic analysis of the running time worked successfully. We discuss several aspects, as the primal and dual interpretation of the shadow vertex algorithm and we demonstrate how this algorithm is realized numerically.

After that we present in chapter 3 the essential principles and logical steps in the smoothed analysis of the running time for the Simplex Method done by Spielman and Teng [ST04] and by Vershynin [Ver09]. Here we try to show the state of the art and by the way we give a motivation for our investigations in chapters 4 and 5. The essentials are described here concisely.

In their article [ST04], Spielman and Teng have published the first smoothed analysis of the Simplex Method and there they presented the proof of polynomial smoothed running time for the variant under consideration. Their work subdivides into two parts. In the first part they derive an upper bound for the expected number of so-called shadow vertices of a perturbed polyhedron. In part two they develop a special adjusted form of the Simplex Method based on the shadow vertex algorithm. After that they calculate its smoothed running time, making use of the upper bound from the first part. With regard to the method constructed and analyzed in part two some issues should be discussed. What they (finally) present and evaluate is a so called randomized algorithm. That means that the real calculation varies in each application as a result of stochastic decisions. Spielman and Teng used this randomization with the intention to keep the upper bound in the smoothed analysis rather low. A corresponding “derandomized” variant would also be evaluable, but for that procedure the upper bound of order $\mathcal{O}(m^{86}d^{55}\sigma^{-30})$ could not hold resp. could not be proved. In this formula logarithmic factors are ignored. Despite the accepted randomization the upper bound still is of a tremendous order even though it is polynomial. So the significance of that evaluation is rather qualitative than quantitative. Further details will be given in the first section of chapter 3. At this point we want to summarize: Spielman and Teng investigate a randomized form of the Simplex Method. Hence the running time and the upper bound for that is not only a result of the perturbations (which are the essence of smoothed analysis) but also on decisions by chance about how the algorithm will proceed.

In augmentation to the result of Spielman and Teng an improved investigation was published by Vershynin in [Ver06] and in [Ver09]. The essential aspects of that will be discussed in detail in the second section of chapter 3. As seen in the work of Spielman and Teng, also the work of Vershynin consists of two components. In the first part he applies a refined geometrical study and he succeeds in obtaining a better upper bound for the number of shadow vertices. In the second part he develops a method for the solution of linear optimization problems which can be analyzed much simpler than the approach of Spielman and Teng. For this reason Vershynin is able to derive a significantly improved upper bound. But as we shall see in chapter 3, the method applied by Vershynin is obviously a randomized procedure. Here the randomization is not chosen strategically, to keep the bounds low, but it is essential for the functioning. So Vershynin gains his better upper bound by an improved shadow vertex analysis and by the acceptance of a complete randomization. This upper bound for the smoothed running time amounts to an order of $\mathcal{O}(\max\{d^5(\ln m)^2, d^9(\ln d)^4, d^3\sigma^{-4}\})$, which is considerably lower than Spielman’s and Teng’s bound.

This concisely described state of the art with regard to the smoothed analysis of the Sim-

plex Method is the motivation for the first part of this work. We are going to present a deterministic form of the Simplex Method on the basis of the dimension-by-dimension algorithm in chapter 5. After that we evaluate the smoothed running time of that method. This amounts to an upper bound of (essential) order $\mathcal{O}(\max\{d^6(\ln m)^2, d^4\sigma^{-4}\})$. In comparison with the upper bound derived by Vershynin, we observe a clear similarity, which is disturbed only by the fact, that now d runs of the shadow-vertex-algorithm must be carried out. So it can be shown that such a low upper bound can be achieved without the necessity and the use of randomization. And we avoid any impact of randomization on the bounds itself. Here the smoothed running time is affected only by the way of perturbation of input data. Nevertheless we make use of the fundamental estimation of the number of shadow vertices found by Vershynin. Since our method works successively in dimensions $k = 2, \dots, d$, and since Spielman, Teng and Vershynin derived their fundamental results only for $k \geq 3$ we are in need for a respective result for $d = 2$. (This is essentially no conflict, but the mentioned authors had used coordinate transformations which can be done only in dimension 3 or higher). So we derive and prove an analogous result for $d = 2 = k$ on our own in chapter 4 in detail. So this chapter is a preparation and augmentation for the following total summing up in chapter 5 . There we get the desired smoothed running time result for the dimension-by-dimension algorithm.

The second part of this work is put in chapter 6 and it has strong connections with the algorithmic investigation in chapter 5 . If one wants to study the expected running time of the shadow-vertex-algorithm in the framework of a probabilistic analysis - this is the case for smoothed analysis and average-case analysis as well - then the expected number of visited shadow vertices under certain fixed stochastic conditions plays the crucial role. For that reason one is limited to very specific algorithmic steps - as the use of randomization by Spielman and Teng and Vershynins or e.g, the use of the procedure in chapter 5. Failing to meet those limits would prohibit us from using results from stochastic geometry (expected numbers of) for our proof of total expected running time. As a consequence, our results would not hold for an algorithmic behaviour (observed in practice) to do a simple Phase 1 by finding any vertex and then immediately starting Phase 2 from that vertex. Here the problem is that this action does not guarantee, that the start of Phase 2 is stochastically independent of the input data. And then we cannot apply our stochastic results. In other words: a start at an optimal vertex to an auxiliary direction \mathbf{u} is feasible, if \mathbf{u} was chosen independently from the restrictions. But the delivery of any start vertex to Phase 2 generates strong dependencies and this destroys any rigorous proof. This problem of the distinction between practical (efficient?) behaviour and meeting the theoretical rules on the other side and the comparison of the empirical behaviour in both cases form the question investigated in this chapter: In case that we do not meet the independence rules and conditions for the choice of the starting vertex for Phase 2 - are then the theoretically obtained bounds for the running time of Phase 2 nevertheless valid (although we cannot prove this) or is the behaviour then completely different?

To give an answer, we carry out an empirical Average-Case Analysis. For that purpose we use the rotation symmetry model as the stochastic principle. We explain the basic

statistical method of the investigation and after that we present the empirical results numerically and graphically. These results confirm that under ignorance of the theoretically required independency conditions the running time does not change significantly. For that reason it becomes very plausible (although this cannot be proved theoretically) that the results of the theoretical Average-Case-Analysis hold for the more efficient behaviour of practitioners, too. In this empirical investigation we have observed some additional interesting effects. They are discussed in detail at the end of chapter 6 .

Summarizing: we remark that we augment the smoothed analysis of the Simplex Method by an investigation of a deterministic variant. In addition we clarify empirically, that the results of the Average-Case-Behaviour hold even when the independency conditions for the start vertex are not fulfilled. In chapter 7 we summarize and give some final remarks.

2 Fundamentals

This chapter lists all the fundamentals, which we are going to use in this thesis.

2.1 Notation

Here are the details of the notation.

Scalars and sets

Scalars are denoted by the use of Greek lower case letters, e.g. λ or μ . When it will be necessary to deviate from that, we shall give a hint. For sets in \mathbb{R}^d we use Latin upper case letters as X or Y . The boundary of a set X is denoted by ∂X . In case that we want to emphasize the geometrical shape of a set G , for instance a straight line, we use caligraphic lettering and write \mathcal{G} instead of G . In case of a finite set Δ its number of elements (cardinality) will be denoted by $\#(\Delta)$.

For a point $\mathbf{x} \in \mathbb{R}^d$ and a set $M \subset \mathbb{R}^d$ let $\mathbf{x} + M$ stand for the shifting of M by \mathbf{x} . I.e. $\mathbf{x} + M := \{\mathbf{x} + \mathbf{y} : \mathbf{y} \in M\}$.

Vectors and matrices

Vectors are denoted by boldface lowercase letters, e.g. \mathbf{a} . If not explained otherwise, we regard any vector \mathbf{a} as a column vector. The corresponding row vector is denoted by \mathbf{a}^T . For a vector $\mathbf{a} \in \mathbb{R}^d$ let a^1, \dots, a^d be its d components. Let $\mathbf{a}, \mathbf{b} \in \mathbb{R}^d$ be two vectors. Then we write for a possible comparison: $\mathbf{a} \geq \mathbf{b} \Leftrightarrow a^i \geq b^i$ for all $i = 1, \dots, d$. In the following we sometimes augment a vector \mathbf{a} by an additional component \tilde{a} (first or last). For simplification we write in that case (\tilde{a}, \mathbf{a}) resp. (\mathbf{a}, \tilde{a}) , but the meaning is still that augmented column vector.

In contrast to vectors matrices are denoted by boldface capital letters. Let $\mathbf{A} = (\mathbf{a}_1, \dots, \mathbf{a}_m)^T \in \mathbb{R}^{m \times d}$. This matrix obviously consists of the row vectors $\mathbf{a}_1^T, \dots, \mathbf{a}_m^T$. In addition consider an index set $\Delta = \{\Delta^1, \dots, \Delta^n\} \subset \{1, \dots, m\}$. Then \mathbf{A}_Δ denotes the matrix consisting of those row vectors whose indices belong to $\Delta^1, \dots, \Delta^n$. In shortform

$$\mathbf{A}_\Delta = \begin{pmatrix} \mathbf{a}_{\Delta^1}^T \\ \vdots \\ \mathbf{a}_{\Delta^n}^T \end{pmatrix} \in \mathbb{R}^{n \times d}.$$

So we can regard \mathbf{A}_Δ as a part of the matrix of \mathbf{A} . Analogously we will apply that convention to vectors .

In addition \mathbf{E}_d will denote the unit matrix in $\mathbb{R}^{d \times d}$.

Scalar product and norm

$\langle \cdot, \cdot \rangle$ denotes the standard scalar product. For two vectors $\mathbf{x}, \mathbf{y} \in \mathbb{R}^d$ we have $\langle \mathbf{x}, \mathbf{y} \rangle := \sum_{i=1}^d x^i \cdot y^i$. That scalar product induces the Euclidean norm $\|\cdot\|$.

Distance and angle

For two vectors $\mathbf{x}, \mathbf{y} \in \mathbb{R}^d$ we write $\mathbf{dist}(\mathbf{x}, \mathbf{y})$ for the distance between both vectors. Consequently $\mathbf{dist}(\mathbf{x}, \mathbf{y}) = \|\mathbf{x} - \mathbf{y}\|$. In addition let $M \subset \mathbb{R}^d$. Then the distance between \mathbf{x} and M is defined as follows

$$\mathbf{dist}(\mathbf{x}, M) := \inf_{\mathbf{y} \in M} \mathbf{dist}(\mathbf{x}, \mathbf{y}).$$

For $M = \emptyset$ let $\mathbf{dist}(\mathbf{x}, M) = \infty$. In addition $\mathbf{arc}(\mathbf{x}, \mathbf{y})$ denotes the angle between \mathbf{x} and \mathbf{y} , i.e.

$$\mathbf{arc}(\mathbf{x}, \mathbf{y}) := \arccos \left(\frac{\langle \mathbf{x}, \mathbf{y} \rangle}{\|\mathbf{x}\| \cdot \|\mathbf{y}\|} \right).$$

Analogously we define the angle between a point \mathbf{x} and a set M :

$$\mathbf{arc}(\mathbf{x}, M) := \inf_{\mathbf{y} \in M} \mathbf{arc}(\mathbf{x}, \mathbf{y})$$

and $\mathbf{arc}(\mathbf{x}, M) = \infty$, if $M = \emptyset$.

Ball, sphere and Lebesgue measure

By $\Omega_d(r)$ we shall denote the d -dimensional ball about the origin of radius $r \geq 0$, i.e.

$$\Omega_d(r) := \{ \mathbf{x} \in \mathbb{R}^d : \|\mathbf{x}\| \leq r \}.$$

Analogously $\omega_d(r)$ shall denote the sphere in \mathbb{R}^d of radius $r \geq 0$, i.e. the volume of the surface of $\Omega_d(r)$. So we have

$$\omega_d(r) := \{ \mathbf{x} \in \mathbb{R}^d : \|\mathbf{x}\| = r \}.$$

This has dimension $(d-1)$. For $r = 1$ let $\Omega_d(r)$ and $\omega_d(r)$ simply be denoted by Ω_d resp. ω_d . Further let $\lambda_d(\cdot)$ stand for the d -dimensional Lebesgue measure. In our context that means

$$\lambda_d(\Omega_d(r)) = r^d \cdot \frac{\pi^{\frac{d}{2}}}{\Gamma\left(\frac{d}{2} + 1\right)}$$

as well as

$$\lambda_{d-1}(\omega_d(r)) = 2r^{d-1} \cdot \frac{\pi^{\frac{d}{2}}}{\Gamma\left(\frac{d}{2}\right)}.$$

Here Γ is the Gammafunction $\Gamma : (0, \infty) \rightarrow \mathbb{R}$ with

$$\Gamma(x) = \int_0^\infty e^{-t} t^{x-1} dt.$$

Convex, affine, conical and linear hull

Consider m vectors $\mathbf{x}_1, \dots, \mathbf{x}_m$. Based on that we introduce $\mathbf{KH}(\mathbf{x}_1, \dots, \mathbf{x}_m)$ for the convex hull of the vectors $\mathbf{x}_1, \dots, \mathbf{x}_m$, i.e.

$$\mathbf{KH}(\mathbf{x}_1, \dots, \mathbf{x}_m) := \{ \lambda_1 \mathbf{x}_1 + \dots + \lambda_m \mathbf{x}_m : \lambda_1, \dots, \lambda_m \geq 0, \lambda_1 + \dots + \lambda_m = 1 \}.$$

Further we denote the convex hull of a point $\mathbf{x} \in \mathbb{R}^d$ and a set $M \subset \mathbb{R}^d$ as follows

$$\mathbf{KH}(\mathbf{x}, M) := \{ \lambda \mathbf{x} + (1 - \lambda) \mathbf{y} : \lambda \in [0, 1] \text{ and } \mathbf{y} \in M \}.$$

Let $\mathbf{AH}(\mathbf{x}_1, \dots, \mathbf{x}_m)$ stand for the affine hull

$$\mathbf{AH}(\mathbf{x}_1, \dots, \mathbf{x}_m) := \{ \lambda_1 \mathbf{x}_1 + \dots + \lambda_m \mathbf{x}_m : \lambda_1 + \dots + \lambda_m = 1 \},$$

$\mathbf{KK}(\mathbf{x}_1, \dots, \mathbf{x}_m)$ for the conical hull

$$\mathbf{KK}(\mathbf{x}_1, \dots, \mathbf{x}_m) := \{ \lambda_1 \mathbf{x}_1 + \dots + \lambda_m \mathbf{x}_m : \lambda_1, \dots, \lambda_m \geq 0 \}$$

und $\mathbf{LH}(\mathbf{x}_1, \dots, \mathbf{x}_m)$ for the linear hull

$$\mathbf{LH}(\mathbf{x}_1, \dots, \mathbf{x}_m) := \{ \lambda_1 \mathbf{x}_1 + \dots + \lambda_m \mathbf{x}_m : \lambda_1, \dots, \lambda_m \in \mathbb{R} \}.$$

Random variable and notation from probability theory

For the notion of random variables and of random vectors we make use of two different notations. In this first chapter we use capital letters as Z for random variables and \mathbf{Z} for random vectors. In the course of the thesis sometimes data vectors \mathbf{a} will appear, which are affected by some stochastic influence. In that context, we shall (for simplification) also use \mathbf{a} as a random vector. In each context the meaning will be clarified.

For the determination of more notation let a random variable X and two random events A, B be available. Then $\mathbb{E}[X]$ stands for the expected value of X and $\mathbb{P}[A]$ is the probability that the event A will occur. If $\mathbb{P}[B] > 0$, then $\mathbb{P}[A|B]$ denotes the conditional probability of A under the condition (or given) B . Hence

$$\mathbb{P}[A|B] := \frac{\mathbb{P}[A \wedge B]}{\mathbb{P}[B]}.$$

Furthermore let $\mathbb{1}[A]$ be the indicator function for the event A , i.e.

$$\mathbb{1}[A] := \begin{cases} 1, & \text{if the event } A \text{ has occurred} \\ 0, & \text{else.} \end{cases}$$

For a random variable X and an event A with $\mathbb{P}[A] > 0$ let $\mathbb{E}[X | A]$ stand for the conditional expected value of X , given A . In detail:

$$\mathbb{E}[X | A] := \frac{\mathbb{E}[X \cdot \mathbf{1}[A]]}{\mathbb{P}[A]}.$$

Logarithm

$\ln(\cdot)$ denotes the natural logarithm and $\lg(\cdot)$ is the logarithm to basis 2.

2.2 Probability Theory

This section contains results from stochastics, which will be exploited in the following. Most of them can be found in textbooks as [Geo04] or [Kle08]. More special results are proven or we have inserted a corresponding reference.

2.2.1 Transformation Of Density Functions

Let us consider density functions. Compare section 1.1.2 and Proposition 9.1 in [Geo04].

Lemma 2.2.1 (Transformation of density functions).

Let $X \subset \mathbb{R}^d$ be open and let P be a probability measure on (X, \mathfrak{B}_X^d) (\mathfrak{B}_X^d denotes the Borel σ -algebra on X) with density function f . Let further $Y \subset \mathbb{R}^d$ be open and $\Phi : X \rightarrow Y$ be a diffeomorphism, i.e. a continuously differentiable bijection with Jacobian determinant $\det\left(\frac{\partial}{\partial \mathbf{x}}\Phi(\mathbf{x})\right) \neq 0$ for all $\mathbf{x} \in X$. Then the distribution $P \circ \Phi^{-1}$ of Φ on Y has the density function

$$g(\mathbf{y}) = f(\Phi^{-1}(\mathbf{y})) \cdot \left| \det\left(\frac{\partial}{\partial \mathbf{y}}\Phi^{-1}(\mathbf{y})\right) \right|$$

for all $\mathbf{y} \in Y$.

2.2.2 The Gaussian or Normal Distribution

This section deals with the normal distribution (Gaussian distribution). It is extremely important for the investigations in connection with Smoothed Analysis, since there one has fixed the principle that the deviations follow normally distributed deviations from the original data. For further details compare [Geo04] and [Kle08].

A random variable Z is normally distributed with expectation value μ and variance $\sigma^2 > 0$, i.e. $Z \sim \mathcal{N}(\mu, \sigma^2)$, if Z possesses the density function

$$f_Z(z) = \frac{1}{\sqrt{2\pi}\sigma} \cdot e^{-\frac{(z-\mu)^2}{2\sigma^2}}$$

That principle can be transferred to random vectors. Let a positive definite and symmetrical matrix $\mathbf{M} \in \mathbb{R}^{d \times d}$ as well as a vector $\boldsymbol{\mu} \in \mathbb{R}^d$ be given. Then we call a random vector $\mathbf{Z} = (Z_1, \dots, Z_d)^T$ d -dimensional normally distributed with center $\boldsymbol{\mu}$ and covariance matrix \mathbf{M} , if \mathbf{Z} has the density function

$$f_{\mathbf{Z}}(\mathbf{z}) = \frac{1}{\sqrt{(2\pi)^d \det(\mathbf{M})}} \cdot e^{-\frac{1}{2}(\mathbf{z}-\boldsymbol{\mu})^T \mathbf{M}^{-1}(\mathbf{z}-\boldsymbol{\mu})}$$

for $\mathbf{z} \in \mathbb{R}^d$. Shortly we write $\mathbf{Z} \sim \mathcal{N}_d(\boldsymbol{\mu}, \mathbf{M})$ and we speak of a multivariate and multi-dimensional normal distribution.

In context with the multivariate normal distribution the following special case will be interesting for us. Let $\boldsymbol{\mu} \in \mathbb{R}^d$ as before and for the covariance matrix let $\mathbf{M} = \sigma^2 \mathbf{E}_d$ with $\sigma > 0$ and unit matrix \mathbf{E}_d . If $\mathbf{Z} \sim \mathcal{N}_d(\boldsymbol{\mu}, \sigma^2 \mathbf{E}_d)$, then \mathbf{Z} has the density function

$$f_{\mathbf{Z}}(\mathbf{z}) = \left(\frac{1}{\sqrt{2\pi}\sigma} \right)^d \cdot e^{-\frac{\|\mathbf{z}-\boldsymbol{\mu}\|^2}{2\sigma^2}}$$

for $\mathbf{z} \in \mathbb{R}^d$. In that case \mathbf{Z} will be called a normally distributed random vector with center $\boldsymbol{\mu} = (\mu^1, \dots, \mu^d)^T$ and standard deviation σ . Further the components Z_i of \mathbf{Z} are independently normally distributed random variables with expectation value μ^i and standard deviation σ . So we have $Z_i \sim \mathcal{N}(\mu^i, \sigma^2)$ for all $i = 1, \dots, d$. If in particular $\sigma = 1$, then we call \mathbf{Z} a multivariate (standard-)normally distributed random vector in dimension d . This definition of a normally distributed random vector can be analogously transferred on the construction of a normally distributed random matrix

An important feature of the normal distribution for our purpose comes from the affine transformation of normally distributed random vectors. Here the question is, how large is the impact of such a transformation on the distribution of the random vector. An answer is given in the following Lemma.

Lemma 2.2.2 (Affine transformation of multivariate normal distributions).

Let \mathbf{Z} be a normally distributed random vector in \mathbb{R}^d about $\boldsymbol{\mu}$ with covariance matrix \mathbf{M} , i.e. $\mathbf{Z} \sim \mathcal{N}_d(\boldsymbol{\mu}, \mathbf{M})$. In addition let for $k \leq d$ a real $(k \times d)$ -Matrix \mathbf{P} of full rank as well as a vector $\mathbf{p} \in \mathbb{R}^k$ be given. Then the k -dimensional random vector $\mathbf{W} = \mathbf{P}\mathbf{Z} + \mathbf{p}$ follows a normal distribution with center $\mathbf{P}\boldsymbol{\mu} + \mathbf{p}$ and covariance matrix $\mathbf{P}\mathbf{M}\mathbf{P}^T$ as well. Hence

$$\mathbf{W} \sim \mathcal{N}_k(\mathbf{P}\boldsymbol{\mu} + \mathbf{p}, \mathbf{P}\mathbf{M}\mathbf{P}^T).$$

Proof. Compare [Geo04, Satz 9.5]. □

In the style of [ST04, Lemma 2.15] we formulate the following result, which gives a description of the smoothness of the normal distribution. This will be useful in the following.

Lemma 2.2.3 (Smoothness of the normal distribution).

Given a density function f of a one-dimensional normal distribution with standard deviation σ and expectation value μ . Furthermore let $\delta, \eta \geq 0$ and let two values z_1, z_2 be available with $|z_1 - \mu| \leq \delta$ and $|z_1 - z_2| \leq \eta$. Then

$$\frac{f(z_1)}{f(z_2)} \leq e^{\frac{2\delta\eta + \eta^2}{2\sigma^2}}.$$

Proof. The density function in explicit form is

$$f(z) = \frac{1}{\sqrt{2\pi}\sigma} \cdot e^{-\frac{(z-\mu)^2}{2\sigma^2}}.$$

For further considerations we set $w_1 := z_1 - \mu$ and $w_2 := z_2 - \mu$. Then

$$\begin{aligned} |w_2| &= |z_2 - \mu| \\ &= |z_2 - z_1 + z_1 - \mu| \\ &= |z_2 - z_1 + w_1| \\ &\leq |z_2 - z_1| + |w_1| \\ &\leq \eta + |w_1| \end{aligned}$$

as well as

$$|w_1| = |z_1 - \mu| \leq \delta.$$

So we can conclude

$$\begin{aligned} \frac{f(z_1)}{f(z_2)} &= \frac{e^{-\frac{(z_1-\mu)^2}{2\sigma^2}}}{e^{-\frac{(z_2-\mu)^2}{2\sigma^2}}} \\ &= \frac{e^{-\frac{w_1^2}{2\sigma^2}}}{e^{-\frac{w_2^2}{2\sigma^2}}} \\ &= e^{-\frac{w_1^2}{2\sigma^2}} \cdot e^{\frac{w_2^2}{2\sigma^2}} \\ &\leq e^{-\frac{w_1^2}{2\sigma^2}} \cdot e^{\frac{(\eta+|w_1|)^2}{2\sigma^2}} \\ &= e^{-\frac{w_1^2}{2\sigma^2}} \cdot e^{\frac{w_1^2 + 2|w_1|\eta + \eta^2}{2\sigma^2}} \\ &= e^{\frac{2|w_1|\eta + \eta^2}{2\sigma^2}} \\ &\leq e^{\frac{2\delta\eta + \eta^2}{2\sigma^2}}. \end{aligned}$$

This proves the proposition of the Lemma. □

2.2.3 Chi-Quadrat-Distribution

Closely connected with the normal distribution is the Chi-Square-Distribution, which is defined on the basis of [FKPT07]. After that we present some fundamental properties.

Z_1, \dots, Z_n may be independently and identically normally distributed random variables. So $Z_i \sim \mathcal{N}(0, 1)$ für $i = 1, \dots, n$. On that basis we define

$$W = (Z_1)^2 + \dots + (Z_n)^2.$$

Then we call their distribution Chi-Square-Distribution with n degrees of freedom (shortly: $\chi^2(n)$ -distribution). W is $\chi^2(n)$ -distributed (shortly: $W \sim \chi^2(n)$).

The following relationship is useful: For $\mathbf{U} = (U_1, \dots, U_d)^T$ with $\mathbf{U} \sim \mathcal{N}_d(\mathbf{0}, \mathbf{E}_d)$ we consider :

$$\|\mathbf{U}\|^2 = (U_1)^2 + \dots + (U_d)^2.$$

From $U_i \sim \mathcal{N}(0, 1)$ for $i = 1, \dots, d$ we derive $\|\mathbf{U}\|^2 \sim \chi^2(d)$. So it holds: The squared norm of a normally distributed random vector $\mathbf{U} \sim \mathcal{N}_d(\mathbf{0}, \mathbf{E}_d)$ follows a Chi-Square-distribution with d degrees of freedom.

In the following we focus on the special case $d = 2$, since we are obligated to do some smoothed analysis for that case on our own without having predecessor results as for $d \geq 3$.

Lemma 2.2.4.

Let \mathbf{U} be a two dimensional normally distributed vector with $\mathbf{U} \sim \mathcal{N}_2(\mathbf{0}, \mathbf{E}_2)$. Then

$$\mathbb{P}[\|\mathbf{U}\|^2 \geq \epsilon^2] = \mathbb{P}[\|\mathbf{U}\| \geq \epsilon] = e^{-\frac{\epsilon^2}{2}}$$

for all $\epsilon \geq 0$. Here $\|\mathbf{U}\|^2 \sim \chi^2(2)$.

Proof. As known \mathbf{U} possesses the density function $f(\mathbf{u}) = \frac{1}{2\pi} \cdot e^{-\frac{u_1^2+u_2^2}{2}}$. Besides we see that for each $\mathbf{w} \in \mathbb{R}^2$ with $\|\mathbf{w}\| = \epsilon$ the density attains the value

$$f(\mathbf{w}) = \frac{1}{2\pi} \cdot e^{-\frac{\epsilon^2}{2}}$$

The set of all points \mathbf{y} with $\|\mathbf{y}\| = \epsilon$ forms a circle with radius ϵ about the origin. It has circumference $2\pi\epsilon$. So we can calculate the radial density function

$$\tilde{f}(\epsilon) = 2\pi\epsilon \cdot \frac{1}{2\pi} \cdot e^{-\frac{\epsilon^2}{2}} = \epsilon \cdot e^{-\frac{\epsilon^2}{2}}$$

and the probability will be

$$\mathbb{P}[\|\mathbf{U}\| \geq \epsilon] = \int_{\epsilon}^{\infty} \tilde{f}(r) dr = \int_{\epsilon}^{\infty} r \cdot e^{-\frac{r^2}{2}} dr = \left[-e^{-\frac{r^2}{2}} \right]_{\epsilon}^{\infty} = e^{-\frac{\epsilon^2}{2}}.$$

Since obviously $\mathbb{P}[\|\mathbf{U}\|^2 \geq \epsilon^2] = \mathbb{P}[\|\mathbf{U}\| \geq \epsilon]$ this concludes the proof. \square

From that we may draw the following consequences.

Corollary 2.2.5.

Ler \mathbf{U} be a twodimensional normally distributed random vector with center in the origin and standard deviation $\sigma > 0$, i.e. $\mathbf{U} \sim \mathcal{N}_2(\mathbf{0}, \sigma^2 \mathbf{E}_2)$. Then

$$\mathbb{P}[\|\mathbf{U}\| \geq \epsilon\sigma] = e^{-\frac{\epsilon^2}{2}}$$

for all $\epsilon \geq 0$.

Proof. Set $\mathbf{U} = \sigma \mathbf{W}$ with $\mathbf{W} \sim \mathcal{N}_2(\mathbf{0}, \mathbf{E}_2)$. Then

$$\mathbb{P}[\|\mathbf{U}\| \geq \epsilon\sigma] = \mathbb{P}[\|\sigma \mathbf{W}\| \geq \epsilon\sigma] = \mathbb{P}[\sigma \|\mathbf{W}\| \geq \epsilon\sigma] \stackrel{(*)}{=} \mathbb{P}[\|\mathbf{W}\| \geq \epsilon] = e^{-\frac{\epsilon^2}{2}}.$$

The equation $(*)$ holds because of $\sigma > 0$ and the last equation is a consequence of Lemma 2.2.4. This concludes the proof. \square

Corollary 2.2.6.

Let $\mathbf{U} \sim \mathcal{N}_2(\boldsymbol{\mu}, \sigma^2 \mathbf{E}_2)$ with $\|\boldsymbol{\mu}\| \leq 1$. Then

$$\mathbb{P}[\|\mathbf{U}\| \geq 1 + \epsilon\sigma] \leq e^{-\frac{\epsilon^2}{2}}.$$

Proof. Set $\mathbf{U} = \boldsymbol{\mu} + \mathbf{W}$ mit $\mathbf{W} \sim \mathcal{N}_2(\mathbf{0}, \sigma^2 \mathbf{E}_2)$. Hence

$$\begin{aligned} & \mathbb{P}[\|\mathbf{U}\| \geq 1 + \epsilon\sigma] \\ &= \mathbb{P}[\|\boldsymbol{\mu} + \mathbf{W}\| \geq 1 + \epsilon\sigma] \\ &\leq \mathbb{P}[\|\boldsymbol{\mu}\| + \|\mathbf{W}\| \geq 1 + \epsilon\sigma] \quad (\text{da } \|\boldsymbol{\mu} + \mathbf{W}\| \leq \|\boldsymbol{\mu}\| + \|\mathbf{W}\|) \\ &= \mathbb{P}[\|\mathbf{W}\| \geq 1 - \|\boldsymbol{\mu}\| + \epsilon\sigma] \\ &\leq \mathbb{P}[\|\mathbf{W}\| \geq \epsilon\sigma] \quad (\text{da } 1 - \|\boldsymbol{\mu}\| \geq 0) \\ &= e^{-\frac{\epsilon^2}{2}}. \end{aligned} \tag{Corollary 2.2.5}$$

which shows the proposition. \square

As a final step we extend our considerations to a set of m normally distributed random variables $\mathbf{U}_1, \dots, \mathbf{U}_m$. In that context we can obtain the following result..

Lemma 2.2.7.

Let m ($m \geq 2$) independently and normally distributed random vectors $\mathbf{U}_1, \dots, \mathbf{U}_m$ with $\mathbf{U}_i \sim \mathcal{N}_2(\boldsymbol{\mu}_i, \sigma^2 \mathbf{E}_2)$ be given. For the centers we assume that $\|\boldsymbol{\mu}_i\| \leq 1$ for all i and for the standard deviation we may have $\sigma \leq \frac{1}{2\sqrt{\ln(m)}}$. Then it holds:

$$\mathbb{P}\left[\max_{i=1,\dots,m} \|\mathbf{U}_i\| \geq 2\right] \leq \frac{1}{m}.$$

Proof. First consider

$$\begin{aligned}
 & \mathbb{P} \left[\max_{i=1,\dots,m} \|\mathbf{U}_i\| \geq 2 \right] \\
 &= \mathbb{P} [(\|\mathbf{U}_1\| \geq 2) \vee \dots \vee (\|\mathbf{U}_m\| \geq 2)] \\
 &\leq \sum_{i=1}^m \mathbb{P} [\|\mathbf{U}_i\| \geq 2] \\
 &\leq m \cdot \max_{i=1,\dots,m} \mathbb{P} [\|\mathbf{U}_i\| \geq 2].
 \end{aligned}$$

It will suffice to show that for arbitrary $j \in \{1, \dots, m\}$:

$$\mathbb{P} [\|\mathbf{U}_j\| \geq 2] \leq m^{-2}.$$

For ensuring that estimation we apply Corollary 2.2.6. Therefore we choose $\epsilon = 2\sqrt{\ln(m)}$ and we remember that $\sigma \leq \frac{1}{2\sqrt{\ln(m)}}$. So we obtain:

$$\begin{aligned}
 & \mathbb{P} [\|\mathbf{U}_j\| \geq 2] \\
 &\leq \mathbb{P} \left[\|\mathbf{U}_j\| \geq 1 + 2\sqrt{\ln(m)}\sigma \right] \quad (\text{since } 2\sqrt{\ln(m)}\sigma \leq 1) \\
 &\leq e^{-\frac{(2\sqrt{\ln(m)})^2}{2}} \quad (\text{Corollary 2.2.6}) \\
 &= e^{-2\ln(m)} \\
 &= m^{-2}.
 \end{aligned}$$

This bounds the probability. □

2.3 The Simplex Method

In this section we explain the basic functionality of the Simplex Method and we discuss the numerical realization by means of the so-called Tableau-Method. Further information can be got from [Bor01].

2.3.1 The Essential Functionality

For preparing the content of this thesis we introduce the principle of the Simplex Method for the solution of Linear Optimization Problems of the following kind:

$$\begin{aligned}
 & \text{maximize } \langle \mathbf{v}, \mathbf{x} \rangle \\
 & \text{s.t. } \langle \mathbf{a}_1, \mathbf{x} \rangle \leq b^1 \\
 & \quad \vdots \\
 & \quad \langle \mathbf{a}_m, \mathbf{x} \rangle \leq b^m
 \end{aligned} \tag{LP}$$

by finding an \mathbf{x} with $\mathbf{a}_1, \dots, \mathbf{a}_m, \mathbf{v} \in \mathbb{R}^d$ and $\mathbf{b} = (b^1, \dots, b^m)^T \in \mathbb{R}^m$. The feasible region, which is polyhedron, is denoted by X . For simplification we set $\mathbf{A} := (\mathbf{a}_1, \dots, \mathbf{a}_m)^T$. In the following problems of that kind will be denoted by (LP).

The concept of the Simplex Method exploits the following two insights from polyhedral theory and from the theory of linear optimization problems.

Conclusion 2.3.1.

Let the feasible region X of (LP) be nonempty and it may have at least one vertex. Then the set X_{opt} of optimal points of (LP) is nonempty, so it contains at least one vertex of X .

Conclusion 2.3.2.

The feasible region X of (LP) may be nonempty and it may have one vertex \mathbf{x} at least. Then at \mathbf{x} the following cases are possible:

1. *The vertex \mathbf{x} is optimal for (LP).*
2. *There is an adjacent vertex to \mathbf{x} called \mathbf{y} with greater objective value, i.e. $\langle \mathbf{v}, \mathbf{y} \rangle > \langle \mathbf{v}, \mathbf{x} \rangle$.*
3. *There is an unbounded edge originating from \mathbf{x} improving the objective. In that case (LP) has no optimal point. The objective is unbounded from above.*

We explain the functionality of the Simplex Method. Assume that we have a vertex \mathbf{x} of the feasible region X . Then either we can stop the treatment at \mathbf{x} (in case of optimality or if unboundedness of the objective becomes apparent) or there is an edge from \mathbf{x} to an adjacent vertex \mathbf{y} featuring a greater objective value. Since the number of vertices of X is finite (the maximal number can be calculated) such a procedure of edge-walks terminates after finitely many steps. This procedure just described is called Phase 2 of the Simplex Method.

In order to start this Phase 2 procedure, we are in need of a start vertex \mathbf{x} of X . For this purpose we apply a so-called Phase 1. This procedure shall clarify whether X is nonempty at all. If Yes, then this procedure is able to determine one of the vertices of X . And that vertex can then be used for the start of Phase 2. The essential way how this procedure works is similar to that of Phase 2.

So the principal course of action is as follows

Phase 1 Find a vertex \mathbf{x}_0 of X or assure, that the feasible region is empty. In the latter case we can abort the procedure, because a solution to the problem cannot exist.

Phase 2 Starting from \mathbf{x}_0 construct a sequence $\mathbf{x}_0, \mathbf{x}_1, \dots, \mathbf{x}_s$ of successively adjacent vertices with the following two properties: For sequential vertices \mathbf{x}_k and \mathbf{x}_{k+1} we have $\langle \mathbf{v}, \mathbf{x}_k \rangle < \langle \mathbf{v}, \mathbf{x}_{k+1} \rangle$. In addition \mathbf{x}_s either is an optimal point or it becomes obvious at \mathbf{x}_s that the problem is unsolvable because of unboundedness of the objective.

Besides that classical partition into a first and a second Phase we are going to study differing partitions, which enable us to obtain improving results.

Remark 2.3.3.

Potentially there are several vertices adjacent to \mathbf{x}_k and exhibiting a better objective value than \mathbf{x}_k . All these could take the role of the successor vertex \mathbf{x}_{k+1} . To make a deterministic decision how to continue and to select a unique successor vertex, one has to apply a chosen pivot rule. The choice of such a pivot rule determines what we call a (special) variant of the Simplex Method. Such a special variant, the so-called shadow-vertex algorithm, is located in the focus in the theory of probabilistic analysis of the running time of the Simplex Method. And this includes all the attempts to carry out a smoothed analysis.

2.3.2 The Tableau Method

For the clear and understandable execution of the Simplex Method it is very helpful to organize the relevant data in Tableau-form . Some aspects of that Tableau-form and of the Tableau-method will be presented and discussed in this subsection. A complete demonstration and explanation can be found in [Bor01, S. 83-110], where also the following excerpts are from.

For our problem the Tableau has the following structure.

	\mathbf{a}_1	\cdots	\mathbf{a}_j	\cdots	\mathbf{a}_r	\cdots	\mathbf{a}_m	$-\mathbf{e}_1$	\cdots	$-\mathbf{e}_i$	\cdots	$-\mathbf{e}_d$	\mathbf{v}
\mathbf{a}_{Δ^1}	α_1^1	\cdots	α_j^1	\cdots	0	\cdots	α_m^1	γ_1^1	\cdots	γ_i^1	\cdots	γ_d^1	ν^1
\vdots	\vdots		\vdots		\vdots		\vdots	\vdots		\vdots		\vdots	\vdots
\mathbf{a}_{Δ^k}	α_1^k	\cdots	α_j^k	\cdots	0	\cdots	α_m^k	γ_1^k	\cdots	γ_i^k	\cdots	γ_d^k	ν^k
\vdots	\vdots		\vdots		\vdots		\vdots	\vdots		\vdots		\vdots	\vdots
$\mathbf{a}_{\Delta^s} = \mathbf{a}_r$	α_1^s	\cdots	α_j^s	\cdots	1	\cdots	α_m^s	γ_1^s	\cdots	γ_i^s	\cdots	γ_d^s	ν^s
\vdots	\vdots		\vdots		\vdots		\vdots	\vdots		\vdots		\vdots	\vdots
\mathbf{a}_{Δ^d}	α_1^d	\cdots	α_j^d	\cdots	0	\cdots	α_m^d	γ_1^d	\cdots	γ_i^d	\cdots	γ_d^d	ν^d
	β^1	\cdots	β^j	\cdots	0	\cdots	β^m	x^1	\cdots	x^i	\cdots	x^d	$-Q$

Tableau 2.1: General Tableau-Structure in componentwise illustration

There are in total $m+d+1$ columns, where the first m represent the regular restrictions $\langle \mathbf{a}_1, \mathbf{x} \rangle \leq b^1, \dots, \langle \mathbf{a}_m, \mathbf{x} \rangle \leq b^m$. The next d columns are dedicated to the additional (and sometimes artificial) restrictions $\langle -\mathbf{e}_1, \mathbf{x} \rangle \leq 0, \dots, \langle -\mathbf{e}_d, \mathbf{x} \rangle \leq 0$ and the last column corresponds to the hypothetical restriction $\langle \mathbf{v}, \mathbf{x} \rangle \leq 0$.

The first d of the $(d+1)$ rows of the Tableau are reserved for the coordinate-representations of the vectors $\mathbf{a}_1, \dots, \mathbf{a}_m, -\mathbf{e}_1, \dots, -\mathbf{e}_d$ and \mathbf{v} with respect to a basis consisting of d

restriction vectors $\mathbf{a}_{\Delta^1}, \dots, \mathbf{a}_{\Delta^d}$.¹ On the left side or boundary of the Tableau it is specified which original vectors take (at this moment) the role of the according basis vectors. The index set $\Delta = \{\Delta^1, \dots, \Delta^d\} \subset \{1, \dots, m\}$ is according to its functionality in the Simplex Method not an arbitrary set. Instead it is chosen in a way that the corresponding basic solution $\mathbf{x}_\Delta = \mathbf{A}_\Delta^{-1} \mathbf{b}_\Delta$ is a vertex of the feasible region X .

In the lowermost row of the Tableau one finds the differences between the right-hand sides of the restrictions and the present value of the restriction functions at the vertex under consideration \mathbf{x} . For the first m columns according to this it holds that $\beta^j = b^j - \langle \mathbf{a}_j, \mathbf{x} \rangle$. For the restrictions corresponding to $-\mathbf{e}_1, \dots, -\mathbf{e}_d$ we obtain $x^i = 0 - \langle -\mathbf{e}_i, \mathbf{x} \rangle$. There - as shown in the Tableau above - one finds just the coordinates of the present vertex. The entry in the column to \mathbf{v} is calculated as $-Q = 0 - \langle \mathbf{v}, \mathbf{x} \rangle = -\langle \mathbf{v}, \mathbf{x} \rangle$. Here Q denotes the value of the objective function at the present vertex. These observations can be formulated in concise form by using a formulation in terms of matrices under use of the index set Δ .

	\mathbf{a}_1	\dots	\mathbf{a}_m	$-\mathbf{e}_1$	\dots	$-\mathbf{e}_d$	\mathbf{v}
\mathbf{a}_{Δ^1}							
\vdots			$(\mathbf{A}\mathbf{A}_\Delta^{-1})^T$			$-(\mathbf{A}_\Delta^{-1})^T$	$(\mathbf{A}_\Delta^{-1})^T \mathbf{v}$
\mathbf{a}_{Δ^d}							
			$(\mathbf{b} - \mathbf{A}\mathbf{A}_\Delta^{-1}\mathbf{b}_\Delta)^T$		$(\mathbf{A}_\Delta^{-1}\mathbf{b}_\Delta)^T$		$-\mathbf{v}^T \mathbf{A}_\Delta^{-1} \mathbf{b}_\Delta$

Tableau 2.2: General Tableau-representation in matrix-notation

Now we are going to discuss the three essential operations handling the Tableau data. Without proving this, we state the following: The choice of the edge emanating from \mathbf{x} , used for the iteration to the next vertex, structurally determines the pivot row. Potential pivot rows are those \mathbf{a}_{Δ^k} for which the entry ν^k in the \mathbf{v} -column is strictly negative.

Detection of optimality

If $\nu^1, \dots, \nu^d \geq 0$ for all entries in the \mathbf{v} -column of the Tableau, then we have optimality at the present vertex \mathbf{x} . This is a direct consequence of the polar cone theorem.

Theorem 2.3.4 (polar cone theorem).

Let \mathbf{x} a feasible point for (LP) such that $\mathbf{A}_I = \mathbf{b}_I$ and $\mathbf{A}_J < \mathbf{b}_J$ for $I \cup J = \{1, \dots, m\}$. Then \mathbf{x} is an optimal solution for (LP) if and only if

$$\mathbf{v} \in \mathbf{KK}(\mathbf{a}_i : i \in I)$$

¹We assume that the vectors $\mathbf{a}_{\Delta^1}, \dots, \mathbf{a}_{\Delta^d}$ are linearly independent..

Detection of Unboundedness:

Assume that we have already chosen the pivot row \mathbf{a}_{Δ^k} . Then we identify unboundedness of the objective by observing that for the corresponding entries in the first m columns of the Tableau $\alpha_1^k, \dots, \alpha_m^k \geq 0$ holds.

Execution of a pivot step:

Let again \mathbf{a}_{Δ^k} be the pivot row already chosen. We assume that the criterion for unboundedness is not valid. Now one has to determine an index j such that

$$\frac{\beta^j}{-\alpha_j^k} = \min \left\{ \frac{\beta^l}{-\alpha_l^k} : \alpha_l^k < 0, l \notin \Delta \right\}.$$

This index determines in the pivot row with index Δ^k just the pivot element α_j^k . It is framed in the following Tableau.

	\mathbf{a}_1	\cdots	\mathbf{a}_j	\cdots	\mathbf{a}_r	\cdots	\mathbf{a}_m	$-\mathbf{e}_1$	\cdots	$-\mathbf{e}_i$	\cdots	$-\mathbf{e}_d$	\mathbf{v}
\mathbf{a}_{Δ^1}	α_1^1	\cdots	α_j^1	\cdots	0	\cdots	α_m^1	γ_1^1	\cdots	γ_i^1	\cdots	γ_d^1	v^1
\vdots	\vdots		\vdots		\vdots		\vdots	\vdots		\vdots		\vdots	\vdots
\mathbf{a}_{Δ^k}	α_1^k	\cdots	$\boxed{\alpha_j^k}$	\cdots	0	\cdots	α_m^k	γ_1^k	\cdots	γ_i^k	\cdots	γ_d^k	v^k
\vdots	\vdots		\vdots		\vdots		\vdots	\vdots		\vdots		\vdots	\vdots
$\mathbf{a}_{\Delta^s} = \mathbf{a}_r$	α_1^s	\cdots	α_j^s	\cdots	1	\cdots	α_m^s	γ_1^s	\cdots	γ_i^s	\cdots	γ_d^s	v^s
\vdots	\vdots		\vdots		\vdots		\vdots	\vdots		\vdots		\vdots	\vdots
\mathbf{a}_{Δ^d}	α_1^d	\cdots	α_j^d	\cdots	0	\cdots	α_m^d	γ_1^d	\cdots	γ_i^d	\cdots	γ_d^d	v^d
	β^1	\cdots	β^j	\cdots	0	\cdots	β^m	x^1	\cdots	x^i	\cdots	x^d	$-Q$

Tableau 2.3: Tableau with pivot element for the execution of a pivot step

Now the Tableau for the successor vertex \mathbf{x}' can be calculated by application of the Gauß-Algorithmus to the available Tableau such that the entry of the pivot element gets the value 1 and all the remaining entries of that column get the value 0.

At a later point we shall demonstrate how the shadow vertex algorithm works. Therefore it seems to be helpful to remark:

Remark 2.3.5 (Adding a new restriction).

With little effort it is possible to insert and to integrate a new resp. additional restriction for our problem $\langle \mathbf{a}_{m+1}, \mathbf{x} \rangle \leq b^{m+1}$ in the Tableau. For that it is only necessary to calculate the values

$$(\mathbf{A}_{\Delta}^{-1})^T \mathbf{a}_{m+1}$$

as well as

$$b^{m+1} - \langle \mathbf{a}_{m+1}, \mathbf{x} \rangle$$

and we have to record these values in an additional column of the Tableau. The necessary inverse matrix as well as the actual point can be seen directly in the Tableau 2.2.

2.3.3 Fundamental Considerations On The Computation Time

On the basis of the functionality of the Simplex Method as presented in the two previous sections 2.3.1 and 2.3.2 we want to build a connection to the argumentation in chapter 1. There we had presented the essential different views on the complexity in general form. For preparation of the content of this work it makes sense to state some points more precisely.

For our complexity criterion \mathcal{C}_A in the respective form A of the Simplex Method we use always the number of pivot steps carried out. This makes sense, since it essentially determines the arithmetical effort. We shall use the criteria with respect to the solution process for

$$\begin{aligned} & \text{maximize } \langle \mathbf{v}, \mathbf{x} \rangle \\ \text{s.t. } & \langle \mathbf{a}_1, \mathbf{x} \rangle \leq b^1 \\ & \vdots \\ & \langle \mathbf{a}_m, \mathbf{x} \rangle \leq b^m. \end{aligned}$$

The problem-defining data can be stored in a vector of dimension $n := m(d + 1) + d$. But for the impact on the number of pivot steps the two single and separate figures m and d have the greatest relevance. Consequently the functions $f(n)$, $g(n)$ and $h(n, \sigma)$ for the different complexity types from the introduction chapter should – in our case – be replaced by functions of the form $f(m, d)$, $g(m, d)$ and $h(m, d, \sigma)$.

The following sections deal with the shadow-vertex-algorithm, a special variant of the Simplex Algorithm .

2.4 The Shadow Vertex Algorithm

The content of this section comes from [Bor87] and everything is proved there in detail. Therefore we concentrate on the presentation of the results and we do without deriving them. Also the kind of presentation is taken from that source.

2.4.1 The Primal Shadow Vertex Algorithm

We shall exhibit the functionality of the shadow vertex algorithm for the solution of problems like:²

$$\begin{aligned} & \text{maximize } \langle \mathbf{v}, \mathbf{x} \rangle \\ & \text{s.t. } \langle \mathbf{a}_1, \mathbf{x} \rangle \leq 1 \\ & \quad \vdots \\ & \quad \langle \mathbf{a}_m, \mathbf{x} \rangle \leq 1. \end{aligned} \tag{EP}$$

Here $\mathbf{v}, \mathbf{x}, \mathbf{a}_1, \dots, \mathbf{a}_m \in \mathbb{R}^d$ and $m \geq d$. In the course of this work we shall call problems in the above mentioned form unit problems and abbreviate it by (EP). A restriction from the system of inequalities will consequently be called unit restriction and X stands for the feasible region.

In the following let us concentrate on Phase 2. Assume that we have a vertex \mathbf{x}_0 of X , which is optimal with respect to the objective direction $\mathbf{u} \in \mathbb{R}^d$. Furthermore we assume that:

Assumption 2.4.1 (Condition of nondegeneracy).

Each d -element subset of $\{\mathbf{a}_1, \dots, \mathbf{a}_m, \mathbf{u}, \mathbf{v}\}$ shall be linearly independent and each subset of $(d+1)$ elements from $\{\mathbf{a}_1, \dots, \mathbf{a}_m\}$ shall be in general position..

Under the stochastic models used in our investigations we can presume the validity of that condition of nondegeneracy in this work. In that case each vertex of X is the unique solution \mathbf{x}_Δ of a system of equations

$$\langle \mathbf{a}_{\Delta^1}, \mathbf{x} \rangle = 1, \dots, \langle \mathbf{a}_{\Delta^d}, \mathbf{x} \rangle = 1$$

with $\Delta = \{\Delta^1, \dots, \Delta^d\}$. In addition this is a feasible point, i.e. $\langle \mathbf{a}_j, \mathbf{x} \rangle \leq 1$ for all $j = 1, \dots, m$.

Now we can present the principle of the shadow vertex pivot-rule. Consider the orthogonal projection $\Gamma(X)$ of the polyhedron X on the two-dimensional plane $\mathbf{LH}(\mathbf{u}, \mathbf{v})$. Then the shadow vertices are just those vertices of X , whose images $\Gamma(\mathbf{x})$ are vertices of the polygon $\Gamma(X)$. We can make the following statement.

Lemma 2.4.2.

Let \mathbf{x}_Δ be a vertex of X . Then nondegeneracy makes the following three conditions equivalent.

- (a) \mathbf{x}_Δ is a shadow vertex.
- (b) $\Gamma(\mathbf{x}_\Delta) \in \partial\Gamma(X)$ (boundary of $\Gamma(X)$)

²In principle the shadow vertex algorithm can be used to solve arbitrary linear optimization problems. But an investigation on the basis of the dual perspective, as exploited later, is possible only for this type of problem .

(c) There is a vector $\mathbf{w} \in \mathbf{LH}(\mathbf{u}, \mathbf{v}) \setminus \{\mathbf{0}\}$, such that $\langle \mathbf{w}, \mathbf{x}_\Delta \rangle = \max_{\mathbf{x} \in X} \langle \mathbf{w}, \mathbf{x} \rangle$.

In consequence of that equivalence we come to the following algorithmic principle. We take the vector \mathbf{u} and rotate it in direction of \mathbf{v} . Simultaneously we determine the optimal solutions on X for all intermediate directions \mathbf{w} . These are the directions traversed during our rotation. The Lemma declares that by the way we create a sequence of vertices, that are all shadow vertices. Furthermore the vertices $\Gamma(\mathbf{x}_i)$ and $\Gamma(\mathbf{x}_{i+1})$ in $\Gamma(X)$ are adjacent. Of course such a sequence can also be constructed, if in direction \mathbf{v} unboundedness is valid. In that case \mathbf{x}_s is optimal with respect to the last $\mathbf{w} \in \mathbf{KK}(\mathbf{u}, \mathbf{v})$, for which boundedness was true. In this case our vertex is adjacent to an unbounded edge not improving this last \mathbf{w} -objective, but strictly improving the \mathbf{v} -objective.

At this point we do not yet know whether the sequence $\mathbf{x}_0, \dots, \mathbf{x}_s$ describes a Simplex-path. For an answer we should clarify two questions.

1. Is it true that two successive vertices \mathbf{x}_i and \mathbf{x}_{i+1} are adjacent in any case?
2. Will the move from \mathbf{x}_i to \mathbf{x}_{i+1} strictly increase the objective value?

An answer is given in the following Lemma.

Lemma 2.4.3.

Let \mathbf{x}_i and \mathbf{x}_{i+1} be vertices. If $\Gamma(\mathbf{x}_i)$ and $\Gamma(\mathbf{x}_{i+1})$ in $\Gamma(X)$ are adjacent, then this applies to \mathbf{x}_i and \mathbf{x}_{i+1} in X as well.

Lemma 2.4.4.

Let $\mathbf{x}_0, \mathbf{x}_1, \dots, \mathbf{x}_s$ be the optimal vertices with respect to the objective directions $\mathbf{w}_0, \mathbf{w}_1, \dots, \mathbf{w}_s$, where $\mathbf{w}_0 = \mathbf{u}$ and $\text{arc}(\mathbf{w}_i, \mathbf{v}) > \text{arc}(\mathbf{w}_{i+1}, \mathbf{v})$ for $i = 0, \dots, s-1$. Then:

$$\langle \mathbf{v}, \mathbf{x}_{i+1} \rangle > \langle \mathbf{v}, \mathbf{x}_i \rangle$$

für $i = 0, \dots, s-1$.

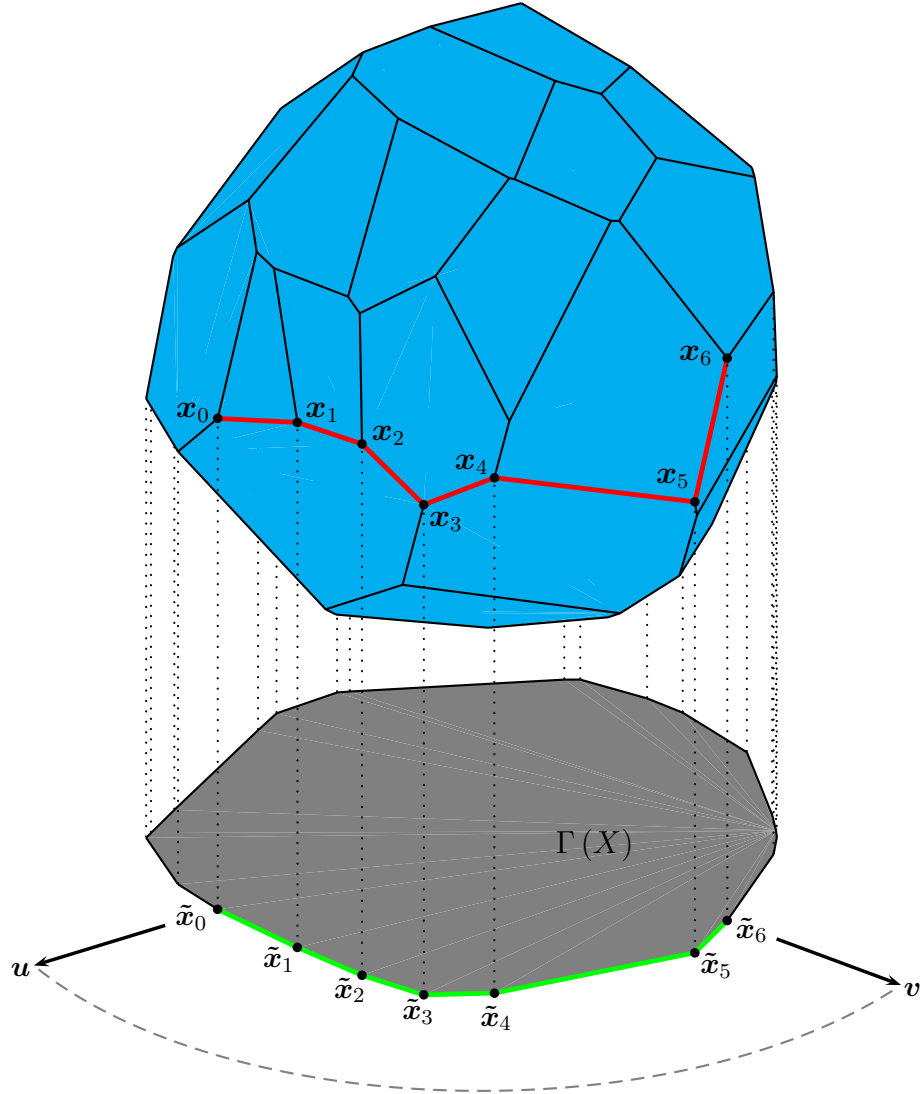


Figure 2.1: Graphical illustration of the functionality of the primal shadow-vertex-algorithm

So the method described before does indeed construct a Simplex Path. In figure 2.1 one finds a graphical illustration of the functionality of the shadow vertex algorithm. For simplification of the notation in the figure we set $\tilde{\mathbf{x}}_i := \Gamma(\mathbf{x}_i)$. First we consider the orthogonal projection of X on the plane $\mathbf{LH}(\mathbf{u}, \mathbf{v})$. This delivers the polygon drawn in grey. We start from the vertex $\tilde{\mathbf{x}}_0$ von $\Gamma(X)$. This vertex is optimal with respect to the objective direction \mathbf{u} . Now we rotate the vector \mathbf{u} in direction \mathbf{v} . By the way we obtain a chain of edges $\tilde{\mathbf{x}}_0, \dots, \tilde{\mathbf{x}}_6$, where $\tilde{\mathbf{x}}_6$ is optimal with respect to \mathbf{v} . This chain of edges corresponds to the Simplex Path $\mathbf{x}_0, \dots, \mathbf{x}_6$ on the original originalen polyhedron X . The start vertex \mathbf{x}_0 is optimal with respect to the auxiliary objective direction \mathbf{u} and \mathbf{x}_6 is the optimal solution for the original problem.

2.4.2 The Dual Shadow Vertex Algorithm

In this section we discuss the shadow vertex algorithm under the so called dual perspective. This viewpoint grants the advantage that all interesting events can be expressed directly by means of the vectors $\mathbf{a}_1, \dots, \mathbf{a}_m, \mathbf{u}, \mathbf{v}$. This simplifies the considerations, since these are the random variables dominating the game. Now we deal with the polyhedron Y , which is dual to X , and is defined as follows:

$$Y := \{ \mathbf{y} \in \mathbb{R}^d : \langle \mathbf{x}, \mathbf{y} \rangle \leq 1 \text{ for all } \mathbf{x} \in X \}.$$

We can show that this polyhedron has the following form:

Lemma 2.4.5.

$$Y = \{ \mathbf{y} \in \mathbb{R}^d : \langle \mathbf{x}, \mathbf{y} \rangle \leq 1 \text{ for all } \mathbf{x} \in X \} = \mathbf{K}\mathbf{H}(\mathbf{0}, \mathbf{a}_1, \dots, \mathbf{a}_m).$$

As before $\Delta := \{\Delta^1, \dots, \Delta^d\} \subset \{1, \dots, m\}$ shall be a d -element index set. Since the condition of nondegeneracy is valid (2.4.1), we have an obvious 1-to-1-relation between Δ and the solution \mathbf{x}_Δ of the system of equations

$$\langle \mathbf{a}_{\Delta^1}, \mathbf{x} \rangle = 1, \dots, \langle \mathbf{a}_{\Delta^d}, \mathbf{x} \rangle = 1.$$

On the other side there is also a 1-to-1-relation between Δ and the $(d-1)$ -dimensional simplex $\mathbf{K}\mathbf{H}(\mathbf{a}_{\Delta^1}, \dots, \mathbf{a}_{\Delta^d})$. Hence in total we have the 1-to-1-relation:

$$\mathbf{x}_\Delta \longleftrightarrow \Delta \longleftrightarrow \mathbf{K}\mathbf{H}(\mathbf{a}_{\Delta^1}, \dots, \mathbf{a}_{\Delta^d}) =: \Sigma(\Delta). \quad (2.1)$$

At this point it should be clarified, how the property of having a vertex \mathbf{x}_Δ of X affects $\Sigma(\Delta)$ and vice versa. An answer is given in the following Lemma.

Lemma 2.4.6.

\mathbf{x}_Δ is a vertex of X if and only $\Sigma(\Delta)$ is a facet³ of Y .

In connection with the 1-to-1-relation (2.1) we recognize a unique correspondence between the vertices of the primal polyhedron X and the facets of the dual polytope Y not containing the origin.

A further significant point is to clarify, how the property of being a shadow vertex can be recognized in the dual perspective. An answer is given in the following Lemma.

Lemma 2.4.7.

Let \mathbf{x}_Δ be a vertex of X and let us have a $\mathbf{w} \in \mathbb{R}^d$ with $\mathbf{w} \neq \mathbf{0}$. Then \mathbf{x}_Δ is optimal on X with respect to the objective \mathbf{w} if and only if

$$\mathbb{R}^+ \mathbf{w} \cap \Sigma(\Delta) \neq \emptyset.$$

Here $\mathbb{R}^+ \mathbf{w} := \{ \lambda \mathbf{w} : \lambda > 0 \}$.

³What we mean is a $(d-1)$ -dimensional face .

Hence a vertex \mathbf{x}_Δ is a shadow vertex if and only if the corresponding facet $\Sigma(\Delta)$ of the polyhedron Y is intersected by the plane $\mathbf{LH}(\mathbf{u}, \mathbf{v})$. Besides we want to call the facet $\Sigma(\Delta)$ start-facet, if it is intersected by the ray $\mathbb{R}^+ \mathbf{u}$. Analogously $\Sigma(\Delta)$ will be called optimal facet, if it is intersected by the ray $\mathbb{R}^+ \mathbf{v}$.

In contrast to the primal perspective, where we are interested in a sequence of vertices, in the dual perspective our interest turns to a sequence of facets. But common to both perspectives is the interest in the length of both sequences. The following Lemma gives further important information.

Lemma 2.4.8.

The facets of Y intersected by $\mathbf{KK}(\mathbf{u}, \mathbf{v}) \subset \mathbf{LH}(\mathbf{u}, \mathbf{v})$ can be ordered uniquely in a sequence $\Sigma(\Delta_0), \dots, \Sigma(\Delta_s)$ such that

1. $\Delta_i \neq \Delta_j$ for $i \neq j$,
2. Δ_i und Δ_{i+1} differ in exactly one index
3. $\text{arc}(\mathbf{z}_i, \mathbf{v}) \geq \text{arc}(\mathbf{z}_{i+1}, \mathbf{v})$ for each pair $(\mathbf{z}_i, \mathbf{z}_{i+1})$ with $\mathbf{z}_i \in \Sigma(\Delta_i) \cap \mathbf{LH}(\mathbf{u}, \mathbf{v})$ and $\mathbf{z}_{i+1} \in \Sigma(\Delta_{i+1}) \cap \mathbf{LH}(\mathbf{u}, \mathbf{v})$.

Now we come to the last result, describing the relation between primal and dual perspective.

Lemma 2.4.9.

There is a unique relation between the constructed sequence of facets of Y and a sequence $\mathbf{x}_{\Delta_0}, \dots, \mathbf{x}_{\Delta_s}$ of shadow vertices of X , which stands for a valid Simplex-Path.

Finally in figure 2.2 there is a graphical illustration for the dual interpretation of the shadow vertex algorithm on the polytope Y . For simplification of the notation we set $F_i := \Sigma(\Delta_i)$.

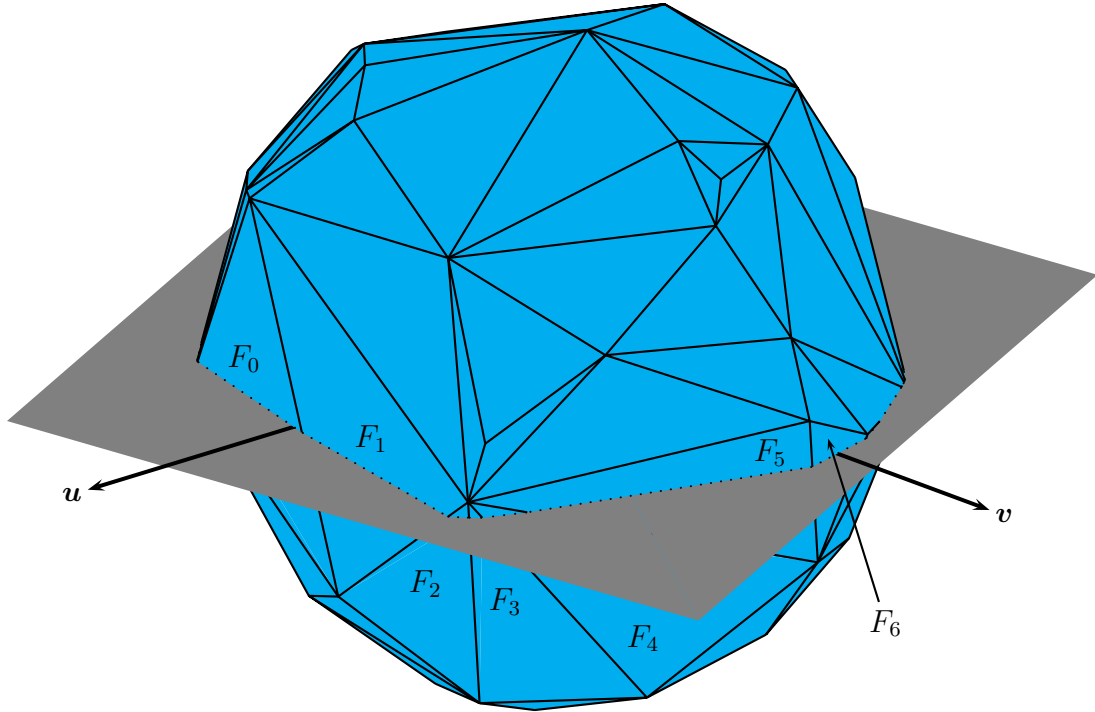


Figure 2.2: Graphical illustration of the dual interpretation of the shadow-vertex-algorithm

F_0 is a facet for starting the algorithm. Emanating from there we rotate the vector \mathbf{u} in direction \mathbf{v} constructing the sequence F_0, F_1, \dots, F_6 of successively intersected facets. Finally F_6 is the desired optimal facet. Here F_0, \dots, F_6 corresponds with a sequence $\mathbf{x}_0, \dots, \mathbf{x}_6$ of shadow vertices, which are traversed (in the primal perspective) on the polyhedron X .

2.4.3 Numerical Realization Of The Shadow Vertex Algorithm

In this subsection we discuss the numerical realization of the shadow vertex algorithm in Tableau-form. In particular we have to focus on the determination of the pivot element for the upcoming pivot step.

We should remark that the rotation of \mathbf{u} in direction \mathbf{v} is realized in the shadow vertex algorithm in the following way: Consider starting from $\mu = 0$ the objective directions $\mathbf{u} + \mu \cdot \mathbf{v}$ für $\mu \rightarrow \infty$.

For demonstrating one pivot step assume that we have the vertex \mathbf{x}_q of the primal polyhedron X and the corresponding Tableau at hand.

	\mathbf{a}_1	\cdots	\mathbf{a}_m	$-\mathbf{e}_1$	\cdots	$-\mathbf{e}_d$	\mathbf{v}	\mathbf{u}
\mathbf{a}_{Δ^1}	α_1^1	\cdots	α_m^1	γ_1^1	\cdots	γ_d^1	ν^1	ξ^1
\vdots	\vdots	\ddots	\vdots	\vdots	\ddots	\vdots	\vdots	\vdots
\mathbf{a}_{Δ^d}	α_1^d	\cdots	α_m^d	γ_1^d	\cdots	γ_d^d	ν^d	ξ^d
	β^1	\cdots	β^m	x_q^1	\cdots	x_q^d	$-Q_v$	$-Q_u$

Tableau 2.4: Tableau for execution of the shadow vertex algorithm

The additional \mathbf{u} -column results from the fact, that we need an auxiliary objective direction \mathbf{u} to realize the shadow vertex algorithm. Moreover let \mathbf{x}_q be optimal with respect to the direction $\mathbf{q} := \mathbf{u} + \bar{\mu} \cdot \mathbf{v}$ such that $\bar{\mu} \geq 0$.⁴ Here we have

$$\bar{\mu} \cdot \nu^k + \xi^k \geq 0$$

for all $k = 1, \dots, d$. If in addition $\nu^1, \dots, \nu^d \geq 0$ for all entries of the \mathbf{v} -columns, then we can stop. In that case we would have optimality at \mathbf{x}_q also for the objective direction \mathbf{v} .

If alternatively \mathbf{x}_q is not optimal, then there are entries $\nu^k < 0$. We shall see, that among these negative entries in the \mathbf{v} -column the pivot row has to be chosen according to a certain rule. To realize that principle, we increase the value of μ beginning from $\bar{\mu}$. By the way we rotate the vector $\mathbf{u} + \mu \cdot \mathbf{v}$ more and more in direction of \mathbf{v} . For sufficiently great values of μ the vector $\mathbf{u} + \mu \cdot \mathbf{v}$ will leave the polar cone of \mathbf{x}_q and \mathbf{x}_q will lose its optimality. Against this background we distinguish between four possible sign-combinations for the pairs (ν^k, ξ^k) :

1. $\nu^k > 0, \xi^k < 0$

This case does not cause problems, since $\mu \cdot \nu^k + \xi^k$ remains positive for all $\mu \geq \bar{\mu}$.

2. $\nu^k < 0, \xi^k < 0$

This combination cannot appear because of $\bar{\mu} \cdot \nu^k + \xi^k \geq 0$ with $\bar{\mu} \geq 0$.

3. $\nu^k > 0, \xi^k > 0$

This combination is not problematic in the same way as the case 1 was not.

4. $\nu^k < 0, \xi^k > 0$

That combination is the most interesting, because for $\mu_k = -\frac{\xi^k}{\nu^k}$ the term $\mu_k \cdot \nu^k + \xi^k$ attains the value 0 and it gets negative for further increasing μ_k .

In order to guarantee that $\mathbf{u} + \mu \cdot \mathbf{v}$ for $\mu \geq \bar{\mu}$ remains in the polar cone of \mathbf{x}_q it is necessary that

$$\mu \leq \min_{\nu^k < 0} \left(-\frac{\xi^k}{\nu^k} \right) = -\frac{\xi^j}{\nu^j} =: \mu' \quad (2.2)$$

⁴A choice of $\bar{\mu} = 0$ would lead us to the start vertex \mathbf{x}_0 of the Simplex Path.

will be satisfied. For $\mu = \mu'$ the hybrid direction $\mathbf{u} + \mu \cdot \mathbf{v}$ is just located in the face

$$\mathbf{KK}(\mathbf{a}_{\Delta^1}, \dots, \mathbf{a}_{\Delta^{j-1}}, \mathbf{a}_{\Delta^{j+1}}, \dots, \mathbf{a}_{\Delta^d})$$

of the polar cone $\mathbf{KK}(\mathbf{a}_{\Delta^1}, \dots, \mathbf{a}_{\Delta^d})$ to \mathbf{x}_q . For iteration to the next vertex the restriction vector \mathbf{a}_{Δ^j} consequently has to be replaced. Hence the row belonging to \mathbf{a}_{Δ^j} must be the pivot row.

Now we can use the principle of section 2.3.2 for determining the pivot column. And so we obtain the pivot element needed to proceed to the next vertex during the iteration.

Remark 2.4.10.

The arithmetic procedure as it is described here in form of the shadow vertex algorithm corresponds to the procedure in the parametric Simplex-Variant [GS55] introduced by Gass und Saaty. This was given exclusively in arithmetical form without any geometrical interpretation. The geometrical interpretation as of following the shadow boundary stems from Borgwardt. Also the algorithmic interpretation under the dual perspective (which has been presented above) is due to Borgwardt's thesis [Bor77]. This mathematical tool turns out to be essential for all stochastically motivated investigations of the running time of the Simplex Method carried out successfully up to now. And no other variant of the Simplex Method has permitted investigations which are likewise successful.

3 Hitherto Existing Smoothed Analysis Approaches For The Simplex Method

In this chapter we present the fundamental principles from the hitherto existing investigations of smoothed analysis of the Simplex Method done by Spielman und Teng and Vershynin. Presenting the algorithmic procedures we build a bridge to the master's thesis [Sch12], where the treatment of Phase 1 in both approaches is studied in detail. We want to emphasize that this chapter is only a sketch of both works. Its main purpose is to give an impression and fundamental information on the methods used there. This is important, since we shall make use of many of the results achieved there.

3.1 The Work Of Spielman And Teng

In 2001 Spielman und Teng presented the principle of Smoothed Analysis in combination with a first investigation according to that principle for the Simplex Method in [ST01]. The final analysis from [ST04], was published in 2004. It is the basis of our following presentation.

3.1.1 The Geometrical Fundamental Result

The variant of the Simplex Method analyzed by Spielman und Teng in [ST04] makes extensive use of the shadow vertex algorithm, which we have explained in section 2.4. For that reason the total running time analysis is closely connected to the number of shadow vertices of a perturbed polyhedron. This number or figure will play a dominating role in the course of this section.

First of all let a unit problem

$$\begin{aligned} & \text{maximize } \langle \mathbf{v}, \mathbf{x} \rangle \\ & \text{s.t. } \langle \mathbf{a}_1, \mathbf{x} \rangle \leq 1 \\ & \quad \vdots \\ & \quad \langle \mathbf{a}_m, \mathbf{x} \rangle \leq 1 \end{aligned} \tag{EP}$$

be given. In addition assume that we have a vertex \mathbf{x}_0 of the feasible region X . Moreover let \mathbf{x}_0 be optimal with respect to an objective direction \mathbf{u} . On that starting position we can apply the shadow vertex algorithm in order to solve (EP). The insights

gained in section 2.4 show that the number of pivot steps carried out can be bounded from above by the number of shadow vertices $S(\mathbf{a}_1, \dots, \mathbf{a}_m, \mathbf{u}, \mathbf{v})$ of X with respect to the plane $\mathbf{LH}(\mathbf{u}, \mathbf{v})$. Changing to the dual point of view demonstrates that the number of shadow vertices corresponds to the number of those facets of the polytope $Y = \mathbf{KH}(\mathbf{0}, \mathbf{a}_1, \dots, \mathbf{a}_m)$, which are generated by d original restriction vectors (not $\mathbf{0}$) and which are intersected by the twodimensional plane $\mathbf{LH}(\mathbf{u}, \mathbf{v})$. We have illustrated this relation in the following figure from section 2.4.2 .

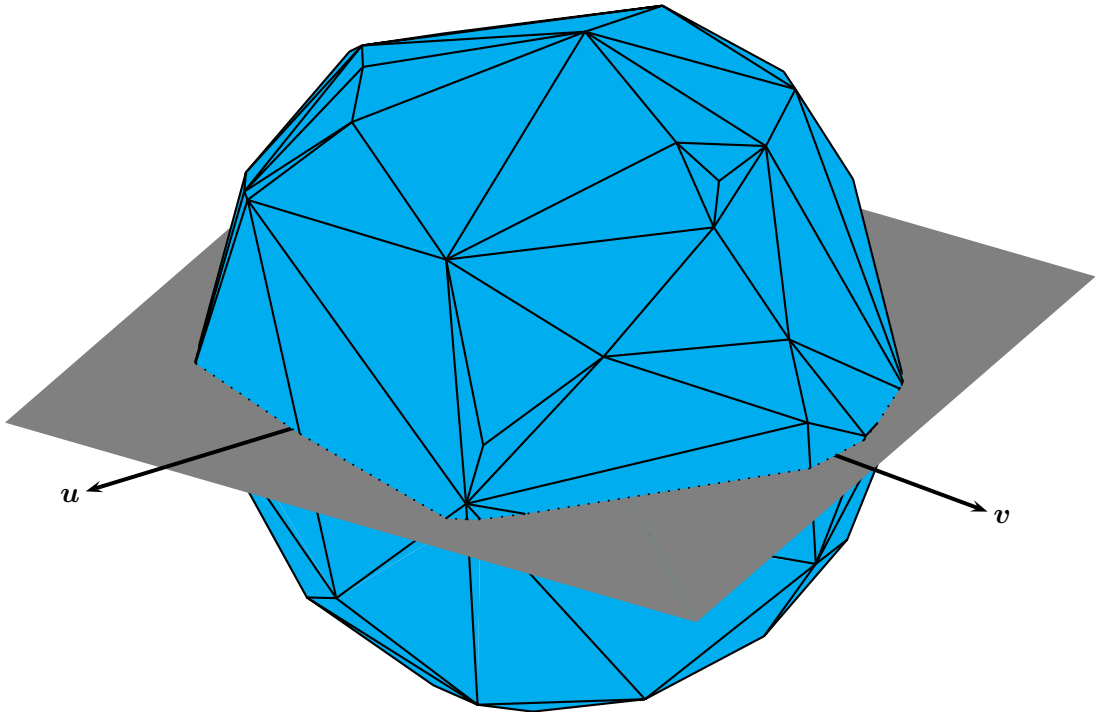


Figure 3.1: Graphical illustration of the number of shadow vertices in the dual perspective

Since X shall be a perturbed polyhedron, the restriction vectors $\mathbf{a}_1, \dots, \mathbf{a}_m$ are not fixed, but they are distributed according to the following stochastic principle:

$$\mathbf{a}_i \sim \mathcal{N}_d(\bar{\mathbf{a}}_i, \sigma^2 \cdot \mathbf{E}_d)$$

with $\sigma > 0$ and $\|\bar{\mathbf{a}}_i\| \leq 1$ for all $i = 1, \dots, m$. So $S := S(\mathbf{a}_1, \dots, \mathbf{a}_m, \mathbf{u}, \mathbf{v})$ becomes a random variable and the condition of nondegeneracy 2.4.1 is satisfied with probability 1. From, the basis of that configuration Spielman and Teng derive the following result. This is the geometrical fundatum of all the following algorithmic investigations..

Theorem 3.1.1 (Shadow of a perturbed polyhedron).

Let $d \geq 3$ and $m > d$. \mathbf{u}, \mathbf{v} shall be linearly independent vectors and $\mathbf{a}_1, \dots, \mathbf{a}_m$ shall be normally distributed random vectors with standard deviations $\sigma > 0$ and centers $\bar{\mathbf{a}}_1, \dots, \bar{\mathbf{a}}_m$ of norm at most 1. Let the random variable S stand for the number of

shadow vertices of $X = \{ \mathbf{x} : \langle \mathbf{a}_i, \mathbf{x} \rangle \leq 1 \forall i = 1, \dots, m \}$ with respect to the two-dimensional plane $\mathbf{LH}(\mathbf{u}, \mathbf{v})$. Then it holds that

$$\mathbb{E}[S] \leq \frac{58.888.678md^3}{\min\left(\sigma, \frac{1}{3\sqrt{d\ln(m)}}\right)^6}.$$

In the following we present (in a very concise way) the essentials of the proof-strategy in the proof of Theorem 3.1.1.

First one recognizes that without loss of generality $\sigma \leq 1/\left(3\sqrt{d\ln(m)}\right)$ can be assumed. In the case $\sigma > 1/\left(3\sqrt{d\ln(m)}\right)$, one scales all restriction vectors down in such a way that $\sigma = 1/\left(3\sqrt{d\ln(m)}\right)$ is achieved. As a consequence the norms of the centers of distributions become smaller. And this does not impact the validity of the theorem. In the following let in addition two orthogonal vectors $\mathbf{u}_1, \mathbf{u}_2$ of length 1 from the plane $\mathbf{LH}(\mathbf{u}, \mathbf{v})$ be given. Now one observes for values $\theta \in (0, 2\pi]$ the vectors $\mathbf{q}_\theta := \mathbf{u}_1 \cdot \sin(\theta) + \mathbf{u}_2 \cdot \cos(\theta)$.

Furthermore it is helpful to introduce for the vector $\mathbf{q} \in \mathbb{R}^d$ the notation $\text{optSimp}_{\mathbf{q}}(\mathbf{a}_1, \dots, \mathbf{a}_m)$. This notation stands for the system of all index sets $\Delta = \{ \Delta^1, \dots, \Delta^d \} \subset \{1, \dots, m\}$, for which the following condition holds: The vectors $\mathbf{a}_{\Delta^1}, \dots, \mathbf{a}_{\Delta^d}$ are linearly independent, the convex hull $\mathbf{KH}(\mathbf{a}_{\Delta^1}, \dots, \mathbf{a}_{\Delta^d})$ is a facet of Y and $\mathbf{q} \in \mathbf{KK}(\mathbf{a}_{\Delta^1}, \dots, \mathbf{a}_{\Delta^d})$. That means that we select all the index sets to the optimal points on X with respect to the direction \mathbf{q} and use that notation for that system of sets. Since we deal with perturbations, the term $\text{optSimp}_{\mathbf{q}}(\mathbf{a}_1, \dots, \mathbf{a}_m)$ is almost surely empty or it is an index set. Against this background it is useful for the following considerations in this section to identify $\text{optSimp}_{\mathbf{q}}(\mathbf{a}_1, \dots, \mathbf{a}_m)$ with the corresponding index set resp. with the empty set.

In the next step one considers for $\ell \in \mathbb{N}$ the set $\left\{ \frac{1 \cdot 2\pi}{\ell}, \frac{2 \cdot 2\pi}{\ell}, \dots, \frac{\ell \cdot 2\pi}{\ell} \right\}$ of angles out of the interval $(0, 2\pi]$ and one replaces the plane $\mathbf{LH}(\mathbf{u}, \mathbf{v})$ by the ℓ vectors $\mathbf{q}_1, \dots, \mathbf{q}_\ell$ such that $\mathbf{q}_i := \mathbf{u}_1 \cdot \sin\left(\frac{i \cdot 2\pi}{\ell}\right) + \mathbf{u}_2 \cdot \cos\left(\frac{i \cdot 2\pi}{\ell}\right)$. A graphical illustration of that discretization can be found in figure 3.2.

Instead of considering all facets of Y , that are intersected by the plane $\mathbf{LH}(\mathbf{u}, \mathbf{v})$, one concentrates on those facets that are hit by some directions out of $\{\mathbf{q}_1, \dots, \mathbf{q}_\ell\}$. If that discretization is chosen sufficiently tight or fine, i.e $\ell \rightarrow \infty$, then every desired facet will be recognized and identified by that way. So we have the equation

$$\mathbb{E}[S] = \lim_{\ell \rightarrow \infty} \mathbb{E} \left[\# \left(\bigcup_{i \in \{1, \dots, \ell\}} \{\text{optSimp}_{\mathbf{q}_i}(\mathbf{a}_1, \dots, \mathbf{a}_m)\} \right) \right].$$

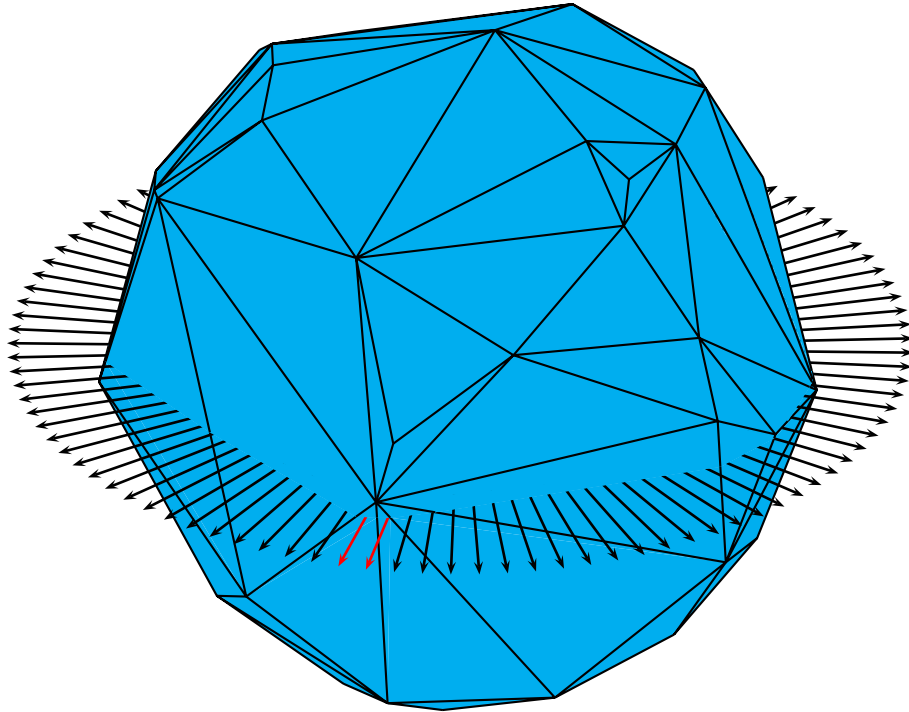


Figure 3.2: Discretization of the shadow plane

The term

$$\# \left(\bigcup_{i \in \{1, \dots, \ell\}} \{ \text{optSimp}_{\mathbf{q}_i}(\mathbf{a}_1, \dots, \mathbf{a}_m) \} \right)$$

denotes the number of those facets that are hit by any of the ℓ vectors. For the calculation and determination of that term one also has an alternative chance: One counts how often the following case will occur: two successive directions \mathbf{q}_i and \mathbf{q}_{i+1} hit different facets. In that context we set $\mathbf{q}_{\ell+1} = \mathbf{q}_1$. In figure 3.2 we have emphasized that configuration by two red-colored directions. Based on that consideration one can introduce the indicator variable $W_i := W_i(\mathbf{a}_1, \dots, \mathbf{a}_m)$ for $i = 1, \dots, \ell$:

$$W_i := \begin{cases} 1, & \text{if } \emptyset \neq \text{optSimp}_{\mathbf{q}_i}(\mathbf{a}_1, \dots, \mathbf{a}_m) \neq \text{optSimp}_{\mathbf{q}_{i+1}}(\mathbf{a}_1, \dots, \mathbf{a}_m) \\ 0, & \text{else.} \end{cases}$$

So one obtains

$$\mathbb{E}[S] = \lim_{\ell \rightarrow \infty} \mathbb{E} \left[\sum_{i=1}^{\ell} W_i \right].$$

For the next steps one needs the set P , which is defined as follows:

$$P := \{ (\mathbf{p}_1, \dots, \mathbf{p}_m) \in \mathbb{R}^{d \times m} : \|\mathbf{p}_i\| \leq 2 \text{ for all } i = 1, \dots, m \}.$$

In combination with property $\sigma \leq 1 / (3\sqrt{d \ln(m)})$ one can show that

$$\mathbb{P}[(\mathbf{a}_1, \dots, \mathbf{a}_m) \in P] \geq 1 - m^{-2,9d+1}. \quad (3.1)$$

The following remarks will clarify, that on the basis of the estimation (3.1) it is possible, to focus only on those configurations of restriction vectors, for which each single vector is located in the ball of radius 2 about the origin. In view of figure 3.3 and formulated in a somehow different way one concentrates on those configurations of restriction vectors $\mathbf{a}_1, \dots, \mathbf{a}_m$, which generate a dual polyhedron Y completely belonging to the ball of radius 2 about the origin.

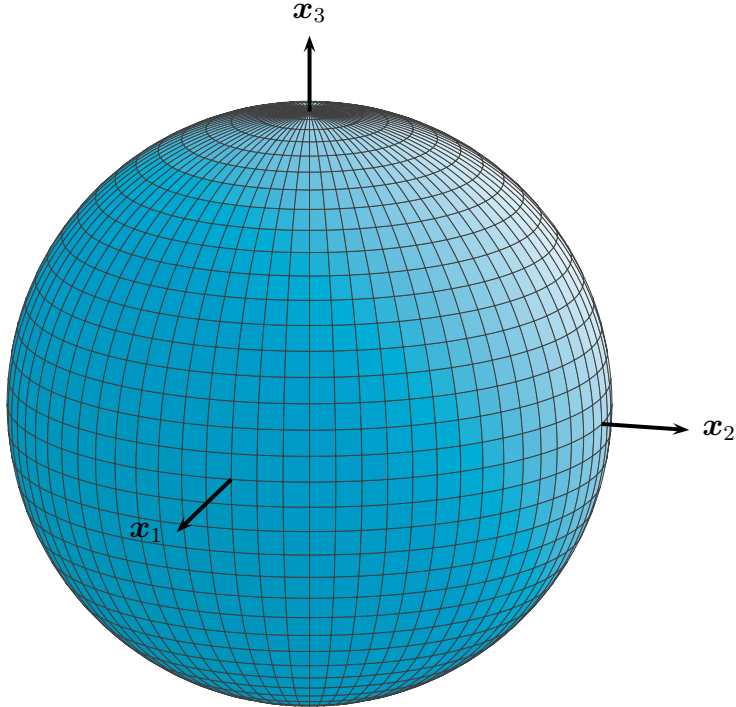


Figure 3.3: Graphical illustration of the ball containing all further configurations

For simplification of the notation we shall abbreviate the event $(\mathbf{a}_1, \dots, \mathbf{a}_m) \in P$ with the notation P and accordingly we denote the complementary event by $\neg P$. Because of $\mathbb{P}[P], \mathbb{P}[\neg P] > 0$ one can achieve the following estimation by a partition in two conditional expectation values:

$$\begin{aligned} \mathbb{E} \left[\sum_{i=1}^{\ell} W_i \right] &= \mathbb{E} \left[\sum_{i=1}^{\ell} W_i \middle| P \right] \cdot \mathbb{P}[P] + \mathbb{E} \left[\sum_{i=1}^{\ell} W_i \middle| \neg P \right] \cdot \mathbb{P}[\neg P] \\ &\leq \mathbb{E} \left[\sum_{i=1}^{\ell} W_i \middle| P \right] + \binom{m}{d} \cdot m^{-2,9d+1} \end{aligned}$$

$$\leq \mathbb{E} \left[\sum_{i=1}^{\ell} W_i \mid P \right] + 1.$$

For the conditional expectation value $\mathbb{E} \left[\sum_{i=1}^{\ell} W_i \mid P \right]$ we have as known

$$\mathbb{E} \left[\sum_{i=1}^{\ell} W_i \mid P \right] = \frac{\mathbb{E} \left[\sum_{i=1}^{\ell} W_i \cdot \mathbf{1}[P] \right]}{\mathbb{P}[P]}.$$

Further we can concentrate on the estimation of $\mathbb{E} \left[\sum_{i=1}^{\ell} W_i \mid P \right]$. On the basis of the definition of the indicator variable W_i it is clear, that in the case of $W_i = 1$ we will always meet the event

$$\emptyset \neq \text{optSimp}_{\mathbf{q}_i}(\mathbf{a}_1, \dots, \mathbf{a}_m) \neq \text{optSimp}_{\mathbf{q}_{i+1}}(\mathbf{a}_1, \dots, \mathbf{a}_m).$$

So while changing from \mathbf{q}_i to \mathbf{q}_{i+1} one hits or meets a new facet. Since we know that the angles of both vectors differ by $\frac{2\pi}{\ell}$, one concludes that the angle between \mathbf{q}_i and the boundary of $\Sigma(\text{optSimp}_{\mathbf{q}_i}(\mathbf{a}_1, \dots, \mathbf{a}_m))$ is less than $\frac{2\pi}{\ell}$. In summary the following implication holds:

$$W_i = 1 \Rightarrow \text{arc}(\mathbf{q}_i, \partial\Sigma(\text{optSimp}_{\mathbf{q}_i}(\mathbf{a}_1, \dots, \mathbf{a}_m))) < \frac{2\pi}{\ell}.$$

This enables the estimation

$$W_i \leq \mathbf{1} \left[\text{arc}(\mathbf{q}_i, \partial\Sigma(\text{optSimp}_{\mathbf{q}_i}(\mathbf{a}_1, \dots, \mathbf{a}_m))) < \frac{2\pi}{\ell} \right],$$

where $\mathbf{1}[\cdot]$ stands as already stated for the indicator function. Exploiting the monotony of the expectation value one can state:

$$\mathbb{E}[S] \leq \lim_{\ell \rightarrow \infty} \mathbb{E} \left[\sum_{i=1}^{\ell} \mathbf{1} \left[\text{arc}(\mathbf{q}_i, \partial\Sigma(\text{optSimp}_{\mathbf{q}_i}(\mathbf{a}_1, \dots, \mathbf{a}_m))) < \frac{2\pi}{\ell} \right] \mid P \right] + 1.$$

If one in addition applies the linearity of the expectation value, then one achieves:

$$\begin{aligned} \mathbb{E}[S] &\leq \lim_{\ell \rightarrow \infty} \sum_{i=1}^{\ell} \mathbb{E} \left[\mathbf{1} \left[\text{arc}(\mathbf{q}_i, \partial\Sigma(\text{optSimp}_{\mathbf{q}_i}(\mathbf{a}_1, \dots, \mathbf{a}_m))) < \frac{2\pi}{\ell} \right] \mid P \right] + 1 \\ &= \lim_{\ell \rightarrow \infty} \sum_{i=1}^{\ell} \mathbb{P} \left[\text{arc}(\mathbf{q}_i, \partial\Sigma(\text{optSimp}_{\mathbf{q}_i}(\mathbf{a}_1, \dots, \mathbf{a}_m))) < \frac{2\pi}{\ell} \mid P \right] + 1. \end{aligned} \quad (3.2)$$

Now we can focus on the estimation of probability

$$\mathbb{P} \left[\text{arc}(\mathbf{q}, \partial\Sigma(\text{optSimp}_{\mathbf{q}}(\mathbf{a}_1, \dots, \mathbf{a}_m))) < \epsilon \mid P \right]$$

for an arbitrary $\mathbf{q} \in \omega_d$. Suitable transformations enable the authors to deduce for that aim an upper bound of the following kind:

$$\begin{aligned} \mathbb{P} [\text{arc}(\mathbf{q}, \partial\Sigma(\text{optSimp}_{\mathbf{q}}(\mathbf{a}_1, \dots, \mathbf{a}_m))) < \epsilon \mid P] &\leq \frac{d}{(1 - m^{-2,9d+1})^2} \\ &\cdot \max_{\substack{j=1, \dots, d \\ \Delta \subset \{1, \dots, m\} \\ \#(\Delta)=d}} \mathbb{P} [\text{arc}(\mathbf{q}, \mathbf{KH}(\mathbf{a}_{\Delta^1}, \dots, \mathbf{a}_{\Delta^{j-1}}, \mathbf{a}_{\Delta^{j+1}}, \dots, \mathbf{a}_{\Delta^d})) < \epsilon \mid \\ &\quad P_{\Delta}^j \wedge \text{optSimp}_{\mathbf{q}}(\mathbf{a}_1, \dots, \mathbf{a}_m) = \Delta]. \end{aligned} \quad (3.3)$$

Here P_{Δ}^j with $\Delta := \{\Delta^1, \dots, \Delta^d\} \subset \{1, \dots, m\}$ und $j \in \{1, \dots, d\}$ is the set of all $\mathbf{a}_{\Delta^1}, \dots, \mathbf{a}_{\Delta^d}$, satisfying:

1. For all \mathbf{q} it results that $s \leq 2$ in case of $\text{optSimp}_{\mathbf{q}}(\mathbf{a}_1, \dots, \mathbf{a}_m) \neq \emptyset$. Here s is chosen in such a way, that $s\mathbf{q} \in \Sigma(\text{optSimp}_{\mathbf{q}}(\mathbf{a}_1, \dots, \mathbf{a}_m))$ holds.
2. $\text{dist}(\mathbf{a}_i, \mathbf{a}_k) \leq 4$ für $i, k \in \Delta \setminus \{\Delta^j\}$.
3. $\text{dist}(\mathbf{a}_{\Delta^j}, \mathbf{AH}(\{\mathbf{a}_{\Delta^1}, \dots, \mathbf{a}_{\Delta^d}\} \setminus \{\mathbf{a}_{\Delta^j}\})) \leq 4$.
4. $\text{dist}(\mathbf{a}_{\Delta^j}^{\perp}, \mathbf{a}_i) \leq 4$ for all $i \in \Delta \setminus \{\Delta^j\}$. Here $\mathbf{a}_{\Delta^j}^{\perp}$ is the orthogonal projection of \mathbf{a}_{Δ^j} on $\mathbf{AH}(\{\mathbf{a}_{\Delta^1}, \dots, \mathbf{a}_{\Delta^d}\} \setminus \{\mathbf{a}_{\Delta^j}\})$.

In utilization of that very technical definition one can show that $P \subset P_{\Delta}^j$. We remark that in the probability above the term P_{Δ}^j should be seen as an event like in the case P .

The fundamental geometrical idea in the term on the right side of the estimation in (3.3) is the following: In question is the probability that the intersection of the Y boundary with the cone with angle ϵ about the vector \mathbf{q} is not completely contained in the facet, conditioned on the case that the corresponding facet has been hit anyway. A graphical illustration of the complementary configuration can be seen in figure 3.4.

A further evaluation of the probability

$$\begin{aligned} \max_{\substack{j=1, \dots, d \\ \Delta \subset \{1, \dots, m\} \\ \#(\Delta)=d}} \mathbb{P} [\text{arc}(\mathbf{q}, \mathbf{KH}(\mathbf{a}_{\Delta^1}, \dots, \mathbf{a}_{\Delta^{j-1}}, \mathbf{a}_{\Delta^{j+1}}, \dots, \mathbf{a}_{\Delta^d})) < \epsilon \mid \\ &\quad P_{\Delta}^j \wedge \text{optSimp}_{\mathbf{q}}(\mathbf{a}_1, \dots, \mathbf{a}_m) = \Delta] \end{aligned} \quad (3.4)$$

is technically very complicated. This results mainly from the appearance of the angle-term

$$\text{arc}(\mathbf{q}, \mathbf{KH}(\mathbf{a}_{\Delta^1}, \dots, \mathbf{a}_{\Delta^{j-1}}, \mathbf{a}_{\Delta^{j+1}}, \dots, \mathbf{a}_{\Delta^d})).$$

In the approach of Spielman and Teng they focus on the set P_{Δ}^j and by the way they

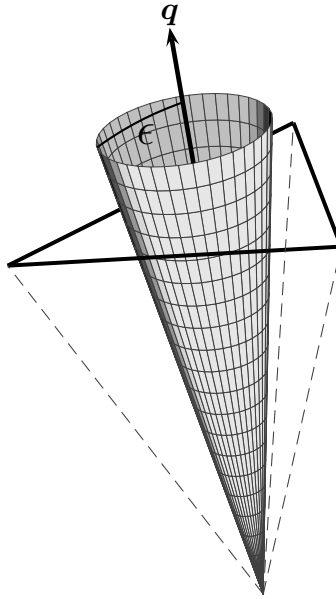


Figure 3.4: Graphical illustration of the cone about the vector \mathbf{q}

can prove the following upper bound :

$$\begin{aligned} & \max_{\substack{j=1, \dots, d \\ \Delta \subset \{1, \dots, m\} \\ \#(\Delta)=d}} \mathbb{P}[\text{arc}(\mathbf{q}, \mathbf{K}\mathbf{H}(\mathbf{a}_{\Delta^1}, \dots, \mathbf{a}_{\Delta^{j-1}}, \mathbf{a}_{\Delta^{j+1}}, \dots, \mathbf{a}_{\Delta^d})) < \epsilon \mid \\ & \quad P_{\Delta}^j \wedge \text{optSimp}_{\mathbf{q}}(\mathbf{a}_1, \dots, \mathbf{a}_m) = \Delta] \\ & \leq \frac{9.371.990 m d^2}{\sigma^6} \epsilon. \end{aligned}$$

Combinig this insight with the estimation (3.3) and taking into regard the information from (3.2), yields (under use of further transformations) the long desired result:

$$\mathbb{E}[S] \leq \frac{58.888.678 m d^3}{\sigma^6}.$$

This finishes the sketch of the proof for Theorem 3.1.1. In the next section we shall see how this geometrical result corresponds to an algorithmic procedure and gives information of the algorithmic complexity.

3.1.2 The Algorithmic Realization

Here as already announced we discuss the principal steps of the algorithmical realization as in [ST04]. Thereto we are going to present the variant of the Simplex Method as investigated by both researchers. This variant is used in their paper to solve general linear optimization problems of the form

$$\begin{aligned} & \text{maximize } \langle \mathbf{v}, \mathbf{x} \rangle \\ & \text{s.t. } \mathbf{A}\mathbf{x} \leq \mathbf{b} \end{aligned} \tag{LP}$$

with $\mathbf{A} = (\mathbf{a}_1, \dots, \mathbf{a}_m)^T \in \mathbb{R}^{m \times d}$, $\mathbf{b} = (b^1, \dots, b^m)^T \in \mathbb{R}^m$ and $m > d \geq 3$. In the context of Spielman's and Teng's perturbation principle each restriction vector \mathbf{a}_i is a normally distributed random vector with center $\bar{\mathbf{a}}_i \in \mathbb{R}^d$ and standard deviation $\sigma \max_{i=1,\dots,m} \|(\bar{\mathbf{a}}_i, \bar{b}^i)\|$. Moreover each righthand side value b^i is a normally distributed random variable with expectation value $\bar{b}^i \in \mathbb{R}$ and the same standard deviation. Herefrom we get in addition the matrix $\bar{\mathbf{A}} = (\bar{\mathbf{a}}_1, \dots, \bar{\mathbf{a}}_m)^T$ as well as the vector $\bar{\mathbf{b}} = (\bar{b}^1, \dots, \bar{b}^m)^T$. The appearance of $\max_{i=1,\dots,m} \|(\bar{\mathbf{a}}_i, \bar{b}^i)\|$ besides the parameter σ in the standard deviation can thus be explained: Scaling of the vector (\mathbf{a}_i, b^i) with value $(\max_{i=1,\dots,m} \|(\bar{\mathbf{a}}_i, \bar{b}^i)\|)^{-1}$ (let without loss of generality this be positive), produces a normally distributed random vector with standard deviation σ and a center of norm at most 1. Having the conditions of Theorem 3.1.1 from the previous section in mind this will be very helpful.

We have already explained that the shadow vertex algorithm in its dual interpretation can only be analyzed in the application on unit problems. For that reason Spielman und Teng introduce in the definition of their Phase-1-problem positive righthand sides $\hat{b}^1, \dots, \hat{b}^m$, which replace the primary values b^1, \dots, b^m . After that any relaxed restriction $\langle \mathbf{a}_i, \mathbf{x} \rangle \leq \hat{b}^i$ can via division by \hat{b}^i be transformed in a unit restriction. For the construction of the relaxed values $\hat{b}^1, \dots, \hat{b}^m$ one needs foremost an index set $\Delta = \{\Delta^1, \dots, \Delta^d\} \subset \{1, \dots, m\}$. Afterwards one defines the values

$$M := 2^{\lceil \lg(\max_{i=1,\dots,m} \|(\mathbf{a}_i, b^i)\|) \rceil + 2}$$

$$\tau := 2^{\lfloor \lg(s_{\min}(\mathbf{A}_\Delta)) \rfloor}.$$

Here $s_{\min}(\mathbf{A}_\Delta)$ denotes the smallest singular value of \mathbf{A}_Δ , i.e.

$$s_{\min}(\mathbf{A}_\Delta) := \min_{\mathbf{x} \neq 0} \frac{\|\mathbf{A}_\Delta \mathbf{x}\|}{\|\mathbf{x}\|}. \quad (3.5)$$

Herefrom one determines the relaxed righthand sides, which are positive, in the following way:

$$\hat{b}^i := \begin{cases} M, & \text{for } i \in \Delta \\ \frac{\sqrt{d}M^2}{4\tau}, & \text{else.} \end{cases}$$

Now the Phase-1-problem can be formulated:

$$\begin{aligned} & \text{maximize } \langle \mathbf{v}, \mathbf{x} \rangle \\ & \text{s.t. } \langle \mathbf{a}_1, \mathbf{x} \rangle \leq \hat{b}^1 \\ & \quad \vdots \\ & \quad \langle \mathbf{a}_m, \mathbf{x} \rangle \leq \hat{b}^m. \end{aligned} \quad (\widehat{\text{LP}})$$

For simplification one sets $\hat{\mathbf{b}} := (\hat{b}^1, \dots, \hat{b}^m)^T$. Here the relaxed righthand sides are chosen in such a way that the basic solution $\hat{\mathbf{x}}_\Delta = (\mathbf{A}_\Delta)^{-1} \hat{\mathbf{b}}_\Delta$ belonging to the index

set Δ is a vertex of the feasible region \hat{X} of $(\widehat{\text{LP}})$. A graphical illustration for that can be found in figures 3.5 and 3.6:

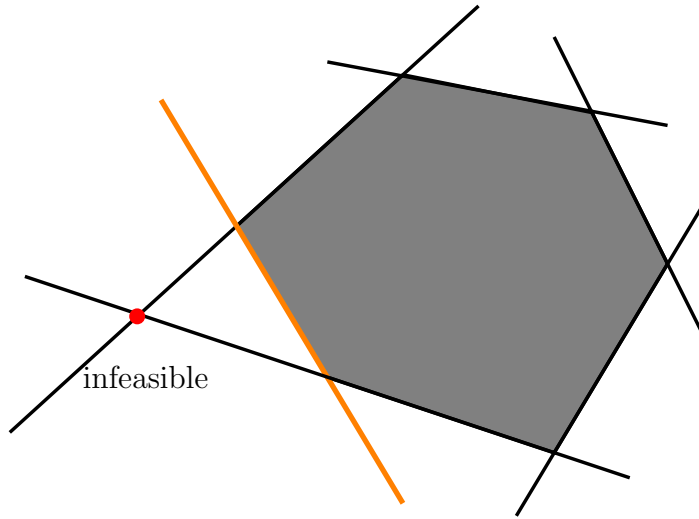


Figure 3.5: The basic solution in red is not feasible as long as the orange restriction is not relaxed

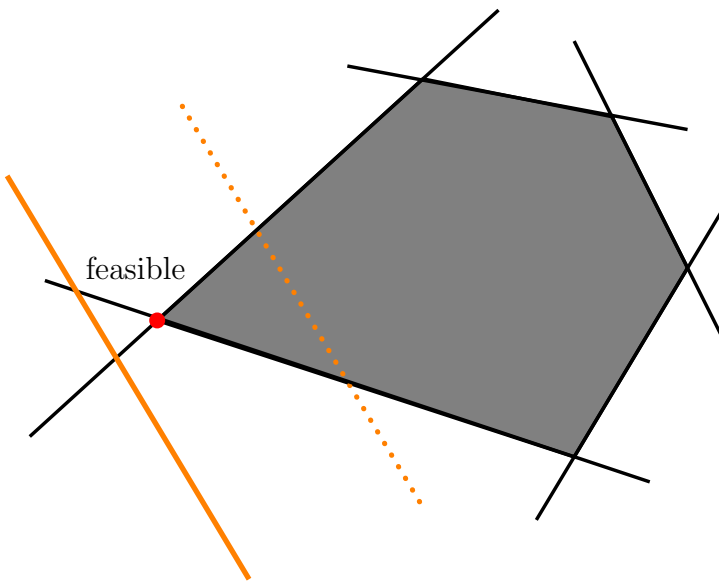


Figure 3.6: The basic solution in red - which had been infeasible before - becomes an edge after relaxation of the orange restriction

On that basis we can proceed to the determination of problem of Phase 2, which interpolates between $(\widehat{\text{LP}})$ and (LP) . For that aim one needs an additional interpolation variable $-1 \leq x^0 \leq 1$ and for each original restriction we introduce the following new

and artificial restriction:

$$\langle \mathbf{a}_i, \mathbf{x} \rangle \leq \left(\frac{1+x^0}{2} \right) b^i + \left(\frac{1-x^0}{2} \right) \hat{b}^i.$$

For $x^0 = -1$ one consequently obtains the restrictions of the Phase-1-program $(\widehat{\text{LP}})$ and for $x^0 = 1$ we receive the restrictions of the original problem (LP) . By means of according transformations the interpolation problem can be represented in the following way.

$$\begin{aligned} & \text{maximize } \langle (1, 0, \dots, 0), (x^0, \mathbf{x}) \rangle \\ & \text{s.t. } \langle (-1, 0, \dots, 0), (x^0, \mathbf{x}) \rangle \leq 1 \\ & \quad \langle (1, 0, \dots, 0), (x^0, \mathbf{x}) \rangle \leq 1 \\ & \quad \langle \left(\frac{(\hat{b}^1 - b^1)}{2}, \mathbf{a}_1 \right), (x^0, \mathbf{x}) \rangle \leq \frac{(\hat{b}^1 + b^1)}{2} \quad (\widetilde{\text{LP}}) \\ & \quad \vdots \\ & \quad \langle \left(\frac{(\hat{b}^m - b^m)}{2}, \mathbf{a}_m \right), (x^0, \mathbf{x}) \rangle \leq \frac{(\hat{b}^m + b^m)}{2} \end{aligned}$$

The righthand sides of the restrictions are positive again. So they can by means of division be converted into unit restrictions. Furthermore let the notation \tilde{X} stand for the feasible region of $(\widetilde{\text{LP}})$. If we find an optimal vertex in the course of executing Phase 1 named $\hat{\mathbf{x}}^*$ of $(\widehat{\text{LP}})$, then one can from it construct the vertex $(-1, \hat{\mathbf{x}}^*)$ of \tilde{X} . Emanating from that one tries to reach a vertex of the original problem. Therefore one uses the objective direction $(1, 0, \dots, 0)^T$. If at the end of handling $(\widetilde{\text{LP}})$ a solution in the form $(1, \tilde{\mathbf{x}}^*)$ is available, then it can be shown that $\tilde{\mathbf{x}}^*$ is a solution for the original problem (LP) . Also all remaining cases, which are so far not discussed here in detail, as for instance infeasibility, will be treated in the algorithm accordingly. In addition the procedure in step 1 implies an additional routine, that is not absolutely necessary for the solution of the problem. But its value lies in the fact that it facilitates a better estimation for the running time. This comes from the fact that out of a collection of potential starting bases one chooses that one having the best features. For simplification of the notation the restrictions of $(\widetilde{\text{LP}})$ will be marked according to their appearance with $\tilde{\mathbf{a}}_{-1}, \tilde{\mathbf{a}}_0, \tilde{\mathbf{a}}_1, \dots, \tilde{\mathbf{a}}_m$. Accordingly the righthand sides will be named $\tilde{b}^{-1}, \tilde{b}^0, \tilde{b}^1, \dots, \tilde{b}^m$.

Algorithm 3.1.2 (Two-Phase-Variant of the shadow vertex algorithm).

Input: $\mathbf{A} = (\mathbf{a}_1, \dots, \mathbf{a}_m)^T$, $\mathbf{b} = (b^1, \dots, b^m)^T$ and \mathbf{v}

Procedure:

1. Let $\mathcal{I} = \{\Delta_1, \dots, \Delta_{3md \ln(m)}\}$ be a collection of randomly chosen index sets such that $\Delta_i \subset \{1, \dots, m\}$ and $\#(\Delta_i) = d$ for all i . Let $\Delta \in \mathcal{I}$ be that index set with maximal $s_{\min}(\mathbf{A}_\Delta)$. Here $s_{\min}(\mathbf{A}_\Delta)$ stands for the smallest singular value of \mathbf{A}_Δ as defined in (3.5).

2. Set $M := 2^{\lceil \lg(\max_{i=1,\dots,m} \|(\mathbf{a}_i, b^i)\|) \rceil + 2}$ und $\tau := 2^{\lfloor \lg(s_{\min}(\mathbf{A}_{\Delta})) \rfloor}$.
3. Set $\hat{b}^i := \begin{cases} M, & \text{for } i \in \Delta \\ \frac{\sqrt{d}M^2}{4\tau} & \text{else.} \end{cases}$
4. Choose $\mathbf{t} \in \mathbb{R}^d$ randomly and uniformly distributed from the set $\left\{ \mathbf{t} : \sum_{i=1}^d t^i = 1, t^i \geq \frac{1}{d^2} \forall i \right\}$.
Set $\mathbf{u} := (\mathbf{A}_{\Delta})^T \mathbf{t}$.
5. Start the shadow vertex algorithm for solving (\widehat{LP}) under use of the start basis Δ and of the auxiliary objective direction \mathbf{u} . If one detects unboundedness, then this is true for the starting problem, too. Then one can stop. Else let $\hat{\Delta}$ be the index set to the optimal solution just derived.
6. Let $\zeta > 0$ be such that
$$\{-1\} \cup \hat{\Delta} \in \mathbf{optSimp}_{(-\zeta, \mathbf{v})} \left(\frac{\tilde{\mathbf{a}}_{-1}}{\tilde{b}_{-1}}, \dots, \frac{\tilde{\mathbf{a}}_m}{\tilde{b}_m} \right).$$
7. Let $\tilde{\Delta}$ be the index set of the solution of (\widetilde{LP}) , which has been determined by the shadow vertex algorithm starting with an optimal basis $\{-1\} \cup \hat{\Delta}$ for the objective $(-\zeta, \mathbf{v})$.
8. Determine the solution $(\tilde{x}^0, \tilde{\mathbf{x}}^*)$ of the system of equations $\langle (x^0, \mathbf{x}), \tilde{\mathbf{a}}_i \rangle = \tilde{b}^i$ for $i \in \tilde{\Delta}$.
9. For $\tilde{x}^0 < 1$ the problem is infeasible and in the case of $\tilde{x}^0 = 1$ we have an optimal solution $\tilde{\mathbf{x}}^*$.

Output:

If the algorithm has stopped in step 5, then report “problem unbounded”. In case of $\tilde{x}^0 < 1$ the report should be “problem infeasible”. Otherwise $\tilde{\mathbf{x}}^*$ is the optimal point and should be reported.

For the purpose of a smoothed analysis of that method Spielman and Teng investigated all steps with a focus on step 5 and step 7. The first step can, as already mentioned, be seen as a preparation routine. Here one compares all elements of the group $\mathcal{I} = \{\Delta_1, \dots, \Delta_{3md \ln(m)}\}$ and one tries to make a best possible choice among the $\binom{m}{d}$ available candidates. In the fourth step one draws a direction from the polar cone associated to the start basis Δ . This choice simulates a uniform distribution over a certain inner region of the polar cone. The chosen direction will serve as auxiliary objective direction for the solution of the Phase-1-problem in step 5. If thereby an optimal basis $\hat{\Delta}$ can be found, then herefrom the basis $\{-1\} \cup \hat{\Delta}$ to a vertex \tilde{X} will be constructed in step 6 and an auxiliary objective direction in the associated polar cone will be determined. Finally in step 7 the Phase-2-problem can be treated. This is done to solve the original problem at last.

In the following we look at steps 5 and 7 in detail and we speak about the essential challenges in connection with the smoothed analysis. And we give some ideas how to overcome those difficulties.

Phase 1:

For the solution of the Phase-1-problem (\widehat{LP}) one uses (as known) $\mathbf{LH}(\mathbf{u}, \mathbf{v})$ with $\mathbf{u} = (\mathbf{A}_\Delta)^T \mathbf{t}$ as the projection plane for the application of the shadow vertex algorithm. The vector \mathbf{v} may be seen as a fixed exogen input. In contrast one uses for the construction of \mathbf{u} a subset of the restriction vectors $\mathbf{a}_1, \dots, \mathbf{a}_m$. For that reason the projection plane is not fixed and on the other side it is stochastically dependent of the problem data. The bound in Theorem 3.1.1 is for this reason not suitable and confirmed for the estimation of the necessary number of pivot steps in the solution process of problem (\widehat{LP}) . This is the first challenge appearing during the investigation of the running time of Phase 1. In order to overcome those difficulties, Spielman and Teng play according to the principle described below. Their first aim is to show that under the condition

$$s_{min}(\bar{\mathbf{A}}_\Delta) \geq \frac{\tau_0}{2} \quad (3.6)$$

for a constant τ_0 and in the case of a perturbation of moderate size the expected number of shadow vertices of \hat{X} with respect to the actually used projection plane $\mathbf{LH}((\mathbf{A}_\Delta)^T \mathbf{t}, \mathbf{v})$ is at most larger by a constant factor than the expectation value for the number of shadow vertices of \hat{X} with respect to the fixed plane $\mathbf{LH}((\bar{\mathbf{A}}_\Delta)^T \bar{\mathbf{t}}, \mathbf{v})$ with $\bar{\mathbf{A}} = (\bar{\mathbf{a}}_1, \dots, \bar{\mathbf{a}}_m)^T$. Here $\bar{\mathbf{t}} \in \mathbb{R}^d$ is a fixed vector with $\bar{\mathbf{t}} \geq \mathbf{0}$ and with $\sum_{i=1}^d \bar{t}^i = 1$. However for a fixed matrix $\bar{\mathbf{A}}$ the property

$$s_{min}(\bar{\mathbf{A}}_\Delta) \geq \frac{\tau_0}{2}$$

cannot be presumed. For that reason Spielman and Teng make use of the additivity of the normal distribution. And they partition the disturbance term $\mathbf{g}_i \sim \mathcal{N}_d(\mathbf{0}, \sigma^2 \cdot \mathbf{E}_d)$, belonging to the restriction vector \mathbf{a}_i in two parts: The perturbation $\mathbf{g}_i^{(1)}$ with standard deviation ς_1 and the perturbation $\mathbf{g}_i^{(2)}$ with standard deviation ς_2 . Here ς_1 and ς_2 are basically chosen in a way, that in total $\sigma^2 = (\varsigma_1)^2 + (\varsigma_2)^2$ is satisfied. After that they set

$$\begin{aligned} \check{\mathbf{a}}_i &:= \bar{\mathbf{a}}_i + \mathbf{g}_i^{(1)} \text{ and} \\ \mathbf{a}_i &:= \check{\mathbf{a}}_i + \mathbf{g}_i^{(2)}. \end{aligned}$$

Analogously we obtain the matrix $\check{\mathbf{A}}$. The same principle can also be applied to the righthand sides, which are subject to a perturbation as well.

$$\begin{aligned} \check{\mathbf{b}} &:= \bar{\mathbf{b}} + \mathbf{h}^{(1)} \text{ and} \\ \mathbf{b} &:= \check{\mathbf{b}} + \mathbf{h}^{(2)}. \end{aligned}$$

The reason for that partition is as follows: The first perturbation enables Spielman and Teng to base their ideas on the configuration $s_{min}(\check{\mathbf{A}}_\Delta) \geq \frac{\tau_0}{2}$. The property for the

occurrence of $s_{min}(\check{\mathbf{A}}_\Delta) < \frac{\tau_0}{2}$ is extremely small, so that case allows may modify the number of pivot steps at most by a constant 1. If we interpret $\check{\mathbf{A}}$ and $\check{\mathbf{b}}$ as the new centers, then the condition from (3.6) can be regarded as satisfied. This permits the associated estimation.

Further we must keep in mind that the righthand sides of the restrictions from (\widehat{LP}) in fact are positive, however they usually fail to be of value 1. As known it holds:

$$\hat{b}^i := \begin{cases} M, & \text{for } i \in \Delta \\ \frac{\sqrt{d}M^2}{4\tau}, & \text{else} \end{cases}$$

with $M := 2^{\lceil \lg(\max_{i=1,\dots,m} \|(\mathbf{a}_i, b^i)\|) \rceil + 2}$ and $\tau := 2^{\lfloor \lg(s_{min}(\mathbf{A}_\Delta)) \rfloor}$. To transform the restriction

$$\langle \mathbf{a}_i, \mathbf{x} \rangle \leq \hat{b}^i$$

into unit form, one can divide by \hat{b}^i . However, since the relaxed righthand sides are correlated with the rest of the input data via the variables M and τ , the scaled restriction vectors would not necessarily be normally distributed. An application of the bound for the number of shadow vertices from section 3.1.1 would not be allowed in that case. This complication is treated and resolved by Spielman and Teng conceptually as follows: Since M and τ are defined as discrete figures, one can show that with high probability both attain only a small number of different values (the converse case consequently can influence the number of pivots only by a value 1). This feature is transferred also on the relaxed righthand sides. If one concentrates on a fixed configuration of M and $\frac{\sqrt{d}M^2}{4\tau}$ for $\hat{b}^1, \dots, \hat{b}^m$, then the righthand sides may be regarded as fixed. Hence the transformation into unit restrictions is possible without accepting the loss of the normal distribution. So the bound for shadow vertices from Theorem 3.1.1 remains applicable. If one carries out that argumentation for each possible configuration of values and if one sums up the single upper bounds (there is a small number of summands, so the result is not deteriorated significantly), then one obtains an upper bound for the expectation value of the number of necessary pivot steps for the solution of Phase 1.

Phase 2:

For the solution of (\widetilde{LP}) in the second Phase one uses the plane $\mathbf{LH}((- \zeta, \mathbf{v}), (1, 0, \dots, 0))$ as projection plane during the application of the shadow vertex algorithm. These vectors are fixed, so we do not get into trouble. Nevertheless some challenges will appear, as we will recognize soon. As a reminder we list the restriction data of the program (\widetilde{LP}) once more:

$$\begin{aligned} \tilde{\mathbf{a}}_{-1} &= (-1, 0, \dots, 0), & \tilde{b}^{-1} &= 1 \\ \tilde{\mathbf{a}}_0 &= (1, 0, \dots, 0), & \tilde{b}^0 &= 1 \\ \tilde{\mathbf{a}}_i &= (\frac{(\hat{b}^i - b^i)}{2}, \mathbf{a}_i), & \tilde{b}^i &= \frac{(\hat{b}^i + b^i)}{2} \quad (*) \end{aligned}$$

for $i = 1, \dots, m$. The two fixed vectors $\tilde{\mathbf{a}}_{-1}$ and $\tilde{\mathbf{a}}_0$ are located in the shadow plane and have only a little impact on the number of shadow vertices. So it is permitted to

disregard them in following considerations. A precise view on the restriction data that are marked with (*) shows that \tilde{b}^i is influenced by the corresponding relaxed righthand side \hat{b}^i from Phase 1. This makes it clear that the righthand sides from (\widetilde{LP}) are in the same way correlated with the original problem data. Here the same complications and difficulties arise as in the analysis of Phase 1. These can be resolved by an analogous treatment. For the upcoming considerations we may assume that the values $\hat{b}^1, \dots, \hat{b}^m$ are fixed. But still the bound on the number of shadow vertices 3.1.1 cannot be applied. For that aim the restrictions of (\widetilde{LP}) must be transformed in unit form by means of division. This produces the scaled restriction vectors

$$\frac{\tilde{\mathbf{a}}_1}{\tilde{b}^1}, \dots, \frac{\tilde{\mathbf{a}}_m}{\tilde{b}^m}. \quad (3.7)$$

A new view on (*) shows, that for fixed \hat{b}^i the righthand side \tilde{b}^i becomes a normally distributed random variable. This is the reason why the vectors in (3.7) do not possess a normal distribution. To clarify that difficulty, Spielman und Teng show that the distribution of an arbitrary

$$\frac{\tilde{\mathbf{a}}_i}{\tilde{b}^i}$$

in every neighbourhood (chosen small enough) be approximated by a normal distribution. Exploiting the obvious interrelation between the actual distribution and that newly constructed distribution delivers an estimation for the number of pivot steps. An important issue in that procedure is given – like in the investigation of the first Phase – the exploitation of the additivity of the normal distribution. For the local approximation the disturbance term belonging to \mathbf{a}_i , precisely $\mathbf{g}_i \sim \mathcal{N}_d(\mathbf{0}, \sigma^2 \cdot \mathbf{E}_d)$ is partitioned in two parts $\mathbf{g}_i = \mathbf{g}_i^{(1)} + \mathbf{g}_i^{(2)}$. Here $\mathbf{g}_i^{(1)}$ has the standard deviation ρ_1 and $\mathbf{g}_i^{(2)}$ has the standard deviation ρ_2 and in total $(\rho_1)^2 + (\rho_2)^2 = \sigma^2$. The same partition is then done for the right hand sides \tilde{b}^i . In the remaining argumentation the first perturbation dominates and it determines – loosely spoken – the region of the local approximation. On basis of that principal approach the authors manage to achieve an upper bound by use of a very technical analysis.

Combining the investigations of Phase 1 and Phase 2 and of their upper bounds, Spielman und Teng can derive the following result.

Theorem 3.1.3 (Smoothed running time of the Two-Phase-Algorithm).

There exists a polynomial \mathcal{P} and a constant σ_0 , such that for each $m > d \geq 3$, $\bar{\mathbf{A}} = (\bar{\mathbf{a}}_1, \dots, \bar{\mathbf{a}}_m)^T \in \mathbb{R}^{m \times d}$, $\bar{\mathbf{b}} \in \mathbb{R}^m$, $\mathbf{v} \in \mathbb{R}^d$ und $\sigma > 0$ it holds that:

$$\mathbb{E}_{\mathbf{A}, \mathbf{b}} [\mathcal{C}(\mathbf{A}, \mathbf{b}, \mathbf{v})] \leq \min \left\{ \mathcal{P} \left(d, m, \frac{1}{\min(\sigma, \sigma_0)} \right), \binom{m}{d} + \binom{m}{d+1} + 2 \right\}.$$

Here \mathbf{A} is a normally distributed random matrix with center $\bar{\mathbf{A}}$ and standard deviation $\sigma \max_i(\|(\bar{\mathbf{a}}_i, \bar{b}^i)\|)$ and \mathbf{b} is a normally distributed random vector with the same standard deviation and with the center $\bar{\mathbf{b}}$. Moreover $\mathcal{C}(\bar{\mathbf{A}}, \bar{\mathbf{b}}, \mathbf{v})$ stands for the average number of pivot steps in the algorithm after input of the fixed problem data $\bar{\mathbf{A}}$, $\bar{\mathbf{b}}$ und \mathbf{v} .

Remark 3.1.4 (degree of the polynomial).

Calculating the polynomial \mathcal{P} explicitly delivers:

$$\begin{aligned} \mathcal{P}\left(d, m, \frac{1}{\sigma}\right) &= C_1 \cdot d^{55} \cdot m^{86} \cdot (\ln m)^{16} \cdot \frac{1}{\sigma^{24}} \cdot \lg\left(\frac{dm}{\sigma}\right) \\ &\quad + C_2 \cdot (d+1)^{36} \cdot m^{85} \cdot (\ln m)^{15} \cdot \frac{1}{\sigma^{30}} \cdot \lg\left(\frac{dm}{\sigma}\right) + m + 2. \end{aligned}$$

Here C_1 and C_2 are absolute constants.

After reading the information of this section one recognizes the enormous effort, which was made by Spielman und Teng for the derivation of the above stated result. The introduction of an alternative approach by Vershynin in [Ver09] lead to a significantly simpler and more elegant analysis. This will be the issue in the following section.

3.2 The Contribution Of Vershynin

In this section we present the contribution by Vershynin to the smoothed analysis of the Simplex Method. It was first presented as a conference talk [Ver06] and in 2009 it was published in more detail as a journal article [Ver09]. Vershynins approach consists at first of an improved estimation method of the expectation value for the number of shadow vertices of a perturbed polyhedron and in addition of a new algorithmic realization of the Phase 1 – Phase 2 composition, which makes a simplified running-time analysis possible.

3.2.1 Improvement Of The Geometrical Fundamental Result

For the expected value of the number of shadow vertices of a perturbed polyhedron Vershynin derives the bound given in the following Theorem. The formulation directly addresses the dual perspective.

Theorem 3.2.1 (Intersections of perturbed polytopes and planes).

Let $d \geq 3$. And let $\mathbf{a}_1, \dots, \mathbf{a}_m$ be (independent) normally distributed random vectors in \mathbb{R}^d with centers of norm at most 1 and standard deviation $\sigma \leq 1/(6\sqrt{d \ln(m)})$. Consider a fixed two-dimensional plane E in \mathbb{R}^d and the perturbed polytope $V = \mathbf{KH}(\mathbf{a}_1, \dots, \mathbf{a}_m)$. The random variable K stands for the number of those facets of V , that are intersected by the pland E . Then:

$$\mathbb{E}[K] \leq \text{Const} \cdot \frac{d^3}{\sigma^4}.$$

Const is an absolute constant.

Remark 3.2.2.

Vershynin does not introduce the condition $d \geq 3$ for the dimension explicitly. But the reason for that necessary limitation becomes obvious for the following reason. At

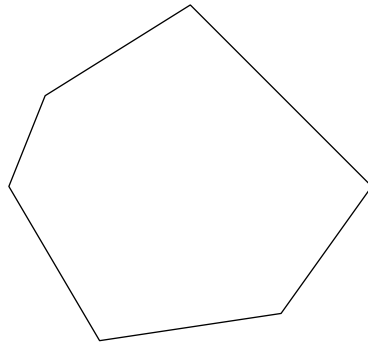
a certain stage in his estimation-appproach Vershynin [Ver09] makes use of a so-called *distance-result* originating from the paper [ST04]. For the derivation of that distance-result Spielman und Teng did apply a twofold coordinate transformation on some of the original restriction data $\mathbf{a}_1, \dots, \mathbf{a}_m$. After those transformations they work with new vector-representations $\mathbf{c}_2, \dots, \mathbf{c}_d \in \mathbb{R}^{d-2}$. This approach is only justified for $d \geq 3$. For the running time investigation of the Simplex Method the constraint $d \geq 3$ is not essential. And the interest in the Simplex Method surely focuses on higher dimensions d . Nevertheless we shall deal with the twodimensional case in a more precise and detailed matter in order to have for that case an upper bound of the same size as in Theorem 3.2.1. For our goal of a smoothed analysis of the dimension-by-dimension algorithm this will be essential. The reason is that in this algorithm for solving a d -dimensional problem d stages $k = 1, \dots, d$ have to be performed. And in each stage a problem of according dimension has to be solved by use of the shadow vertex algorithm. Now $k = 1$ is trivial, but $k = 2$ could generate unforseeable difficulties. So we should have a closer look at it. This will pay in the context of the smoothed analysis of that dimension-by-dimension algorithm in chapter 5.

Now we present the fundamental approach of Vershynin for the derivation and we discuss and lay a focus on the essential differences to the approach of Spielman and Teng.

As annonced in section 3.1.1, Spielman's und Teng's investigation of the number of shadow vertices of a perturbed polyhedron relies on the observation under the dual perspective. One is interested in the number of facets of the dual polyhedron $Y = \mathbf{K}\mathbf{H}(\mathbf{0}, \mathbf{a}_1, \dots, \mathbf{a}_m)$, which are generated by d original restriction vectors and which are intersected by the plane $E = \mathbf{L}\mathbf{H}(\mathbf{u}, \mathbf{v})$. One discretizes the plane by ℓ equidistant directions and then one is at the starting point of the analysis. For graphical illustration have a look at figures 3.1 and 3.2.

Vershynin's interpretation of the situation is a little different. Consider the perturbed polytope $V = \mathbf{K}\mathbf{H}(\mathbf{a}_1, \dots, \mathbf{a}_m)$.¹ Now one recognizes that the number of facets of V , that are intersected by the plane E , equals the number of edges of the polygon $V \cap E$. In figure 3.7 one observes an example for such an intersection.

¹Dealing with $V = \mathbf{K}\mathbf{H}(\mathbf{a}_1, \dots, \mathbf{a}_m)$ instead of $Y = \mathbf{K}\mathbf{H}(\mathbf{0}, \mathbf{a}_1, \dots, \mathbf{a}_m)$ is only a technical modification and has no significant meaning.


 Figure 3.7: An example for an intersection $V \cap E$

Further considerations rely on that twodimensional configuration. The principle of Spielman and Teng demands the following procedure: One looks consecutively from the origin in all ℓ discrete directions $\mathbf{q}_1, \dots, \mathbf{q}_\ell$ and one determines the number of facets intersected or hit in this way. Moreover one makes the discretization more and more tight or capillary ($\ell \rightarrow \infty$), to avoid disregarding an edge. An illustration can be seen in figure 3.8.

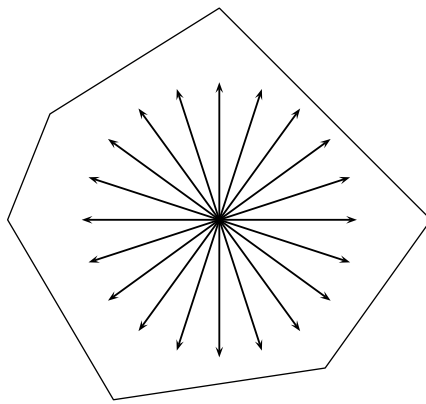


Figure 3.8: Calculation of the number of edges according to Spielman and Teng

In contrast to that Vershynin follows another principle. First of all concentrate on those configurations of the restriction vectors $\mathbf{a}_1, \dots, \mathbf{a}_m$, that are contained in the set

$$P_r := \{(\mathbf{p}_1, \dots, \mathbf{p}_m) \in \mathbb{R}^{d \times m} : \|\mathbf{p}_i\| \leq r \text{ für alle } i = 1, \dots, m\}$$

for $r = 2$. So one can assume that the intersection polygon $V \cap E = \mathbf{KH}(\mathbf{b}_1, \dots, \mathbf{b}_N) =: W$ is contained in the circle disk of radius 2 in the plane E . Now we avoid counting all edges of the polygon from the origin as viewpoint. Instead one uses an alternative method: Let an equilateral triangle with center of gravity in the origin be given. Its vertices $\mathbf{o}_1, \mathbf{o}_2, \mathbf{o}_3$ shall all have norm 8. They will serve as observation points for counting the edges of $W = \mathbf{KH}(\mathbf{b}_1, \dots, \mathbf{b}_N)$. This is possible because of the following insight, gained by Vershynin: For each edge $\mathbf{KH}(\mathbf{b}_j, \mathbf{b}_k)$ of W there is at least

one viewpoint \mathbf{o}_i , such that $\mathbf{KH}(\mathbf{b}_j, \mathbf{b}_k)$ is an edge of $\mathbf{KH}(\mathbf{o}_i, \mathbf{b}_1, \dots, \mathbf{b}_N)$ and that $\text{dist}(\mathbf{o}_i, \mathbf{AH}(\mathbf{b}_j, \mathbf{b}_k)) \geq 2$ holds. A graphical illustration is given in figure 3.9, which is similar to [Ver09, Figure 7.2].

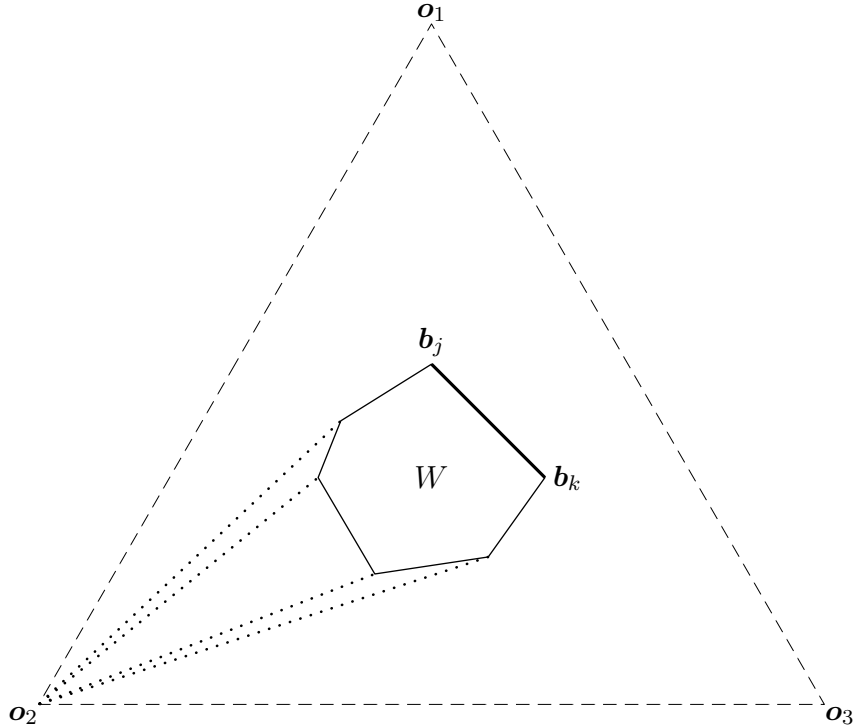


Figure 3.9: The Three-Viewpoints-Principle

Exploiting that perception about the distance and transforming the origin in the point \mathbf{o}_i , enables to establish for an arbitrary pair of points $\mathbf{x}_1, \mathbf{x}_2$ on the edge $\mathbf{KH}(-\mathbf{o}_i + \mathbf{b}_j, -\mathbf{o}_i + \mathbf{b}_k)$ that there is a proportionality between angle and Euclidean distance.

$$c \cdot \text{dist}(\mathbf{x}_1, \mathbf{x}_2) \leq \text{arc}(\mathbf{x}_1, \mathbf{x}_2) \leq \text{dist}(\mathbf{x}_1, \mathbf{x}_2).$$

c is an absolute constant. In total we can draw the conclusion: Each edge of W can be seen by one point \mathbf{o}_i from $\{\mathbf{o}_1, \mathbf{o}_2, \mathbf{o}_3\}$ under an angle, that differs at most by a constant factor from the length of the edge. In addition the edge is preserved under the change to the polygon $\mathbf{KH}(\mathbf{o}_i, W)$ erhalten.²

Let us have a look at the counting principle of Vershynin. First we have to agree on a certain notation. For a polytope of the form $Y = \mathbf{KH}(\mathbf{0}, \mathbf{a}_1, \dots, \mathbf{a}_m)$ and for a vector $\mathbf{q} \in \mathbb{R}^d$ the term $\mathbf{facet}_Y(\mathbf{q})$ will denote the family of all d -element sets $\Delta \subset \{1, \dots, m\}$, such that the convex hull $\mathbf{KH}(\mathbf{a}_{\Delta^1}, \dots, \mathbf{a}_{\Delta^d})$ is a facet of Y and such that it is intersected by the ray $\mathbf{KK}(\mathbf{q})$. The according intersection point will

²In chapter 4, we shall in detail deal with this Three-Viewpoint-Argument again, when we try to get an estimation of the expected number of vertices of a perturbed polygon.

be denoted by \mathbf{q}_Y . If the vector \mathbf{q} is in general position, then $\mathbf{facet}_Y(\mathbf{q})$ either is the empty set or it consists of only one element. In that case $\mathbf{Facet}_Y(\mathbf{q})$ denotes the corresponding geometrical facet.

As known one is interested in the expectation value $\mathbb{E}[K]$ of the number of facets of $V = \mathbf{KH}(\mathbf{a}_1, \dots, \mathbf{a}_m)$, that are intersected by the twodimensional plane E . For that purpose one starts with partitioning the potential configurations of the restriction vectors $\mathbf{a}_1, \dots, \mathbf{a}_m$ in the above mentioned set P_2 and in the complementary set. For simplicity we denote the events of belonging or not to the sets by P_2 or $\neg P_2$. On that basis the following partition resp. estimation of the expectation value can be done:³

$$\begin{aligned}\mathbb{E}[K] &= \mathbb{E}[K \cdot \mathbf{1}[P_2]] + \mathbb{E}[K \cdot \mathbf{1}[\neg P_2]] \\ &\leq \mathbb{E}[K \cdot \mathbf{1}[P_2]] + 1.\end{aligned}$$

For the remaining expectation value one can use the Three-Viewpoints-Principle. This is justified by the limitation of the configurations of $\mathbf{a}_1, \dots, \mathbf{a}_m$ on the set P_2 . We shall give a sketch of ist application. Let $\mathbf{o}_1, \mathbf{o}_2, \mathbf{o}_3$ be the vertices of an equilateral triangle in the plane E with center of gravity in the origin and with $\|\mathbf{o}_1\| = \|\mathbf{o}_2\| = \|\mathbf{o}_3\| = 8$. Moreover let $W_i = \mathbf{KH}(\mathbf{0}, -\mathbf{o}_i + W)$. Using the fact that each edge of the polygon $W = V \cap E$ is preserved for at least one of the three viewpoints one obtains:⁴

$$\mathbb{E}[K] \leq \mathbb{E}[\#\{\mathbf{facet}_{W_i}(\mathbf{q}_\theta) : \theta \in (0, 2\pi], i = 1, 2, 3\} \cdot \mathbf{1}[P_{10}]] + 1.$$

Here $\mathbf{q}_\theta := \mathbf{u}_1 \cdot \sin(\theta) + \mathbf{u}_2 \cdot \cos(\theta)$ and $\mathbf{u}_1, \mathbf{u}_2$ are orthogonal vectors of length 1 from E . One uses the set $Z_\ell = \{\mathbf{q}_\theta : \theta = \frac{2\pi}{\ell}, \dots, \frac{\ell \cdot 2\pi}{\ell}\}$ of directions in the same way as Spielman and Teng did in order to discretize the problem:

$$\mathbb{E}[K] \leq \lim_{\ell \rightarrow \infty} \mathbb{E}[\#\{\mathbf{facet}_{W_i}(\mathbf{q}) : \mathbf{q} \in Z_\ell, i = 1, 2, 3\} \cdot \mathbf{1}[P_{10}]] + 1. \quad (3.8)$$

Now the case can occur, that an edge of $W = V \cap E$ under view from \mathbf{o}_i is hit by several discrete directions. In that case one keeps only that direction $\mathbf{q} \in Z_\ell$, which belongs to the largest angle θ aus $\{\frac{2\pi}{\ell}, \dots, \frac{\ell \cdot 2\pi}{\ell}\}$. This implies that for the angle between \mathbf{q} and the boundary of the edge $\mathbf{Facet}_{W_i \cap E}(\mathbf{q})$ it holds that:

$$\text{arc}(\mathbf{q}, \partial \mathbf{Facet}_{W_i \cap E}(\mathbf{q})) \leq \frac{2\pi}{\ell}. \quad (3.9)$$

Moreover the Three-Viewpoints-Principle enables us to restrict the incorporation of the viewpoint \mathbf{o}_i to those configurations, where for an arbitrary pair of points $\mathbf{x}_1, \mathbf{x}_2$ on the edge $\mathbf{Facet}_{W_i \cap E}(\mathbf{q})$ the known proportionality-condition is satisfied:

$$c \cdot \text{dist}(\mathbf{x}_1, \mathbf{x}_2) \leq \text{arc}(\mathbf{x}_1, \mathbf{x}_2) \leq \text{dist}(\mathbf{x}_1, \mathbf{x}_2). \quad (3.10)$$

³All the configurations not belonging to P_2 , can have an impact of at most 1 on the expected value.

⁴Here and further we identify $\mathbf{facet}_{W_i}(\mathbf{q})$ with the corresponding index set. Since the according polytope is in general position almost surely, $\mathbf{facet}_{W_i}(\mathbf{q})$ contains at most one index set.

Combining the results from (3.9) and from (3.10), yields the following finding : It is sufficient to take the index set $\mathbf{facet}_{W_i}(\mathbf{q})$ into regard for the discretized expected value (3.8) , if

$$\mathbf{dist} (\mathbf{q}_{W_i}, \partial \mathbf{Facet}_{W_i} (\mathbf{q})) \leq \frac{2\pi}{c \cdot \ell} =: \frac{C}{\ell}$$

holds. Instead of an angle-condition we now have a distance-condition. In total we obtain

$$\begin{aligned} \mathbb{E}[K] &\leq \lim_{\ell \rightarrow \infty} \mathbb{E} \left[\# \left(\left\{ \mathbf{facet}_{W_i}(\mathbf{q}) : \mathbf{dist} (\mathbf{q}_{W_i}, \partial \mathbf{Facet}_{W_i} (\mathbf{q})) \leq \frac{C}{\ell}, \right. \right. \right. \\ &\quad \left. \left. \left. \mathbf{q} \in Z_\ell, i = 1, 2, 3 \right\} \right) \cdot \mathbf{1}[P_{10}] \right] + 2. \end{aligned}$$

Further considerations lead to the estimation

$$\begin{aligned} \mathbb{E}[K] &\leq 3 \cdot \sup_{\mathbf{b}_1, \dots, \mathbf{b}_m} \lim_{\ell \rightarrow \infty} \ell \cdot \max_{\substack{\mathbf{q} \in Z_\ell \\ \Delta \subset \{1, \dots, m\} \\ \#(\Delta) = d}} \mathbb{P} \left[\mathbf{dist} (\mathbf{q}_Y, \partial \mathbf{KH}(\mathbf{b}_{\Delta^1}, \dots, \mathbf{b}_{\Delta^d})) \leq \frac{C}{\ell} \right. \\ &\quad \left. \text{und } P_{10} \left| \mathbf{facet}_Y(\mathbf{q}) = \Delta \right. \right] + 2. \end{aligned}$$

The supremum will be taken over all normally distributed random vectors $\mathbf{b}_1, \dots, \mathbf{b}_m$ with centers of norm at most 9 and with standard deviation σ , as known from the original vectors $\mathbf{a}_1, \dots, \mathbf{a}_m$. Besides that we have $Y = \mathbf{KH}(\mathbf{0}, \mathbf{b}_1, \dots, \mathbf{b}_m)$. A demonstration of the appearing probability in this seemingly very complicated term is possible as follows: One asks for the probability that the intersection of the ϵ -ball about the point \mathbf{q}_Y with the surface of the polytope Y is not completely contained in the facet being hit. A graphical illustration of the complementary configuration is given in figure 3.10.

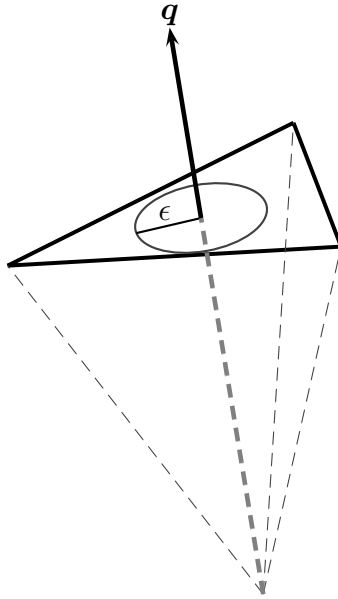


Figure 3.10: Graphical illustration of the distance-probability

In contrast to the investigation by Spielman and Teng for the probability (3.4) of small angles Vershynin can concentrate on the investigation of the probability for small distances. This simplifies the technical evaluation and yields an improved result

$$\mathbb{E}[K] \leq \text{Const} \cdot \frac{d^3}{\sigma^4}.$$

Here we finish the description of Vershynin's approach for estimating the number of shadow vertices of a perturbed polyhedron. From Theorem 3.2.1 we deduce a Corollary , that makes a certifying statement for arbitrary standard deviation values σ .

Corollary 3.2.3 (Number of shadow vertices of a perturbed polyhedron).

Let $d \geq 3$. $\mathbf{a}_1, \dots, \mathbf{a}_m$ shall be (independent) normally distributed random vectors in \mathbb{R}^d with centers of norm at most 1 and standard deviation σ . Let E be a fixed twodimensional plane in \mathbb{R}^d and observe the perturbed polyhedron

$X = \{\mathbf{x} : \langle \mathbf{a}_1, \mathbf{x} \rangle \leq 1, \dots, \langle \mathbf{a}_m, \mathbf{x} \rangle \leq 1\}$. The random variable S may stand for the number of shadow vertices of X with respect to the plane E . Then:

$$\mathbb{E}[S] \leq \text{Const} \cdot \left(\frac{d^3}{\sigma^4} + d^5 \cdot (\ln m)^2 \right).$$

Const is an absolute constant.

Proof. First consider the function $T : \mathbb{R}^d \times \dots \times \mathbb{R}^d \rightarrow \mathbb{N}$, defined as follows : For m vectors $\mathbf{z}_1, \dots, \mathbf{z}_m$ the term $T(\mathbf{z}_1, \dots, \mathbf{z}_m)$ stands for the number of facets of the polytope $Y = \mathbf{KH}(\mathbf{0}, \mathbf{z}_1, \dots, \mathbf{z}_m)$, not containing the origin, which are intersected by the plane E . From 2.4.2 we know the dual perspective. This helps us to understand the following equivalency for the random variable S : $S \equiv T(\mathbf{a}_1, \dots, \mathbf{a}_m)$. Regarding

the random variable K , also appearing in Theorem 3.2.1, then the following estimation becomes obvious: $T(\mathbf{a}_1, \dots, \mathbf{a}_m) \leq K$. By use of the monotony of the expectation value we obtain:

$$\mathbb{E}_{\mathbf{a}_1, \dots, \mathbf{a}_m} [T(\mathbf{a}_1, \dots, \mathbf{a}_m)] \leq \mathbb{E}_{\mathbf{a}_1, \dots, \mathbf{a}_m} [K].$$

As indicated, the expected value is taken over the random vectors $\mathbf{a}_1, \dots, \mathbf{a}_m$. Now we take advantage of a distinction of cases.

Case 1: $\sigma \leq 1/(6\sqrt{d \ln(m)})$. Here we directly can apply Theorem 3.2.1:

$$\mathbb{E}[S] \leq \mathbb{E}[K] \leq \text{Const} \cdot \frac{d^3}{\sigma^4}.$$

Case 2: $\sigma > 1/(6\sqrt{d \ln(m)})$. In that case one scales the vectors $\mathbf{a}_1, \dots, \mathbf{a}_m$ down in a way that the resulting normally distributed random vectors, called $\mathbf{b}_1, \dots, \mathbf{b}_m$, get the standard deviations $\sigma' = 1/(6\sqrt{d \ln(m)})$. Since by the way the norms of the centers also become smaller, we can apply the estimation from Theorem 3.2.1 to the vectors $\mathbf{b}_1, \dots, \mathbf{b}_m$. It holds:

$$\mathbb{E}_{\mathbf{b}_1, \dots, \mathbf{b}_m} [T(\mathbf{b}_1, \dots, \mathbf{b}_m)] \leq \text{Const} \cdot 6^4 \cdot d^5 \cdot (\ln m)^2.$$

Moreover the equality

$$\mathbb{E}_{\mathbf{a}_1, \dots, \mathbf{a}_m} [T(\mathbf{a}_1, \dots, \mathbf{a}_m)] = \mathbb{E}_{\mathbf{b}_1, \dots, \mathbf{b}_m} [T(\mathbf{b}_1, \dots, \mathbf{b}_m)]$$

can be shown easily. Therefore use the fact that the vectors $\mathbf{b}_1, \dots, \mathbf{b}_m$ were generated by scaling from $\mathbf{a}_1, \dots, \mathbf{a}_m$. And remember the property of T : $T(\mathbf{z}_1, \dots, \mathbf{z}_m) = T(\lambda \mathbf{z}_1, \dots, \lambda \mathbf{z}_m)$ for arbitrary $\mathbf{z}_1, \dots, \mathbf{z}_m \in \mathbb{R}^d$ and $\lambda > 0$. One deduces:

$$\mathbb{E}_{\mathbf{a}_1, \dots, \mathbf{a}_m} [S] = \mathbb{E}_{\mathbf{a}_1, \dots, \mathbf{a}_m} [T(\mathbf{a}_1, \dots, \mathbf{a}_m)] \leq \text{Const} \cdot 6^4 \cdot d^5 \cdot (\ln m)^2.$$

Combining both cases yields

$$\begin{aligned} \mathbb{E}_{\mathbf{a}_1, \dots, \mathbf{a}_m} [S] &\leq \max \left\{ \text{Const} \cdot \frac{d^3}{\sigma^4}, \text{Const} \cdot 6^4 \cdot d^5 \cdot (\ln m)^2 \right\} \\ &\leq \text{Const} \cdot \frac{d^3}{\sigma^4} + \text{Const} \cdot 6^4 \cdot d^5 \cdot (\ln m)^2 \\ &\leq \text{Const} \cdot 6^4 \cdot \left(\frac{d^3}{\sigma^4} + d^5 \cdot (\ln m)^2 \right). \end{aligned}$$

This proves the proposition. □

3.2.2 New Algorithmic Proposals

In this subsection we introduce the fundamental principle of the method created by Vershynin, which he has analyzed. We will leave some technical details out in order to be somehow concise. After that we study the impact on the smoothed analysis.

Vershynin's method is designed to solve linear optimization problems of the following form

$$\begin{aligned} & \text{maximize } \langle \mathbf{v}, \mathbf{x} \rangle \\ & \text{s.t. } \mathbf{A}\mathbf{x} \leq \mathbf{b} \end{aligned} \tag{LP}$$

with $\mathbf{A} = (\mathbf{a}_1, \dots, \mathbf{a}_m)^T \in \mathbb{R}^{m \times d}$, $\mathbf{b} = (b^1, \dots, b^m)^T \in \mathbb{R}^m$ and $m > d \geq 3$.

For that purpose one starts with considering the corresponding unit problem

$$\begin{aligned} & \text{maximize } \langle \mathbf{v}, \mathbf{x} \rangle \\ & \text{s.t. } \mathbf{A}\mathbf{x} \leq \mathbf{1} \end{aligned} \tag{EP}$$

Now one calculates a solution point for that problem. For achieving that goal, Vershynin suggests a randomized procedure. The fundamental idea behind that is: Instead of determining a vertex of the feasible region X_{EP} von (EP), one adjoins an artificial vertex. This vertex can serve as a starting point for the shadow vertex path. Now we present the principle for adjoining that vertex. In that context the dual perspective as presented in section 2.4.2 is very helpful. It is known that $Y = \mathbf{K}\mathbf{H}(\mathbf{0}, \mathbf{a}_1, \dots, \mathbf{a}_m)$ is the dual polyhedron to X_{EP} . Adjoining a vertex to X_{EP} is equivalent to adjoin a facet to Y . We can manage that task as described: Select first a direction \mathbf{u} uniformly distributed in the unit sphere ω_d . Now create in the hyperplane $\{\mathbf{x} : \langle \mathbf{u}, \mathbf{x} \rangle = 0\}$ a regular simplex whose center of gravity is located in the origin. Now we want to transform that simplex in a facet of Y . Therefore we add the vector $\eta\mathbf{u}$ with $\eta = e^{\lceil \ln(\max_{i=1,\dots,m} \|\mathbf{a}_i\|) \rceil}$ to each of the simplex-vertices $\mathbf{b}_1, \dots, \mathbf{b}_d$. This ensures that each of the transformed vertices emerges from the set Y . Thus we have got the additional vectors $\mathbf{a}_{m+1}, \dots, \mathbf{a}_{m+d}$.⁵ On the basis of the described construction it is assured that $\mathbf{K}\mathbf{H}(\mathbf{a}_{m+1}, \dots, \mathbf{a}_{m+d})$ is a facet of $Y^+ := \mathbf{K}\mathbf{H}(\mathbf{0}, \mathbf{a}_1, \dots, \mathbf{a}_{m+d})$. Consequently the restrictions corresponding to the vectors $\mathbf{a}_{m+1}, \dots, \mathbf{a}_{m+d}$ generate a vertex of the modified (primal) feasible polyhedron

$$X_{EP}^+ := \{\mathbf{x} : \langle \mathbf{a}_1, \mathbf{x} \rangle \leq 1, \dots, \langle \mathbf{a}_{m+d}, \mathbf{x} \rangle \leq 1\}.$$

In the dual view it may occur that in consequence of the appearance of the additional vectors more than one new facets are created. And it may happen as well that hitherto existing facets disappear.⁶ A graphical illustration is given in figure 3.11. Our actions have adjoined the red facet to Y . By the way the orange colored facets were generated as well. On the contrary the two grey colored (dashed) facets disappear. This modification transforms Y into Y^+ . The primal meaning is that three new vertices arise and two hitherto existing vertices become infeasible.

⁵Some details about the construction of $\mathbf{a}_{m+1}, \dots, \mathbf{a}_{m+d}$ are omitted. This is because they are very technical and they do not concern the fundamental principle.

⁶In this context we speak of a facet only if the origin is not involved.

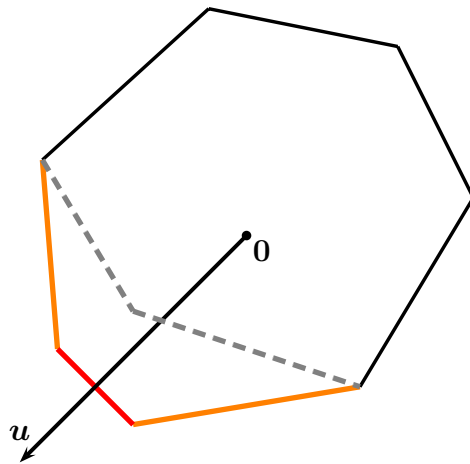


Figure 3.11: Augmentation of an additional facet to Y

Taking the newly generated restriction vectors into regard one can construct the extended matrix $\mathbf{A}^+ := (\mathbf{a}_1, \dots, \mathbf{a}_{m+d})^T$. Using this matrix one can formulate the modified problem

$$\begin{aligned} & \text{maximize } \langle \mathbf{v}, \mathbf{x} \rangle \\ & \text{s.t. } \mathbf{A}^+ \mathbf{x} \leq \mathbf{1}. \end{aligned} \tag{EP^+}$$

For that problem we know one vertex according to the construction. This vertex is yet optimal with respect to the direction \mathbf{u} . Hence the shadow vertex algorithm can be started at that vertex in order to solve the problem.

It may happen that (EP⁺) due to the additional restrictions has another resp. different optimal point than (EP). Algorithmically this difficulty can be treated as follows. At first one solves the modified problem (EP⁺) and after that one checks, which of the three following cases has occurred.

1. If (EP⁺) has unbounded objective, then this holds for (EP), too. In that case we can stop.
2. If for (EP⁺) an optimal point \mathbf{x}^* has been found, where none of the artificial restriction vectors $\mathbf{a}_{m+1}, \dots, \mathbf{a}_{m+d}$ is involved, then \mathbf{x}^* is definitely a solution also for (EP).
3. If we have found a solution for (EP⁺), where some of the artificial vectors $\mathbf{a}_{m+1}, \dots, \mathbf{a}_{m+d}$ are active and involved, then one cannot draw any conclusions on the solution of (EP). In that case the vectors $\mathbf{a}_{m+1}, \dots, \mathbf{a}_{m+d}$ have failed their purpose. They should be dropped. Instead one tries with another selection of an additional facet anywhere else. This construction process should be started from scratch.

The procedure described above is nothing else but Vershynin's fundamental principle for solving (EP). It is stated below in algorithmic notation.

Algorithm 3.2.4 (Randomized principle for the solution of (EP)).

Input: $\mathbf{A} = (\mathbf{a}_1, \dots, \mathbf{a}_m)^T$ and \mathbf{v}

Procedure: Repeat resp. iterate the steps 1 und 2, until one of the following cases occurs.

1. The index set Δ^+ belonging to the optimal \mathbf{x}^+ of (EP^+) of tight restrictions does not contain any element from the accessory set $\{m + 1, \dots, m + d\}$.
2. The problem (EP^+) is unbounded.

Step 1 According to the demonstrated principle construct the additional restriction vectors $\mathbf{a}_{m+1}, \dots, \mathbf{a}_{m+d}$ and use the extended matrix $\mathbf{A}^+ = (\mathbf{a}_1, \dots, \mathbf{a}_{m+d})^T$ to formulate the modified unit problem (EP^+) . Then the vertex \mathbf{x}_u corresponding to the index set $\{m + 1, \dots, m + d\}$ is an optimal solution on the feasible set of (EP^+) for the objective direction \mathbf{u} .

Step 2 Make use of the shadow vertex algorithm in the following way. Start at \mathbf{x}_u and use the auxiliary objective direction \mathbf{u} in order to find an optimal solution for (EP^+) . If that objective is not unbounded for that problem, then let Δ^+ be the index set belonging to the solution \mathbf{x}^+ .

Output: If the iteration loop above has been aborted because of unboundedness of (EP^+) , then one has to send the message “problem unbounded”. Else the output should be the optimal solution \mathbf{x}^+ .

Now it is the intention, to integrate that principle into a solution process for the original (LP). To achieve that goal one interpolates between the problems (LP) and (EP). For that purpose one introduces the interpolation variable $t \in [0, 1]$ and one defines the restrictions

$$\mathbf{Ax} \leq t \cdot \mathbf{b} + (1 - t) \cdot \mathbf{1}.$$

Moreover we should have the possibility to lay stress on certain values of t . Therefore one introduces a parameter $\lambda \in \mathbb{R}$ and one changes the objective function to $\langle \mathbf{v}, \mathbf{x} \rangle + \lambda t$. So one is in the position to formulate a linear optimization problem that interpolates between (LP) and (EP):

$$\begin{aligned} & \text{maximize } \langle \mathbf{v}, \mathbf{x} \rangle + \lambda t \\ & \text{s.t. } \mathbf{Ax} \leq t \cdot \mathbf{b} + (1 - t) \cdot \mathbf{1}, \quad 0 \leq t \leq 1. \end{aligned} \tag{Int LP}$$

For fixed $\lambda \in \mathbb{R}$ the problem (Int LP) behaves in case of $t = 1$ like the original problem (LP), since λ is a constant and for $t = 0$ it behaves like the corresponding unit problem

(EP). For $\lambda \rightarrow -\infty$ one can attach importance to $t = 0$ and for $\lambda \rightarrow \infty$ accordingly to $t = 1$. Furthermore (Int LP) can be formulated as a unit problem in \mathbb{R}^{d+1} :⁷

$$\begin{aligned} & \text{maximize } \langle (\mathbf{v}, \lambda), (\mathbf{x}, t) \rangle \\ & \text{s.t. } \langle (\mathbf{0}, -\infty), (\mathbf{x}, t) \rangle \leq 1 \\ & \quad \langle (\mathbf{0}, 1), (\mathbf{x}, t) \rangle \leq 1 \\ & \quad \langle (\mathbf{a}_i, 1 - b^i), (\mathbf{x}, t) \rangle \leq 1, \quad i = 1, \dots, m. \end{aligned} \tag{Int EP}$$

Now we have the ability to formulate a procedure for solving general linear optimization problems.

Algorithm 3.2.5 (Two Phase version of the Simplex Method for (LP)).

Input : $\mathbf{A} = (\mathbf{a}_1, \dots, \mathbf{a}_m)^T$, \mathbf{b} and \mathbf{v}

Procedure:

Phase 1 Solve (EP) by means of algorithm 3.2.4. If this reports that the problem is unbounded, then (LP) does not have an optimal solution and one can stop. Else the just calculated optimal point $\hat{\mathbf{x}}^*$ of (EP) and $t = 0$ delivers a limit solution of (Int LP) for $\lambda \rightarrow -\infty$. Use that solution as a starting point for Phase 2.

Phase 2 Use the shadow vertex algorithm in order to determine a limit solution (\mathbf{x}^*, t^*) of (Int LP) for $\lambda \rightarrow +\infty$. If $t^* < 1$, then (LP) is infeasible. Elsewise \mathbf{x}^* is a solution of (LP).

Output: Report according to the achieved insight either the optimal point \mathbf{x}^* or alternatively the message “problem has no solution.”.

Vershynin uses limit solutions for determining the algorithm. Nevertheless he makes clear that in practical applications the use of the limit solutions is not necessary. He explains this as follows: A solution for $\lambda \rightarrow -\infty$ is optimal for the feasible region of (Int LP) with respect to the objective $(\mathbf{0}, -1)$. In almost the same manner one obtains the optimality with respect to the vector $(\mathbf{0}, 1)$ for $\lambda \rightarrow \infty$. However both vectors are linearly dependent and consequently they do not span a twodimensional plane. Remember that we need such a plane for the execution of the shadow vertex algorithm. For that reason one is in need of an additional vector. According considerations enable Vershynin to show that the vector $(\mathbf{v}, 0)$ is suitable for that purpose. Hence we use the projection plane $\mathbf{LH}((\mathbf{v}, 0), (\mathbf{0}, 1))$ in Phase 2.

So we have learned about the fundamental principle of Vershynins algorithmic method. For additional aspects and details we refer to the original paper. Now we have to clarify, which impacts of that method on the smoothed analysis can be observed. Here the restriction data $(\mathbf{a}_1, b^1), \dots, (\mathbf{a}_m, b^m)$ are not fixed, but they are normally distributed

⁷Vershynin explains in detail in [Ver09, Section 3.2] how to deal with vectors of the form $(\mathbf{0}, -\infty)$.

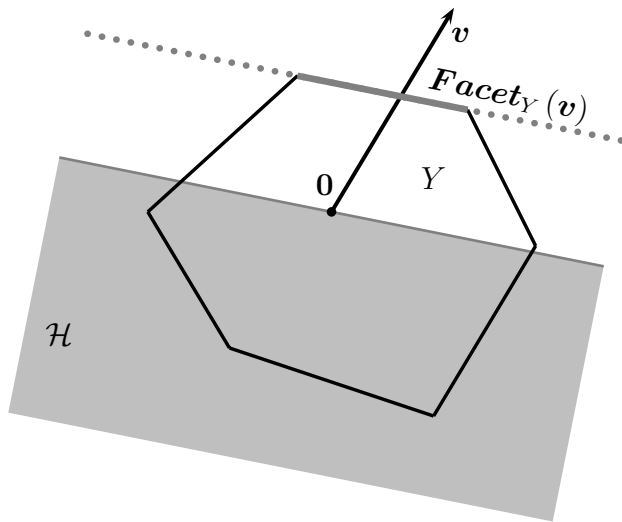
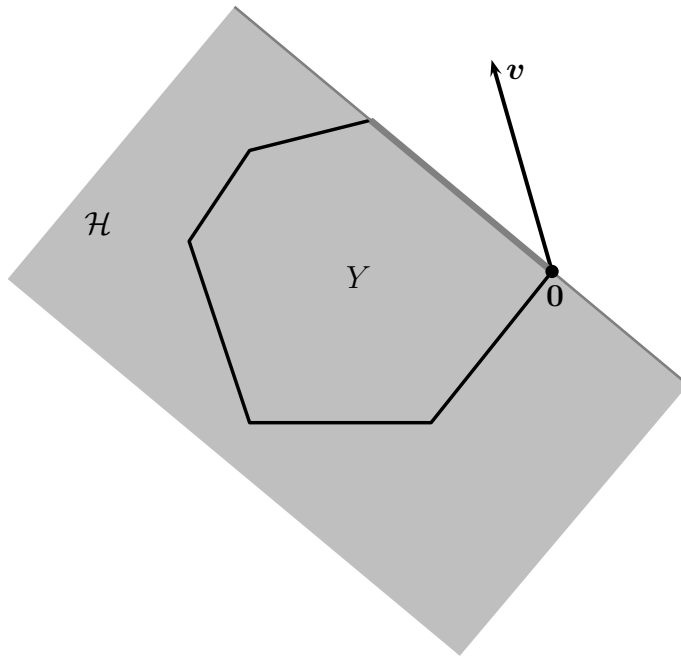
random vectors with standard deviation σ and centers of norm at most 2. Phases 1 and 2 from algorithm 3.2.5 can still be investigated separately. Furthermore we should remark that the upper bound on the number of shadow vertices from Theorem 3.2.1 serves as a geometrical basis for the investigation of the algorithmic running time.

Phase 1:

For the investigation of Phase 1 it is helpful to consider algorithm 3.2.4 in detail. There the first and the second step will be executed one after another, until unboundedness becomes obvious or until a solution of (EP) is available. From the viewpoint of the running time analysis the question arises, how many iterations resp. loops have to be run through. As an answer Vershynin can determine an expected value. We present and discuss the essential ideas. Before some notations should be clarified: A halfspace in \mathbb{R}^d is a set of the form $\{\mathbf{x} : \langle \mathbf{z}, \mathbf{x} \rangle \leq 0\}$, where $\mathbf{z} \neq \mathbf{0}$ may be an arbitrary vector. For an affine halfspace we need in addition a number s and we get $\{\mathbf{x} : \langle \mathbf{z}, \mathbf{x} \rangle \leq s\}$. The definitions for a hyperplane resp. an affine hyperplane are likely. Here only the inequalities are replaced by equations.

Furthermore we have to explain the term *numb set* as introduced and used by Vershynin. This is the set of vectors \mathbf{a} , such that the addition of the restriction $\langle \mathbf{a}, \mathbf{x} \rangle \leq 1$ to the original restrictions of (EP) does not change the optimal solution resp. does not change the property of unboundedness. For that set Vershynin can show that in any case this numb set will contain a half space. We are going to explain and to illustrate the according argumentation. If (EP) is bounded, then for instance the *numb set* (in the dual perspective) is that affine halfspace, which is bounded by $\mathbf{AH}(\mathbf{Facet}_Y(\mathbf{v}))$ and which contains the origin. Hence the *numb set* contains a half space, which will be denoted by \mathcal{H} . A graphical illustration for that can be found in figure 3.12, which uses the dual dual perspective. The grey highlighted facet of Y , which is intersected by the direction \mathbf{v} , is $\mathbf{Facet}_Y(\mathbf{v})$ and the dashed extension represents the hyperplane $\mathbf{AH}(\mathbf{Facet}_Y(\mathbf{v}))$, which bounds the *numb set* from above. Plotted in grey is the halfspace \mathcal{H} , a subset of the *numb set*.

In case of unboundedness the illustration of *numb set* is more complicated. Nevertheless it pays to look at the illustration in figure 3.13. We see a dual polytope Y , which corresponds to an unbounded primal feasibility region X . We recognize this by the fact that the origin belongs to the boundary of Y . Since furthermore the objective direction does not hit any facet \mathbf{v} , that does not contain the origin, we can conclude that the objective can be improved arbitrarily on the primal polyhedron X . This means that unboundedness is at hand. The halfspace given in grey \mathcal{H} is contained in the *numb set*. This can be perceived by the following consideration: If one adds an arbitrary vector from the grey region to the convex hull $Y = \mathbf{KH}(\mathbf{0}, \mathbf{a}_1, \dots, \mathbf{a}_m)$, then the configuration just described remains as it is. Besides we recognize that the objective direction \mathbf{v} and the polytope Y are located on different sides of the hyperplane bounding the halfspace \mathcal{H} .


 Figure 3.12: Graphical illustration of the *numb set* under boundedness

 Figure 3.13: Graphical illustration of a subset of the *numb set* in case of unboundedness

This characterization just mentioned holds in general in the case of unboundedness. The *numb set* contains a halfspace \mathcal{H} , bounded by a hyperplane, which on one hand separates \mathbf{v} from Y , and which on the other hand is determined by a facet of Y containing the origin. It is very difficult to make statements about the size of the *numb set* in general. Essential and sufficient is the perception that the *numb set* contains some half space \mathcal{H} . In the following course of the argumentation we can –in the case

of boundedness and in the case of unboundedness as well – make use of the existence of such a halfspace.

Drawing the auxiliary objective vector \mathbf{u} from a uniform distribution over the unit sphere ω_d , as announced at the begin of this section, it becomes obvious that this vector belongs to the halfspace \mathcal{H} with probability $\frac{1}{2}$. The application of methods from geometrical functional analysis enables Vershynin to conclude in addition, that with probability $p' \geq \frac{1}{4}$ also the vectors $\mathbf{a}_{m+1}, \dots, \mathbf{a}_{m+d}$, whose location is strongly influenced by the direction of \mathbf{u} , also are contained in \mathcal{H} ⁸. Exploiting that \mathcal{H} is contained in *numb set*, it results, that with probability $p \geq \frac{1}{4}$ the problems (EP) und (EP⁺) either have the identical optimal solution or both are unbounded. The consequence is that in algorithm 3.2.4 on the average at most four iterations are carried out until the final vertex is reached and the iteration can be aborted. For that reason it is permitted to concentrate on one representative iteration. After that one should multiply the result resp. the number of pivot steps by the factor 4.

Let us direct our attention on one single run of such a loop in algorithm 3.2.4. In step 1 we construct – as explained – an additional artificial vertex. This is done in a way that it becomes optimal with respect to the coobjective direction \mathbf{u} . And from that vertex one starts the optimization process in direction \mathbf{v} . According considerations enable Vershynin to show, that in the view of the conditions for Theorem 3.2.1 the use of the projection plane $\mathbf{LH}(\mathbf{u}, \mathbf{v})$ does not at all create significant complications for the application of the shadow vertex algorithm. Nevertheless we should focus on the construction of the modified problem (EP⁺). Here we first create vectors $\mathbf{b}_1, \dots, \mathbf{b}_d$ and after that they are shifted by the vector $\eta\mathbf{u}$ with $\eta = e^{\lceil \ln(\max_{i=1, \dots, m} \|\mathbf{a}_i\|) \rceil}$. So we obtain the additional vectors $\mathbf{a}_{m+1}, \dots, \mathbf{a}_{m+d}$. These are necessary for the construction of (EP⁺). In that context we should take three points into regard:

1. There are d additional and artificial vectors $\mathbf{a}_{m+1}, \dots, \mathbf{a}_{m+d}$.
2. These vectors are dependent on \mathbf{u} due to the rules for their construction.
3. Moreover the vectors are also correlated with the original restriction vectors $\mathbf{a}_1, \dots, \mathbf{a}_m$ via the condition $\eta = e^{\lceil \ln(\max_{i=1, \dots, m} \|\mathbf{a}_i\|) \rceil}$.

The second point does not cause great difficulties. Roughly spoken Vershynin's approach does not make significant conditions with respect to the vector \mathbf{u} , which are necessary for the construction of $\mathbf{a}_{m+1}, \dots, \mathbf{a}_{m+d}$.

For the third point the following ascertainment ist important: The variable $\eta = e^{\lceil \ln(\max_{i=1, \dots, m} \|\mathbf{a}_i\|) \rceil}$ does attain only discrete values. On that basis one can show that with very high probability η attains values from a set M with low cardinality. For that reason it is possible to disregard all cases, for which η attains a value outside of M . This holds, because they can influence the expected value for the number of pivot steps at most by the value of 1. For a fixed value $\eta \in M$ there is no correlation, such that

⁸Compare for a graphical illustration once more in figure 3.11

the discussed difficulty can be dissolved via the separated consideration of all values in M .

Roughly spoken, the concern from point 1 is met by Vershynin by artificially perturbing the additional vectors $\mathbf{a}_{m+1}, \dots, \mathbf{a}_{m+d}$. So he can treat them in principle in the same way as the original restriction vectors. .

The approach described finally leads to a point, where one is able to apply the upper bound for the number of shadow vertices from Theorem 3.2.1. So one is in the position to gain an upper bound for the expectation value of the number of pivot steps for solving 1. Now we come to the final discussion of Phase 2.

Phase 2:

As already mentioned, we use the fixed projection plane $\mathbf{LH}((\mathbf{v}, 0), (\mathbf{0}, 1))$ in the application of the shadow vertex algorithm for the solution of Phase 2. Moreover the restriction vectors $(\mathbf{a}_1, 1 - b^1), \dots, (\mathbf{a}_m, 1 - b^m)$ of the interpolation problem (Int EP) are normally distributed. So we do not get into trouble. The two fixed vectors $(\mathbf{0}, -\infty)$ und $(\mathbf{0}, 1)$ should be considered more carefully. Since they are located in the projection plane $\mathbf{LH}((\mathbf{v}, 0), (\mathbf{0}, 1))$, a little additional consideration suffices to be permitted to disregard them. Hence the upper bound for shadow vertices from Theorem 3.2.1 can be applied and an estimation for the average number of pivot steps for the solution of Phase 2 can be obtained.

On the basis of the presented algorithmic principle and of the sketched approach in the analysis of the running time, Vershynin can prove the final result:

Theorem 3.2.6 (Smoothed running time of the Two-Phase-Simplex-Algorithm).
For an arbitrary linear optimization problem with $d \geq 3$ variables⁹ and $m > d$ restrictions Algorithmus 3.2.5 requires on the average not more than

$$\mathcal{O}((\ln m)^2 \cdot \ln(\ln(m)) \cdot (d^3 \sigma^{-4} + d^5 \cdot (\ln m)^2 + d^9 \cdot (\ln d)^4))$$

pivot steps for the solution of the corresponding perturbed linear optimization problem.

By presentation of the smoothed analysis for the Simplex Method under the approach of Spielman and Teng on one side and of Vershynin on the other side we have learned about the main studies done until now in that field.

⁹Vershynin formulates at this place the condition $d > 3$. For the exclusion of $d = 3$ there is no evident reason. After consulting the author, this formulation it is probable that this was caused by a typing error.

4 Smoothed Analysis Of Polyhedra In Dimension 2

In this chapter we shall – based on the methods of [Ver09], [ST04] and [Bor87] – derive an upper bound for the expected number of vertices of a perturbed polyhedron in dimension 2. By the way we supplement the estimation for this quantity derived by Vershynin (compare section 3.2.1) by clarifying the case of dimension 2. That seemingly discrete geometric result is necessary for our purpose, since we want to have a smoothed analysis for the dimension-by-dimension algorithm in chapter 5. And the first stage of that algorithm is an application of the shadow vertex algorithm in dimension 2. This chapter is organized as follows: After some introducing remarks we describe the problem for our investigation explicitly. Then we explain a coordinate transformation, which will be useful for further considerations. It will assist us when we deal with the estimation of the probability of small edges in the next section. In the fourth part of this chapter we make use of the so-called Three-Viewpoints-Principle from [Ver09]. Finally we summarize in order to obtain the desired estimation for the number of vertices.

4.1 Formulation Of The Problem

As stated before, we care about a Smoothed Analysis of polyhedra in dimension 2. More precisely we want to obtain knowledge about the expected number of vertices of a two-dimensional polyhedron defined like :

$$X = \{ \mathbf{x} : \langle \mathbf{a}_1, \mathbf{x} \rangle \leq 1, \dots, \langle \mathbf{a}_m, \mathbf{x} \rangle \leq 1 \}.$$

In the context of Smoothed Analysis the restriction vectors $\mathbf{a}_1, \dots, \mathbf{a}_m$ are not fixed, but they follow a normal distribution having these features:

$$\mathbf{a}_i \sim \mathcal{N}_2(\bar{\mathbf{a}}_i, \sigma^2 \cdot \mathbf{E}_2)$$

and $\|\bar{\mathbf{a}}_i\| \leq 1$ for all $i = 1, \dots, m$ as well as $\sigma \leq \frac{1}{2\sqrt{\ln(m)}}$.

In view of our goal to get an estimation for the expected number of vertices it is advantageous to change from the primal point of view to the dual perspective. Therefore we remember the results from section 2.4.2 and we look at the polyhedron dual to X

$$Y := \{ \mathbf{y} \in \mathbb{R}^2 : \langle \mathbf{y}, \mathbf{x} \rangle \leq 1 \ \forall \mathbf{x} \in X \} = \mathbf{K}\mathbf{H}(\mathbf{0}, \mathbf{a}_1, \dots, \mathbf{a}_m).$$

As a consequence of the nondegeneracy condition 2.4.1, which applies for our perturbation principle with probability 1, there is a 1-to-1-relation between the vertices of X

and those edges of Y , which join two vectors \mathbf{a}_j and \mathbf{a}_k .¹ Such edges will be identified as *proper* edges . In order to calculate the number of vertices of X , it is sufficient to determine the number of proper edges Y . Let V be the random variable denoting just that number.

Based on the insight that $Y = \mathbf{K}\mathbf{H}(\mathbf{0}, \mathbf{a}_1, \dots, \mathbf{a}_m)$, we consider the slightly modified polygon

$$P = \mathbf{K}\mathbf{H}(\mathbf{a}_1, \dots, \mathbf{a}_m).$$

All the edges of this polygon P are created by pairs of restriction vectors $\mathbf{a}_1, \dots, \mathbf{a}_m$ and the random variable K shall denote the number of edges in P . It is useful to know that each proper edge of Y automatically is an edge of P , too. Hence $V \leq K$ and the monotony of the expected value delivers

$$\mathbb{E}[V] \leq \mathbb{E}[K].$$

So for getting an upper bound for the expected value of V we are allowed to concentrate on the evaluation of $\mathbb{E}[K]$. In that context we gain the following result. That statement will be proven as a theorem 4.5.1 in section 4.5.

Theorem 4.1.1 (Number of edges of a perturbed polygon).

Let $\mathbf{a}_1, \dots, \mathbf{a}_m$ be independent and normally distributed random variables in \mathbb{R}^2 with centers $\bar{\mathbf{a}}_1, \dots, \bar{\mathbf{a}}_m$ of norm at most 1 and with standard deviation $\sigma \leq \frac{1}{2\sqrt{\ln(m)}}$. Furthermore the random variable K shall stand for the number of edges $P = \mathbf{K}\mathbf{H}(\mathbf{a}_1, \dots, \mathbf{a}_m)$. Then under the mentioned perturbation model it holds:

$$\mathbb{E}[K] \leq \text{Const} \cdot \frac{1}{\sigma^2}.$$

The expected value is calculated over the random $\mathbf{a}_1, \dots, \mathbf{a}_m$ and Const is an absolute constant value.

An illustration for the meaning of that theorem is given in 4.1.

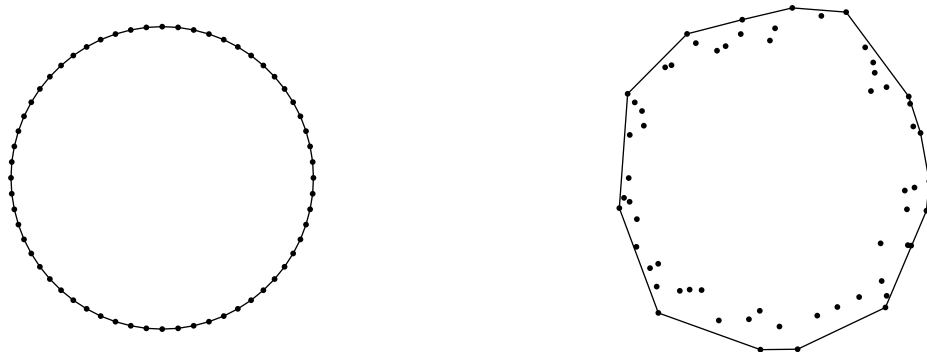


Figure 4.1: Original polygon with 60 edges and polygon generated through perturbation

¹Usually one calls those the facets of 1st kind

In combination with the considerations mentioned above we can prove the following corollary.

Corollary 4.1.2 (Number of vertices of a twodimensional perturbed polygon).

Let $\mathbf{a}_1, \dots, \mathbf{a}_m$ be independent and normally distributed random vectors in \mathbb{R}^2 with centers $\bar{\mathbf{a}}_1, \dots, \bar{\mathbf{a}}_m$ of norm at most 1 and with standard deviation σ . Furthermore let the random variable V denote the number of vertices of the twodimensional polyhedron $X = \{ \mathbf{x} : \langle \mathbf{a}_1, \mathbf{x} \rangle \leq 1, \dots, \langle \mathbf{a}_m, \mathbf{x} \rangle \leq 1 \}$. Then under our perturbation model it holds:

$$\mathbb{E}[V] \leq \text{Const} \cdot \left(\frac{1}{\sigma^2} + \ln(m) \right).$$

That expected value is calculated over the random vectors $\mathbf{a}_1, \dots, \mathbf{a}_m$ and Const is an absolute constant.

Proof. First consider the function $T : \mathbb{R}^2 \times \dots \times \mathbb{R}^2 \rightarrow \mathbb{N}$, which is defined like that: For m vectors $\mathbf{z}_1, \dots, \mathbf{z}_m$ the function $T(\mathbf{z}_1, \dots, \mathbf{z}_m)$ stands for the number of those edges of the polygon $Y = \mathbf{KH}(\mathbf{0}, \mathbf{z}_1, \dots, \mathbf{z}_m)$, where the origin is not involved. By the help of the dual perspective, known from 2.4.2, one recognizes for the random variable V the following equivalence: $V \equiv T(\mathbf{a}_1, \dots, \mathbf{a}_m)$. For the random variable K used in 4.1.1 in addition the following estimation holds: $T(\mathbf{a}_1, \dots, \mathbf{a}_m) \leq K$. Taking the monotony of the expected value into regard, we see:

$$\mathbb{E}_{\mathbf{a}_1, \dots, \mathbf{a}_m}[T(\mathbf{a}_1, \dots, \mathbf{a}_m)] \leq \mathbb{E}_{\mathbf{a}_1, \dots, \mathbf{a}_m}[K].$$

As already mentioned, the expected value is in each time calculated over the random vectors $\mathbf{a}_1, \dots, \mathbf{a}_m$. The following distinction of cases will be useful for further considerations.

Case 1: $\sigma \leq 1/(2\sqrt{\ln(m)})$. Here we can directly apply theorem 4.1.1 and one obtains

$$\mathbb{E}[V] \leq \mathbb{E}[K] \leq \text{Const} \cdot \frac{1}{\sigma^2}.$$

Case 2: $\sigma > 1/(2\sqrt{\ln(m)})$. In that case one should downscale the vectors $\mathbf{a}_1, \dots, \mathbf{a}_m$ so far, that the resulting normally distributed random vectors $\mathbf{b}_1, \dots, \mathbf{b}_m$ exhibit the random deviation $\sigma' = 1/(2\sqrt{\ln(m)})$. Since during that procedure the norms of the centers decrease too, we can now apply the estimation from theorem 4.1.1 to the vectors $\mathbf{b}_1, \dots, \mathbf{b}_m$. One obtains:

$$\mathbb{E}_{\mathbf{b}_1, \dots, \mathbf{b}_m}[T(\mathbf{b}_1, \dots, \mathbf{b}_m)] \leq \text{Const} \cdot 2^2 \cdot \ln(m).$$

In addition the equality

$$\mathbb{E}_{\mathbf{a}_1, \dots, \mathbf{a}_m}[T(\mathbf{a}_1, \dots, \mathbf{a}_m)] = \mathbb{E}_{\mathbf{b}_1, \dots, \mathbf{b}_m}[T(\mathbf{b}_1, \dots, \mathbf{b}_m)]$$

can easily be ensured. For that purpose let $\mathbf{b}_1, \dots, \mathbf{b}_m$ and $\mathbf{a}_1, \dots, \mathbf{a}_m$ be a result of rescaling and use the insight about T : $T(\mathbf{z}_1, \dots, \mathbf{z}_m) = T(\lambda \mathbf{z}_1, \dots, \lambda \mathbf{z}_m)$ for arbitrary $\mathbf{z}_1, \dots, \mathbf{z}_m \in \mathbb{R}^d$ and $\lambda > 0$. By the way one obtains

$$\mathbb{E}_{\mathbf{a}_1, \dots, \mathbf{a}_m} [V] = \mathbb{E}_{\mathbf{a}_1, \dots, \mathbf{a}_m} [T(\mathbf{a}_1, \dots, \mathbf{a}_m)] \leq \text{Const} \cdot 2^2 \cdot \ln(m).$$

Combination of both cases delivers:

$$\begin{aligned} \mathbb{E}_{\mathbf{a}_1, \dots, \mathbf{a}_m} [V] &\leq \max \left\{ \text{Const} \cdot \frac{1}{\sigma^2}, \text{Const} \cdot 2^2 \cdot \ln(m) \right\} \\ &\leq \text{Const} \cdot \frac{1}{\sigma^2} + \text{Const} \cdot 2^2 \cdot \ln(m) \\ &\leq \text{Const} \cdot 2^2 \cdot \left(\frac{1}{\sigma^2} + \ln(m) \right). \end{aligned}$$

This concludes the proof. \square

This corollary will be very helpful during the Smoothed Analysis of the dimension-by-dimension algorithm in chapter 5.

Remark 4.1.3.

In purely geometrical context other authors have already dealt with similar questions in compatible form in [Dam06] and [DGG13]. The closest relationship to our considerations exists in the methods and results of [Dam06]. The reason is the fact that there also the basis is a normal distribution of the perturbation. But if one translates things into our situation one sees that there are different conditions on the centers of the distributions $\bar{\mathbf{a}}_1, \dots, \bar{\mathbf{a}}_m$ of the random vectors. These are points in the unit square, $[0, 1]^2$. In order to have a consistent application of the results obtained so far for the Smoothed Analysis of the dimension-by-dimension algorithm we need to have the results exactly in our desired form.

After a short introduction we have given an exact formulation of the problem, which we want to discuss and to solve in the course of this and the next chapter. Our next aim will be to carry out an advantageous coordinate transformation.

4.2 The Transformation Of Coordinates Under Use

Before starting with the description of the transformation of coordinates, we remark that Spielman and Teng work in their Smoothed Analysis [ST04] of the Simplex Method with an analogous method, which is applicable also in higher dimensions. For that reason our final results with regard to the functional determinant coincides with the result of Corollary 2.28 for $d = 2$ obtained in their analysis. However the technique for the reasoning after having transformed coordinates cannot be transferred directly to the situation in \mathbb{R}^2 . So we should show our way to do that for $d = 2$.

Consider two vectors \mathbf{a}_j and \mathbf{a}_k in the plane. As a consequence of the condition of nondegeneracy 2.4.1, which is valid with probability 1, we may assume that \mathbf{a}_j and \mathbf{a}_k are linearly independent. On that basis we observe the straight line $\mathcal{G} := \mathbf{AH}(\mathbf{a}_j, \mathbf{a}_k)$, which is determined by these two points. In addition consider a vector $\mathbf{v} \in \omega_2$, which generates the straight line $\mathcal{H} := \mathbf{LH}(\mathbf{v})$. Now and in the following we act on the assumption that the straight lines \mathcal{G} and \mathcal{H} intersect each other, i.e. $\mathcal{G} \cap \mathcal{H} \neq \emptyset$. This means no significant loss of generality, since all configurations of \mathbf{a}_j and \mathbf{a}_k , which generate a line \mathcal{G} parallel to \mathcal{H} , form a nullset and therefore do not influence the expectation values.

For the description of the location of the two \mathbf{a}_j and \mathbf{a}_k we will do without cartesian coordinates. Instead we first fix the position of the straight line \mathcal{G} . For that purpose we need two variables:

- The variable t with $t \in \mathbb{R}$ locates the point $t \cdot \mathbf{v}$, where the lines \mathcal{G} and \mathcal{H} intersect each other. This point is used as a reference point in the line.
- Besides we need the φ such that $-\frac{\pi}{2} \leq \varphi < \frac{\pi}{2}$. This variable tells us the angle between the normal vector $\boldsymbol{\omega}$ of \mathcal{G} and the direction of \mathbf{v} . We measure the angle anti-clockwise. $\boldsymbol{\omega}$ shall be that one of the two possible normal vectors, which exhibits a nonnegative scalar product with \mathbf{v} .

In addition two more coordinates are required. They should locate the two points \mathbf{a}_j and \mathbf{a}_k on \mathcal{G} . Therefore we use the following notation:

- for the determination of the location of \mathbf{a}_j and \mathbf{a}_k on the straight line \mathcal{G} we use the real variables b_j and b_k .

It remains to determine the direction in the straight line \mathcal{G} until we have the final coordinates b_j and b_k . Before clarifying that point we want to illustrate the situation graphically. Have a look at Figure 4.2.

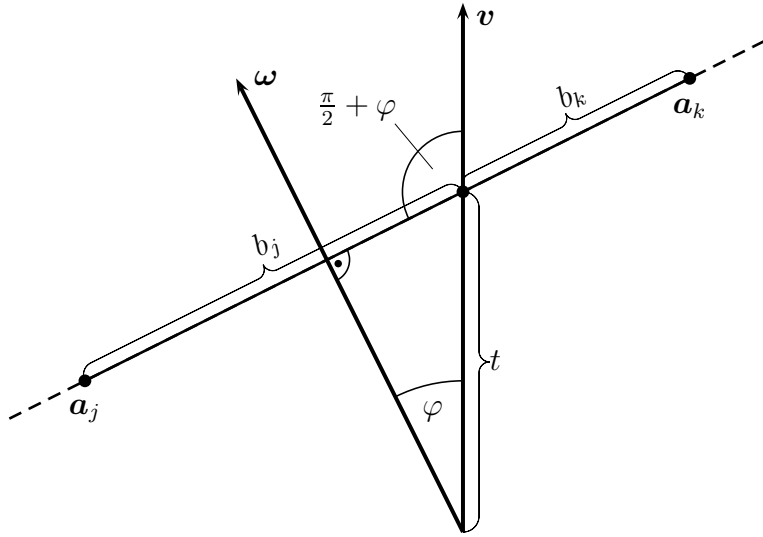


Figure 4.2: Graphical illustration of the change of coordinates

Now it becomes essential how the location of \mathbf{a}_j and \mathbf{a}_k can be derived from the coordinates t, φ, b_j, b_k . For that purpose we need a direction vector spanning \mathcal{G} . As one can see in figure 4.2 it is for instance possible to obtain that direction by a rotation of \mathbf{v} through an angle $(\frac{\pi}{2} + \varphi)$ anti-clockwise. The rotation matrix for that is then:

$$\mathbf{R}_\varphi = \begin{pmatrix} \cos(\frac{\pi}{2} + \varphi) & -\sin(\frac{\pi}{2} + \varphi) \\ \sin(\frac{\pi}{2} + \varphi) & \cos(\frac{\pi}{2} + \varphi) \end{pmatrix}.$$

Exploliting that

$$\begin{aligned} \cos\left(\frac{\pi}{2} + \varphi\right) &= -\sin(\varphi) \\ \sin\left(\frac{\pi}{2} + \varphi\right) &= \cos(\varphi) \end{aligned}$$

we obtain

$$\mathbf{R}_\varphi = \begin{pmatrix} -\sin(\varphi) & -\cos(\varphi) \\ \cos(\varphi) & -\sin(\varphi) \end{pmatrix}.$$

It is easy to see, that the columns of that matrix form an orthonormal basis of \mathbb{R}^2 . These considerations enable us to describe the position of both points in the new coordinates:

$$\mathbf{a}_j = t \cdot \mathbf{v} + \underbrace{(\mathbf{R}_\varphi \cdot \mathbf{v}) \cdot b_j}_{=: \mathbf{v}_\varphi},$$

$$\mathbf{a}_k = t \cdot \mathbf{v} + \mathbf{v}_\varphi \cdot b_k.$$

Finally we should know the functional determinant of the change of coordinates. The answer can be found in the following Lemma.

Lemma 4.2.1.

The functional determinant of the transformation of coordinates described above is

$$\left| \det \left(\frac{\partial(\mathbf{a}_j, \mathbf{a}_k)}{\partial(\varphi, t, b_j, b_k)} \right) \right| = \cos(\varphi) \cdot |b_j - b_k|.$$

Proof. First we give the representation of \mathbf{a}_j and \mathbf{a}_k in terms of the new coordinates once more in detail:²

$$\begin{aligned} \mathbf{a}_j &= t \begin{pmatrix} v_1 \\ v_2 \end{pmatrix} + \left[\begin{pmatrix} -\sin(\varphi) & -\cos(\varphi) \\ \cos(\varphi) & -\sin(\varphi) \end{pmatrix} \begin{pmatrix} v_1 \\ v_2 \end{pmatrix} \right] \cdot b_j \\ &= \begin{pmatrix} t \cdot v_1 + (-\sin(\varphi) \cdot v_1 - \cos(\varphi) \cdot v_2) \cdot b_j \\ t \cdot v_2 + (\cos(\varphi) \cdot v_1 - \sin(\varphi) \cdot v_2) \cdot b_j \end{pmatrix}, \\ \mathbf{a}_k &= t \begin{pmatrix} v_1 \\ v_2 \end{pmatrix} + \left[\begin{pmatrix} -\sin(\varphi) & -\cos(\varphi) \\ \cos(\varphi) & -\sin(\varphi) \end{pmatrix} \begin{pmatrix} v_1 \\ v_2 \end{pmatrix} \right] \cdot b_k \\ &= \begin{pmatrix} t \cdot v_1 + (-\sin(\varphi) \cdot v_1 - \cos(\varphi) \cdot v_2) \cdot b_k \\ t \cdot v_2 + (\cos(\varphi) \cdot v_1 - \sin(\varphi) \cdot v_2) \cdot b_k \end{pmatrix}. \end{aligned}$$

Now we are able to determine the corresponding Jacobi-matrix.

$$\frac{\partial(\mathbf{a}_j, \mathbf{a}_k)}{\partial(\varphi, t, b_j, b_k)} = \begin{pmatrix} (1) & v_1 & (5) & 0 \\ (2) & v_2 & (6) & 0 \\ (3) & v_1 & 0 & (5) \\ (4) & v_2 & 0 & (6) \end{pmatrix}$$

With

- (1) $(-\cos(\varphi) \cdot v_1 + \sin(\varphi) \cdot v_2) \cdot b_j,$
- (2) $(-\sin(\varphi) \cdot v_1 - \cos(\varphi) \cdot v_2) \cdot b_j,$
- (3) $(-\cos(\varphi) \cdot v_1 + \sin(\varphi) \cdot v_2) \cdot b_k,$
- (4) $(-\sin(\varphi) \cdot v_1 - \cos(\varphi) \cdot v_2) \cdot b_k,$
- (5) $(-\sin(\varphi) \cdot v_1 - \cos(\varphi) \cdot v_2)$ und
- (6) $(\cos(\varphi) \cdot v_1 - \sin(\varphi) \cdot v_2).$

²Since we argue with powers in the proof, we denote for simplicity the components of \mathbf{v} by v_1 and v_2 instead of v^1, v^2 .

Let us think about the determinant of that matrix. We exploit the structure of the third column and we obtain according to the determinant rules:

$$\det \left(\frac{\partial(\mathbf{a}_j, \mathbf{a}_k)}{\partial(\varphi, t, b_j, b_k)} \right) = (5) \cdot \underbrace{\det \begin{pmatrix} (2) & v_2 & 0 \\ (3) & v_1 & (5) \\ (4) & v_2 & (6) \end{pmatrix}}_{(*)} - (6) \cdot \underbrace{\det \begin{pmatrix} (1) & v_1 & 0 \\ (3) & v_1 & (5) \\ (4) & v_2 & (6) \end{pmatrix}}_{(**)}.$$

For (*) we get:

$$\begin{aligned} & (-\sin(\varphi) \cdot v_1 - \cos(\varphi) \cdot v_2) \cdot b_j \cdot \cos(\varphi) \cdot \underbrace{[(v_1)^2 + (v_2)^2]}_{=1} \\ & - v_2 [(-\cos(\varphi) \cdot v_1 + \sin(\varphi) \cdot v_2) \cdot b_k \cdot (\cos(\varphi) \cdot v_1 - \sin(\varphi) \cdot v_2) \\ & - b_k \cdot (\sin(\varphi) \cdot v_1 + \cos(\varphi) \cdot v_2)^2] \\ & = (-\sin(\varphi) \cdot v_1 - \cos(\varphi) \cdot v_2) \cdot b_j \cdot \cos(\varphi) \\ & - v_2 \cdot b_k \cdot \underbrace{[-(\cos \varphi)^2 \cdot (v_1)^2 - (\sin \varphi)^2 \cdot (v_2)^2 - (\sin \varphi)^2 \cdot (v_1)^2 - (\cos \varphi)^2 \cdot (v_2)^2]}_{=-1} \\ & = (-\sin(\varphi) \cdot v_1 - \cos(\varphi) \cdot v_2) \cdot b_j \cdot \cos(\varphi) + v_2 \cdot b_k. \end{aligned}$$

For (**) we obtain:

$$\begin{aligned} & (-\cos(\varphi) \cdot v_1 + \sin(\varphi) \cdot v_2) \cdot b_j \cdot \cos(\varphi) \cdot \underbrace{[(v_1)^2 + (v_2)^2]}_{=1} \\ & - v_1 [(-\cos(\varphi) \cdot v_1 + \sin(\varphi) \cdot v_2) \cdot b_k \cdot (\cos(\varphi) \cdot v_1 - \sin(\varphi) \cdot v_2) \\ & - b_k \cdot (\sin(\varphi) \cdot v_1 + \cos(\varphi) \cdot v_2)^2] \\ & = (-\cos(\varphi) \cdot v_1 + \sin(\varphi) \cdot v_2) \cdot b_j \cdot \cos(\varphi) \\ & - v_1 \cdot b_k \cdot \underbrace{[-(\cos \varphi)^2 \cdot (v_1)^2 - (\sin \varphi)^2 \cdot (v_2)^2 - (\sin \varphi)^2 \cdot (v_1)^2 - (\cos \varphi)^2 \cdot (v_2)^2]}_{=-1} \\ & = (-\cos(\varphi) \cdot v_1 + \sin(\varphi) \cdot v_2) \cdot b_j \cdot \cos(\varphi) + v_1 \cdot b_k. \end{aligned}$$

So we have for the determinant in total:

$$\begin{aligned}
 & (-\sin(\varphi) \cdot v_1 - \cos(\varphi) \cdot v_2) [(-\sin(\varphi) \cdot v_1 - \cos(\varphi) \cdot v_2) \cdot b_j \cdot \cos(\varphi) + v_2 \cdot b_k] \\
 & + (-\cos(\varphi) \cdot v_1 + \sin(\varphi) \cdot v_2) [(-\cos(\varphi) \cdot v_1 + \sin(\varphi) \cdot v_2) \cdot b_j \cdot \cos(\varphi) + v_1 \cdot b_k] \\
 & = b_j \cdot \cos(\varphi) \underbrace{[(-\sin(\varphi) \cdot v_1 - \cos(\varphi) \cdot v_2)^2 + (-\cos(\varphi) \cdot v_1 + \sin(\varphi) \cdot v_2)^2]}_{=1} \\
 & + b_k \underbrace{[(-\sin(\varphi) \cdot v_1 - \cos(\varphi) \cdot v_2) \cdot v_2 + (-\cos(\varphi) \cdot v_1 + \sin(\varphi) \cdot v_2) \cdot v_1]}_{= -\cos(\varphi)} \\
 & = b_j \cdot \cos(\varphi) - b_k \cdot \cos(\varphi) \\
 & = (b_j - b_k) \cdot \cos(\varphi).
 \end{aligned}$$

For $-\frac{\pi}{2} \leq \varphi < \frac{\pi}{2}$ holds $\cos(\varphi) \geq 0$ and finally we have the proposition

$$\left| \det \left(\frac{\partial(\mathbf{a}_j, \mathbf{a}_k)}{\partial(\varphi, t, b_j, b_k)} \right) \right| = \cos(\varphi) \cdot |b_j - b_k|.$$

□

The issue of this chapter was the description of the coordinate transformation, which we will use in the next section in order to gain the desired upper bounds. In addition we have calculated the functional determinant. We shall come back to that useful knowledge in the following.

4.3 An Estimation Of The Probability For Short Edges

The subject of this section is the derivation of an estimation for the probability that edges have a small length in the context of twodimensional perturbed convex hulls. To reach that goal we shall orientate ourselves at the approach in [ST04], where Spielman and Teng derive an analogical probability in the case of higher dimensions. Therefore we make use of several principles which have been exploited there (e.g. the coordinate transformation of the last section). However there is one significant difference insofar as we work with integral formulas that are in a stronger way similar to those used in the Average-Case Analysis [Bor87] and which do not appear in that form in the paper of Spielman and Teng. Besides some methodical principles and definitions of [Ver09] and [Bor87] are incorporated in our considerations

Before starting the theoretical considerations, we have to introduce some basic ideas and concepts. Here it makes sense to remember that we have got $m \geq 3$ twodimensional random vectors $\mathbf{a}_1, \dots, \mathbf{a}_m$ featuring the following distribution:

$$\mathbf{a}_i \sim \mathcal{N}_2(\bar{\mathbf{a}}_i, \sigma^2 \mathbf{E}_2).$$

For all $i = 1, \dots, m$ it further holds that $\|\bar{\mathbf{a}}_i\| \leq 1$ as well as $\sigma \leq \frac{1}{2\sqrt{\ln(m)}}$. That means that in explicit form each \mathbf{a}_i has the density function

$$f_i(\mathbf{a}_i) = \left(\frac{1}{\sqrt{2\pi}\sigma} \right)^2 \cdot e^{-\frac{\|\mathbf{a}_i - \bar{\mathbf{a}}_i\|^2}{2\sigma^2}}.$$

Relying on that we look at the perturbed polygon

$$Y = \mathbf{K}\mathbf{H}(\mathbf{0}, \mathbf{a}_1, \dots, \mathbf{a}_m)$$

in the rest of this section. Now we shall present some definitions which will turn out to be helpful and used several times in later considerations.

Definition 4.3.1 (\mathbf{v}_Y).

As known we deal with vectors $\mathbf{v}, \mathbf{a}_1, \dots, \mathbf{a}_m \in \mathbb{R}^2$. We study $Y = \mathbf{K}\mathbf{H}(\mathbf{0}, \mathbf{a}_1, \dots, \mathbf{a}_m)$. Then \mathbf{v}_Y will on that basis denote the point

$$\mathbf{KK}(\mathbf{v}) \cap \partial Y,$$

which is the intersection point of the ray $\mathbf{KK}(\mathbf{v})$ with the boundary of the polytope Y .

Helpful is also the following definition.

Definition 4.3.2 (kante** / **Kante**).**

For $\mathbf{v}, \mathbf{a}_1, \dots, \mathbf{a}_m \in \mathbb{R}^2$ let $\mathbf{kante}_Y(\mathbf{v})$ denote the index³ $\Delta = \{j, k\} \subset \{1, \dots, m\}$ such that:

1. \mathbf{a}_j and \mathbf{a}_k are linearly independent vectors,
2. $\mathbf{K}\mathbf{H}(\mathbf{a}_j, \mathbf{a}_k)$ is an edge of Y and
3. there are $\lambda_j, \lambda_k > 0$, for which $\mathbf{v} = \lambda_j \cdot \mathbf{a}_j + \lambda_k \cdot \mathbf{a}_k$ holds.

If those three conditions cannot be met, then $\mathbf{kante}_Y(\mathbf{v}) = \emptyset$. In case of $\mathbf{kante}_Y(\mathbf{v}) \neq \emptyset$ then $\mathbf{Kante}_Y(\mathbf{v})$ will denote the edge itself (as a geometrical subject).

In figure 4.3 one finds a graphical illustration for that definition.

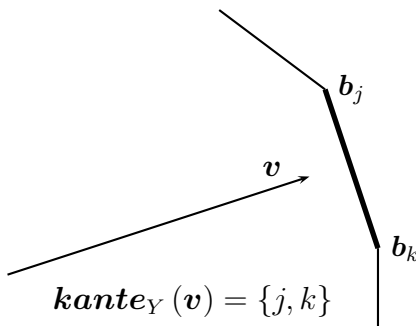


Figure 4.3: Graphical illustration of definition 4.3.2

Finally we give some additional definitions.

³Due to the nondegeneracy assumption there is at most one index set with the required property.

Definition 4.3.3 (R_δ).

Let R_δ denote the set of all configurations $(\mathbf{a}_1, \dots, \mathbf{a}_m) \in \mathbb{R}^{2 \times m}$, such that

$$\|\mathbf{a}_i\| \leq \delta$$

holds for all $i = 1, \dots, m$. More formally R_δ can be described as follows:

$$R_\delta := \{(\mathbf{a}_1, \dots, \mathbf{a}_m) \in \mathbb{R}^{2 \times m} : \|\mathbf{a}_i\| \leq \delta \ \forall i = 1, \dots, m\}.$$

For our perturbation model we can combine that definition with the insight from Lemma 2.2.7 and we realize:

$$\mathbb{P}[(\mathbf{a}_1, \dots, \mathbf{a}_m) \notin R_2] \leq \frac{1}{m}.$$

Events of the form $(\mathbf{a}_1, \dots, \mathbf{a}_m) \in R_\delta$ resp. $(\mathbf{a}_1, \dots, \mathbf{a}_m) \notin R_\delta$ will appear frequently in this chapter, so we are going to simplify the denotation to R_δ resp. $\neg R_\delta$. For instance it holds that

$$\mathbb{P}[(\mathbf{a}_1, \dots, \mathbf{a}_m) \notin R_\delta] = \mathbb{P}[\neg R_\delta].$$

The remaining aim of this section is to prove the following Lemma.

Lemma 4.3.4 (small distances).

Let $\mathbf{a}_1, \dots, \mathbf{a}_m \in \mathbb{R}^2$ be normally distributed random vectors with $\mathbf{a}_i \sim \mathcal{N}_2(\bar{\mathbf{a}}_i, \sigma^2 \cdot \mathbf{E}_2)$ and with density functions f_1, \dots, f_m . Moreover let $\|\bar{\mathbf{a}}_i\| \leq 1$. For all $i = 1, \dots, m$ and $\sigma \leq \frac{1}{2\sqrt{\ln(m)}}$ hold. Then

$$\mathbb{P}[(\text{dist}(\mathbf{v}_Y, \partial Kante_Y(\mathbf{v})) \leq \epsilon) \wedge R_2 \mid kante_Y(\mathbf{v}) = \Delta] \leq 4e^5 \cdot \frac{\epsilon}{\sigma^2}$$

for an arbitrary index set $\Delta = \{j, k\} \subset \{1, \dots, m\}$, where the random vectors feature the common density

$$\prod_{i=1}^m f_i(\mathbf{a}_i).$$

The proof of Lemma 4.3.4, which is divided in five steps, requires a lot of technical precision work. For that reason we give in advance a crude description with the important points and the obtained results. After that the reader will find the elaborated proof in detail.

As known we are interested in an upper bound for the probability

$$\mathbb{P}[(\text{dist}(\mathbf{v}_Y, \partial Kante_Y(\mathbf{v})) \leq \epsilon) \wedge R_2 \mid kante_Y(\mathbf{v}) = \Delta]$$

for an index set $\Delta = \{j, k\}$. Our approach works as follows:

Step1:

First we apply the coordinate transformation from 4.2 on the vectors \mathbf{a}_j and \mathbf{a}_k belonging to the index set Δ . By the way we get the variables t, φ, b_j, b_k . The two values t and φ determine the position of the straight line $\mathbf{AH}(\mathbf{a}_j, \mathbf{a}_k)$ and b_j, b_k can be interpreted as the local coordinates of $\mathbf{a}_j, \mathbf{a}_k$ in the line. For an illustration have a look at figure 4.2.

Because we are dealing now with the new coordinates t, φ, b_j, b_k instead of $\mathbf{a}_j, \mathbf{a}_k$, we must formulate the interesting events in a new way. Let us start with the set R_2 , for which we know that

$$R_2 = \{(\mathbf{a}_1, \dots, \mathbf{a}_m) \in \mathbb{R}^{2 \times m} : \|\mathbf{a}_i\| \leq 2 \ \forall i = 1, \dots, m\}.$$

We translate that into a set Q , containing all configurations of φ, t, b_j, b_k and \mathbf{a}_i such that $i \neq j, k$, for which it is true that:

1. $\|\mathbf{a}_i\| \leq 2 \ \forall i \neq j, k,$
2. $|b_j|, |b_k| \leq 4,$
3. $-\frac{\pi}{2} \leq \varphi < \frac{\pi}{2}$ and
4. $t \leq 2.$

This is not a direct translation, but we know that we have an inclusion “ $R_2 \subset Q$ ”. This means: For an arbitrary element $(\mathbf{a}_1, \dots, \mathbf{a}_m) \in R_2$ we can find respective values for the variables $\varphi, t, b_j, b_k, \mathbf{a}_{i \neq j, k}$ belonging to the set Q . Using these variables we are able to display and describe the original vectors $\mathbf{a}_1, \dots, \mathbf{a}_m$.

Besides we formulate in the first step the event appearing in the probability formula $\text{dist}(\mathbf{v}_Y, \partial \mathbf{Kante}_Y(\mathbf{v})) \leq \epsilon$ using the new variables. We understand that under the condition $\mathbf{kante}_Y(\mathbf{v}) = \Delta$ it holds that:

$$\text{dist}(\mathbf{v}_Y, \partial \mathbf{Kante}_Y(\mathbf{v})) \leq \epsilon \Leftrightarrow |b_j| \leq \epsilon \vee |b_k| \leq \epsilon.$$

Furthermore we can reformulate the condition $\mathbf{kante}_Y(\mathbf{v}) = \Delta$ following the same ideas by use of the variables $\varphi, t, b_j, b_k, \mathbf{a}_{i \neq j, k}$:

$$\mathbf{kante}_Y(\mathbf{v}) = \Delta \Leftrightarrow \begin{cases} t \geq 0, \\ (b_j < 0 \wedge b_k > 0) \vee (b_j > 0 \wedge b_k < 0) \text{ and} \\ \langle \boldsymbol{\omega}, \mathbf{a}_i \rangle \leq t \cdot \cos(\varphi) \text{ for all } i \neq j, k. \end{cases}$$

Here $\boldsymbol{\omega}$ is the normal vector on the straight line $\mathbf{AH}(\mathbf{a}_j, \mathbf{a}_k)$ and φ is the angle between $\boldsymbol{\omega}$ and \mathbf{v} . Based on the introduced translation we may formulate a relation between

the original probability and the new formulated probability using φ, t, b_j, b_k and $\mathbf{a}_{i \neq j, k}$:

$$\begin{aligned}
 & \mathbb{P}[(\text{dist}(\mathbf{v}_Y, \partial Kante_Y(\mathbf{v})) \leq \epsilon) \wedge R_2 | kante_Y(\mathbf{v}) = \Delta] \\
 & \leq \mathbb{P}[(|b_j| \leq \epsilon \vee |b_k| \leq \epsilon) \wedge Q | ((b_j < 0 \wedge b_k > 0) \vee (b_j > 0 \wedge b_k < 0)) \wedge \\
 & \quad \wedge (\langle \boldsymbol{\omega}, \mathbf{a}_i \rangle \leq t \cdot \cos(\varphi) \quad \forall i \neq j, k) \wedge (t \geq 0)] \\
 & = \mathbb{P}[(|b_j| \leq \epsilon \vee |b_k| \leq \epsilon) \wedge Q | ((b_j \leq 0 \wedge b_k \geq 0) \vee (b_j \geq 0 \wedge b_k \leq 0)) \wedge \\
 & \quad \wedge (\langle \boldsymbol{\omega}, \mathbf{a}_i \rangle \leq t \cdot \cos(\varphi) \quad \forall i \neq j, k) \wedge (t \geq 0)].
 \end{aligned}$$

The inequality comes from the inclusion “ $R_2 \subset Q$ ”. So we have achieved the goal of the first step.

Step 2:

In the second step we mainly deal with the question, how the common density of the variables φ, t, b_j, b_k , which originate from \mathbf{a}_j and \mathbf{a}_k , can be expressed. The densities of \mathbf{a}_j and of \mathbf{a}_k are according to the assumption of normal distribution

$$\begin{aligned}
 f_j(\mathbf{a}_j) &= \left(\frac{1}{\sqrt{2\pi}\sigma} \right)^2 \cdot e^{-\frac{\|\mathbf{a}_j - \bar{\mathbf{a}}_j\|^2}{2\sigma^2}} \\
 f_k(\mathbf{a}_k) &= \left(\frac{1}{\sqrt{2\pi}\sigma} \right)^2 \cdot e^{-\frac{\|\mathbf{a}_k - \bar{\mathbf{a}}_k\|^2}{2\sigma^2}}
 \end{aligned}$$

and $\|\bar{\mathbf{a}}_j\|, \|\bar{\mathbf{a}}_k\| \leq 1$. Having a look at both density functions, one detects that the essential point is to express the quantities $\|\mathbf{a}_j - \bar{\mathbf{a}}_j\|^2$ and $\|\mathbf{a}_k - \bar{\mathbf{a}}_k\|^2$. Figure 4.4 may help to understand this relation and this wish.

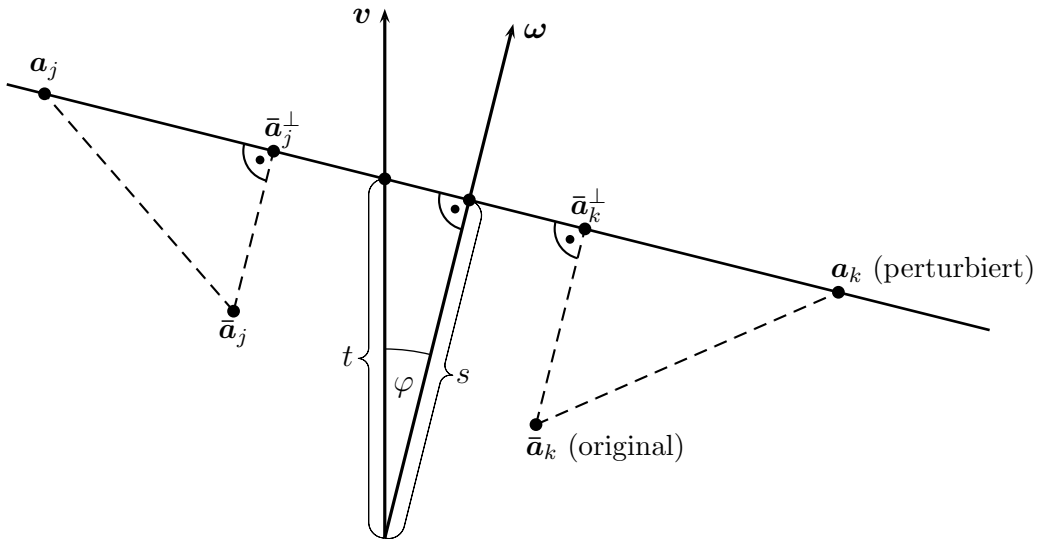


Figure 4.4: Useful illustration for the replacement of original by perturbed vectors

It can be seen that in order to determine $\|\mathbf{a}_k - \bar{\mathbf{a}}_k\|^2$ one can concentrate due to the theorem of Pythagoras on the size of $\|\mathbf{a}_k - \bar{\mathbf{a}}_k^\perp\|^2$ and $\|\bar{\mathbf{a}}_k^\perp - \bar{\mathbf{a}}_k\|^2$. For the term

$\|\mathbf{a}_k - \bar{\mathbf{a}}_k^\perp\|$ we see after some considerations, that

$$\|\mathbf{a}_k - \bar{\mathbf{a}}_k^\perp\| = |\bar{b}_k - b_k|.$$

Here \bar{b}_k denotes (analogously as for b_k) the local coordinate of $\bar{\mathbf{a}}_k^\perp$ in the straight line $\mathbf{AH}(\mathbf{a}_j, \mathbf{a}_k)$. Moreover we can show that

$$\|\mathbf{a}_k^\perp - \bar{\mathbf{a}}_k\| = |t \cdot \cos(\varphi) - \langle \boldsymbol{\omega}, \bar{\mathbf{a}}_k \rangle|.$$

In the case of the second vector the analogous result follows.

$$\|\mathbf{a}_j - \bar{\mathbf{a}}_j\|^2 = (b_j - \bar{b}_j)^2 + (t \cdot \cos(\varphi) - \langle \boldsymbol{\omega}, \bar{\mathbf{a}}_j \rangle)^2.$$

Informally written, we get as reformulations for the density functions of \mathbf{a}_j and \mathbf{a}_k :

$$f_k(\mathbf{a}_k) = \left(\frac{1}{\sqrt{2\pi}\sigma} \right)^2 \cdot e^{-\frac{(b_k - \bar{b}_k)^2}{2\sigma^2}} \cdot e^{-\frac{(t \cdot \cos(\varphi) - \langle \boldsymbol{\omega}, \bar{\mathbf{a}}_k \rangle)^2}{2\sigma^2}}$$

$$f_j(\mathbf{a}_j) = \left(\frac{1}{\sqrt{2\pi}\sigma} \right)^2 \cdot e^{-\frac{(b_j - \bar{b}_j)^2}{2\sigma^2}} \cdot e^{-\frac{(t \cdot \cos(\varphi) - \langle \boldsymbol{\omega}, \bar{\mathbf{a}}_j \rangle)^2}{2\sigma^2}}.$$

Now take into regard that we know the functional determinant $\cos(\varphi) \cdot |b_j - b_k|$ for the change of coordinates from 4.2. Then the common density of the new variables is in exact formulation:

$$g(\varphi, t, b_j, b_k) = \left(\frac{1}{\sqrt{2\pi}\sigma} \right)^4 \cdot \cos(\varphi) \cdot |b_j - b_k| \cdot \prod_{i \in \{j, k\}} e^{-\frac{(b_i - \bar{b}_i)^2}{2\sigma^2}} \cdot e^{-\frac{(t \cdot \cos(\varphi) - \langle \boldsymbol{\omega}, \bar{\mathbf{a}}_i \rangle)^2}{2\sigma^2}}.$$

This settles the essential issue of the second step. Since we want to evaluate the probability under consideration in more detail, the following insight is important. For an arbitrary configuration of $0 \leq t \leq 2$ and $-\frac{\pi}{2} \leq \varphi < \frac{\pi}{2}$ it holds that

$$|\bar{b}_j|, |\bar{b}_k| \leq 3.$$

This will be assured at the end of this step, too.

Step 3:

At the beginning of that step we reformulate the representation of the desired probability from step 1 once more. Now it will be written as a sum of four summands. So the new formulation is:

$$\mathbb{P} [(|b_j| \leq \epsilon \vee |b_k| \leq \epsilon) \wedge Q \mid ((b_j \leq 0 \wedge b_k \geq 0) \vee (b_j \geq 0 \wedge b_k \leq 0)) \wedge \langle \boldsymbol{\omega}, \mathbf{a}_i \rangle \leq t \cdot \cos(\varphi) \quad \forall i \neq j, k) \wedge (t \geq 0)].$$

Due to the two grand *or*-symbols (emphasized in gray) we can estimate the probability by a sum of four separate probabilities

$$\begin{aligned} \mathbb{P} [(\| b_j \| \leq \epsilon) \wedge Q \mid (b_j \leq 0 \wedge b_k \geq 0) \wedge \\ \wedge (\langle \boldsymbol{\omega}, \mathbf{a}_i \rangle \leq t \cdot \cos(\varphi) \quad \forall i \neq j, k) \wedge (t \geq 0)] \end{aligned} \quad (4.1)$$

$$\begin{aligned} + \mathbb{P} [(\| b_k \| \leq \epsilon) \wedge Q \mid (b_j \leq 0 \wedge b_k \geq 0) \wedge \\ \wedge (\langle \boldsymbol{\omega}, \mathbf{a}_i \rangle \leq t \cdot \cos(\varphi) \quad \forall i \neq j, k) \wedge (t \geq 0)] \end{aligned} \quad (4.2)$$

$$\begin{aligned} + \mathbb{P} [(\| b_j \| \leq \epsilon) \wedge Q \mid (b_j \geq 0 \wedge b_k \leq 0) \wedge \\ \wedge (\langle \boldsymbol{\omega}, \mathbf{a}_i \rangle \leq t \cdot \cos(\varphi) \quad \forall i \neq j, k) \wedge (t \geq 0)] \end{aligned} \quad (4.3)$$

$$\begin{aligned} + \mathbb{P} [(\| b_k \| \leq \epsilon) \wedge Q \mid (b_j \geq 0 \wedge b_k \leq 0) \wedge \\ \wedge (\langle \boldsymbol{\omega}, \mathbf{a}_i \rangle \leq t \cdot \cos(\varphi) \quad \forall i \neq j, k) \wedge (t \geq 0)] \end{aligned} \quad (4.4)$$

This is the first important point to be clarified in step 3. The second point consists of the guarantee, that for the conditions appearing in the two probabilities from above the listed estimations hold:

$$\mathbb{P} [(b_j \leq 0 \wedge b_k \geq 0) \wedge (\langle \boldsymbol{\omega}, \mathbf{a}_i \rangle \leq t \cdot \cos(\varphi) \quad \forall i \neq j, k) \wedge (t \geq 0)] > 0$$

and

$$\mathbb{P} [(b_j \geq 0 \wedge b_k \leq 0) \wedge (\langle \boldsymbol{\omega}, \mathbf{a}_i \rangle \leq t \cdot \cos(\varphi) \quad \forall i \neq j, k) \wedge (t \geq 0)] > 0.$$

Hence it is clear that the four conditional probabilities from (4.1) to (4.4) are defined well. For that purpose we obtain for the first probability (the second shall be treated likewise) the integral formula

$$\begin{aligned} \left(\frac{1}{\sqrt{2\pi}\sigma} \right)^4 \cdot \int_{-\frac{\pi}{2}}^{\frac{\pi}{2}} \int_0^{\infty} \int_0^{\infty} \int_{-\infty}^0 \left(\prod_{i \neq j, k} \int_{\mathbb{R}^2} \mathbf{1} [\langle \boldsymbol{\omega}, \mathbf{a}_i \rangle \leq t \cdot \cos(\varphi)] f_i(\mathbf{a}_i) d\mathbf{a}_i \right) \cdot \\ \cdot \cos(\varphi) \cdot |b_j - b_k| \cdot \prod_{i=j, k} e^{-\frac{(b_i - \bar{b}_i)^2}{2\sigma^2}} \cdot \prod_{i=j, k} e^{-\frac{(t \cdot \cos(\varphi) - \langle \boldsymbol{\omega}, \bar{\mathbf{a}}_i \rangle)^2}{2\sigma^2}} db_j db_k dt d\varphi \end{aligned}$$

We can show that it has a positive value by deriving an estimation from below. The result implies

$$\mathbb{P} [\mathbf{kante}_Y(\mathbf{v}) = \Delta] > 0,$$

which guarantees that the conditional probability in Lemma 4.3.4 is reasonably defined. This question had not been discussed so far.

Step 4:

In this step the probabilities from (4.1) to (4.4) will be evaluated separately. We study only the first, because the others can be treated essentially in the same way. For the

estimation we first derive an integral formula giving an upper bound. Since this is a conditional probability, we obtain a quotient:

$$\begin{aligned}
 & \mathbb{P} [(|b_j| \leq \epsilon) \wedge Q \mid (b_j \leq 0 \wedge b_k \geq 0) \wedge \\
 & \quad \wedge (\langle \boldsymbol{\omega}, \mathbf{a}_i \rangle \leq t \cdot \cos(\varphi) \quad \forall i \neq j, k) \wedge (t \geq 0)] \\
 & \leq \frac{\int_{-\frac{\pi}{2}}^{\frac{\pi}{2}} \int_0^2 \int_0^4 \int_{-\epsilon}^0 \left(\prod_{i \neq j, k} \int_{\mathbb{R}^2} \mathbf{1} [\langle \boldsymbol{\omega}, \mathbf{a}_i \rangle \leq t \cdot \cos(\varphi)] f_i(\mathbf{a}_i) d\mathbf{a}_i \right)}{\int_{-\frac{\pi}{2}}^{\frac{\pi}{2}} \int_0^2 \int_0^\infty \int_{-\infty}^0 \left(\prod_{i \neq j, k} \int_{\mathbb{R}^2} \mathbf{1} [\langle \boldsymbol{\omega}, \mathbf{a}_i \rangle \leq t \cdot \cos(\varphi)] f_i(\mathbf{a}_i) d\mathbf{a}_i \right)} \\
 & \quad \cdot \cos(\varphi) \cdot |b_j - b_k| \cdot \prod_{i=j,k} e^{-\frac{(b_i - \bar{b}_i)^2}{2\sigma^2}} \cdot \prod_{i=j,k} e^{-\frac{(t \cdot \cos(\varphi) - \langle \boldsymbol{\omega}, \bar{\mathbf{a}}_i \rangle)^2}{2\sigma^2}} db_j db_k dt d\varphi \\
 & \quad \cdot \cos(\varphi) \cdot |b_j - b_k| \cdot \prod_{i=j,k} e^{-\frac{(b_i - \bar{b}_i)^2}{2\sigma^2}} \cdot \prod_{i=j,k} e^{-\frac{(t \cdot \cos(\varphi) - \langle \boldsymbol{\omega}, \bar{\mathbf{a}}_i \rangle)^2}{2\sigma^2}} db_j db_k dt d\varphi. \tag{4.5}
 \end{aligned}$$

Now we can apply the result from step 2, that $|\bar{b}_j|, |\bar{b}_k| \leq 3$. This makes it possible to bound the quotient in (4.5) from above by the strongly simplified term

$$\sup_{|\bar{b}_j|, |\bar{b}_k| \leq 3} \frac{\int_0^4 \int_{-\epsilon}^0 |b_j - b_k| \cdot \prod_{i=j,k} e^{-\frac{(b_i - \bar{b}_i)^2}{2\sigma^2}} db_j db_k}{\int_0^\infty \int_{-\infty}^0 |b_j - b_k| \cdot \prod_{i=j,k} e^{-\frac{(b_i - \bar{b}_i)^2}{2\sigma^2}} db_j db_k}.$$

For further evaluations let the values of \bar{b}_j, \bar{b}_k with $|\bar{b}_j|, |\bar{b}_k| \leq 3$ be arbitrary. Then we can show the estimations

$$\begin{aligned} & \frac{\int_0^4 \int_{-\epsilon}^0 |b_j - b_k| \cdot \prod_{i=j,k} e^{-\frac{(b_i - \bar{b}_i)^2}{2\sigma^2}} db_j db_k}{\int_0^\infty \int_{-\infty}^0 |b_j - b_k| \cdot \prod_{i=j,k} e^{-\frac{(b_i - \bar{b}_i)^2}{2\sigma^2}} db_j db_k} \\ & \leq \underbrace{\sup_{-\epsilon \leq b_j \leq 0} e^{-\frac{(b_j - \bar{b}_j)^2}{2\sigma^2}}}_{(*)} \cdot \underbrace{\frac{\int_0^4 e^{-\frac{(b_k - \bar{b}_k)^2}{2\sigma^2}} \int_{-\epsilon}^0 |b_j - b_k| db_j db_k}{\int_0^4 e^{-\frac{(b_k - \bar{b}_k)^2}{2\sigma^2}} \int_{-t_0}^0 |b_j - b_k| db_j db_k}}_{(**)}. \end{aligned}$$

The value t_0 satisfies $t_0 \geq \epsilon$. A detailed study of $(*)$ delivers a constant upper bound e^5 and for $(**)$ similar thoughts lead to the estimation $\frac{\epsilon}{\sigma^2}$. In total we obtain as a result for the probability (4.1):

$$\begin{aligned} \mathbb{P} [(|b_j| \leq \epsilon) \wedge Q \mid (b_j \leq 0 \wedge b_k \geq 0) \wedge \\ \wedge (\langle \omega, a_i \rangle \leq t \cdot \cos(\varphi) \quad \forall i \neq j, k) \wedge (t \geq 0)] \leq e^5 \cdot \frac{\epsilon}{\sigma^2}. \end{aligned}$$

For the remaining three probabilities (4.2), (4.3) and (4.4) analogous methods deliver the same upper bounds.

Step 5:

This final step summarizes the different partial upper bounds. So we get as result:

$$\mathbb{P} [(\text{dist}(\mathbf{v}_Y, \partial \mathbf{Kante}_Y(\mathbf{v})) \leq \epsilon) \wedge R_2 \mid \mathbf{kante}_Y(\mathbf{v}) = \Delta] \leq 4e^5 \cdot \frac{\epsilon}{\sigma^2}.$$

This is just the proposition of Lemma 4.3.4.

Now we have announced the essential steps in the proof of Lemma 4.3.4. In the rest of this section we are going to explain the details.

Before starting with the elaborate proof of the Lemma, we state an auxiliary result about conditional probabilities.

Lemma 4.3.5.

Let A, B, C be events such that $\mathbb{P}[B], \mathbb{P}[C] > 0$. Then

$$\mathbb{P}[A \mid B \vee C] \leq \mathbb{P}[A \mid B] + \mathbb{P}[A \mid C].$$

Proof.

$$\begin{aligned}
 \mathbb{P}[A | B \vee C] &= \frac{\mathbb{P}[A \wedge (B \vee C)]}{\mathbb{P}[B \vee C]} \\
 &= \frac{\mathbb{P}[(A \wedge B) \vee (A \wedge C)]}{\mathbb{P}[B \vee C]} \\
 &\leq \frac{\mathbb{P}[A \wedge B]}{\mathbb{P}[B \vee C]} + \frac{\mathbb{P}[A \wedge C]}{\mathbb{P}[B \vee C]} \\
 &\leq \frac{\mathbb{P}[A \wedge B]}{\mathbb{P}[B]} + \frac{\mathbb{P}[A \wedge C]}{\mathbb{P}[C]} \\
 &= \mathbb{P}[A | B] + \mathbb{P}[A | C].
 \end{aligned}$$

This proves the proposition. \square

Now let us start with the proof of Lemma 4.3.4.

Proof of Lemma 4.3.4.

We want to make some remarks about the concept of the arguments following: Everything is listed in extremal detail. To keep the clarity anyway, we have subdivided the proof in several steps as apparent. Further some considerations are combined in Lemmata. They should not be seen as isolated statements, but only be interpreted under the present context.

Let an index set $\Delta = \{j, k\} \subset \{1, \dots, m\}$ be given. Our aim is the derivation of an upper bound for the probability

$$\mathbb{P}[(\mathbf{dist}(\mathbf{v}_Y, \partial \mathbf{Kante}_Y(\mathbf{v})) \leq \epsilon) \wedge R_2 | \mathbf{kante}_Y(\mathbf{v}) = \Delta]. \quad (4.6)$$

Step 1:

The essential points in this step are:

- First we apply the coordinate transformation from 4.2 on the vectors $\mathbf{a}_j, \mathbf{a}_k$. So we obtain a representation using the variables t, φ, b_j, b_k .
- After that we translate the event R_2 in the language of the new coordinates.
- Then we formulate $\mathbf{dist}(\mathbf{v}_Y, \partial \mathbf{Kante}_Y(\mathbf{v})) \leq \epsilon$ as well as the condition $\mathbf{kante}_Y(\mathbf{v}) = \Delta$ by means of the new variables.
- Based on these considerations we find a formulation of the probability in the new variables.

Let us apply the coordinate transformation on the vectors \mathbf{a}_j and \mathbf{a}_k . As known the position of straight line $\mathbf{AH}(\mathbf{a}_j, \mathbf{a}_k)$ is determined by the t and φ and b_j, b_k can be seen as the local coordinates of $\mathbf{a}_j, \mathbf{a}_k$ in the line. Have a second look at the representation

in figure 4.2. We are going to derive ranges for t, φ, b_j, b_k , implicated by the event R_2 . Here we rely on the proven fact that the event $\mathbf{kante}_Y(\mathbf{v}) = \Delta$ is valid.

The above mentioned condition justifies to concentrate on those configurations of \mathbf{a}_j and \mathbf{a}_k for which \mathbf{v} is directed towards the straight line $\mathbf{AH}(\mathbf{a}_j, \mathbf{a}_k)$. Hence we have $t \geq 0$. Moreover we are allowed to assume that $\mathbf{v} \in \mathbf{KK}(\mathbf{a}_j, \mathbf{a}_k) \Leftrightarrow \mathbf{KK}(\mathbf{v}) \cap \mathbf{KH}(\mathbf{a}_j, \mathbf{a}_k) \neq \emptyset$. This enables us to derive a further estimation for the variable t : Because of the event R_2 both $\|\mathbf{a}_j\| \leq 2$ and $\|\mathbf{a}_k\| \leq 2$ are satisfied. Hence it is clear, that also $\|\mathbf{KK}(\mathbf{v}) \cap \mathbf{KH}(\mathbf{a}_j, \mathbf{a}_k)\| \leq 2$. On the other hand t is always chosen in a way that $t \cdot \mathbf{v} = \mathbf{KK}(\mathbf{v}) \cap \mathbf{KH}(\mathbf{a}_j, \mathbf{a}_k)$ holds. Combined with $\|\mathbf{v}\| = 1$ we have the estimation

$$2 \geq \|t \cdot \mathbf{v}\| = t \cdot \|\mathbf{v}\| = t.$$

For the set $[-\frac{\pi}{2}, \frac{\pi}{2})$ of possible values for the variable φ we cannot make further restrictions. Anymore it is clear that $\|\mathbf{a}_i\| \leq 2 \forall i \neq j, k$ remains valid. Now we should think about the possible values of b_j and b_k . For that purpose we remember that we had derived a representation of \mathbf{a}_j resp. \mathbf{a}_k in terms of the new variables in the course of the introduction of the coordinate transformation in section 4.2. This gives for $i = j, k$:

$$\mathbf{a}_i = t \cdot \mathbf{v} + \mathbf{v}_\varphi \cdot b_i.$$

Rearranging leads to

$$\mathbf{v}_\varphi \cdot b_i = \mathbf{a}_i - t \cdot \mathbf{v}$$

and so

$$\begin{aligned} \|\mathbf{v}_\varphi \cdot b_i\| &= \|\mathbf{a}_i - t \cdot \mathbf{v}\| \\ &\leq \|\mathbf{a}_i\| + \|t \cdot \mathbf{v}\| \\ &\leq \|\mathbf{a}_i\| + t \cdot \|\mathbf{v}\| && (t \geq 0) \\ &\leq 2 + t && (\|\mathbf{a}_i\| \leq 2, \|\mathbf{v}\| = 1) \\ &\leq 4. && (0 \leq t \leq 2) \end{aligned}$$

Inclusion of $\|\mathbf{v}_\varphi\| = 1$ in our consideration finally delivers $|b_i| \leq 4$.

In total we see the “inclusion of sets”:

$$R_2 = \{(\mathbf{a}_1, \dots, \mathbf{a}_m) \in \mathbb{R}^{2 \times m} : \|\mathbf{a}_i\| \leq 2 \ \forall i = 1, \dots, m\} \subset Q,$$

where Q is the set of all configurations of φ, t, b_j, b_k and \mathbf{a}_i mit $i \neq j, k$ such that:

1. $\|\mathbf{a}_i\| \leq 2 \ \forall i \neq j, k$,
2. $|b_j|, |b_k| \leq 4$,
3. $-\frac{\pi}{2} \leq \varphi < \frac{\pi}{2}$ and

4. $t \leq 2$.

Our point 4 lacks the condition $t \geq 0$. This has the reason that this restriction resulted from the **kante** condition and not from focusing on R_2 . For that reason we do not want to rely on $t \geq 0$ in Q , but instead in the following reformulation of the **kante**-condition in the new variables. The inclusion mentioned above should be understood in the following way: For an arbitrary realization $(\mathbf{a}_1, \dots, \mathbf{a}_m) \in R_2$ we can find respective values for the variables φ, t, b_j and b_k , which belong to the set Q and which enable a representation in the form

$$\mathbf{a}_i = t \cdot \mathbf{v} + \mathbf{v}_\varphi \cdot b_i$$

for $i = j, k$. For all other points \mathbf{a}_l everything is clear.

At the end of step 1 we are going to formulate $\text{dist}(\mathbf{v}_Y, \partial \mathbf{Kante}_Y(\mathbf{v})) \leq \epsilon$ as well as the condition $\mathbf{kante}_Y(\mathbf{v}) = \Delta$ by means of the new variables. Here we observe: In the straight line $\mathbf{AH}(\mathbf{a}_j, \mathbf{a}_k)$ the new origin is \mathbf{v}_Y . Further we know

$$\mathbf{kante}_Y(\mathbf{v}) = \Delta \Leftrightarrow \begin{cases} \mathbf{v}_Y \in \mathbf{KH}(\mathbf{a}_j, \mathbf{a}_k), \mathbf{v}_Y \neq \mathbf{a}_j, \mathbf{a}_k \text{ and} \\ \mathbf{KH}(\mathbf{a}_j, \mathbf{a}_k) \text{ is an edge of } Y. \end{cases}$$

Combining both findings it becomes clear that we may replace

$$\mathbf{v}_Y \in \mathbf{KH}(\mathbf{a}_j, \mathbf{a}_k) \wedge \mathbf{v}_Y \neq \mathbf{a}_j, \mathbf{a}_k$$

in the original coordinates by

$$0 \in \mathbf{KH}(b_j, b_k) \wedge b_j, b_k \neq 0 \wedge t \geq 0$$

in the new variables. In addition we see that $\mathbf{KH}(\mathbf{a}_j, \mathbf{a}_k)$ becomes an edge of Y exactly if all other points \mathbf{a}_i are located on the same side of the straight line $\mathbf{AH}(\mathbf{a}_j, \mathbf{a}_k)$ as the origin. We can simply express that condition, if we remember that the angle between normal vector $\boldsymbol{\omega}$ of the straight line and \mathbf{v} has value

$$\text{arc}(\boldsymbol{\omega}, \mathbf{v}) = \varphi,$$

as we know that the point $t \cdot \mathbf{v}$ lies on the straight line. So we obtain:

$$\begin{aligned} \mathbf{KH}(\mathbf{a}_j, \mathbf{a}_k) \text{ is an edge of } Y \\ \Leftrightarrow \\ \langle \boldsymbol{\omega}, \mathbf{a}_i \rangle \leq \langle \boldsymbol{\omega}, t\mathbf{v} \rangle = t \cdot \langle \boldsymbol{\omega}, \mathbf{v} \rangle = t \cdot \cos(\varphi) \quad \text{for all } i \neq j, k. \end{aligned}$$

Remark 4.3.6.

At this point we see, that the event depends on the values φ, t , which determine the position of the straight line, and on the vectors \mathbf{a}_i with $i \neq j, k$. The local variables in the straight line b_j and b_k do not have any relevance. This fact will turn out to be helpful.

Moreover the coordinate transformation yields

$$\text{dist}(\mathbf{v}_Y, \partial Kante_Y(\mathbf{v})) = \text{dist}(0, \partial \mathbf{KH}(b_j, b_k)).$$

After the considerations made so far we obtain the following upper bound for our probability in new variables:

$$\begin{aligned} & \mathbb{P}[(\text{dist}(\mathbf{v}_Y, \partial Kante_Y(\mathbf{v})) \leq \epsilon) \wedge R_2 \mid kante_Y(\mathbf{v}) = \Delta] \\ & \stackrel{(*)}{\leq} \mathbb{P}[(\text{dist}(0, \partial \mathbf{KH}(b_j, b_k)) \leq \epsilon) \wedge Q \mid (0 \in \mathbf{KH}(b_j, b_k)) \wedge b_j, b_k \neq 0 \wedge \\ & \quad \wedge (\langle \boldsymbol{\omega}, \mathbf{a}_i \rangle \leq t \cdot \cos(\varphi) \quad \forall i \neq j, k) \wedge (t \geq 0)]. \end{aligned}$$

Inequality $(*)$ results from the fact $R_2 \subset Q$ discussed above. Now we have a first formulation for the probability in new variables. It is possible to do one more simplification by exploiting the following two equivalencies:

$$\text{dist}(0, \partial \mathbf{KH}(b_j, b_k)) \leq \epsilon \Leftrightarrow |b_j| \leq \epsilon \vee |b_k| \leq \epsilon$$

and

$$0 \in \mathbf{KH}(b_j, b_k) \wedge b_j, b_k \neq 0 \Leftrightarrow (b_j < 0 \wedge b_k > 0) \vee (b_j > 0 \wedge b_k < 0).$$

This makes an important reformulation possible

$$\begin{aligned} & \mathbb{P}[(\text{dist}(0, \partial \mathbf{KH}(b_j, b_k)) \leq \epsilon) \wedge Q \mid (0 \in \mathbf{KH}(b_j, b_k)) \wedge \\ & \quad \wedge (\langle \boldsymbol{\omega}, \mathbf{a}_i \rangle \leq t \cdot \cos(\varphi) \quad \forall i \neq j, k) \wedge (t \geq 0)] \\ & = \mathbb{P}[(|b_j| \leq \epsilon \vee |b_k| \leq \epsilon) \wedge Q \mid ((b_j < 0 \wedge b_k > 0) \vee (b_j > 0 \wedge b_k < 0)) \wedge \\ & \quad \wedge (\langle \boldsymbol{\omega}, \mathbf{a}_i \rangle \leq t \cdot \cos(\varphi) \quad \forall i \neq j, k) \wedge (t \geq 0)] \\ & \stackrel{(*)}{=} \mathbb{P}[(|b_j| \leq \epsilon \vee |b_k| \leq \epsilon) \wedge Q \mid ((b_j \leq 0 \wedge b_k \geq 0) \vee (b_j \geq 0 \wedge b_k \leq 0)) \wedge \\ & \quad \wedge (\langle \boldsymbol{\omega}, \mathbf{a}_i \rangle \leq t \cdot \cos(\varphi) \quad \forall i \neq j, k) \wedge (t \geq 0)]. \end{aligned}$$

The equality $(*)$ results from the null-set property of $b_j = b_k = 0$ under our stochastic model. So we have carried out a specific coordinate transformation and have formulated the probability in new variables. This was the goal of step 1.

Step 2:

In the first step we have tried to express the probability in question in terms of the new variables. In order to evaluate that expression we have to work with an integral-formula. We now concentrate on the question: How can the common density of \mathbf{a}_j and \mathbf{a}_k be expressed in the new variables? For that purpose it makes sense to remember the representations for \mathbf{a}_j and \mathbf{a}_k from section 4.2:

$$\begin{aligned} \mathbf{a}_j &= t \cdot \mathbf{v} + \mathbf{v}_\varphi \cdot b_j, \\ \mathbf{a}_k &= t \cdot \mathbf{v} + \mathbf{v}_\varphi \cdot b_k. \end{aligned} \tag{4.7}$$

To continue we shall determine the normal vector ω on the straight line $AH(\mathbf{a}_j, \mathbf{a}_k)$ based on these considerations: Both vectors ω and \mathbf{v} are of length 1 and the vector ω results from \mathbf{v} which is rotated by the angle φ anti-clockwise. With the help of the insights of section 4.2 we obtain for the respective rotation matrix:

$$\tilde{\mathbf{R}}_\varphi = \begin{pmatrix} \cos(\varphi) & -\sin(\varphi) \\ \sin(\varphi) & \cos(\varphi) \end{pmatrix}.$$

So we have:

$$\omega = \tilde{\mathbf{R}}_\varphi \cdot \mathbf{v} = \begin{pmatrix} \cos(\varphi) & -\sin(\varphi) \\ \sin(\varphi) & \cos(\varphi) \end{pmatrix} \begin{pmatrix} v^1 \\ v^2 \end{pmatrix} = \begin{pmatrix} v^1 \cos(\varphi) - v^2 \sin(\varphi) \\ v^1 \sin(\varphi) + v^2 \cos(\varphi) \end{pmatrix}.$$

On that fundamentum we aim for a formulation of the density functions f_j, f_k of \mathbf{a}_j and \mathbf{a}_k in terms of the variables φ, t, b_j, b_k . In addition we want to make some transformations and estimations which will turn out to be useful for the evaluation.

Let us have a look at the density of \mathbf{a}_j . It is:

$$f_j(\mathbf{a}_j) = \left(\frac{1}{\sqrt{2\pi}\sigma} \right)^2 \cdot e^{-\frac{\|\mathbf{a}_j - \bar{\mathbf{a}}_j\|^2}{2\sigma^2}}.$$

It is getting clear that it will be essential to know the formulation of $\|\mathbf{a}_j - \bar{\mathbf{a}}_j\|^2$ by use of the new variables. Here the illustration in figure 4.5 can be helpful.

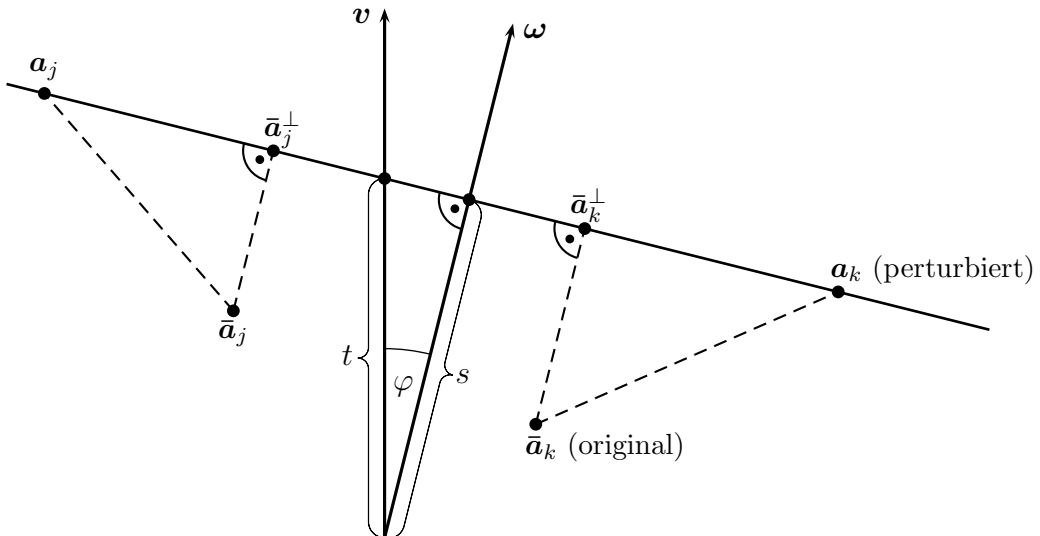


Figure 4.5: Useful illustration for the replacement of original by perturbed vectors

Looking on the drawing in figure 4.5 we see that $\bar{\mathbf{a}}_j$ is projected orthogonally on the straight line through \mathbf{a}_j and \mathbf{a}_k . This generates the point $\bar{\mathbf{a}}_j^\perp$. Since this is a point on the line, it can be represented in the form

$$\bar{\mathbf{a}}_j^\perp = t \cdot \mathbf{v} + \mathbf{v}_\varphi \cdot \bar{b}_j \quad (4.8)$$

for a \bar{b}_j as it is known for \mathbf{a}_j and \mathbf{a}_k . Our construction permits the application of the theorem of Pythagoras:

$$\|\mathbf{a}_j - \bar{\mathbf{a}}_j\|^2 = \|\mathbf{a}_j - \bar{\mathbf{a}}_j^\perp\|^2 + \|\bar{\mathbf{a}}_j^\perp - \bar{\mathbf{a}}_j\|^2. \quad (4.9)$$

Now we try to express the figures $\|\mathbf{a}_j - \bar{\mathbf{a}}_j^\perp\|$ and $\|\bar{\mathbf{a}}_j^\perp - \bar{\mathbf{a}}_j\|$ in terms of the new variables. For $\|\mathbf{a}_j - \bar{\mathbf{a}}_j^\perp\|$ this is easily possible, as a calculation shows. We use the representations for \mathbf{a}_j and for $\bar{\mathbf{a}}_j^\perp$ from (4.7) and from (4.8):

$$\begin{aligned} \|\mathbf{a}_j - \bar{\mathbf{a}}_j^\perp\| &= \|(\mathbf{t} \cdot \mathbf{v} + \mathbf{v}_\varphi \cdot b_j) - (\mathbf{t} \cdot \mathbf{v} + \mathbf{v}_\varphi \cdot \bar{b}_j)\| \\ &= \|\mathbf{v}_\varphi \cdot b_j - \mathbf{v}_\varphi \cdot \bar{b}_j\| \\ &= \|\mathbf{v}_\varphi \cdot (b_j - \bar{b}_j)\| \\ &= |b_j - \bar{b}_j| \cdot \|\mathbf{v}_\varphi\| \\ &= |b_j - \bar{b}_j|. \end{aligned}$$

The last equation relies on the obvious fact $\|\mathbf{v}_\varphi\| = 1$. Now we concentrate on the term $\|\bar{\mathbf{a}}_j^\perp - \bar{\mathbf{a}}_j\|$ in new variables. This is less simple. Looking at figure 4.5 we see that

$$\bar{\mathbf{a}}_j^\perp = \bar{\mathbf{a}}_j + u \cdot \boldsymbol{\omega}$$

for a certain factor u . A simple consideration leads us to :

$$u = \langle \boldsymbol{\omega}, \mathbf{a}_j \rangle - \langle \boldsymbol{\omega}, \bar{\mathbf{a}}_j \rangle = \langle \boldsymbol{\omega}, \mathbf{a}_j - \bar{\mathbf{a}}_j \rangle.$$

We can certify the validity of that result simply, because a calculation shows that the point $\bar{\mathbf{a}}_j + \langle \boldsymbol{\omega}, \mathbf{a}_j - \bar{\mathbf{a}}_j \rangle \cdot \boldsymbol{\omega}$ is located on the straight line $\mathbf{AH}(\mathbf{a}_j, \mathbf{a}_k)$:

$$\begin{aligned} \langle \boldsymbol{\omega}, \bar{\mathbf{a}}_j + \langle \boldsymbol{\omega}, \mathbf{a}_j - \bar{\mathbf{a}}_j \rangle \cdot \boldsymbol{\omega} \rangle &= \langle \boldsymbol{\omega}, \bar{\mathbf{a}}_j \rangle + \langle \boldsymbol{\omega}, \langle \boldsymbol{\omega}, \mathbf{a}_j - \bar{\mathbf{a}}_j \rangle \cdot \boldsymbol{\omega} \rangle \\ &= \langle \boldsymbol{\omega}, \bar{\mathbf{a}}_j \rangle + \langle \boldsymbol{\omega}, \mathbf{a}_j - \bar{\mathbf{a}}_j \rangle \cdot \underbrace{\langle \boldsymbol{\omega}, \boldsymbol{\omega} \rangle}_{=1} \\ &= \langle \boldsymbol{\omega}, \bar{\mathbf{a}}_j \rangle + \langle \boldsymbol{\omega}, \mathbf{a}_j \rangle - \langle \boldsymbol{\omega}, \bar{\mathbf{a}}_j \rangle \\ &= \langle \boldsymbol{\omega}, \mathbf{a}_j \rangle. \end{aligned}$$

This leads to a new representation for $\|\bar{\mathbf{a}}_j^\perp - \bar{\mathbf{a}}_j\|$:

$$\|\bar{\mathbf{a}}_j^\perp - \bar{\mathbf{a}}_j\| = \|\bar{\mathbf{a}}_j + \langle \boldsymbol{\omega}, \mathbf{a}_j - \bar{\mathbf{a}}_j \rangle \cdot \boldsymbol{\omega} - \bar{\mathbf{a}}_j\| = |\langle \boldsymbol{\omega}, \mathbf{a}_j - \bar{\mathbf{a}}_j \rangle| \cdot \|\boldsymbol{\omega}\| = |\langle \boldsymbol{\omega}, \mathbf{a}_j - \bar{\mathbf{a}}_j \rangle|.$$

Again we have taken into regard that $\|\boldsymbol{\omega}\| = 1$. In total we conclude:

$$\|\mathbf{a}_j - \bar{\mathbf{a}}_j\|^2 = (b_j - \bar{b}_j)^2 + \langle \boldsymbol{\omega}, \mathbf{a}_j - \bar{\mathbf{a}}_j \rangle^2. \quad (4.10)$$

In the above expression (4.10) the vector \mathbf{a}_j still occurs. This should be represented by use of the new variables, too. Therefore we use the well-known representation $\mathbf{a}_j = t \cdot \mathbf{v} + \mathbf{v}_\varphi \cdot b_j$ and we insert it into $\langle \boldsymbol{\omega}, \mathbf{a}_j - \bar{\mathbf{a}}_j \rangle$. So we obtain:

$$\begin{aligned}\langle \boldsymbol{\omega}, \mathbf{a}_j - \bar{\mathbf{a}}_j \rangle^2 &= \langle \boldsymbol{\omega}, t \cdot \mathbf{v} + \mathbf{v}_\varphi \cdot b_j - \bar{\mathbf{a}}_j \rangle^2 \\ &= (t \cdot \langle \boldsymbol{\omega}, \mathbf{v} \rangle + \langle \boldsymbol{\omega}, \mathbf{v}_\varphi \cdot b_j \rangle - \langle \boldsymbol{\omega}, \bar{\mathbf{a}}_j \rangle)^2 \\ &= (t \cdot \cos(\varphi) + b_j \cdot \langle \boldsymbol{\omega}, \mathbf{v}_\varphi \rangle - \langle \boldsymbol{\omega}, \bar{\mathbf{a}}_j \rangle)^2 \\ &= (t \cdot \cos(\varphi) - \langle \boldsymbol{\omega}, \bar{\mathbf{a}}_j \rangle)^2.\end{aligned}$$

Finally we have:

$$\|\mathbf{a}_j - \bar{\mathbf{a}}_j\|^2 = (b_j - \bar{b}_j)^2 + (t \cdot \cos(\varphi) - \langle \boldsymbol{\omega}, \bar{\mathbf{a}}_j \rangle)^2. \quad (4.11)$$

Remark 4.3.7.

The term $(t \cdot \cos(\varphi) - \langle \boldsymbol{\omega}, \bar{\mathbf{a}}_j \rangle)^2$ could be evaluated even more precisely. But having our further aims in mind for us only the following insight is relevant. Only the variables φ and t will appear and b_j resp. b_k will not appear.

If we make use of equation (4.11), then we get a formulation for the density function of \mathbf{a}_j in terms of new variables:

$$\begin{aligned}f_j(\mathbf{a}_j) &= f_j(t \cdot \mathbf{v} + \mathbf{v}_\varphi \cdot b_j) \\ &= \left(\frac{1}{\sqrt{2\pi}\sigma} \right)^2 \cdot e^{-\frac{(b_j - \bar{b}_j)^2 + (t \cdot \cos(\varphi) - \langle \boldsymbol{\omega}, \bar{\mathbf{a}}_j \rangle)^2}{2\sigma^2}} \\ &= \left(\frac{1}{\sqrt{2\pi}\sigma} \right)^2 \cdot e^{-\frac{(b_j - \bar{b}_j)^2}{2\sigma^2}} \cdot e^{-\frac{(t \cdot \cos(\varphi) - \langle \boldsymbol{\omega}, \bar{\mathbf{a}}_j \rangle)^2}{2\sigma^2}}.\end{aligned}$$

Analogously we get for \mathbf{a}_k :

$$\begin{aligned}f_k(\mathbf{a}_k) &= f_k(t \cdot \mathbf{v} + \mathbf{v}_\varphi \cdot b_k) \\ &= \left(\frac{1}{\sqrt{2\pi}\sigma} \right)^2 \cdot e^{-\frac{(b_k - \bar{b}_k)^2}{2\sigma^2}} \cdot e^{-\frac{(t \cdot \cos(\varphi) - \langle \boldsymbol{\omega}, \bar{\mathbf{a}}_k \rangle)^2}{2\sigma^2}}.\end{aligned}$$

Besides in section 4.2 we have calculated the functional determinant of the coordinate transformation. Taking its value $\cos(\varphi) \cdot |b_j - b_k|$ into regard, we can conclude that the common density of \mathbf{a}_j and \mathbf{a}_k expressed in new variables is:

$$g(\varphi, t, b_j, b_k) = \left(\frac{1}{\sqrt{2\pi}\sigma} \right)^4 \cdot \cos(\varphi) \cdot |b_j - b_k| \cdot \prod_{i \in \{j, k\}} e^{-\frac{(b_i - \bar{b}_i)^2}{2\sigma^2}} \cdot e^{-\frac{(t \cdot \cos(\varphi) - \langle \boldsymbol{\omega}, \bar{\mathbf{a}}_i \rangle)^2}{2\sigma^2}}.$$

Now we have achieved the main goal of step 2. Nevertheless we want to study the variables \bar{b}_j and \bar{b}_k even more precisely. Their specific values are in spite of the fixed

centers $\bar{\mathbf{a}}_j, \bar{\mathbf{a}}_k$ still variable, since the projections $\bar{\mathbf{a}}_j^\perp$ and $\bar{\mathbf{a}}_k^\perp$ depend on the values φ and t . One more look at figure 4.5 will confirm that insight. Motivated by that remark, we shall give estimations for both variables.⁴ They will prove useful in the evaluation of the probability.

Lemma 4.3.8.

For an arbitrary configuration of $0 \leq t \leq 2$ as well as $-\frac{\pi}{2} \leq \varphi < \frac{\pi}{2}$ it holds:

$$|\bar{b}_j|, |\bar{b}_k| \leq 3.$$

Proof. Let us look at representations for \mathbf{a}_j , $\bar{\mathbf{a}}_j^\perp$ and $\bar{\mathbf{a}}_j$ on the basis of the normal vector $\boldsymbol{\omega}$ to the line $\mathbf{AH}(\mathbf{a}_j, \mathbf{a}_k)$ for certain, but not explicitly specified values c_j, \bar{c}_j and r :

$$\begin{aligned}\mathbf{a}_j &= s \cdot \boldsymbol{\omega} + c_j \cdot \mathbf{v}_\varphi = (t \cdot \cos(\varphi)) \cdot \boldsymbol{\omega} + c_j \cdot \mathbf{v}_\varphi, \\ \bar{\mathbf{a}}_j^\perp &= s \cdot \boldsymbol{\omega} + \bar{c}_j \cdot \mathbf{v}_\varphi = (t \cdot \cos(\varphi)) \cdot \boldsymbol{\omega} + \bar{c}_j \cdot \mathbf{v}_\varphi, \\ \bar{\mathbf{a}}_j &= r \cdot \boldsymbol{\omega} + \bar{c}_j \cdot \mathbf{v}_\varphi.\end{aligned}$$

The factor \bar{c}_j appears both in $\bar{\mathbf{a}}_j$ and in $\bar{\mathbf{a}}_j^\perp$, since

$$\bar{\mathbf{a}}_j^\perp = \bar{\mathbf{a}}_j + (t \cdot \cos(\varphi) - \langle \boldsymbol{\omega}, \bar{\mathbf{a}}_j \rangle) \cdot \boldsymbol{\omega}$$

and besides $\boldsymbol{\omega} \perp \mathbf{v}_\varphi$ hold. Moreover we can with the help of $\boldsymbol{\omega} \perp \mathbf{v}_\varphi$ also conclude

$$\|\bar{\mathbf{a}}_j\|^2 = r^2 \cdot \|\boldsymbol{\omega}\|^2 + (\bar{c}_j)^2 \cdot \|\mathbf{v}_\varphi\|^2 = r^2 + (\bar{c}_j)^2.$$

Combined with the condition $\|\bar{\mathbf{a}}_j\| \leq 1$ we obtain:

$$(\bar{c}_j)^2 \leq 1 - r^2 \leq 1. \quad (4.12)$$

That perception can be exploited for gaining another estimation. Therefore we need the two alternative representations.

$$\begin{aligned}\bar{\mathbf{a}}_j^\perp &= t \cdot \cos(\varphi) \cdot \boldsymbol{\omega} + \bar{c}_j \cdot \mathbf{v}_\varphi, \\ \bar{\mathbf{a}}_j &= t \cdot \mathbf{v} + \bar{b}_j \cdot \mathbf{v}_\varphi.\end{aligned}$$

Herefrom we get the system of equations:

$$t \cdot \cos(\varphi) \cdot \boldsymbol{\omega} + \bar{c}_j \cdot \mathbf{v}_\varphi = t \cdot \mathbf{v} + \bar{b}_j \cdot \mathbf{v}_\varphi.$$

Take $\bar{b}_j \cdot \mathbf{v}_\varphi$ on one side:

$$\bar{b}_j \cdot \mathbf{v}_\varphi = t \cdot (\cos(\varphi) \cdot \boldsymbol{\omega} - \mathbf{v}) + \bar{c}_j \cdot \mathbf{v}_\varphi.$$

⁴ Spielman and Teng use and derive for the evaluation of the probability also such an estimation.

This leads to

$$\begin{aligned}
 |\bar{b}_j| &= |\bar{b}_j| \cdot \|\mathbf{v}_\varphi\| \\
 &= \|\bar{b}_j \cdot \mathbf{v}_\varphi\| \\
 &= \|t \cdot (\cos(\varphi) \cdot \boldsymbol{\omega} - \mathbf{v}) + \bar{c}_j \cdot \mathbf{v}_\varphi\| \\
 &\leq \|t \cdot (\cos(\varphi) \cdot \boldsymbol{\omega} - \mathbf{v})\| + \|\bar{c}_j \cdot \mathbf{v}_\varphi\| \\
 &= t \cdot \|\cos(\varphi) \cdot \boldsymbol{\omega} - \mathbf{v}\| + |\bar{c}_j| \cdot \|\mathbf{v}_\varphi\| \quad (\text{since } t \geq 0) \\
 &= t \cdot \|\cos(\varphi) \cdot \boldsymbol{\omega} - \mathbf{v}\| + |\bar{c}_j| \quad (\text{since } \|\mathbf{v}_\varphi\| = 1) \\
 &\leq t \cdot \|\cos(\varphi) \cdot \boldsymbol{\omega} - \mathbf{v}\| + 1 \quad [\text{compare estimation (4.12)}] \\
 &\leq t + 1 \quad (*) \\
 &\leq 3. \quad (\text{since } t \leq 2)
 \end{aligned}$$

Estimation $(*)$ is valid, since

$$\begin{aligned}
 \|\cos(\varphi) \cdot \boldsymbol{\omega} - \mathbf{v}\| &= \sqrt{\langle \cos(\varphi) \cdot \boldsymbol{\omega} - \mathbf{v}, \cos(\varphi) \cdot \boldsymbol{\omega} - \mathbf{v} \rangle} \\
 &= \sqrt{(\cos \varphi)^2 \langle \boldsymbol{\omega}, \boldsymbol{\omega} \rangle - 2 \cos(\varphi) \langle \boldsymbol{\omega}, \mathbf{v} \rangle + \langle \mathbf{v}, \mathbf{v} \rangle} \\
 &= \sqrt{(\cos \varphi)^2 - 2(\cos \varphi)^2 + 1} \\
 &= \sqrt{-(\cos \varphi)^2 + 1} \\
 &= |\sin(\varphi)| \\
 &\leq 1.
 \end{aligned}$$

Analogously this estimation can be deduced for \bar{b}_k . For an arbitrary configuration $-\frac{\pi}{2} \leq \varphi < \frac{\pi}{2}$ and $0 \leq t \leq 2$ also holds

$$|\bar{b}_j|, |\bar{b}_k| \leq 3.$$

This shows the validity of the Lemma □

Remark 4.3.9.

We want to remark once more that $\bar{\mathbf{a}}_j^\perp, \bar{\mathbf{a}}_k^\perp$ and in consequence \bar{b}_j, \bar{b}_k depend on the specific values of φ and t . For the purpose of the desired evaluation of the probability we are not interested in the specific values. In contrast we work for simplification with the estimation presented above.

The essential issue of this step was the formulation of the probability using the new variables. Besides we have obtained a useful estimation for the values \bar{b}_j and \bar{b}_k . Let us go to the next step.

Step 3:

The main goal of this step is to transform the probability-representation in new variables once more and to subdivide it into single summands. These single summands should permit an evaluation. In addition we will have a second look at the condition $\mathbf{kante}_Y(\mathbf{v}) = \Delta$ resp. its new formulation. We shall show that this condition is fulfilled with positive probability. This will be essential and necessary, because we want to condition on events of that kind.

The present available formulation for the probability resulting from step 1 is:

$$\mathbb{P}[(|b_j| \leq \epsilon \vee |b_k| \leq \epsilon) \wedge Q \mid ((b_j \leq 0 \wedge b_k \geq 0) \vee (b_j \geq 0 \wedge b_k \leq 0)) \wedge \wedge (\langle \boldsymbol{\omega}, \mathbf{a}_i \rangle \leq t \cdot \cos(\varphi) \quad \forall i \neq j, k) \wedge (t \geq 0)]. \quad (4.13)$$

The findings from step 2 allow us to give an evaluable integral expression for the probability mentioned above (4.13). But in order to make the notation and the estimations a bit easier, we are first going to make some reformulations. First consider the condition in the probability and write it down in the following way:

$$\begin{aligned} & ((b_j \leq 0 \wedge b_k \geq 0) \vee (b_j \geq 0 \wedge b_k \leq 0)) \wedge (\langle \boldsymbol{\omega}, \mathbf{a}_i \rangle \leq t \cdot \cos(\varphi) \quad \forall i \neq j, k) \wedge (t \geq 0) \\ &= [(b_j \leq 0 \wedge b_k \geq 0) \wedge (\langle \boldsymbol{\omega}, \mathbf{a}_i \rangle \leq t \cdot \cos(\varphi) \quad \forall i \neq j, k) \wedge (t \geq 0)] \\ &\quad \vee [(b_j \geq 0 \wedge b_k \leq 0) \wedge (\langle \boldsymbol{\omega}, \mathbf{a}_i \rangle \leq t \cdot \cos(\varphi) \quad \forall i \neq j, k) \wedge (t \geq 0)]. \end{aligned}$$

This enables us to apply Lemma 4.3.5 and to conclude for the probability in (4.13):

$$\begin{aligned} & \mathbb{P}\left[(|b_j| \leq \epsilon \vee |b_k| \leq \epsilon) \wedge Q \mid \left(\boxed{(b_j \leq 0 \wedge b_k \geq 0)} \vee \boxed{(b_j \geq 0 \wedge b_k \leq 0)} \right) \wedge \right. \\ & \quad \left. \wedge (\langle \boldsymbol{\omega}, \mathbf{a}_i \rangle \leq t \cdot \cos(\varphi) \quad \forall i \neq j, k) \wedge (t \geq 0) \right] \\ & \leq \mathbb{P}\left[(|b_j| \leq \epsilon \vee |b_k| \leq \epsilon) \wedge Q \mid \boxed{(b_j \leq 0 \wedge b_k \geq 0)} \wedge \right. \\ & \quad \left. \wedge (\langle \boldsymbol{\omega}, \mathbf{a}_i \rangle \leq t \cdot \cos(\varphi) \quad \forall i \neq j, k) \wedge (t \geq 0) \right] \\ & \quad + \mathbb{P}\left[(|b_j| \leq \epsilon \vee |b_k| \leq \epsilon) \wedge Q \mid \boxed{(b_j \geq 0 \wedge b_k \leq 0)} \wedge \right. \\ & \quad \left. \wedge (\langle \boldsymbol{\omega}, \mathbf{a}_i \rangle \leq t \cdot \cos(\varphi) \quad \forall i \neq j, k) \wedge (t \geq 0) \right]. \end{aligned}$$

Both probabilities can be bounded from above another time:

$$\begin{aligned} & \mathbb{P}[(|b_j| \leq \epsilon \vee |b_k| \leq \epsilon) \wedge Q \mid (b_j \leq 0 \wedge b_k \geq 0) \wedge \\ & \quad \wedge (\langle \boldsymbol{\omega}, \mathbf{a}_i \rangle \leq t \cdot \cos(\varphi) \quad \forall i \neq j, k) \wedge (t \geq 0)] \\ & \leq \mathbb{P}[(|b_j| \leq \epsilon) \wedge Q \mid (b_j \leq 0 \wedge b_k \geq 0) \wedge (\langle \boldsymbol{\omega}, \mathbf{a}_i \rangle \leq t \cdot \cos(\varphi) \quad \forall i \neq j, k) \wedge (t \geq 0)] \\ & \quad + \mathbb{P}[(|b_k| \leq \epsilon) \wedge Q \mid (b_j \leq 0 \wedge b_k \geq 0) \wedge (\langle \boldsymbol{\omega}, \mathbf{a}_i \rangle \leq t \cdot \cos(\varphi) \quad \forall i \neq j, k) \wedge (t \geq 0)] \end{aligned}$$

as well as

$$\begin{aligned} & \mathbb{P}[(|b_j| \leq \epsilon \vee |b_k| \leq \epsilon) \wedge Q \mid (b_j \geq 0 \wedge b_k \leq 0) \wedge \\ & \quad \wedge (\langle \boldsymbol{\omega}, \mathbf{a}_i \rangle \leq t \cdot \cos(\varphi) \quad \forall i \neq j, k) \wedge (t \geq 0)] \\ & \leq \mathbb{P}[(|b_j| \leq \epsilon) \wedge Q \mid (b_j \geq 0 \wedge b_k \leq 0) \wedge (\langle \boldsymbol{\omega}, \mathbf{a}_i \rangle \leq t \cdot \cos(\varphi) \quad \forall i \neq j, k) \wedge (t \geq 0)] \\ & \quad + \mathbb{P}[(|b_k| \leq \epsilon) \wedge Q \mid (b_j \geq 0 \wedge b_k \leq 0) \wedge (\langle \boldsymbol{\omega}, \mathbf{a}_i \rangle \leq t \cdot \cos(\varphi) \quad \forall i \neq j, k) \wedge (t \geq 0)]. \end{aligned}$$

In total we have the upper bound :

$$\begin{aligned} & \mathbb{P}[(|b_j| \leq \epsilon \vee |b_k| \leq \epsilon) \wedge Q \mid ((b_j \leq 0 \wedge b_k \geq 0) \vee (b_j \geq 0 \wedge b_k \leq 0)) \wedge \\ & \quad \wedge (\langle \boldsymbol{\omega}, \mathbf{a}_i \rangle \leq t \cdot \cos(\varphi) \quad \forall i \neq j, k) \wedge (t \geq 0)] \\ & \leq \mathbb{P}[(|b_j| \leq \epsilon) \wedge Q \mid (b_j \leq 0 \wedge b_k \geq 0) \wedge \\ & \quad \wedge (\langle \boldsymbol{\omega}, \mathbf{a}_i \rangle \leq t \cdot \cos(\varphi) \quad \forall i \neq j, k) \wedge (t \geq 0)] \end{aligned} \tag{4.14}$$

$$+ \mathbb{P}[(|b_k| \leq \epsilon) \wedge Q \mid (b_j \leq 0 \wedge b_k \geq 0) \wedge \\ \wedge (\langle \boldsymbol{\omega}, \mathbf{a}_i \rangle \leq t \cdot \cos(\varphi) \quad \forall i \neq j, k) \wedge (t \geq 0)] \tag{4.15}$$

$$+ \mathbb{P}[(|b_j| \leq \epsilon) \wedge Q \mid (b_j \geq 0 \wedge b_k \leq 0) \wedge \\ \wedge (\langle \boldsymbol{\omega}, \mathbf{a}_i \rangle \leq t \cdot \cos(\varphi) \quad \forall i \neq j, k) \wedge (t \geq 0)] \tag{4.16}$$

$$+ \mathbb{P}[(|b_k| \leq \epsilon) \wedge Q \mid (b_j \geq 0 \wedge b_k \leq 0) \wedge \\ \wedge (\langle \boldsymbol{\omega}, \mathbf{a}_i \rangle \leq t \cdot \cos(\varphi) \quad \forall i \neq j, k) \wedge (t \geq 0)]. \tag{4.17}$$

Each of the four probabilities in (4.14) up to (4.17) will be estimated in step 4. During the rest of the third step we want to think about a fact which has not got into the focus so far. As known, our essential aim is an estimation for the probability

$$\mathbb{P}[(\text{dist}(\mathbf{v}_Y, \partial \mathbf{Kante}_Y(\mathbf{v})) \leq \epsilon) \wedge R_2 \mid \mathbf{kante}_Y(\mathbf{v}) = \Delta].$$

Here we meet a condition on the event

$$\mathbf{kante}_Y(\mathbf{v}) = \Delta$$

with $\Delta = \{j, k\}$. The definition of that probability is according to this reasonable only if the event occurs with positive probability. We want to ensure that this is the case. Using the change of variables we have already obtained the reformulation for this event:

$$\begin{aligned} & \mathbf{kante}_Y(\mathbf{v}) = \Delta \\ & \Leftrightarrow \\ & [(b_j < 0 \wedge b_k > 0) \wedge (\langle \boldsymbol{\omega}, \mathbf{a}_i \rangle \leq t \cdot \cos(\varphi) \quad \forall i \neq j, k) \wedge (t \geq 0)] \vee \end{aligned} \tag{4.18}$$

$$\vee [(b_j > 0 \wedge b_k < 0) \wedge (\langle \boldsymbol{\omega}, \mathbf{a}_i \rangle \leq t \cdot \cos(\varphi) \quad \forall i \neq j, k) \wedge (t \geq 0)]. \tag{4.19}$$

The term in (4.18) appears just in the two first of the four probabilities and the term in (4.19) appears in the two last ones. The splitting in the partial conditions (4.18) and (4.19) is a consequence of the application of Lemma 4.3.5. To make the application of that Lemma possible, we have implicitly presumed that

$$\begin{aligned} & \mathbb{P}[(b_j < 0 \wedge b_k > 0) \wedge (\langle \boldsymbol{\omega}, \mathbf{a}_i \rangle \leq t \cdot \cos(\varphi) \quad \forall i \neq j, k) \wedge (t \geq 0)] \\ &= \mathbb{P}[(b_j \leq 0 \wedge b_k \geq 0) \wedge (\langle \boldsymbol{\omega}, \mathbf{a}_i \rangle \leq t \cdot \cos(\varphi) \quad \forall i \neq j, k) \wedge (t \geq 0)] > 0 \end{aligned}$$

and

$$\begin{aligned} & \mathbb{P}[(b_j > 0 \wedge b_k < 0) \wedge (\langle \boldsymbol{\omega}, \mathbf{a}_i \rangle \leq t \cdot \cos(\varphi) \quad \forall i \neq j, k) \wedge (t \geq 0)] \\ &= \mathbb{P}[(b_j \geq 0 \wedge b_k \leq 0) \wedge (\langle \boldsymbol{\omega}, \mathbf{a}_i \rangle \leq t \cdot \cos(\varphi) \quad \forall i \neq j, k) \wedge (t \geq 0)] > 0. \end{aligned}$$

Now we want to assure that this is actually the case. A direct consequence is then

$$\mathbb{P}[\mathbf{kante}_Y(\mathbf{v}) = \Delta] > 0,$$

So the probability has a meaningful definition. The following estimations are again summarized in an own Lemma.

Lemma 4.3.10.

So far we have

$$\mathbb{P}[(b_j \leq 0 \wedge b_k \geq 0) \wedge (\langle \boldsymbol{\omega}, \mathbf{a}_i \rangle \leq t \cdot \cos(\varphi) \quad \forall i \neq j, k) \wedge (t \geq 0)] > 0$$

and

$$\mathbb{P}[(b_j \geq 0 \wedge b_k \leq 0) \wedge (\langle \boldsymbol{\omega}, \mathbf{a}_i \rangle \leq t \cdot \cos(\varphi) \quad \forall i \neq j, k) \wedge (t \geq 0)] > 0.$$

Proof. For the proof we formulate the integral representations for the probabilities in question. Afterwards we demonstrate that their values are strictly positive.

The considerations made so far directly permit a representation and an estimation for

the first probability.

$$\begin{aligned}
 & \mathbb{P}[(b_j \leq 0 \wedge b_k \geq 0) \wedge (\langle \boldsymbol{\omega}, \mathbf{a}_i \rangle \leq t \cdot \cos(\varphi) \quad \forall i \neq j, k) \wedge (t \geq 0)] \\
 &= \left(\frac{1}{\sqrt{2\pi}\sigma} \right)^4 \cdot \int_{-\frac{\pi}{2}}^{\frac{\pi}{2}} \int_0^{\frac{\pi}{2}} \int_0^\infty \int_{-\infty}^0 \left(\prod_{i \neq j, k} \int_{\mathbb{R}^2} \mathbf{1}[\langle \boldsymbol{\omega}, \mathbf{a}_i \rangle \leq t \cdot \cos(\varphi)] f_i(\mathbf{a}_i) d\mathbf{a}_i \right) \cdot \\
 &\quad \cdot \cos(\varphi) \cdot |b_j - b_k| \cdot \prod_{i=j, k} e^{-\frac{(b_i - \bar{b}_i)^2}{2\sigma^2}} \cdot \prod_{i=j, k} e^{-\frac{(t \cdot \cos(\varphi) - \langle \boldsymbol{\omega}, \bar{\mathbf{a}}_i \rangle)^2}{2\sigma^2}} db_j db_k dt d\varphi \\
 &\stackrel{(*)}{\geq} \left(\frac{1}{\sqrt{2\pi}\sigma} \right)^4 \cdot \int_{-\frac{\pi}{2}}^{\frac{\pi}{2}} \int_0^2 \int_0^\infty \int_{-\infty}^0 \left(\prod_{i \neq j, k} \int_{\mathbb{R}^2} \mathbf{1}[\langle \boldsymbol{\omega}, \mathbf{a}_i \rangle \leq t \cdot \cos(\varphi)] f_i(\mathbf{a}_i) d\mathbf{a}_i \right) \cdot \\
 &\quad \cdot \cos(\varphi) \cdot |b_j - b_k| \cdot \prod_{i=j, k} e^{-\frac{(b_i - \bar{b}_i)^2}{2\sigma^2}} \cdot \prod_{i=j, k} e^{-\frac{(t \cdot \cos(\varphi) - \langle \boldsymbol{\omega}, \bar{\mathbf{a}}_i \rangle)^2}{2\sigma^2}} db_j db_k dt d\varphi \quad (4.20) \\
 &\geq \left(\frac{1}{\sqrt{2\pi}\sigma} \right)^4 \cdot \prod_{i \neq j, k} \left(\inf_{\substack{-\frac{\pi}{2} \leq \varphi < \frac{\pi}{2} \\ 0 \leq t \leq 2}} \int_{\mathbb{R}^2} \mathbf{1}[\langle \boldsymbol{\omega}, \mathbf{a}_i \rangle \leq t \cdot \cos(\varphi)] f_i(\mathbf{a}_i) d\mathbf{a}_i \right) \cdot \int_{-\frac{\pi}{2}}^{\frac{\pi}{2}} \int_0^2 \int_0^\infty \int_{-\infty}^0 \\
 &\quad \cos(\varphi) \cdot |b_j - b_k| \cdot \prod_{i=j, k} e^{-\frac{(b_i - \bar{b}_i)^2}{2\sigma^2}} \cdot \prod_{i=j, k} e^{-\frac{(t \cdot \cos(\varphi) - \langle \boldsymbol{\omega}, \bar{\mathbf{a}}_i \rangle)^2}{2\sigma^2}} db_j db_k dt d\varphi \\
 &\stackrel{(*)}{\geq} \left(\frac{1}{\sqrt{2\pi}\sigma} \right)^4 \cdot \prod_{i \neq j, k} \left(\inf_{\substack{-\frac{\pi}{2} \leq \varphi < \frac{\pi}{2} \\ 0 \leq t \leq 2}} \int_{\mathbb{R}^2} \mathbf{1}[\langle \boldsymbol{\omega}, \mathbf{a}_i \rangle \leq t \cdot \cos(\varphi)] f_i(\mathbf{a}_i) d\mathbf{a}_i \right) \cdot \int_{-\frac{\pi}{3}}^{\frac{\pi}{3}} \int_0^2 \int_1^3 \int_{-3}^{-1} \\
 &\quad \cos(\varphi) \cdot |b_j - b_k| \cdot \prod_{i=j, k} e^{-\frac{(b_i - \bar{b}_i)^2}{2\sigma^2}} \cdot \prod_{i=j, k} e^{-\frac{(t \cdot \cos(\varphi) - \langle \boldsymbol{\omega}, \bar{\mathbf{a}}_i \rangle)^2}{2\sigma^2}} db_j db_k dt d\varphi. \quad (4.21)
 \end{aligned}$$

The estimations labeled with $(*)$ base upon a diminishment of the integration range. This is possible, since for all feasible values of φ , t , b_j and b_k the integrand will stay to be nonnegative.

The following considerations help us to show that the main integral in (4.21) has a positive value. We start by showing that the integrand is positive everywhere in the integration range. For that purpose it is sufficient to clarify that each of the factors remains positive everywhere. For the first and the second factor it is easy to see that:

- The values $\varphi \in [-\frac{\pi}{3}, \frac{\pi}{3}]$ lead to $\cos(\varphi) > 0$.
- For $b_j \in [-3, -1]$ and $b_k \in [1, 3]$ one obtains $|b_j - b_k| > 0$.

Looking at the third factor we remember that $|\bar{b}_j| \leq 3$ and $|\bar{b}_k| \leq 3$. In combination with the feasible values for b_j and b_k this leads to $(b_j - \bar{b}_j)^2 \leq 36$ and $(b_k - \bar{b}_k)^2 \leq 36$. So we have:

$$\prod_{i=j,k} e^{-\frac{(b_i - \bar{b}_i)^2}{2\sigma^2}} \geq \left(e^{-\frac{36}{2\sigma^2}}\right)^2 > 0.$$

For the fourth factor we remember the following facts:

- $0 \leq t \leq 2$,
- $0 \leq \cos(\varphi) \leq 1$ für $\varphi \in [-\frac{\pi}{3}, \frac{\pi}{3}]$,
- $\|\boldsymbol{\omega}\| = 1$,
- $\|\bar{\mathbf{a}}_j\|, \|\bar{\mathbf{a}}_k\| \leq 1$.

Hence $(t \cdot \cos(\varphi) - \langle \boldsymbol{\omega}, \bar{\mathbf{a}}_i \rangle)^2 \leq (2+1)^2 = 9$ for $i = j, k$. This implies

$$\prod_{i=j,k} e^{-\frac{(t \cdot \cos(\varphi) - \langle \boldsymbol{\omega}, \bar{\mathbf{a}}_i \rangle)^2}{2\sigma^2}} \geq \left(e^{-\frac{9}{2\sigma^2}}\right)^2 > 0.$$

Combining all these partial results, we see that the figure

$$\cos(\varphi) \cdot |b_j - b_k| \cdot \prod_{i=j,k} e^{-\frac{(b_i - \bar{b}_i)^2}{2\sigma^2}} \cdot \prod_{i=j,k} e^{-\frac{(t \cdot \cos(\varphi) - \langle \boldsymbol{\omega}, \bar{\mathbf{a}}_i \rangle)^2}{2\sigma^2}}$$

from our integral is always positive. In a second step we realize that the set M of those (φ, t, b_j, b_k) , in our integration area, can be written as follows:

$$M = \left\{ (\varphi, t, b_j, b_k) : -\frac{\pi}{3} \leq \varphi \leq \frac{\pi}{3}, 0 \leq t \leq 2, -3 \leq b_j \leq -1, 1 \leq b_k \leq 3 \right\}.$$

This set M obviously has a positive Lebesgue-measure, hence the integral is positive in toto.

In a further step we look at an arbitrary factor of

$$\prod_{i \neq j,k} \left(\inf_{\substack{-\frac{\pi}{2} \leq \varphi < \frac{\pi}{2} \\ 0 \leq t \leq 2}} \int_{\mathbb{R}^2} \mathbb{1} [\langle \boldsymbol{\omega}, \mathbf{a}_i \rangle \leq t \cdot \cos(\varphi)] f_i(\mathbf{a}_i) d\mathbf{a}_i \right) \quad (4.22)$$

and we show that this is positive. Let φ, t and i from the expression above (4.22) be chosen arbitrarily but fixed. We study

$$\int_{\mathbb{R}^2} \mathbb{1} [\langle \boldsymbol{\omega}, \mathbf{a}_i \rangle \leq t \cdot \cos(\varphi)] f_i(\mathbf{a}_i) d\mathbf{a}_i = \mathbb{P} [\langle \boldsymbol{\omega}, \mathbf{a}_i \rangle \leq t \cdot \cos(\varphi)] \quad (4.23)$$

and keep in mind that $\mathbf{a}_i \sim \mathcal{N}_2(\bar{\mathbf{a}}_i, \sigma^2 \cdot \mathbf{E}_2)$ with $\|\bar{\mathbf{a}}_i\| \leq 1$. Since φ can now be seen as a fixed value, $\boldsymbol{\omega}$ turns out to be a fixed vector. Moreover $t \cdot \cos(\varphi)$ is a fixed value, for which $0 \leq t \cdot \cos(\varphi) \leq 2$ holds. Prior to estimating the probability (4.23), we make a small but helpful modification. First we form the matrix $\mathbf{B} := (\boldsymbol{\omega}, \boldsymbol{\eta})$, where the vector $\boldsymbol{\eta}$ is chosen in a way that it forms an orthonormal system together with $\boldsymbol{\omega}$ of \mathbb{R}^2 . In place of \mathbf{a}_i we shall study the transformed vector $\mathbf{b}_i := \mathbf{B}^{-1} \cdot \mathbf{a}_i$. From Lemma 2.2.2 we deduce, that $\mathbf{b}_i = (b_i^1, b_i^2)^T$ is normally distributed with expectation vector $\bar{\mathbf{b}}_i := \mathbf{B}^{-1} \cdot \bar{\mathbf{a}}_i$ and covariance matrix $\sigma^2 \cdot \mathbf{B}^{-1} \mathbf{E}_2 \mathbf{B}^{-T} = \sigma^2 \cdot \mathbf{E}_2$. In addition because of

$$\langle \boldsymbol{\omega}, \mathbf{a}_i \rangle = \langle \mathbf{B}^{-1} \boldsymbol{\omega}, \mathbf{B}^{-1} \mathbf{a}_i \rangle = \langle \mathbf{B}^T \boldsymbol{\omega}, \mathbf{b}_i \rangle = b_i^1$$

we have the equality

$$\mathbb{P}[\langle \boldsymbol{\omega}, \mathbf{a}_i \rangle \leq t \cdot \cos(\varphi)] = \mathbb{P}[b_i^1 \leq t \cdot \cos(\varphi)].$$

Our knowledge about the distribution of \mathbf{b}_i leads to the integral representation :

$$\mathbb{P}[b_i^1 \leq t \cdot \cos(\varphi)] = \int_{-\infty}^{t \cdot \cos(\varphi)} \frac{1}{\sqrt{2\pi}\sigma} \cdot e^{-\frac{(b_i^1 - \bar{b}_i^1)^2}{2\sigma^2}} db_i^1.$$

Moreover

$$\|\bar{\mathbf{b}}_i\| = \|\mathbf{B}^{-1} \bar{\mathbf{a}}_i\| = \|\bar{\mathbf{a}}_i\| \leq 1.$$

This delivers $\bar{b}_i^1 \leq 1$. In combination with $0 \leq t \cdot \cos(\varphi) \leq 2$ we obtain

$$\begin{aligned} \int_{-\infty}^{t \cdot \cos(\varphi)} \frac{1}{\sqrt{2\pi}\sigma} \cdot e^{-\frac{(b_i^1 - \bar{b}_i^1)^2}{2\sigma^2}} db_i^1 &\geq \int_{-\infty}^0 \frac{1}{\sqrt{2\pi}\sigma} \cdot e^{-\frac{(b_i^1 - 1)^2}{2\sigma^2}} db_i^1 \\ &\geq \int_{-1}^0 \frac{1}{\sqrt{2\pi}\sigma} \cdot e^{-\frac{(b_i^1 - 1)^2}{2\sigma^2}} db_i^1 > 0. \end{aligned}$$

Now we see that each factor of the product (4.22) is positive and so is the product, too. In total we recognize that for the probability under investigation

$$\mathbb{P}[(b_j \leq 0 \wedge b_k \geq 0) \wedge (\langle \boldsymbol{\omega}, \mathbf{a}_i \rangle \leq t \cdot \cos(\varphi) \quad \forall i \neq j, k) \wedge (t \geq 0)] > 0$$

holds. This proves the first part of the Lemma. For the second probability we obtain

as representation and estimation:

$$\begin{aligned}
 & \mathbb{P}[(b_j \geq 0 \wedge b_k \leq 0) \wedge (\langle \boldsymbol{\omega}, \mathbf{a}_i \rangle \leq t \cdot \cos(\varphi) \quad \forall i \neq j, k) \wedge (t \geq 0)] \\
 &= \left(\frac{1}{\sqrt{2\pi}\sigma} \right)^4 \cdot \int_{-\frac{\pi}{2}}^{\frac{\pi}{2}} \int_0^{\frac{\pi}{2}} \int_{-\infty}^0 \int_0^\infty \left(\prod_{i \neq j, k} \int_{\mathbb{R}^2} \mathbb{1}[\langle \boldsymbol{\omega}, \mathbf{a}_i \rangle \leq t \cdot \cos(\varphi)] f_i(\mathbf{a}_i) d\mathbf{a}_i \right) \cdot \\
 & \quad \cdot \cos(\varphi) \cdot |b_j - b_k| \cdot \prod_{i=j, k} e^{-\frac{(b_i - \bar{b}_i)^2}{2\sigma^2}} \cdot \prod_{i=j, k} e^{-\frac{(t \cdot \cos(\varphi) - \langle \boldsymbol{\omega}, \bar{\mathbf{a}}_i \rangle)^2}{2\sigma^2}} db_j db_k dt d\varphi \\
 &\geq \left(\frac{1}{\sqrt{2\pi}\sigma} \right)^4 \cdot \int_{-\frac{\pi}{2}}^{\frac{\pi}{2}} \int_0^{\frac{\pi}{2}} \int_{-\infty}^0 \int_0^\infty \left(\prod_{i \neq j, k} \int_{\mathbb{R}^2} \mathbb{1}[\langle \boldsymbol{\omega}, \mathbf{a}_i \rangle \leq t \cdot \cos(\varphi)] f_i(\mathbf{a}_i) d\mathbf{a}_i \right) \cdot \\
 & \quad \cdot \cos(\varphi) \cdot |b_j - b_k| \cdot \prod_{i=j, k} e^{-\frac{(b_i - \bar{b}_i)^2}{2\sigma^2}} \cdot \prod_{i=j, k} e^{-\frac{(t \cdot \cos(\varphi) - \langle \boldsymbol{\omega}, \bar{\mathbf{a}}_i \rangle)^2}{2\sigma^2}} db_j db_k dt d\varphi. \quad (4.24)
 \end{aligned}$$

From this one can analogously show that the probability is strictly positive. This proves the Lemma. \square

In this step we have transformed the fundamental probability once more and we have split it in separate summands. For these summands we shall give upper bounds. In addition we have investigated the condition $\mathbf{kante}_Y(\mathbf{v}) = \Delta$ in detail and by the way we have justified the applicability of Lemma 4.3.5. So we proceed to the next step

Step 4:

The goal of the fourth step is the estimation of the four probabilities (4.14) to (4.17). Let us start with the probability in (4.14). For its evaluation we prove the following Lemma.

Lemma 4.3.11.

On the basis of our arrangements we know:

$$\begin{aligned}
 & \mathbb{P}[(|b_j| \leq \epsilon) \wedge Q \mid (b_j \leq 0 \wedge b_k \geq 0) \wedge \\
 & \quad \wedge (\langle \boldsymbol{\omega}, \mathbf{a}_i \rangle \leq t \cdot \cos(\varphi) \quad \forall i \neq j, k) \wedge (t \geq 0)] \leq e^5 \cdot \frac{\epsilon}{\sigma^2}.
 \end{aligned}$$

Proof. Let us write the probability like that:

$$\begin{aligned}
 & \mathbb{P}[(|b_j| \leq \epsilon) \wedge Q \mid (b_j \leq 0 \wedge b_k \geq 0) \wedge (\langle \boldsymbol{\omega}, \mathbf{a}_i \rangle \leq t \cdot \cos(\varphi) \quad \forall i \neq j, k) \wedge (t \geq 0)] \\
 &= \frac{\mathbb{P}[(|b_j| \leq \epsilon) \wedge Q \wedge (b_j \leq 0 \wedge b_k \geq 0) \wedge}{\mathbb{P}[(b_j \leq 0 \wedge b_k \geq 0) \wedge} \\
 & \quad \wedge (\langle \boldsymbol{\omega}, \mathbf{a}_i \rangle \leq t \cdot \cos(\varphi) \quad \forall i \neq j, k) \wedge (t \geq 0)]}{\wedge (\langle \boldsymbol{\omega}, \mathbf{a}_i \rangle \leq t \cdot \cos(\varphi) \quad \forall i \neq j, k) \wedge (t \geq 0)]}. \quad (4.25)
 \end{aligned}$$

An integral representation for the denominator had been derived above. Still missing is such an integral representation for the numerator. For simplification we make some small modifications.

At the moment, the set Q in its original form is not perfect for our purpose. Therefore we drop the conditions for those \mathbf{a}_i with $i \neq j, k$ and we receive the set Q' with

$$Q' = \left\{ (\varphi, t, b_j, b_k, \mathbf{a}_{i \neq j, k}) : -\frac{\pi}{2} \leq \varphi \leq \frac{\pi}{2}, t \leq 2, |b_j| \leq 4, |b_k| \leq 4 \right\}.$$

Obviously $Q \subset Q'$. We obtain for the numerator in (4.25):

$$\begin{aligned} & \mathbb{P} [(|b_j| \leq \epsilon) \wedge Q \wedge (b_j \leq 0 \wedge b_k \geq 0) \wedge (\langle \boldsymbol{\omega}, \mathbf{a}_i \rangle \leq t \cdot \cos(\varphi) \quad \forall i \neq j, k) \wedge (t \geq 0)] \\ & \leq \mathbb{P} [(|b_j| \leq \epsilon) \wedge Q' \wedge (b_j \leq 0 \wedge b_k \geq 0) \wedge (\langle \boldsymbol{\omega}, \mathbf{a}_i \rangle \leq t \cdot \cos(\varphi) \quad \forall i \neq j, k) \wedge (t \geq 0)] \\ & = \mathbb{P} [(|b_j| \leq \epsilon) \wedge (0 \leq t \leq 2) \wedge (|b_j| \leq 4) \wedge (|b_k| \leq 4) \wedge (b_j \leq 0 \wedge b_k \geq 0) \wedge \\ & \quad \wedge (\langle \boldsymbol{\omega}, \mathbf{a}_i \rangle \leq t \cdot \cos(\varphi) \quad \forall i \neq j, k)] \\ & \stackrel{(*)}{=} \mathbb{P} [(|b_j| \leq \epsilon) \wedge (0 \leq t \leq 2) \wedge (|b_k| \leq 4) \wedge (b_j \leq 0 \wedge b_k \geq 0) \wedge \\ & \quad \wedge (\langle \boldsymbol{\omega}, \mathbf{a}_i \rangle \leq t \cdot \cos(\varphi) \quad \forall i \neq j, k)] \\ & = \mathbb{P} [(-\epsilon \leq b_j \leq 0) \wedge (0 \leq t \leq 2) \wedge (0 \leq b_k \leq 4) \wedge (\langle \boldsymbol{\omega}, \mathbf{a}_i \rangle \leq t \cdot \cos(\varphi) \quad \forall i \neq j, k)] \end{aligned}$$

In order to understand why the equality in $(*)$ holds, it pays to reconsider the statement of Lemma 4.3.4. Here we see that we may assume that $\epsilon \leq 4$, since for $\epsilon > 4$ the given upper bound is trivial. We give an integral expression for the last probability in the chain of estimations.

$$\begin{aligned} & \mathbb{P} [(-\epsilon \leq b_j \leq 0) \wedge (0 \leq t \leq 2) \wedge (0 \leq b_k \leq 4) \wedge (\langle \boldsymbol{\omega}, \mathbf{a}_i \rangle \leq t \cdot \cos(\varphi) \quad \forall i \neq j, k)] \\ & = \left(\frac{1}{\sqrt{2\pi}\sigma} \right)^4 \cdot \int_{-\frac{\pi}{2}}^{\frac{\pi}{2}} \int_0^2 \int_0^4 \int_{-\epsilon}^0 \left(\prod_{i \neq j, k} \int_{\mathbb{R}^2} \mathbb{1} [\langle \boldsymbol{\omega}, \mathbf{a}_i \rangle \leq t \cdot \cos(\varphi)] f_i(\mathbf{a}_i) d\mathbf{a}_i \right) \cdot \\ & \quad \cdot \cos(\varphi) \cdot |b_j - b_k| \cdot \prod_{i=j, k} e^{-\frac{(b_i - \bar{b}_i)^2}{2\sigma^2}} \cdot \prod_{i=j, k} e^{-\frac{(t \cdot \cos(\varphi) - \langle \boldsymbol{\omega}, \bar{\mathbf{a}}_i \rangle)^2}{2\sigma^2}} db_j db_k dt d\varphi. \quad (4.26) \end{aligned}$$

Now we can estimate the probability (4.25) by means of the integral representation

(4.26) for the numerator and of the above derived figure (4.20) for the denominator:

$$\begin{aligned}
 & \frac{\mathbb{P}[(|b_j| \leq \epsilon) \wedge Q \wedge (b_j \leq 0 \wedge b_k \geq 0) \wedge}{\mathbb{P}[(b_j \leq 0 \wedge b_k \geq 0) \wedge} \\
 & \quad \wedge (\langle \boldsymbol{\omega}, \mathbf{a}_i \rangle \leq t \cdot \cos(\varphi) \quad \forall i \neq j, k) \wedge (t \geq 0)] \\
 & \quad \wedge (\langle \boldsymbol{\omega}, \mathbf{a}_i \rangle \leq t \cdot \cos(\varphi) \quad \forall i \neq j, k) \wedge (t \geq 0)] \\
 \leq & \frac{\int_{-\frac{\pi}{2}}^{\frac{\pi}{2}} \int_0^2 \int_0^4 \int_{-\epsilon}^0 \left(\prod_{i \neq j, k} \int_{\mathbb{R}^2} \mathbb{1}[\langle \boldsymbol{\omega}, \mathbf{a}_i \rangle \leq t \cdot \cos(\varphi)] f_i(\mathbf{a}_i) d\mathbf{a}_i \right)}{\int_{-\frac{\pi}{2}}^{\frac{\pi}{2}} \int_0^2 \int_0^\infty \int_{-\infty}^0 \left(\prod_{i \neq j, k} \int_{\mathbb{R}^2} \mathbb{1}[\langle \boldsymbol{\omega}, \mathbf{a}_i \rangle \leq t \cdot \cos(\varphi)] f_i(\mathbf{a}_i) d\mathbf{a}_i \right)} \\
 & \cdot \cos(\varphi) \cdot |b_j - b_k| \cdot \prod_{i=j, k} e^{-\frac{(b_i - \bar{b}_i)^2}{2\sigma^2}} \cdot \prod_{i=j, k} e^{-\frac{(t \cdot \cos(\varphi) - \langle \boldsymbol{\omega}, \bar{\mathbf{a}}_i \rangle)^2}{2\sigma^2}} db_j db_k dt d\varphi \\
 & \cdot \cos(\varphi) \cdot |b_j - b_k| \cdot \prod_{i=j, k} e^{-\frac{(b_i - \bar{b}_i)^2}{2\sigma^2}} \cdot \prod_{i=j, k} e^{-\frac{(t \cdot \cos(\varphi) - \langle \boldsymbol{\omega}, \bar{\mathbf{a}}_i \rangle)^2}{2\sigma^2}} db_j db_k dt d\varphi \\
 = & \frac{\int_{-\frac{\pi}{2}}^{\frac{\pi}{2}} \int_0^2 \left(\prod_{i \neq j, k} \int_{\mathbb{R}^2} \mathbb{1}[\langle \boldsymbol{\omega}, \mathbf{a}_i \rangle \leq t \cdot \cos(\varphi)] f_i(\mathbf{a}_i) d\mathbf{a}_i \right) \cdot \cos(\varphi)}{\int_{-\frac{\pi}{2}}^{\frac{\pi}{2}} \int_0^2 \left(\prod_{i \neq j, k} \int_{\mathbb{R}^2} \mathbb{1}[\langle \boldsymbol{\omega}, \mathbf{a}_i \rangle \leq t \cdot \cos(\varphi)] f_i(\mathbf{a}_i) d\mathbf{a}_i \right) \cdot \cos(\varphi)} \\
 & \cdot \prod_{i=j, k} e^{-\frac{(t \cdot \cos(\varphi) - \langle \boldsymbol{\omega}, \bar{\mathbf{a}}_i \rangle)^2}{2\sigma^2}} \cdot \int_0^4 \int_{-\epsilon}^0 |b_j - b_k| \cdot \prod_{i=j, k} e^{-\frac{(b_i - \bar{b}_i)^2}{2\sigma^2}} db_j db_k dt d\varphi \\
 & \cdot \prod_{i=j, k} e^{-\frac{(t \cdot \cos(\varphi) - \langle \boldsymbol{\omega}, \bar{\mathbf{a}}_i \rangle)^2}{2\sigma^2}} \cdot \int_0^\infty \int_{-\infty}^0 |b_j - b_k| \cdot \prod_{i=j, k} e^{-\frac{(b_i - \bar{b}_i)^2}{2\sigma^2}} db_j db_k dt d\varphi. \tag{4.27}
 \end{aligned}$$

In the last step we have extracted all parts from the b_j - and b_k -integrals, which depend only on the values of φ and t . Now we are able to apply the rule of the so-called

*pointwise comparison*⁵. So we will obtain the following estimation for (4.27):

$$\sup_{\substack{-\frac{\pi}{2} \leq \varphi \leq \frac{\pi}{2} \\ 0 \leq t \leq 2}} \frac{\int_0^4 \int_{-\epsilon}^0 |b_j - b_k| \cdot \prod_{i=j,k} e^{-\frac{(b_i - \bar{b}_i)^2}{2\sigma^2}} db_j db_k}{\int_0^\infty \int_{-\infty}^0 |b_j - b_k| \cdot \prod_{i=j,k} e^{-\frac{(b_i - \bar{b}_i)^2}{2\sigma^2}} db_j db_k}.$$

Looking at the Supremum we want to recapitulate the impact of the values φ and t on the integrals because this seems to be somehow hidden. As mentioned above they affect the concrete value of the centers \bar{b}_j and \bar{b}_k . We remind that for that context we had already stated in Lemma 4.3.8, that for arbitrary $-\frac{\pi}{2} \leq \varphi \leq \frac{\pi}{2}$ and $0 \leq t \leq 2$ the bounds

$$|\bar{b}_j|, |\bar{b}_k| \leq 3$$

hold. So we are able to derive an upper bound .

$$\begin{aligned} & \sup_{\substack{-\frac{\pi}{2} \leq \varphi \leq \frac{\pi}{2} \\ 0 \leq t \leq 2}} \frac{\int_0^4 \int_{-\epsilon}^0 |b_j - b_k| \cdot \prod_{i=j,k} e^{-\frac{(b_i - \bar{b}_i)^2}{2\sigma^2}} db_j db_k}{\int_0^\infty \int_{-\infty}^0 |b_j - b_k| \cdot \prod_{i=j,k} e^{-\frac{(b_i - \bar{b}_i)^2}{2\sigma^2}} db_j db_k} \\ & \leq \sup_{|\bar{b}_j|, |\bar{b}_k| \leq 3} \frac{\int_0^4 \int_{-\epsilon}^0 |b_j - b_k| \cdot \prod_{i=j,k} e^{-\frac{(b_i - \bar{b}_i)^2}{2\sigma^2}} db_j db_k}{\int_0^\infty \int_{-\infty}^0 |b_j - b_k| \cdot \prod_{i=j,k} e^{-\frac{(b_i - \bar{b}_i)^2}{2\sigma^2}} db_j db_k}. \end{aligned} \quad (4.28)$$

Continuing we shall derive an upper bound for the expression (4.28). Let \bar{b}_j and \bar{b}_k such that $|\bar{b}_j|, |\bar{b}_k| \leq 3$ be arbitrary and consider:

$$\frac{\int_0^4 \int_{-\epsilon}^0 |b_j - b_k| \cdot \prod_{i=j,k} e^{-\frac{(b_i - \bar{b}_i)^2}{2\sigma^2}} db_j db_k}{\int_0^\infty \int_{-\infty}^0 |b_j - b_k| \cdot \prod_{i=j,k} e^{-\frac{(b_i - \bar{b}_i)^2}{2\sigma^2}} db_j db_k}$$

⁵A detailed description of that estimation rule can be found in [Bor87].

$$\begin{aligned}
 &= \frac{\int_0^4 \int_{-\epsilon}^0 |b_j - b_k| \cdot e^{-\frac{(b_j - \bar{b}_j)^2}{2\sigma^2}} \cdot e^{-\frac{(b_k - \bar{b}_k)^2}{2\sigma^2}} db_j db_k}{\int_0^\infty \int_0^0 |b_j - b_k| \cdot e^{-\frac{(b_j - \bar{b}_j)^2}{2\sigma^2}} \cdot e^{-\frac{(b_k - \bar{b}_k)^2}{2\sigma^2}} db_j db_k} \\
 &\leq \frac{\int_0^4 \int_{-\epsilon}^0 |b_j - b_k| \cdot e^{-\frac{(b_j - \bar{b}_j)^2}{2\sigma^2}} \cdot e^{-\frac{(b_k - \bar{b}_k)^2}{2\sigma^2}} db_j db_k}{\int_0^4 \int_{-\infty}^0 |b_j - b_k| \cdot e^{-\frac{(b_j - \bar{b}_j)^2}{2\sigma^2}} \cdot e^{-\frac{(b_k - \bar{b}_k)^2}{2\sigma^2}} db_j db_k} \\
 &= \frac{\int_0^4 e^{-\frac{(b_k - \bar{b}_k)^2}{2\sigma^2}} \int_{-\epsilon}^0 |b_j - b_k| \cdot e^{-\frac{(b_j - \bar{b}_j)^2}{2\sigma^2}} db_j db_k}{\int_0^4 e^{-\frac{(b_k - \bar{b}_k)^2}{2\sigma^2}} \int_{-\infty}^0 |b_j - b_k| \cdot e^{-\frac{(b_j - \bar{b}_j)^2}{2\sigma^2}} db_j db_k} \\
 &\leq \frac{\int_0^4 e^{-\frac{(b_k - \bar{b}_k)^2}{2\sigma^2}} \int_{-\epsilon}^0 |b_j - b_k| \cdot e^{-\frac{(b_j - \bar{b}_j)^2}{2\sigma^2}} db_j db_k}{\int_0^4 e^{-\frac{(b_k - \bar{b}_k)^2}{2\sigma^2}} \int_{-t_0}^0 |b_j - b_k| \cdot e^{-\frac{(b_j - \bar{b}_j)^2}{2\sigma^2}} db_j db_k}. \tag{4.29}
 \end{aligned}$$

For t_0 we make the convention $\epsilon \leq t_0 < \infty$. Now we give an upper bound for (4.29):

$$\frac{\sup_{-\epsilon \leq b_j \leq 0} e^{-\frac{(b_j - \bar{b}_j)^2}{2\sigma^2}} \cdot \int_0^4 e^{-\frac{(b_k - \bar{b}_k)^2}{2\sigma^2}} \int_{-\epsilon}^0 |b_j - b_k| db_j db_k}{\underbrace{\inf_{-t_0 \leq b_j \leq 0} e^{-\frac{(b_j - \bar{b}_j)^2}{2\sigma^2}}}_{(*)} \cdot \underbrace{\int_0^4 e^{-\frac{(b_k - \bar{b}_k)^2}{2\sigma^2}} \int_{-t_0}^0 |b_j - b_k| db_j db_k}_{(**)}}. \tag{4.30}$$

First of all we want to study $(*)$ from (4.30) in detail and to derive an upper bound . Since $t_0 \geq \epsilon$ we have in the first instance

$$\frac{\sup_{-\epsilon \leq b_j \leq 0} e^{-\frac{(b_j - \bar{b}_j)^2}{2\sigma^2}}}{\inf_{-t_0 \leq b_j \leq 0} e^{-\frac{(b_j - \bar{b}_j)^2}{2\sigma^2}}} \leq \frac{\sup_{-t_0 \leq c_j \leq 0} e^{-\frac{(c_j - \bar{b}_j)^2}{2\sigma^2}}}{\inf_{-t_0 \leq d_j \leq 0} e^{-\frac{(d_j - \bar{b}_j)^2}{2\sigma^2}}} \tag{4.31}$$

with “free” c_j and d_j . As is known $|\bar{b}_j| \leq 3$. From that fact combined with $-t_0 \leq c_j \leq 0$ and $-t_0 \leq d_j \leq 0$ it follows, that c_j from the numerator is at most $3 + t_0$ distant from \bar{b}_j . In addition it is clear that c_j and d_j from numerator resp. denominator differ at most by t_0 . Now we can apply Lemma 2.2.3 and we conclude that

$$\frac{\sup_{-t_0 \leq c_j \leq 0} e^{-\frac{(c_j - \bar{b}_j)^2}{2\sigma^2}}}{\inf_{-t_0 \leq d_j \leq 0} e^{-\frac{(d_j - \bar{b}_j)^2}{2\sigma^2}}} \leq e^{\frac{2(3+t_0)t_0 + t_0^2}{2\sigma^2}} = e^{\frac{6t_0}{2\sigma^2}} \cdot e^{\frac{3t_0^2}{2\sigma^2}}.$$

An explicit choice for t_0 is still possible. We should make it in a way that in the upper bound just derived, the parameter σ disappears in the denominator. One such suitable choice would be $t_0 := \sigma^2$. Hence:

$$\frac{\sup_{-t_0 \leq c_j \leq 0} e^{-\frac{(c_j - \bar{b}_j)^2}{2\sigma^2}}}{\inf_{-t_0 \leq d_j \leq 0} e^{-\frac{(d_j - \bar{b}_j)^2}{2\sigma^2}}} \leq e^{\frac{6t_0}{2\sigma^2}} \cdot e^{\frac{3t_0^2}{2\sigma^2}} = e^{\frac{6\sigma^2}{2\sigma^2}} \cdot e^{\frac{3\sigma^4}{2\sigma^2}} = e^{\frac{6}{2}} \cdot e^{\frac{3\sigma^2}{2}} \stackrel{(\diamond)}{\leq} e^{\frac{6}{2}} \cdot e^{\frac{3}{2}} \leq e^5, \quad (4.32)$$

where (\diamond) holds because of $\sigma^2 \leq 1$. Now we can deal with the evaluation of the quotient $(**)$ from the term (4.30). We should bear in mind that we have set $t_0 := \sigma^2$:

$$\begin{aligned} & \frac{\int_0^4 e^{-\frac{(b_k - \bar{b}_k)^2}{2\sigma^2}} \int_{-\epsilon}^0 |b_j - b_k| db_j db_k}{\int_0^4 e^{-\frac{(b_k - \bar{b}_k)^2}{2\sigma^2}} \int_{-t_0}^0 |b_j - b_k| db_j db_k} \\ &= \frac{\int_0^4 e^{-\frac{(b_k - \bar{b}_k)^2}{2\sigma^2}} \int_{-\epsilon}^0 (-b_j + b_k) db_j db_k}{\int_0^4 e^{-\frac{(b_k - \bar{b}_k)^2}{2\sigma^2}} \int_{-t_0}^0 (-b_j + b_k) db_j db_k} \end{aligned}$$

$$\begin{aligned}
 &= \frac{\int_0^4 e^{-\frac{(b_k - \bar{b}_k)^2}{2\sigma^2}} \cdot \left[-\frac{1}{2} \cdot b_j^2 + b_j \cdot b_k \right]_{-\epsilon}^0 db_k}{\int_0^4 e^{-\frac{(b_k - \bar{b}_k)^2}{2\sigma^2}} \cdot \left[-\frac{1}{2} \cdot b_j^2 + b_j \cdot b_k \right]_{-t_0}^0 db_k} \\
 &= \frac{\int_0^4 e^{-\frac{(b_k - \bar{b}_k)^2}{2\sigma^2}} \cdot \left(\frac{1}{2} \cdot \epsilon^2 + \epsilon \cdot b_k \right) db_k}{\int_0^4 e^{-\frac{(b_k - \bar{b}_k)^2}{2\sigma^2}} \cdot \left(\frac{1}{2} \cdot t_0^2 + t_0 \cdot b_k \right) db_k} \\
 &= \frac{\frac{1}{2} \cdot \epsilon^2 \cdot \int_0^4 e^{-\frac{(b_k - \bar{b}_k)^2}{2\sigma^2}} db_k + \epsilon \cdot \int_0^4 b_k \cdot e^{-\frac{(b_k - \bar{b}_k)^2}{2\sigma^2}} db_k}{\frac{1}{2} \cdot t_0^2 \cdot \int_0^4 e^{-\frac{(b_k - \bar{b}_k)^2}{2\sigma^2}} db_k + t_0 \cdot \int_0^4 b_k \cdot e^{-\frac{(b_k - \bar{b}_k)^2}{2\sigma^2}} db_k} \\
 &= \frac{\frac{\epsilon}{2} \cdot \int_0^4 e^{-\frac{(b_k - \bar{b}_k)^2}{2\sigma^2}} db_k + \int_0^4 b_k \cdot e^{-\frac{(b_k - \bar{b}_k)^2}{2\sigma^2}} db_k}{\frac{1}{2} \cdot t_0 \cdot \int_0^4 e^{-\frac{(b_k - \bar{b}_k)^2}{2\sigma^2}} db_k + \int_0^4 b_k \cdot e^{-\frac{(b_k - \bar{b}_k)^2}{2\sigma^2}} db_k} \\
 &\leq \frac{\frac{\epsilon}{t_0} \cdot \int_0^4 e^{-\frac{(b_k - \bar{b}_k)^2}{2\sigma^2}} db_k + \int_0^4 b_k \cdot e^{-\frac{(b_k - \bar{b}_k)^2}{2\sigma^2}} db_k}{\frac{1}{2} \cdot t_0 \cdot \int_0^4 e^{-\frac{(b_k - \bar{b}_k)^2}{2\sigma^2}} db_k + \int_0^4 b_k \cdot e^{-\frac{(b_k - \bar{b}_k)^2}{2\sigma^2}} db_k} \quad (\text{since } \epsilon \leq t_0) \\
 &= \frac{\epsilon}{t_0}.
 \end{aligned}$$

Here it is important that $t_0 = \sigma^2$. We achieve the upper bound

$$\frac{\int_0^4 e^{-\frac{(b_k - \bar{b}_k)^2}{2\sigma^2}} \int_{-\epsilon}^0 |b_j - b_k| db_j db_k}{\int_0^4 e^{-\frac{(b_k - \bar{b}_k)^2}{2\sigma^2}} \int_{-t_0}^0 |b_j - b_k| db_j db_k} \leq \frac{\epsilon}{\sigma^2}. \quad (4.33)$$

Combining the two upper bounds just calculated (4.32) and (4.33), leads to the estimation:

$$\begin{aligned} \mathbb{P} [(|b_j| \leq \epsilon) \wedge Q \mid (b_j \leq 0 \wedge b_k \geq 0) \wedge \\ \wedge (\langle \boldsymbol{\omega}, \mathbf{a}_i \rangle \leq t \cdot \cos(\varphi) \quad \forall i \neq j, k) \wedge (t \geq 0)] \leq e^5 \cdot \frac{\epsilon}{\sigma^2}. \end{aligned}$$

This finishes the proof. \square

For the probability (4.15) we prove an analogous Lemma.

Lemma 4.3.12.

On the basis of our conventions it holds:

$$\begin{aligned} \mathbb{P} [(|b_k| \leq \epsilon) \wedge Q \mid (b_j \leq 0 \wedge b_k \geq 0) \wedge \\ \wedge (\langle \boldsymbol{\omega}, \mathbf{a}_i \rangle \leq t \cdot \cos(\varphi) \quad \forall i \neq j, k) \wedge (t \geq 0)] \leq e^5 \cdot \frac{\epsilon}{\sigma^2}. \end{aligned}$$

Proof. For the derivation of that statement we follow essentially the strategy of the proof to Lemma 4.3.11. First we formulate the probability like that:

$$\begin{aligned} & \mathbb{P} [(|b_k| \leq \epsilon) \wedge Q \mid (b_j \leq 0 \wedge b_k \geq 0) \wedge (\langle \boldsymbol{\omega}, \mathbf{a}_i \rangle \leq t \cdot \cos(\varphi) \quad \forall i \neq j, k) \wedge (t \geq 0)] \\ = & \frac{\mathbb{P} [(|b_k| \leq \epsilon) \wedge Q \wedge (b_j \leq 0 \wedge b_k \geq 0) \wedge \\ & \quad \wedge (\langle \boldsymbol{\omega}, \mathbf{a}_i \rangle \leq t \cdot \cos(\varphi) \quad \forall i \neq j, k) \wedge (t \geq 0)]}{\mathbb{P} [(b_j \leq 0 \wedge b_k \geq 0) \wedge \\ & \quad \wedge (\langle \boldsymbol{\omega}, \mathbf{a}_i \rangle \leq t \cdot \cos(\varphi) \quad \forall i \neq j, k) \wedge (t \geq 0)]}. \end{aligned}$$

For the numerator we perform some transformations and estimations. Again we deal with the set

$$Q' = \left\{ (\varphi, t, b_j, b_k, \mathbf{a}_{i \neq j, k}) : -\frac{\pi}{2} \leq \varphi \leq \frac{\pi}{2}, t \leq 2, |b_j| \leq 4, |b_k| \leq 4 \right\}$$

with $Q \subset Q'$. Consider :

$$\begin{aligned} & \mathbb{P} [(|b_k| \leq \epsilon) \wedge Q \wedge (b_j \leq 0 \wedge b_k \geq 0) \wedge (\langle \boldsymbol{\omega}, \mathbf{a}_i \rangle \leq t \cdot \cos(\varphi) \quad \forall i \neq j, k) \wedge (t \geq 0)] \\ \leq & \mathbb{P} [(|b_k| \leq \epsilon) \wedge Q' \wedge (b_j \leq 0 \wedge b_k \geq 0) \wedge (\langle \boldsymbol{\omega}, \mathbf{a}_i \rangle \leq t \cdot \cos(\varphi) \quad \forall i \neq j, k) \wedge (t \geq 0)] \\ = & \mathbb{P} [(|b_k| \leq \epsilon) \wedge (0 \leq t \leq 2) \wedge (|b_j| \leq 4) \wedge (|b_k| \leq 4) \wedge (b_j \leq 0 \wedge b_k \geq 0) \wedge \\ & \quad \wedge (\langle \boldsymbol{\omega}, \mathbf{a}_i \rangle \leq t \cdot \cos(\varphi) \quad \forall i \neq j, k)] \\ \stackrel{(*)}{=} & \mathbb{P} [(|b_k| \leq \epsilon) \wedge (0 \leq t \leq 2) \wedge (|b_j| \leq 4) \wedge (b_j \leq 0 \wedge b_k \geq 0) \wedge \\ & \quad \wedge (\langle \boldsymbol{\omega}, \mathbf{a}_i \rangle \leq t \cdot \cos(\varphi) \quad \forall i \neq j, k)] \\ = & \mathbb{P} [(0 \leq b_k \leq \epsilon) \wedge (0 \leq t \leq 2) \wedge (-4 \leq b_j \leq 0) \wedge (\langle \boldsymbol{\omega}, \mathbf{a}_i \rangle \leq t \cdot \cos(\varphi) \quad \forall i \neq j, k)]. \end{aligned}$$

The equation holds because we could assume (without loss of generality) that $\epsilon \leq 4$ as in the proof to Lemma 4.3.11. An integral expression for the probability in question is deduced as follows:

$$\begin{aligned} & \mathbb{P}[(0 \leq b_k \leq \epsilon) \wedge (0 \leq t \leq 2) \wedge (-4 \leq b_j \leq 0) \wedge (\langle \boldsymbol{\omega}, \mathbf{a}_i \rangle \leq t \cdot \cos(\varphi) \quad \forall i \neq j, k)] \\ &= \left(\frac{1}{\sqrt{2\pi}\sigma} \right)^4 \cdot \int_{-\frac{\pi}{2}}^{\frac{\pi}{2}} \int_0^2 \int_{-4}^0 \int_0^\epsilon \left(\prod_{i \neq j, k} \int_{\mathbb{R}^2} \mathbb{1}[\langle \boldsymbol{\omega}, \mathbf{a}_i \rangle \leq t \cdot \cos(\varphi)] f_i(\mathbf{a}_i) d\mathbf{a}_i \right) \cdot \\ & \quad \cdot \cos(\varphi) \cdot |b_j - b_k| \cdot \prod_{i=j, k} e^{-\frac{(b_i - \bar{b}_i)^2}{2\sigma^2}} \cdot \prod_{i=j, k} e^{-\frac{(t \cdot \cos(\varphi) - \langle \boldsymbol{\omega}, \bar{\mathbf{a}}_i \rangle)^2}{2\sigma^2}} db_k db_j dt d\varphi. \end{aligned} \quad (4.34)$$

With regard to the denominator we exploit the (already obtained) estimation (4.20). In combination with the expression (4.34) we get:

$$\begin{aligned} & \frac{\mathbb{P}[(|b_k| \leq \epsilon) \wedge Q \wedge (b_j \leq 0 \wedge b_k \geq 0) \wedge]}{\mathbb{P}[(b_j \leq 0 \wedge b_k \geq 0) \wedge]} \\ & \quad \frac{\wedge (\langle \boldsymbol{\omega}, \mathbf{a}_i \rangle \leq t \cdot \cos(\varphi) \quad \forall i \neq j, k) \wedge (t \geq 0)]}{\wedge (\langle \boldsymbol{\omega}, \mathbf{a}_i \rangle \leq t \cdot \cos(\varphi) \quad \forall i \neq j, k) \wedge (t \geq 0)]} \\ & \leq \frac{\int_{-\frac{\pi}{2}}^{\frac{\pi}{2}} \int_0^2 \int_{-4}^0 \int_0^\epsilon \left(\prod_{i \neq j, k} \int_{\mathbb{R}^2} \mathbb{1}[\langle \boldsymbol{\omega}, \mathbf{a}_i \rangle \leq t \cdot \cos(\varphi)] f_i(\mathbf{a}_i) d\mathbf{a}_i \right)}{\int_{-\frac{\pi}{2}}^{\frac{\pi}{2}} \int_0^2 \int_{-\infty}^0 \int_0^\infty \left(\prod_{i \neq j, k} \int_{\mathbb{R}^2} \mathbb{1}[\langle \boldsymbol{\omega}, \mathbf{a}_i \rangle \leq t \cdot \cos(\varphi)] f_i(\mathbf{a}_i) d\mathbf{a}_i \right)} \\ & \quad \cdot \cos(\varphi) \cdot |b_j - b_k| \cdot \prod_{i=j, k} e^{-\frac{(b_i - \bar{b}_i)^2}{2\sigma^2}} \cdot \prod_{i=j, k} e^{-\frac{(t \cdot \cos(\varphi) - \langle \boldsymbol{\omega}, \bar{\mathbf{a}}_i \rangle)^2}{2\sigma^2}} db_k db_j dt d\varphi \\ & \quad \cdot \cos(\varphi) \cdot |b_j - b_k| \cdot \prod_{i=j, k} e^{-\frac{(b_i - \bar{b}_i)^2}{2\sigma^2}} \cdot \prod_{i=j, k} e^{-\frac{(t \cdot \cos(\varphi) - \langle \boldsymbol{\omega}, \bar{\mathbf{a}}_i \rangle)^2}{2\sigma^2}} db_k db_j dt d\varphi \\ &= \frac{\int_{-\frac{\pi}{2}}^{\frac{\pi}{2}} \int_0^2 \left(\prod_{i \neq j, k} \int_{\mathbb{R}^2} \mathbb{1}[\langle \boldsymbol{\omega}, \mathbf{a}_i \rangle \leq t \cdot \cos(\varphi)] f_i(\mathbf{a}_i) d\mathbf{a}_i \right) \cdot \cos(\varphi)}{\int_{-\frac{\pi}{2}}^{\frac{\pi}{2}} \int_0^2 \left(\prod_{i \neq j, k} \int_{\mathbb{R}^2} \mathbb{1}[\langle \boldsymbol{\omega}, \mathbf{a}_i \rangle \leq t \cdot \cos(\varphi)] f_i(\mathbf{a}_i) d\mathbf{a}_i \right) \cdot \cos(\varphi)} \end{aligned}$$

$$\begin{aligned} & \cdot \prod_{i=j,k} e^{-\frac{(t \cdot \cos(\varphi) - \langle \omega, \bar{a}_i \rangle)^2}{2\sigma^2}} \cdot \int_{-4}^0 \int_0^\epsilon |b_j - b_k| \cdot \prod_{i=j,k} e^{-\frac{(b_i - \bar{b}_i)^2}{2\sigma^2}} db_k db_j dt d\varphi \\ & \cdot \prod_{i=j,k} e^{-\frac{(t \cdot \cos(\varphi) - \langle \omega, \bar{a}_i \rangle)^2}{2\sigma^2}} \cdot \int_{-\infty}^0 \int_0^\infty |b_j - b_k| \cdot \prod_{i=j,k} e^{-\frac{(b_i - \bar{b}_i)^2}{2\sigma^2}} db_k db_j dt d\varphi \end{aligned} \quad (4.35)$$

During the last step we have again extracted the respective terms from the integrals as far as possible. Application of the *pointwise-comparison*-rule delivers for (4.35):

$$\begin{aligned} & \sup_{\substack{-\frac{\pi}{2} \leq \varphi \leq \frac{\pi}{2} \\ 0 \leq t \leq 2}} \frac{\int_{-4}^0 \int_0^\epsilon |b_j - b_k| \cdot \prod_{i=j,k} e^{-\frac{(b_i - \bar{b}_i)^2}{2\sigma^2}} db_k db_j}{\int_{-\infty}^0 \int_0^\infty |b_j - b_k| \cdot \prod_{i=j,k} e^{-\frac{(b_i - \bar{b}_i)^2}{2\sigma^2}} db_k db_j} \\ & \leq \sup_{|\bar{b}_j|, |\bar{b}_k| \leq 3} \frac{\int_{-4}^0 \int_0^\epsilon |b_j - b_k| \cdot \prod_{i=j,k} e^{-\frac{(b_i - \bar{b}_i)^2}{2\sigma^2}} db_k db_j}{\int_{-\infty}^0 \int_0^\infty |b_j - b_k| \cdot \prod_{i=j,k} e^{-\frac{(b_i - \bar{b}_i)^2}{2\sigma^2}} db_k db_j}. \end{aligned} \quad (4.36)$$

The upper bound (4.36) results from Lemma 4.3.8. This Lemma has the meaning that for the feasible values of φ and t the centers of the distributions \bar{b}_j and \bar{b}_k satisfy $|\bar{b}_j|, |\bar{b}_k| \leq 3$. The term in (4.36) will be evaluated further in the following. For that purpose we study

$$\begin{aligned} & \frac{\int_{-4}^0 \int_0^\epsilon |b_j - b_k| \cdot \prod_{i=j,k} e^{-\frac{(b_i - \bar{b}_i)^2}{2\sigma^2}} db_k db_j}{\int_{-\infty}^0 \int_0^\infty |b_j - b_k| \cdot \prod_{i=j,k} e^{-\frac{(b_i - \bar{b}_i)^2}{2\sigma^2}} db_k db_j} \\ & = \frac{\int_{-4}^0 \int_0^\epsilon |b_j - b_k| \cdot e^{-\frac{(b_j - \bar{b}_j)^2}{2\sigma^2}} \cdot e^{-\frac{(b_k - \bar{b}_k)^2}{2\sigma^2}} db_k db_j}{\int_{-\infty}^0 \int_0^\infty |b_j - b_k| \cdot e^{-\frac{(b_j - \bar{b}_j)^2}{2\sigma^2}} \cdot e^{-\frac{(b_k - \bar{b}_k)^2}{2\sigma^2}} db_k db_j} \end{aligned} \quad (4.37)$$

$$\begin{aligned}
 & \leq \frac{\int_{-4}^0 \int_0^\epsilon |b_j - b_k| \cdot e^{-\frac{(b_j - \bar{b}_j)^2}{2\sigma^2}} \cdot e^{-\frac{(b_k - \bar{b}_k)^2}{2\sigma^2}} db_k db_j}{\int_{-4}^0 \int_0^\infty |b_j - b_k| \cdot e^{-\frac{(b_j - \bar{b}_j)^2}{2\sigma^2}} \cdot e^{-\frac{(b_k - \bar{b}_k)^2}{2\sigma^2}} db_k db_j} \\
 & = \frac{\int_{-4}^0 e^{-\frac{(b_j - \bar{b}_j)^2}{2\sigma^2}} \int_0^\epsilon |b_j - b_k| \cdot e^{-\frac{(b_k - \bar{b}_k)^2}{2\sigma^2}} db_k db_j}{\int_{-4}^0 e^{-\frac{(b_j - \bar{b}_j)^2}{2\sigma^2}} \int_0^\infty |b_j - b_k| \cdot e^{-\frac{(b_k - \bar{b}_k)^2}{2\sigma^2}} db_k db_j} \\
 & \leq \frac{\int_{-4}^0 e^{-\frac{(b_j - \bar{b}_j)^2}{2\sigma^2}} \int_0^\epsilon |b_j - b_k| \cdot e^{-\frac{(b_k - \bar{b}_k)^2}{2\sigma^2}} db_k db_j}{\int_{-4}^0 e^{-\frac{(b_j - \bar{b}_j)^2}{2\sigma^2}} \int_0^{\sigma^2} |b_j - b_k| \cdot e^{-\frac{(b_k - \bar{b}_k)^2}{2\sigma^2}} db_k db_j} \\
 & \leq \underbrace{\sup_{0 \leq b_k \leq \epsilon} e^{-\frac{(b_k - \bar{b}_k)^2}{2\sigma^2}}}_{(*)} \cdot \underbrace{\frac{\int_{-4}^0 e^{-\frac{(b_j - \bar{b}_j)^2}{2\sigma^2}} \int_0^\epsilon |b_j - b_k| db_k db_j}{\int_{-4}^0 e^{-\frac{(b_j - \bar{b}_j)^2}{2\sigma^2}} \int_0^{\sigma^2} |b_j - b_k| db_k db_j}}_{(**)} \cdot \underbrace{\inf_{0 \leq b_k \leq \sigma^2} e^{-\frac{(b_k - \bar{b}_k)^2}{2\sigma^2}}}_{(***)}. \tag{4.38}
 \end{aligned}$$

Now we bound $(*)$ from the term (4.38). We remark that we may assume that $\sigma^2 \geq \epsilon$. Hence:

$$\frac{\sup_{0 \leq b_k \leq \epsilon} e^{-\frac{(b_k - \bar{b}_k)^2}{2\sigma^2}}}{\inf_{0 \leq b_k \leq \sigma^2} e^{-\frac{(b_k - \bar{b}_k)^2}{2\sigma^2}}} \leq \frac{\sup_{0 \leq c_k \leq \sigma^2} e^{-\frac{(c_k - \bar{b}_k)^2}{2\sigma^2}}}{\inf_{0 \leq d_k \leq \sigma^2} e^{-\frac{(d_k - \bar{b}_k)^2}{2\sigma^2}}}. \tag{4.39}$$

Since $|\bar{b}_k| \leq 3$, we know that c_k in the numerator differs at most by $3 + \sigma^2$ from \bar{b}_k . Moreover it is clear that c_k from the numerator and d_k from the denominator differ at most by σ^2 from each other. So we are able to apply Lemma 2.2.3 and we can derive

an upper bound:

$$\frac{\sup_{0 \leq c_k \leq \sigma^2} e^{-\frac{(c_k - \bar{b}_k)^2}{2\sigma^2}}}{\inf_{0 \leq d_k \leq \sigma^2} e^{-\frac{(d_k - \bar{b}_k)^2}{2\sigma^2}}} \leq e^{\frac{2(3+\sigma^2)\sigma^2 + \sigma^4}{2\sigma^2}} = e^{\frac{6\sigma^2}{2\sigma^2}} \cdot e^{\frac{3\sigma^4}{2\sigma^2}} \leq e^5. \quad (4.40)$$

After that we study (**) from (4.38) in detail:

$$\begin{aligned} & \frac{\int_{-4}^0 e^{-\frac{(b_j - \bar{b}_j)^2}{2\sigma^2}} \int_0^\epsilon |b_j - b_k| db_k db_j}{\int_{-4}^0 e^{-\frac{(b_j - \bar{b}_j)^2}{2\sigma^2}} \int_0^{\sigma^2} |b_j - b_k| db_k db_j} \\ &= \frac{\int_{-4}^0 e^{-\frac{(b_j - \bar{b}_j)^2}{2\sigma^2}} \int_0^\epsilon (-b_j + b_k) db_k db_j}{\int_{-4}^0 e^{-\frac{(b_j - \bar{b}_j)^2}{2\sigma^2}} \int_0^{\sigma^2} (-b_j + b_k) db_k db_j} \\ &= \frac{\int_{-4}^0 e^{-\frac{(b_j - \bar{b}_j)^2}{2\sigma^2}} \cdot \left[-b_j \cdot b_k + \frac{1}{2} \cdot b_k^2 \right]_0^\epsilon db_j}{\int_{-4}^0 e^{-\frac{(b_j - \bar{b}_j)^2}{2\sigma^2}} \cdot \left[-b_j \cdot b_k + \frac{1}{2} \cdot b_k^2 \right]_0^{\sigma^2} db_j} \\ &= \frac{\int_{-4}^0 e^{-\frac{(b_j - \bar{b}_j)^2}{2\sigma^2}} \cdot (-b_j \cdot \epsilon + \frac{1}{2} \cdot \epsilon^2) db_j}{\int_{-4}^0 e^{-\frac{(b_j - \bar{b}_j)^2}{2\sigma^2}} \cdot (-b_j \cdot \sigma^2 + \frac{1}{2} \cdot \sigma^4) db_j} \\ &= \frac{\frac{1}{2} \cdot \epsilon^2 \cdot \int_{-4}^0 e^{-\frac{(b_j - \bar{b}_j)^2}{2\sigma^2}} db_j - \epsilon \cdot \int_{-4}^0 b_j \cdot e^{-\frac{(b_j - \bar{b}_j)^2}{2\sigma^2}} db_j}{\frac{1}{2} \cdot \sigma^4 \cdot \int_{-4}^0 e^{-\frac{(b_j - \bar{b}_j)^2}{2\sigma^2}} db_j - \sigma^2 \cdot \int_{-4}^0 b_j \cdot e^{-\frac{(b_j - \bar{b}_j)^2}{2\sigma^2}} db_j} \end{aligned}$$

$$\begin{aligned}
 &= \frac{\epsilon}{\sigma^2} \cdot \frac{\frac{1}{2} \cdot \epsilon \cdot \int_{-4}^0 e^{-\frac{(b_j - \bar{b}_j)^2}{2\sigma^2}} db_j - \int_{-4}^0 b_j \cdot e^{-\frac{(b_j - \bar{b}_j)^2}{2\sigma^2}} db_j}{\frac{1}{2} \cdot \sigma^2 \cdot \int_{-4}^0 e^{-\frac{(b_j - \bar{b}_j)^2}{2\sigma^2}} db_j - \int_{-4}^0 b_j \cdot e^{-\frac{(b_j - \bar{b}_j)^2}{2\sigma^2}} db_j} \\
 &\leq \frac{\epsilon}{\sigma^2} \cdot \frac{\frac{1}{2} \cdot \sigma^2 \cdot \int_{-4}^0 e^{-\frac{(b_j - \bar{b}_j)^2}{2\sigma^2}} db_j - \int_{-4}^0 b_j \cdot e^{-\frac{(b_j - \bar{b}_j)^2}{2\sigma^2}} db_j}{\frac{1}{2} \cdot \sigma^2 \cdot \int_{-4}^0 e^{-\frac{(b_j - \bar{b}_j)^2}{2\sigma^2}} db_j - \int_{-4}^0 b_j \cdot e^{-\frac{(b_j - \bar{b}_j)^2}{2\sigma^2}} db_j} \quad (\text{da } \epsilon \leq \sigma^2) \\
 &= \frac{\epsilon}{\sigma^2}. \tag{4.41}
 \end{aligned}$$

Combining the two just obtained upper bounds (4.40) and (4.41) delivers the estimation:

$$\begin{aligned}
 &\mathbb{P} [(|b_k| \leq \epsilon) \wedge Q \mid (b_j \leq 0 \wedge b_k \geq 0) \wedge \\
 &\quad \wedge (\langle \boldsymbol{\omega}, \mathbf{a}_i \rangle \leq t \cdot \cos(\varphi) \quad \forall i \neq j, k) \wedge (t \geq 0)] \leq e^5 \cdot \frac{\epsilon}{\sigma^2}.
 \end{aligned}$$

This finishes the proof. \square

The next Lemma presents an upper bound for the probability (4.16).

Lemma 4.3.13.

Under our notation and configuration it holds:

$$\begin{aligned}
 &\mathbb{P} [(|b_j| \leq \epsilon) \wedge Q \mid (b_j \geq 0 \wedge b_k \leq 0) \wedge \\
 &\quad \wedge (\langle \boldsymbol{\omega}, \mathbf{a}_i \rangle \leq t \cdot \cos(\varphi) \quad \forall i \neq j, k) \wedge (t \geq 0)] \leq e^5 \cdot \frac{\epsilon}{\sigma^2}.
 \end{aligned}$$

Proof. We design the proof for this Lemma in a similar manner as we have done it for both previous Lemmata 4.3.11 and 4.3.12. Therefore we start with a well-known transformation and an estimation:

$$\begin{aligned}
 &\mathbb{P} [(|b_j| \leq \epsilon) \wedge Q \mid (b_j \geq 0 \wedge b_k \leq 0) \wedge (\langle \boldsymbol{\omega}, \mathbf{a}_i \rangle \leq t \cdot \cos(\varphi) \quad \forall i \neq j, k) \wedge (t \geq 0)] \\
 &= \frac{\mathbb{P} [(|b_j| \leq \epsilon) \wedge Q \wedge (b_j \geq 0 \wedge b_k \leq 0) \wedge (\langle \boldsymbol{\omega}, \mathbf{a}_i \rangle \leq t \cdot \cos(\varphi) \quad \forall i \neq j, k) \wedge (t \geq 0)]}{\mathbb{P} [(b_j \geq 0 \wedge b_k \leq 0) \wedge (\langle \boldsymbol{\omega}, \mathbf{a}_i \rangle \leq t \cdot \cos(\varphi) \quad \forall i \neq j, k) \wedge (t \geq 0)]} \\
 &\leq \frac{\mathbb{P} [(0 \leq b_j \leq \epsilon) \wedge (0 \leq t \leq 2) \wedge (-4 \leq b_k \leq 0) \wedge (\langle \boldsymbol{\omega}, \mathbf{a}_i \rangle \leq t \cdot \cos(\varphi) \quad \forall i \neq j, k)]}{\mathbb{P} [(b_j \geq 0 \wedge b_k \leq 0) \wedge (\langle \boldsymbol{\omega}, \mathbf{a}_i \rangle \leq t \cdot \cos(\varphi) \quad \forall i \neq j, k) \wedge (t \geq 0)]}.
 \end{aligned}$$

The following considerations are based on these three terms. We introduce an integral formula for the probability in the numerator. And for the probability in the denominator we take into regard the known representation for the probability in the denominator in (4.24). So we get to the estimation:

$$\begin{aligned}
 & \mathbb{P} [(|b_j| \leq \epsilon) \wedge Q \mid (b_j \geq 0 \wedge b_k \leq 0) \wedge (\langle \boldsymbol{\omega}, \mathbf{a}_i \rangle \leq t \cdot \cos(\varphi) \quad \forall i \neq j, k) \wedge (t \geq 0)] \\
 & \leq \frac{\int_{-\frac{\pi}{2}}^{\frac{\pi}{2}} \int_0^2 \int_{-4}^0 \int_0^\epsilon \left(\prod_{i \neq j, k} \int_{\mathbb{R}^2} \mathbb{1} [\langle \boldsymbol{\omega}, \mathbf{a}_i \rangle \leq t \cdot \cos(\varphi)] f_i(\mathbf{a}_i) d\mathbf{a}_i \right)}{\int_{-\frac{\pi}{2}}^{\frac{\pi}{2}} \int_0^2 \int_{-\infty}^0 \int_0^\infty \left(\prod_{i \neq j, k} \int_{\mathbb{R}^2} \mathbb{1} [\langle \boldsymbol{\omega}, \mathbf{a}_i \rangle \leq t \cdot \cos(\varphi)] f_i(\mathbf{a}_i) d\mathbf{a}_i \right)} \\
 & \quad \cdot \cos(\varphi) \cdot |b_j - b_k| \cdot \prod_{i=j, k} e^{-\frac{(b_i - \bar{b}_i)^2}{2\sigma^2}} \cdot \prod_{i=j, k} e^{-\frac{(t \cdot \cos(\varphi) - \langle \boldsymbol{\omega}, \bar{\mathbf{a}}_i \rangle)^2}{2\sigma^2}} db_j db_k dt d\varphi \\
 & \quad \cdot \cos(\varphi) \cdot |b_j - b_k| \cdot \prod_{i=j, k} e^{-\frac{(b_i - \bar{b}_i)^2}{2\sigma^2}} \cdot \prod_{i=j, k} e^{-\frac{(t \cdot \cos(\varphi) - \langle \boldsymbol{\omega}, \bar{\mathbf{a}}_i \rangle)^2}{2\sigma^2}} db_j db_k dt d\varphi \\
 & = \frac{\int_{-\frac{\pi}{2}}^{\frac{\pi}{2}} \int_0^2 \left(\prod_{i \neq j, k} \int_{\mathbb{R}^2} \mathbb{1} [\langle \boldsymbol{\omega}, \mathbf{a}_i \rangle \leq t \cdot \cos(\varphi)] f_i(\mathbf{a}_i) d\mathbf{a}_i \right) \cdot \cos(\varphi)}{\int_{-\frac{\pi}{2}}^{\frac{\pi}{2}} \int_0^2 \left(\prod_{i \neq j, k} \int_{\mathbb{R}^2} \mathbb{1} [\langle \boldsymbol{\omega}, \mathbf{a}_i \rangle \leq t \cdot \cos(\varphi)] f_i(\mathbf{a}_i) d\mathbf{a}_i \right) \cdot \cos(\varphi)} \\
 & \quad \cdot \prod_{i=j, k} e^{-\frac{(t \cdot \cos(\varphi) - \langle \boldsymbol{\omega}, \bar{\mathbf{a}}_i \rangle)^2}{2\sigma^2}} \int_{-4}^0 \int_0^\epsilon |b_j - b_k| \cdot \prod_{i=j, k} e^{-\frac{(b_i - \bar{b}_i)^2}{2\sigma^2}} db_j db_k dt d\varphi \\
 & \quad \cdot \prod_{i=j, k} e^{-\frac{(t \cdot \cos(\varphi) - \langle \boldsymbol{\omega}, \bar{\mathbf{a}}_i \rangle)^2}{2\sigma^2}} \int_{-\infty}^0 \int_0^\infty |b_j - b_k| \cdot \prod_{i=j, k} e^{-\frac{(b_i - \bar{b}_i)^2}{2\sigma^2}} db_j db_k dt d\varphi \tag{4.42}
 \end{aligned}$$

Again we make use of the rule of *pointwise comparison* and with the help of Lemma 4.3.8 we achieve the upper bound for the term in (4.42):

$$\begin{aligned}
 & \sup_{\substack{-\frac{\pi}{2} \leq \varphi \leq \frac{\pi}{2} \\ 0 \leq t \leq 2}} \frac{\int_{-4}^0 \int_0^\epsilon |b_j - b_k| \cdot \prod_{i=j, k} e^{-\frac{(b_i - \bar{b}_i)^2}{2\sigma^2}} db_j db_k}{\int_{-\infty}^0 \int_0^\infty |b_j - b_k| \cdot \prod_{i=j, k} e^{-\frac{(b_i - \bar{b}_i)^2}{2\sigma^2}} db_j db_k}
 \end{aligned}$$

$$\leq \sup_{|\bar{b}_j|, |\bar{b}_k| \leq 3} \frac{\int_{-4}^0 \int_0^\epsilon |b_j - b_k| \cdot \prod_{i=j,k} e^{-\frac{(b_i - \bar{b}_i)^2}{2\sigma^2}} db_j db_k}{\int_{-\infty}^0 \int_0^\infty |b_j - b_k| \cdot \prod_{i=j,k} e^{-\frac{(b_i - \bar{b}_i)^2}{2\sigma^2}} db_j db_k}. \quad (4.43)$$

The term (4.43) shall be evaluated more precisely. Let $|\bar{b}_j|, |\bar{b}_k| \leq 3$ be arbitrary. Now we consider

$$\begin{aligned} & \frac{\int_{-4}^0 \int_0^\epsilon |b_j - b_k| \cdot \prod_{i=j,k} e^{-\frac{(b_i - \bar{b}_i)^2}{2\sigma^2}} db_j db_k}{\int_{-\infty}^0 \int_0^\infty |b_j - b_k| \cdot \prod_{i=j,k} e^{-\frac{(b_i - \bar{b}_i)^2}{2\sigma^2}} db_j db_k} \\ &= \frac{\int_{-4}^0 \int_0^\epsilon |b_j - b_k| \cdot e^{-\frac{(b_j - \bar{b}_j)^2}{2\sigma^2}} \cdot e^{-\frac{(b_k - \bar{b}_k)^2}{2\sigma^2}} db_j db_k}{\int_{-\infty}^0 \int_0^\infty |b_j - b_k| \cdot e^{-\frac{(b_j - \bar{b}_j)^2}{2\sigma^2}} \cdot e^{-\frac{(b_k - \bar{b}_k)^2}{2\sigma^2}} db_j db_k} \\ &\leq \frac{\int_{-4}^0 \int_0^\epsilon |b_j - b_k| \cdot e^{-\frac{(b_j - \bar{b}_j)^2}{2\sigma^2}} \cdot e^{-\frac{(b_k - \bar{b}_k)^2}{2\sigma^2}} db_j db_k}{\int_{-4}^0 \int_0^\infty |b_j - b_k| \cdot e^{-\frac{(b_j - \bar{b}_j)^2}{2\sigma^2}} \cdot e^{-\frac{(b_k - \bar{b}_k)^2}{2\sigma^2}} db_j db_k} \\ &= \frac{\int_{-4}^0 e^{-\frac{(b_k - \bar{b}_k)^2}{2\sigma^2}} \int_0^\epsilon |b_j - b_k| \cdot e^{-\frac{(b_j - \bar{b}_j)^2}{2\sigma^2}} db_j db_k}{\int_{-4}^0 e^{-\frac{(b_k - \bar{b}_k)^2}{2\sigma^2}} \int_0^\infty |b_j - b_k| \cdot e^{-\frac{(b_j - \bar{b}_j)^2}{2\sigma^2}} db_j db_k} \\ &\leq \frac{\int_{-4}^0 e^{-\frac{(b_k - \bar{b}_k)^2}{2\sigma^2}} \int_0^\epsilon |b_j - b_k| \cdot e^{-\frac{(b_j - \bar{b}_j)^2}{2\sigma^2}} db_j db_k}{\int_{-4}^0 e^{-\frac{(b_k - \bar{b}_k)^2}{2\sigma^2}} \int_0^{\sigma^2} |b_j - b_k| \cdot e^{-\frac{(b_j - \bar{b}_j)^2}{2\sigma^2}} db_j db_k} \end{aligned}$$

$$\leq \underbrace{\frac{\sup_{0 \leq b_j \leq \epsilon} e^{-\frac{(b_j - \bar{b}_j)^2}{2\sigma^2}}}{\inf_{0 \leq b_j \leq \sigma^2} e^{-\frac{(b_j - \bar{b}_j)^2}{2\sigma^2}}}}_{(*)} \cdot \underbrace{\frac{\int_{-4}^0 e^{-\frac{(b_k - \bar{b}_k)^2}{2\sigma^2}} \int_0^\epsilon |b_j - b_k| db_j db_k}{\int_{-4}^0 e^{-\frac{(b_k - \bar{b}_k)^2}{2\sigma^2}} \int_0^{\sigma^2} |b_j - b_k| db_j db_k}}_{(**)}. \quad (4.44)$$

Estimating (*) in (4.44) delivers under use of Lemma 2.2.3 as before :

$$\frac{\sup_{0 \leq b_j \leq \epsilon} e^{-\frac{(b_j - \bar{b}_j)^2}{2\sigma^2}}}{\inf_{0 \leq b_j \leq \sigma^2} e^{-\frac{(b_j - \bar{b}_j)^2}{2\sigma^2}}} \leq e^5. \quad (4.45)$$

For that reason we go on to deal with (**) from (4.44):

$$\begin{aligned} & \frac{\int_{-4}^0 e^{-\frac{(b_k - \bar{b}_k)^2}{2\sigma^2}} \int_0^\epsilon |b_j - b_k| db_j db_k}{\int_{-4}^0 e^{-\frac{(b_k - \bar{b}_k)^2}{2\sigma^2}} \int_0^{\sigma^2} |b_j - b_k| db_j db_k} \\ &= \frac{\int_{-4}^0 e^{-\frac{(b_k - \bar{b}_k)^2}{2\sigma^2}} \int_0^\epsilon (b_j - b_k) db_j db_k}{\int_{-4}^0 e^{-\frac{(b_k - \bar{b}_k)^2}{2\sigma^2}} \int_0^{\sigma^2} (b_j - b_k) db_j db_k} \\ &= \frac{\int_{-4}^0 e^{-\frac{(b_k - \bar{b}_k)^2}{2\sigma^2}} \cdot \left[\frac{1}{2} \cdot b_j^2 - b_k \cdot b_j \right]_0^\epsilon db_k}{\int_{-4}^0 e^{-\frac{(b_k - \bar{b}_k)^2}{2\sigma^2}} \cdot \left[\frac{1}{2} \cdot b_j^2 - b_k \cdot b_j \right]_0^{\sigma^2} db_k} \\ &= \frac{\int_{-4}^0 e^{-\frac{(b_k - \bar{b}_k)^2}{2\sigma^2}} \cdot \left(\frac{1}{2} \cdot \epsilon^2 - b_k \cdot \epsilon \right) db_k}{\int_{-4}^0 e^{-\frac{(b_k - \bar{b}_k)^2}{2\sigma^2}} \cdot \left(\frac{1}{2} \cdot \sigma^4 - b_k \cdot \sigma^2 \right) db_k} \end{aligned}$$

$$\begin{aligned}
 &= \frac{\frac{1}{2} \cdot \epsilon^2 \cdot \int_{-4}^0 e^{-\frac{(b_k - \bar{b}_k)^2}{2\sigma^2}} db_k - \epsilon \cdot \int_{-4}^0 b_k \cdot e^{-\frac{(b_k - \bar{b}_k)^2}{2\sigma^2}} db_k}{\frac{1}{2} \cdot \sigma^4 \cdot \int_{-4}^0 e^{-\frac{(b_k - \bar{b}_k)^2}{2\sigma^2}} db_k - \sigma^2 \cdot \int_{-4}^0 b_k \cdot e^{-\frac{(b_k - \bar{b}_k)^2}{2\sigma^2}} db_k} \\
 &= \frac{\epsilon}{\sigma^2} \cdot \frac{\frac{1}{2} \cdot \epsilon \cdot \int_{-4}^0 e^{-\frac{(b_k - \bar{b}_k)^2}{2\sigma^2}} db_k - \int_{-4}^0 b_k \cdot e^{-\frac{(b_k - \bar{b}_k)^2}{2\sigma^2}} db_k}{\frac{1}{2} \cdot \sigma^2 \cdot \int_{-4}^0 e^{-\frac{(b_k - \bar{b}_k)^2}{2\sigma^2}} db_k - \int_{-4}^0 b_k \cdot e^{-\frac{(b_k - \bar{b}_k)^2}{2\sigma^2}} db_k} \\
 &\leq \frac{\epsilon}{\sigma^2} \cdot \frac{\frac{1}{2} \cdot \sigma^2 \cdot \int_{-4}^0 e^{-\frac{(b_k - \bar{b}_k)^2}{2\sigma^2}} db_k - \int_{-4}^0 b_k \cdot e^{-\frac{(b_k - \bar{b}_k)^2}{2\sigma^2}} db_k}{\frac{1}{2} \cdot \sigma^2 \cdot \int_{-4}^0 e^{-\frac{(b_k - \bar{b}_k)^2}{2\sigma^2}} db_k - \int_{-4}^0 b_k \cdot e^{-\frac{(b_k - \bar{b}_k)^2}{2\sigma^2}} db_k} \quad (\text{since } \epsilon \leq \sigma^2) \\
 &= \frac{\epsilon}{\sigma^2}. \tag{4.46}
 \end{aligned}$$

Both upper bounds (4.45) and (4.46) together lead to:

$$\begin{aligned}
 \mathbb{P} [(|b_j| \leq \epsilon) \wedge Q \mid (b_j \geq 0 \wedge b_k \leq 0) \wedge \\
 \wedge (\langle \boldsymbol{\omega}, \mathbf{a}_i \rangle \leq t \cdot \cos(\varphi) \quad \forall i \neq j, k) \wedge (t \geq 0)] \leq e^5 \cdot \frac{\epsilon}{\sigma^2}.
 \end{aligned}$$

This completes the proof. \square

Finally we formulate a Lemma for the probability (4.17).

Lemma 4.3.14.

On the basis of our arrangements it holds:

$$\begin{aligned}
 \mathbb{P} [(|b_k| \leq \epsilon) \wedge Q \mid (b_j \geq 0 \wedge b_k \leq 0) \wedge \\
 \wedge (\langle \boldsymbol{\omega}, \mathbf{a}_i \rangle \leq t \cdot \cos(\varphi) \quad \forall i \neq j, k) \wedge (t \geq 0)] \leq e^5 \cdot \frac{\epsilon}{\sigma^2}.
 \end{aligned}$$

Proof. The proof runs in a similar way as for the other Lemmas. At first we need the transformations:

$$\begin{aligned}
 &\mathbb{P} [(|b_k| \leq \epsilon) \wedge Q \mid (b_j \geq 0 \wedge b_k \leq 0) \wedge (\langle \boldsymbol{\omega}, \mathbf{a}_i \rangle \leq t \cdot \cos(\varphi) \quad \forall i \neq j, k) \wedge (t \geq 0)] \\
 &= \frac{\mathbb{P} [(|b_k| \leq \epsilon) \wedge Q \wedge (b_j \geq 0 \wedge b_k \leq 0) \wedge (\langle \boldsymbol{\omega}, \mathbf{a}_i \rangle \leq t \cdot \cos(\varphi) \quad \forall i \neq j, k) \wedge (t \geq 0)]}{\mathbb{P} [(b_j \geq 0 \wedge b_k \leq 0) \wedge (\langle \boldsymbol{\omega}, \mathbf{a}_i \rangle \leq t \cdot \cos(\varphi) \quad \forall i \neq j, k) \wedge (t \geq 0)]}
 \end{aligned}$$

$$\leq \frac{\mathbb{P} [(-\epsilon \leq b_k \leq 0) \wedge (0 \leq t \leq 2) \wedge (0 \leq b_j \leq 4) \wedge (\langle \boldsymbol{\omega}, \mathbf{a}_i \rangle \leq t \cdot \cos(\varphi) \quad \forall i \neq j, k)]}{\mathbb{P} [(b_j \geq 0 \wedge b_k \leq 0) \wedge (\langle \boldsymbol{\omega}, \mathbf{a}_i \rangle \leq t \cdot \cos(\varphi) \quad \forall i \neq j, k) \wedge (t \geq 0)]}.$$

For the numerator we derive an integral representation. For the denominator it pays to have a look at the term (4.24). So we obtain:

$$\begin{aligned} & \mathbb{P} [(|b_k| \leq \epsilon) \wedge Q \mid (b_j \geq 0 \wedge b_k \leq 0) \wedge (\langle \boldsymbol{\omega}, \mathbf{a}_i \rangle \leq t \cdot \cos(\varphi) \quad \forall i \neq j, k) \wedge (t \geq 0)] \\ & \leq \frac{\int_{-\frac{\pi}{2}}^{\frac{\pi}{2}} \int_0^2 \int_0^4 \int_{-\epsilon}^0 \left(\prod_{i \neq j, k} \int_{\mathbb{R}^2} \mathbb{1} [\langle \boldsymbol{\omega}, \mathbf{a}_i \rangle \leq t \cdot \cos(\varphi)] f_i(\mathbf{a}_i) d\mathbf{a}_i \right)}{\int_{-\frac{\pi}{2}}^{\frac{\pi}{2}} \int_0^2 \int_0^\infty \int_{-\infty}^0 \left(\prod_{i \neq j, k} \int_{\mathbb{R}^2} \mathbb{1} [\langle \boldsymbol{\omega}, \mathbf{a}_i \rangle \leq t \cdot \cos(\varphi)] f_i(\mathbf{a}_i) d\mathbf{a}_i \right)} \\ & \quad \cdot \cos(\varphi) \cdot |b_j - b_k| \cdot \prod_{i=j, k} e^{-\frac{(b_i - \bar{b}_i)^2}{2\sigma^2}} \cdot \prod_{i=j, k} e^{-\frac{(t \cdot \cos(\varphi) - \langle \boldsymbol{\omega}, \bar{\mathbf{a}}_i \rangle)^2}{2\sigma^2}} db_k db_j dt d\varphi \\ & \quad \cdot \cos(\varphi) \cdot |b_j - b_k| \cdot \prod_{i=j, k} e^{-\frac{(b_i - \bar{b}_i)^2}{2\sigma^2}} \cdot \prod_{i=j, k} e^{-\frac{(t \cdot \cos(\varphi) - \langle \boldsymbol{\omega}, \bar{\mathbf{a}}_i \rangle)^2}{2\sigma^2}} db_k db_j dt d\varphi \\ & = \frac{\int_{-\frac{\pi}{2}}^{\frac{\pi}{2}} \int_0^2 \left(\prod_{i \neq j, k} \int_{\mathbb{R}^2} \mathbb{1} [\langle \boldsymbol{\omega}, \mathbf{a}_i \rangle \leq t \cdot \cos(\varphi)] f_i(\mathbf{a}_i) d\mathbf{a}_i \right) \cdot \cos(\varphi)}{\int_{-\frac{\pi}{2}}^{\frac{\pi}{2}} \int_0^2 \left(\prod_{i \neq j, k} \int_{\mathbb{R}^2} \mathbb{1} [\langle \boldsymbol{\omega}, \mathbf{a}_i \rangle \leq t \cdot \cos(\varphi)] f_i(\mathbf{a}_i) d\mathbf{a}_i \right) \cdot \cos(\varphi)} \\ & \quad \cdot \prod_{i=j, k} e^{-\frac{(t \cdot \cos(\varphi) - \langle \boldsymbol{\omega}, \bar{\mathbf{a}}_i \rangle)^2}{2\sigma^2}} \int_0^4 \int_{-\epsilon}^0 |b_j - b_k| \cdot \prod_{i=j, k} e^{-\frac{(b_i - \bar{b}_i)^2}{2\sigma^2}} db_k db_j dt d\varphi \\ & \quad \cdot \prod_{i=j, k} e^{-\frac{(t \cdot \cos(\varphi) - \langle \boldsymbol{\omega}, \bar{\mathbf{a}}_i \rangle)^2}{2\sigma^2}} \int_0^\infty \int_{-\infty}^0 |b_j - b_k| \cdot \prod_{i=j, k} e^{-\frac{(b_i - \bar{b}_i)^2}{2\sigma^2}} db_k db_j dt d\varphi. \end{aligned} \tag{4.47}$$

Under use of the *pointwise-comparison*-rule and of Lemma 4.3.8 we arrive at the upper bound for the term (4.47):

$$\begin{aligned} & \sup_{\substack{-\frac{\pi}{2} \leq \varphi \leq \frac{\pi}{2} \\ 0 \leq t \leq 2}} \frac{\int_0^4 \int_{-\epsilon}^0 |b_j - b_k| \cdot \prod_{i=j, k} e^{-\frac{(b_i - \bar{b}_i)^2}{2\sigma^2}} db_k db_j}{\int_0^\infty \int_{-\infty}^0 |b_j - b_k| \cdot \prod_{i=j, k} e^{-\frac{(b_i - \bar{b}_i)^2}{2\sigma^2}} db_k db_j} \end{aligned}$$

$$\leq \frac{\int_0^4 \int_{-\epsilon}^0 |b_j - b_k| \cdot \prod_{i=j,k} e^{-\frac{(b_i - \bar{b}_i)^2}{2\sigma^2}} db_k db_j}{\int_0^\infty \int_0^0 |b_j - b_k| \cdot \prod_{i=j,k} e^{-\frac{(b_i - \bar{b}_i)^2}{2\sigma^2}} db_k db_j}. \quad (4.48)$$

Now we seek for an evaluation of (4.48). Let $|\bar{b}_j|, |\bar{b}_k| \leq 3$ be arbitrarily chosen and consider:

$$\begin{aligned} & \frac{\int_0^4 \int_{-\epsilon}^0 |b_j - b_k| \cdot \prod_{i=j,k} e^{-\frac{(b_i - \bar{b}_i)^2}{2\sigma^2}} db_k db_j}{\int_0^\infty \int_0^0 |b_j - b_k| \cdot \prod_{i=j,k} e^{-\frac{(b_i - \bar{b}_i)^2}{2\sigma^2}} db_k db_j} \\ &= \frac{\int_0^4 \int_{-\epsilon}^0 |b_j - b_k| \cdot e^{-\frac{(b_j - \bar{b}_j)^2}{2\sigma^2}} \cdot e^{-\frac{(b_k - \bar{b}_k)^2}{2\sigma^2}} db_k db_j}{\int_0^\infty \int_0^0 |b_j - b_k| \cdot e^{-\frac{(b_j - \bar{b}_j)^2}{2\sigma^2}} \cdot e^{-\frac{(b_k - \bar{b}_k)^2}{2\sigma^2}} db_k db_j} \\ &\leq \frac{\int_0^4 \int_{-\epsilon}^0 |b_j - b_k| \cdot e^{-\frac{(b_j - \bar{b}_j)^2}{2\sigma^2}} \cdot e^{-\frac{(b_k - \bar{b}_k)^2}{2\sigma^2}} db_k db_j}{\int_0^4 \int_{-\infty}^0 |b_j - b_k| \cdot e^{-\frac{(b_j - \bar{b}_j)^2}{2\sigma^2}} \cdot e^{-\frac{(b_k - \bar{b}_k)^2}{2\sigma^2}} db_k db_j} \\ &= \frac{\int_0^4 e^{-\frac{(b_j - \bar{b}_j)^2}{2\sigma^2}} \int_{-\epsilon}^0 |b_j - b_k| \cdot e^{-\frac{(b_k - \bar{b}_k)^2}{2\sigma^2}} db_k db_j}{\int_0^4 e^{-\frac{(b_j - \bar{b}_j)^2}{2\sigma^2}} \int_{-\infty}^0 |b_j - b_k| \cdot e^{-\frac{(b_k - \bar{b}_k)^2}{2\sigma^2}} db_k db_j} \\ &\leq \frac{\int_0^4 e^{-\frac{(b_j - \bar{b}_j)^2}{2\sigma^2}} \int_{-\epsilon}^0 |b_j - b_k| \cdot e^{-\frac{(b_k - \bar{b}_k)^2}{2\sigma^2}} db_k db_j}{\int_0^4 e^{-\frac{(b_j - \bar{b}_j)^2}{2\sigma^2}} \int_{-\sigma^2}^0 |b_j - b_k| \cdot e^{-\frac{(b_k - \bar{b}_k)^2}{2\sigma^2}} db_k db_j} \end{aligned}$$

$$\leq \underbrace{\frac{\sup_{-\epsilon \leq b_k \leq 0} e^{-\frac{(b_k - \bar{b}_k)^2}{2\sigma^2}}}{\inf_{-\sigma^2 \leq b_k \leq 0} e^{-\frac{(b_k - \bar{b}_k)^2}{2\sigma^2}}} \cdot \underbrace{\frac{\int_0^4 e^{-\frac{(b_j - \bar{b}_j)^2}{2\sigma^2}} \int_{-\epsilon}^0 |b_j - b_k| db_k db_j}{\int_0^4 e^{-\frac{(b_j - \bar{b}_j)^2}{2\sigma^2}} \int_{-\sigma^2}^0 |b_j - b_k| db_k db_j}}}_{(4.49)}$$

For (*) from (4.49) we apply Lemma 2.2.3 and this leads again to :

$$\frac{\sup_{-\epsilon \leq b_k \leq 0} e^{-\frac{(b_k - \bar{b}_k)^2}{2\sigma^2}}}{\inf_{-\sigma^2 \leq b_k \leq 0} e^{-\frac{(b_k - \bar{b}_k)^2}{2\sigma^2}}} \leq e^5. \quad (4.50)$$

For that reason we look at (**) from (4.49):

$$\begin{aligned} & \frac{\int_0^4 e^{-\frac{(b_j - \bar{b}_j)^2}{2\sigma^2}} \int_{-\epsilon}^0 |b_j - b_k| db_k db_j}{\int_0^4 e^{-\frac{(b_j - \bar{b}_j)^2}{2\sigma^2}} \int_{-\sigma^2}^0 |b_j - b_k| db_k db_j} \\ &= \frac{\int_0^4 e^{-\frac{(b_j - \bar{b}_j)^2}{2\sigma^2}} \int_{-\epsilon}^0 (-b_k + b_j) db_k db_j}{\int_0^4 e^{-\frac{(b_j - \bar{b}_j)^2}{2\sigma^2}} \int_{-\sigma^2}^0 (-b_k + b_j) db_k db_j} \\ &= \frac{\int_0^4 e^{-\frac{(b_j - \bar{b}_j)^2}{2\sigma^2}} \cdot \left[-\frac{1}{2} \cdot b_k^2 + b_j \cdot b_k \right]_{-\epsilon}^0 db_j}{\int_0^4 e^{-\frac{(b_j - \bar{b}_j)^2}{2\sigma^2}} \cdot \left[-\frac{1}{2} \cdot b_k^2 + b_j \cdot b_k \right]_{-\sigma^2}^0 db_j} \\ &= \frac{\int_0^4 e^{-\frac{(b_j - \bar{b}_j)^2}{2\sigma^2}} \cdot \left(\frac{1}{2} \cdot \epsilon^2 + b_j \cdot \epsilon \right) db_j}{\int_0^4 e^{-\frac{(b_j - \bar{b}_j)^2}{2\sigma^2}} \cdot \left(\frac{1}{2} \cdot \sigma^4 + b_j \cdot \sigma^2 \right) db_j} \end{aligned}$$

$$\begin{aligned}
 &= \frac{\frac{1}{2} \cdot \epsilon^2 \cdot \int_0^4 e^{-\frac{(b_j - \bar{b}_j)^2}{2\sigma^2}} db_j + \epsilon \cdot \int_0^4 b_j \cdot e^{-\frac{(b_j - \bar{b}_j)^2}{2\sigma^2}} db_j}{\frac{1}{2} \cdot \sigma^4 \cdot \int_0^4 e^{-\frac{(b_j - \bar{b}_j)^2}{2\sigma^2}} db_j + \sigma^2 \cdot \int_0^4 b_j \cdot e^{-\frac{(b_j - \bar{b}_j)^2}{2\sigma^2}} db_j} \\
 &= \frac{\frac{\epsilon}{\sigma^2} \cdot \frac{1}{2} \cdot \epsilon \cdot \int_0^4 e^{-\frac{(b_j - \bar{b}_j)^2}{2\sigma^2}} db_j + \int_0^4 b_j \cdot e^{-\frac{(b_j - \bar{b}_j)^2}{2\sigma^2}} db_j}{\frac{1}{2} \cdot \sigma^2 \cdot \int_0^4 e^{-\frac{(b_j - \bar{b}_j)^2}{2\sigma^2}} db_j + \int_0^4 b_j \cdot e^{-\frac{(b_j - \bar{b}_j)^2}{2\sigma^2}} db_j} \\
 &\leq \frac{\epsilon}{\sigma^2} \cdot \frac{\frac{1}{2} \cdot \sigma^2 \cdot \int_0^4 e^{-\frac{(b_j - \bar{b}_j)^2}{2\sigma^2}} db_j + \int_0^4 b_j \cdot e^{-\frac{(b_j - \bar{b}_j)^2}{2\sigma^2}} db_j}{\frac{1}{2} \cdot \sigma^2 \cdot \int_0^4 e^{-\frac{(b_j - \bar{b}_j)^2}{2\sigma^2}} db_j + \int_0^4 b_j \cdot e^{-\frac{(b_j - \bar{b}_j)^2}{2\sigma^2}} db_j} \\
 &= \frac{\epsilon}{\sigma^2}. \tag{4.51}
 \end{aligned}$$

Combination of both upper bounds (4.50) and (4.51) yields :

$$\begin{aligned}
 &\mathbb{P} [(|b_k| \leq \epsilon) \wedge Q \mid (b_j \geq 0 \wedge b_k \leq 0) \wedge \\
 &\quad \wedge (\langle \boldsymbol{\omega}, \mathbf{a}_i \rangle \leq t \cdot \cos(\varphi) \quad \forall i \neq j, k) \wedge (t \geq 0)] \leq e^5 \cdot \frac{\epsilon}{\sigma^2}.
 \end{aligned}$$

This finishes the proof. \square

At this point the aim of step 4 is achieved. Now let us go to step 5.

Step 5:

In this final step we want to derive the upper bound stated in Lemma 4.3.4. On basis of the findings described so far it is sufficient to combine the upper bounds from the Lemmas 4.3.11, 4.3.12, 4.3.13 and 4.3.14 . Then we arrive at:

$$\mathbb{P} [(\text{dist}(\mathbf{v}_Y, \partial \mathbf{Kante}_Y(\mathbf{v})) \leq \epsilon) \wedge R_2 \mid \mathbf{kante}_Y(\mathbf{v}) = \Delta] \leq 4e^5 \cdot \frac{\epsilon}{\sigma^2}.$$

This proves the proposition. \square

With the end of the proof of Lemma 4.3.4 we are at the end of this section. In the next section we deal with the so-called *Three-Viewpoints argument*. This will be applied to our problem and in combination with the result of this section it will yield an estimation of the number of vertices.

4.4 The Three-Viewpoints-Argument

In this section we introduce the so-called Three-Viewpoints-Argument. It was penned by Roman Vershynin. He used this argument for his Smoothed Analysis of the Simplex Method [Ver09] for the estimation of the expected number of shadow vertices in a perturbed polyhedron.

With regard to our own purpose the Three-Viewpoints-Argument is as useful as in [Ver09]. We are interested in the number of edges of the polygon $P = \mathbf{KH}(\mathbf{a}_1, \dots, \mathbf{a}_m)$. In order to count edges in reality it seems necessary to be able to see them. In the classical approach one uses a fixed observation point (e.g. the origin) and one studies the polygon looking from there. In that configuration it is possible that we look at some of the edges under an extremely small angle. Although such an edge may have a reasonable length, our impression may be that the edge is extremely short. In other words we are unable to guarantee a fixed relation between the actual length of the edge and its seeming length under the angle of observation. This disadvantage must be taken into regard in the estimations and it leads to a tremendous coarsening and deterioration of the results.

As Vershynin shows, this complication can be avoided by using three observation points instead of persisting in one. A skillful choice of the observation points ensures that for each edge we have at least one observation point that reflects the real length of the edge such that the impression differs from reality at most by a certain factor.

This insight will be discussed in detail in the following. It will turn out to be extremely important to get a sharper bound for the number of edges. The Three-Viewpoints-Argument essentially consists of two separate geometrical findings, which are stated in the two following Lemmata.

Lemma 4.4.1 (Three Viewpoints).

Let $P = \mathbf{KH}(\mathbf{b}_1, \dots, \mathbf{b}_N)$ be a polygon, where the points $\mathbf{b}_1, \dots, \mathbf{b}_N$ are in general position⁶. According to our condition of nondegeneracy 2.4.1 this is satisfied when we want to apply the argument and when the points have norm not larger than 2. Let $\mathbf{o}_1, \mathbf{o}_2, \mathbf{o}_3$ be the vertices of an equilateral triangle, whose center of gravity is in the origin. And in addition let $\|\mathbf{o}_1\| = \|\mathbf{o}_2\| = \|\mathbf{o}_3\| = 8$ hold. Then for each edge $\mathbf{KH}(\mathbf{b}_j, \mathbf{b}_k)$ of P there is an $i \in \{1, 2, 3\}$, such that $\mathbf{KH}(\mathbf{b}_j, \mathbf{b}_k)$ is an edge of $\mathbf{KH}(\mathbf{o}_i, P)$ and

$$\text{dist}(\mathbf{o}_i, \mathbf{AH}(\mathbf{b}_j, \mathbf{b}_k)) \geq 2$$

holds.

A graphical illustration is given in figure 4.6. This figure can in original and scaled form be found in [Ver09, Lemma 7.2]. The interpretation of that figure shows the way to prove the result.⁷

⁶That means: three points can never lie on one line

⁷This is adapted to [Ver09, Figure 7.2].

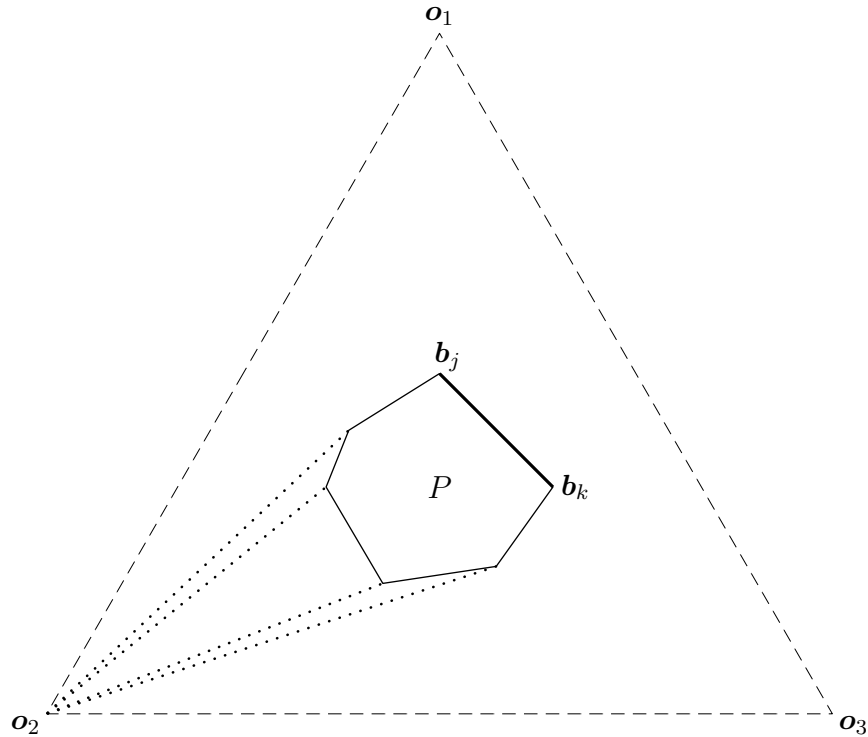


Figure 4.6: Graphical illustration of the Three-Viewpoints-Principle

Proof. Let us start with a general observation. Look at a straight line \mathcal{G} through the origin. Moreover we should have an equilateral triangle with center of gravity in the origin and with vertices $\mathbf{o}_1, \mathbf{o}_2, \mathbf{o}_3$ all in distance r to the origin. Then there are two vertices lying on opposite sides of the line and having a distance of at least $\frac{r}{2}$ to the line. This limit $\frac{r}{2}$ will even be attained if the line is parallel to one of the edges of the triangle. A graphical illustration of that case can be found in figure 4.7.

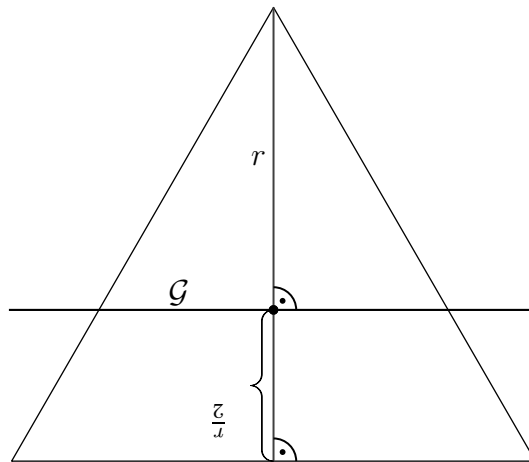


Figure 4.7: Distance of the vertices in the triangle to the straight line \mathcal{G}

With respect to our polygon P let \mathcal{G} be just that line through the origin which runs

parallel to the edge $\mathbf{KH}(\mathbf{b}_j, \mathbf{b}_k)$ von P . From the remark above this leads to the guarantee that among the vertices $\mathbf{o}_1, \mathbf{o}_2, \mathbf{o}_3$ of the triangle there are two vertices lying on opposite sides of \mathcal{G} and whose distance to the line is at least $\frac{8}{2} = 4$. Without loss of generality this may be the pair \mathbf{o}_1 and \mathbf{o}_2 . Moreover the fact that all points $\mathbf{b}_1, \dots, \mathbf{b}_N$ have distance at most 2 to the origin assures that:

$$\text{dist}(\mathcal{G}, \mathbf{AH}(\mathbf{b}_j, \mathbf{b}_k)) \leq \text{dist}(\mathcal{G}, \mathbf{KH}(\mathbf{b}_j, \mathbf{b}_k)) \leq \text{dist}(\mathbf{0}, \mathbf{b}_j) \leq 2.$$

This is visualized in figure 4.8: The two points \mathbf{o}_1 and \mathbf{o}_2 are on different sides of the line and they lie in the dark grey colored regions. These regions are characterized by the fact that all points of those regions exhibit a distance of at least 4 to \mathcal{G} . The line $\mathbf{AH}(\mathbf{b}_j, \mathbf{b}_k)$, which is parallel to \mathcal{G} belongs to the region colored in light grey.

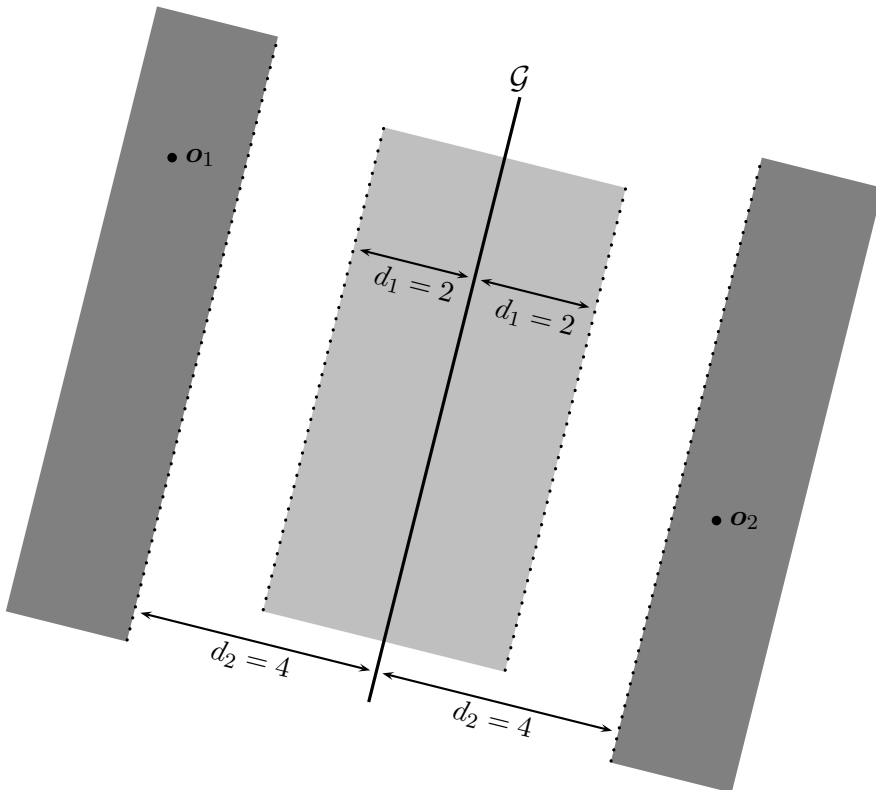


Figure 4.8: Illustration for the proof of 4.4.1

We recognize immediately that \mathbf{o}_1 and \mathbf{o}_2 also lie on opposite sides of the line $\mathbf{AH}(\mathbf{b}_j, \mathbf{b}_k)$ and that moreover

$$\text{dist}(\mathbf{o}_i, \mathbf{AH}(\mathbf{b}_j, \mathbf{b}_k)) \geq 2$$

for $i = 1, 2$ holds. It remains to show that $\mathbf{KH}(\mathbf{b}_j, \mathbf{b}_k)$ for an $i \in \{1, 2\}$ is an edge of $\mathbf{KH}(\mathbf{o}_i, P)$. Under our condition $\mathbf{KH}(\mathbf{b}_j, \mathbf{b}_k)$ is an edge of P . In combination of this insight with the separation property of $\mathbf{AH}(\mathbf{b}_j, \mathbf{b}_k)$ just derived, one realizes that one of the points $\mathbf{o}_1, \mathbf{o}_2$ must belong to the same side of the line $\mathbf{AH}(\mathbf{b}_j, \mathbf{b}_k)$ as the

polygon P . Without loss of generality let this be \mathbf{o}_1 . In other words the situation is as follows: The point \mathbf{o}_1 lies on the same side of the line $\mathbf{AH}(\mathbf{b}_j, \mathbf{b}_k)$ as the polygon P and in addition $\mathbf{KH}(\mathbf{b}_j, \mathbf{b}_k)$ is an edge of P . This means, that $\mathbf{KH}(\mathbf{b}_j, \mathbf{b}_k)$ is an edge of the “extended” polygon $\mathbf{KH}(\mathbf{o}_1, P)$, too. This concludes the proof. \square

Lemma 4.4.2 (Angle and Euclidean Distance).

Let \mathcal{L} be a straight line in the plane such that

$$\mathbf{dist}(\mathbf{0}, \mathcal{L}) \geq 1.$$

Then an arbitrary pair of points $\mathbf{x}_1, \mathbf{x}_2$ on \mathcal{L} with $\|\mathbf{x}_1\|, \|\mathbf{x}_2\| \leq 10$ satisfies:

$$c \cdot \mathbf{dist}(\mathbf{x}_1, \mathbf{x}_2) \leq \mathbf{arc}(\mathbf{x}_1, \mathbf{x}_2) \leq \mathbf{dist}(\mathbf{x}_1, \mathbf{x}_2),$$

where $c = (10^2 + 1)^{-1}$.

Proof. An explicit derivation of this statement can be found in the proof of Lemma 7.3 in [Ver09]. We restrict ourselves to illustrate the fundamental idea of that result by means of figure 4.9.⁸

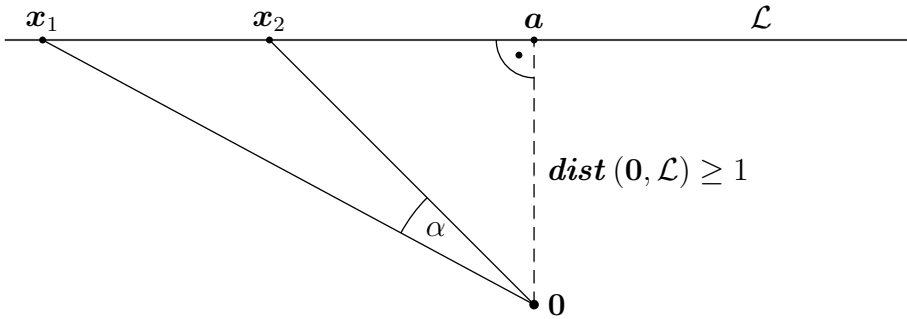


Figure 4.9: Angle between \mathbf{x}_1 and \mathbf{x}_2

Further considerations are supported by taking the two following statements into regard:

1. The distance of the line \mathcal{L} to the origin is at least 1.
2. The distance of \mathbf{x}_1 and of \mathbf{x}_2 to the origin is at most 10. In consequence both points cannot (by moving on the line \mathcal{L}) disappear from the point \mathbf{a} by an arbitrarily high distance.

These two items make it clear that the angle α between both points cannot become arbitrarily smaller than the distance $\mathbf{dist}(\mathbf{x}_1, \mathbf{x}_2)$ itself. Hence $c \cdot \mathbf{dist}(\mathbf{x}_1, \mathbf{x}_2) \leq \mathbf{arc}(\mathbf{x}_1, \mathbf{x}_2)$ for a constant c . The second inequality $\mathbf{arc}(\mathbf{x}_1, \mathbf{x}_2) \leq \mathbf{dist}(\mathbf{x}_1, \mathbf{x}_2)$ can be understood in a similar way. \square

⁸This is adapted to [Ver09, Figure 7.3].

These two Lemmata can be used for giving the following interpretation. For $\mathbf{b}_1, \dots, \mathbf{b}_N \in \mathbb{R}^2$ in general position we observe the polygon $P := \mathbf{KH}(\mathbf{b}_1, \dots, \mathbf{b}_N)$ and further we assume $\|\mathbf{b}_i\| \leq 2$ for all $i = 1, \dots, N$. This polygon is embedded in an equilateral triangle with center of gravity in $\mathbf{0}$ and with vertices all of norm 8. Lemma 4.4.1 implies that we find at least one point of view for each edge, $\mathbf{KH}(\mathbf{b}_j, \mathbf{b}_k)$ of P , namely \mathbf{o}_i ($i = 1, 2, 3$) such that the edge $\mathbf{KH}(\mathbf{b}_j, \mathbf{b}_k)$ under adjoining \mathbf{o}_i to the convex hull remains an edge. So we know that $\mathbf{KH}(\mathbf{b}_j, \mathbf{b}_k)$ is an edge of $\mathbf{KH}(\mathbf{o}_i, P) = \mathbf{KH}(\mathbf{o}_i, \mathbf{b}_1, \dots, \mathbf{b}_N)$. In addition

$$\mathbf{dist}(\mathbf{o}_i, \mathbf{AH}(\mathbf{b}_j, \mathbf{b}_k)) \geq 2. \quad (4.52)$$

For technical reasons we study in the following the convex hull $\mathbf{KH}(\mathbf{o}_i, P) = \mathbf{KH}(\mathbf{o}_i, \mathbf{b}_1, \dots, \mathbf{b}_N)$ shifted by the vector $-\mathbf{o}_i$. So from here on we work under

$$P_i := -\mathbf{o}_i + \mathbf{KH}(\mathbf{o}_i, \mathbf{b}_1, \dots, \mathbf{b}_N) = \mathbf{KH}(\mathbf{0}, \mathbf{b}_1 - \mathbf{o}_i, \dots, \mathbf{b}_N - \mathbf{o}_i).$$

Obviously this does not change the fundamental structure. A descriptive interpretation of P_i is as follows: Instead of looking at P from \mathbf{o}_i , as we are used from using the Three-Viewpoints-Argument, in the case of P_i we study the shifted polytope $-\mathbf{o}_i + P$ looking from the origin $\mathbf{0}$. The edge $\mathbf{KH}(\mathbf{b}_j, \mathbf{b}_k)$ of P changes into

$$\mathbf{KH}(\mathbf{b}_j - \mathbf{o}_i, \mathbf{b}_k - \mathbf{o}_i) = -\mathbf{o}_i + \mathbf{KH}(\mathbf{b}_j, \mathbf{b}_k)$$

and for the line $\mathbf{AH}(\mathbf{b}_j, \mathbf{b}_k)$ we get

$$-\mathbf{o}_i + \mathbf{AH}(\mathbf{b}_j, \mathbf{b}_k).$$

As known from (4.52) we have $\mathbf{dist}(\mathbf{o}_i, \mathbf{AH}(\mathbf{b}_j, \mathbf{b}_k)) \geq 2$. Hence it follows directly that

$$\mathbf{dist}(\mathbf{0}, -\mathbf{o}_i + \mathbf{AH}(\mathbf{b}_j, \mathbf{b}_k)) \geq 2.$$

In addition for the two endpoints of the edges $-\mathbf{o}_i + \mathbf{b}_j$ and $-\mathbf{o}_i + \mathbf{b}_k$ on the line $-\mathbf{o}_i + \mathbf{AH}(\mathbf{b}_j, \mathbf{b}_k)$ we see that:

$$\begin{aligned} \|-\mathbf{o}_i + \mathbf{b}_j\| &\leq \|-\mathbf{o}_i\| + \|\mathbf{b}_j\| \leq 8 + 2 = 10, \\ \|-\mathbf{o}_i + \mathbf{b}_k\| &\leq \|-\mathbf{o}_i\| + \|\mathbf{b}_k\| \leq 8 + 2 = 10. \end{aligned}$$

For that reason we can apply Lemma 4.4.2 and we can conclude, that

$$c \cdot \mathbf{dist}(-\mathbf{o}_i + \mathbf{b}_j, -\mathbf{o}_i + \mathbf{b}_k) \leq \mathbf{arc}(-\mathbf{o}_i + \mathbf{b}_j, -\mathbf{o}_i + \mathbf{b}_k) \leq \mathbf{dist}(-\mathbf{o}_i + \mathbf{b}_j, -\mathbf{o}_i + \mathbf{b}_k)$$

with $c = (10^2 + 1)^{-1}$ holds. That property is transferred on an arbitrary pair of points $\mathbf{x}_1, \mathbf{x}_2 \in -\mathbf{o}_i + \mathbf{KH}(\mathbf{b}_j, \mathbf{b}_k)$. We want to remark that the term $\mathbf{arc}(-\mathbf{o}_i + \mathbf{b}_j, -\mathbf{o}_i + \mathbf{b}_k)$ corresponds just to the angle between \mathbf{b}_j and \mathbf{b}_k under observation from \mathbf{o}_i .

We summarize the observations we have made in a concise form

Conclusion:

For each edge $\mathbf{KH}(\mathbf{b}_j, \mathbf{b}_k)$ of $P = \mathbf{KH}(\mathbf{b}_1, \dots, \mathbf{b}_N)$ we find an observation point out of $\{\mathbf{o}_1, \mathbf{o}_2, \mathbf{o}_3\}$, which contains that edge and which allows an observation under a suitable angle. By suitable we mean that the size of the angle differs from the length of the edge at most by a known (guaranteed) factor. This keeps a kind of proportionality.

Having summarized the fundamental results obtained with the Three-Viewpoints-Argument, we can step forward and use this results in the next section in order to estimate the number of edges.

4.5 An Upper Bound For The Number Of Vertices

The aim of this section is the derivation of an upper bound for the expected value of the number of edges of

$$P = \mathbf{KH}(\mathbf{a}_1, \dots, \mathbf{a}_m)$$

in the case of perturbed vectors $\mathbf{a}_1, \dots, \mathbf{a}_m$. For that purpose we make use of the Three-Viewpoints-Argument, which had been discussed in the previous section. And we combine that with the upper bound from section 4.3 for the probability of short edges. Essentially we follow the proof-strategy of [Ver09], and apply this to our configuration.

More precisely stated we are going to prove the theorem:

Theorem 4.5.1 (Number of Vertices in Dimension 2).

Let $\mathbf{a}_1, \dots, \mathbf{a}_m$ be independently and normally distributed random vectors in \mathbb{R}^2 with centers $\bar{\mathbf{a}}_1, \dots, \bar{\mathbf{a}}_m$, having a norm at most 1 and with standard deviation $\sigma \leq \frac{1}{2\sqrt{\ln(m)}}$.

In addition let the random variable K stand for the number of edges of $P = \mathbf{KH}(\mathbf{a}_1, \dots, \mathbf{a}_m)$. Then under the given perturbation model it holds:

$$\mathbb{E}[K] \leq \text{Const} \cdot \frac{1}{\sigma^2}.$$

This expected value is calculated over the the random vectors $\mathbf{a}_1, \dots, \mathbf{a}_m$ and Const is an absolute constant.

Proof. The subject of our study is the polygon

$$P = \mathbf{KH}(\mathbf{a}_1, \dots, \mathbf{a}_m)$$

and the random variable K stands for the number of edges of P . In very explicit form we can interpret K as a function $K : \mathbb{R}^2 \times \dots \times \mathbb{R}^2 \rightarrow \mathbb{N}$, which is defined as

$$K(\mathbf{z}_1, \dots, \mathbf{z}_m) := \# (\text{Edges of } \mathbf{KH}(\mathbf{z}_1, \dots, \mathbf{z}_m)). \quad (4.53)$$

This function works on the random vectors $\mathbf{a}_1, \dots, \mathbf{a}_m$ as arguments. Moreover we consider the set R_δ , as defined in section 4.3 in the following way:

$$R_\delta := \{(\mathbf{a}_1, \dots, \mathbf{a}_m) \in \mathbb{R}^{2 \times m} : \|\mathbf{a}_i\| \leq \delta \ \forall i = 1, \dots, m\}.$$

For the events $(\mathbf{a}_1, \dots, \mathbf{a}_m) \in R_\delta$ resp. $(\mathbf{a}_1, \dots, \mathbf{a}_m) \notin R_\delta$ we use the abbreviation R_δ bzw. $\neg R_\delta$. From Lemma 2.2.7 it follows that $\mathbb{P}[\neg R_\delta] \leq m^{-1}$. For the indicator function $\mathbf{1}[R_2]$ it is known that:

$$\mathbf{1}[R_2] := \begin{cases} 1, & \text{if } \|\mathbf{a}_i\| \leq 2 \text{ for all } i = 1, \dots, m \\ 0, & \text{else} \end{cases}$$

On the basis of $\mathbf{1}[R_2] + \mathbf{1}[\neg R_2] \equiv 1$ we can split up the expectation value of K :

$$\begin{aligned} \mathbb{E}[K] &= \mathbb{E}[K \cdot \mathbf{1}[R_2]] + \mathbb{E}[K \cdot \mathbf{1}[\neg R_2]] \\ &\leq \mathbb{E}[K \cdot \mathbf{1}[R_2]] + m \cdot \mathbb{E}[\mathbf{1}[\neg R_2]] && (\text{because } K \leq m) \\ &= \mathbb{E}[K \cdot \mathbf{1}[R_2]] + m \cdot \mathbb{P}[\neg R_2] \\ &\leq \mathbb{E}[K \cdot \mathbf{1}[R_2]] + 1. && (\text{because } \mathbb{P}[\neg R_2] \leq m^{-1}). \end{aligned}$$

Using the density functions f_1, \dots, f_m of $\mathbf{a}_1, \dots, \mathbf{a}_m$ and the notation from (4.53) the expected value $\mathbb{E}[K \cdot \mathbf{1}[R_2]]$, can be formulated in the following way:

$$\mathbb{E}[K \cdot \mathbf{1}[R_2]] = \int_{\mathbb{R}^2} \cdots \int_{\mathbb{R}^2} K(\mathbf{a}_1, \dots, \mathbf{a}_m) \cdot \mathbf{1}[R_2] \cdot f_1(\mathbf{a}_1) \cdots f_m(\mathbf{a}_m) d\mathbf{a}_1 \dots d\mathbf{a}_m.$$

That means we are allowed to concentrate on those configurations of $\mathbf{a}_1, \dots, \mathbf{a}_m$, for which each vector has a norm not greater than 2. Now Lemma 4.4.1 based on the Three-Viewpoints-Argument from the previous section is applicable. This enables us to conclude that for each edge $\mathbf{KH}(\mathbf{a}_j, \mathbf{a}_k)$ of $P = \mathbf{KH}(\mathbf{a}_1, \dots, \mathbf{a}_m)$ a viewpoint \mathbf{o}_i can be found, such that $-\mathbf{o}_i + \mathbf{KH}(\mathbf{a}_j, \mathbf{a}_k)$ is an edge of

$$P_i = \mathbf{KH}(\mathbf{0}, -\mathbf{o}_i + P) = \mathbf{KH}(\mathbf{0}, -\mathbf{o}_i + \mathbf{a}_1, \dots, -\mathbf{o}_i + \mathbf{a}_m).$$

Moreover we recognize: If we determine for each P_i those edges, which are defined by two vectors $\mathbf{a}_j, \mathbf{a}_k$, then we obtain all edges of the standard polytope P . Hence the set

$$\{\mathbf{kante}_{P_i}(\mathbf{q}) : \mathbf{q} \in \omega_2, i = 1, 2, 3\} := \bigcup_{i=1,2,3} \bigcup_{\mathbf{q} \in \omega_2} \{\mathbf{kante}_{P_i}(\mathbf{q})\}$$

contains just the index sets corresponding to the edges of P .⁹ The vector \mathbf{q} plays the role of the possible view-directions for the determination of the edges. It may occur that a certain edge will be determined for different P_i . This should not disturb us since we argue in the logic of sets. The consequence is the equality

$$K = \#(\{\mathbf{kante}_{P_i}(\mathbf{q}) : \mathbf{q} \in \omega_2, i = 1, 2, 3\})$$

⁹We remind that the formal definition of $\mathbf{kante}_{P_i}(\mathbf{q})$ can be found in definition 4.3.2.

and so it holds that

$$\mathbb{E}[K \cdot \mathbf{1}[R_2]] = \mathbb{E}[\#(\{\mathbf{kante}_{P_i}(\mathbf{q}) : \mathbf{q} \in \omega_2, i = 1, 2, 3\}) \cdot \mathbf{1}[R_2]].$$

Before proceeding with our considerations, we need the following definition.

Definition 4.5.2 (Discretization of the unit circle).

For a $k \in \mathbb{N}$ we first look at the set of angles

$$W_k = \left\{ \frac{2\pi}{k}, 2 \cdot \frac{2\pi}{k}, 3 \cdot \frac{2\pi}{k}, \dots, k \cdot \frac{2\pi}{k} \right\}.$$

Using that structure we define a discretization of the unit circle:

$$\omega_2^{(k)} = \left\{ \begin{pmatrix} \cos(\varphi) \\ \sin(\varphi) \end{pmatrix} : \varphi \in W_k \right\}.$$

A graphical illustration of this definition can be found in figure 4.10.

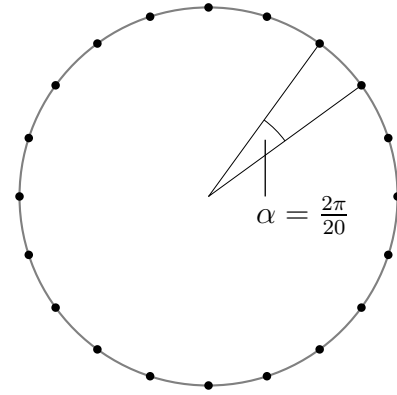


Figure 4.10: Discretization $\omega_2^{(20)}$ of the unit circle

As known we are interested in

$$\mathbb{E}[K \cdot \mathbf{1}[R_2]] = \mathbb{E}[\#(\{\mathbf{kante}_{P_i}(\mathbf{q}) : \mathbf{q} \in \omega_2, i = 1, 2, 3\}) \cdot \mathbf{1}[R_2]].$$

Some pages above we have applied 4.4.1 and asserted, that for each edge $\mathbf{KH}(\mathbf{a}_j, \mathbf{a}_k)$ of P we can find a view-point \mathbf{o}_i such that $-\mathbf{o}_i + \mathbf{KH}(\mathbf{a}_j, \mathbf{a}_k)$ is an edge of P_i . Moreover that Lemma delivers the following insight: We can \mathbf{o}_i choose in such a way that for the corresponding straight line $\mathcal{G} := -\mathbf{o}_i + \mathbf{AH}(\mathbf{a}_j, \mathbf{a}_k)$ it holds that :

$$\mathbf{dist}(\mathbf{0}, \mathcal{G}) \geq 2.$$

In addition we exploit the two estimations

$$\begin{aligned} \|-\mathbf{o}_i + \mathbf{a}_j\| &\leq \|\mathbf{o}_i\| + \|\mathbf{a}_j\| \leq 8 + 2 = 10 \text{ and} \\ \|-\mathbf{o}_i + \mathbf{a}_k\| &\leq \|\mathbf{o}_i\| + \|\mathbf{a}_k\| \leq 8 + 2 = 10, \end{aligned}$$

then Lemma 4.4.2 can be applied and we can conclude that the edge can be observed under the angle

$$\beta := \text{arc}(-\mathbf{o}_i + \mathbf{a}_j, -\mathbf{o}_i + \mathbf{a}_k) \geq (100 + 1)^{-1} \cdot \text{dist}(\mathbf{a}_j, \mathbf{a}_k) > 0.$$

If we choose the value k for the above described discretization of the unit circle large enough, then we have $\frac{2\pi}{k} < \beta$. Hence there is a $\bar{\mathbf{q}} \in \omega_2^{(k)}$ with $\mathbf{kante}_{P_i}(\bar{\mathbf{q}}) = \{j, k\}$. Since this argumentation can be done for each edge of P in the same way, the following discretization is possible:

$$\begin{aligned} & \mathbb{E} [\# (\{ \mathbf{kante}_{P_i}(\mathbf{q}) : \mathbf{q} \in \omega_2, i = 1, 2, 3 \}) \cdot \mathbb{1}[R_2]] \\ &= \lim_{\ell \rightarrow \infty} \mathbb{E} \left[\# \left(\{ \mathbf{kante}_{P_i}(\mathbf{q}) : \mathbf{q} \in \omega_2^{(\ell)}, i = 1, 2, 3 \} \right) \cdot \mathbb{1}[R_2] \right]. \end{aligned}$$

Both figures 4.11 and 4.12 illustrate that principle:

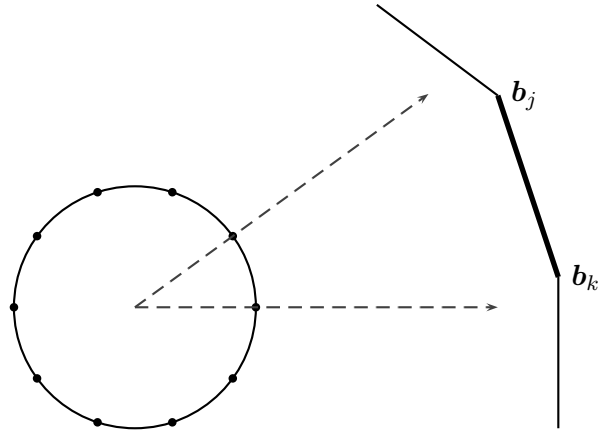


Figure 4.11: edge is not hit under discretization with $k = 10$

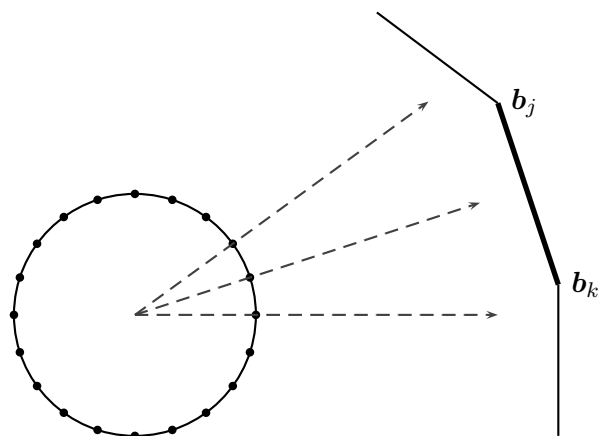


Figure 4.12: edge is hit under discretization with $k = 20$

Remark 4.5.3.

The discretization argument presented above, which is very comprehensible, has been developed and exploited by Spielman and Teng in [ST04] for the purpose of estimating the expectation value of the number of shadow vertices in a perturbed polyhedron. Also Vershynin make use of this principle in his refined geometrical investigation in [Ver09]. A formally even more detailed presentation can be found e.g. in [ST04, Lemma 4.6].

The just mentioned reasoning for the introduction of the discretization can even be used for a further significant conclusion. Without making a point of that so far, we have recognized implicitly that: For ℓ large enough we shall realize an arbitrary edge $\mathbf{KH}(\mathbf{a}_j, \mathbf{a}_k)$ of P as index set $\{j, k\}$ in

$$\left\{ \mathbf{kante}_{P_i}(\mathbf{q}) : \mathbf{q} \in \omega_2^{(\ell)}, i = 1, 2, 3 \right\} \quad (4.54)$$

from a view-point \mathbf{o}_{i_0} , such that for the resulting edge

$$-\mathbf{o}_{i_0} + \mathbf{KH}(\mathbf{a}_j, \mathbf{a}_k) = \mathbf{KH}(-\mathbf{o}_{i_0} + \mathbf{a}_j, -\mathbf{o}_{i_0} + \mathbf{a}_k) =: \mathbf{KH}(\mathbf{c}_j, \mathbf{c}_k)$$

of P_{i_0} it holds that

$$c \cdot \mathbf{dist}(\mathbf{x}_1, \mathbf{x}_2) \leq \mathbf{arc}(\mathbf{x}_1, \mathbf{x}_2) \leq \mathbf{dist}(\mathbf{x}_1, \mathbf{x}_2) \quad (4.55)$$

for arbitrary $\mathbf{x}_1, \mathbf{x}_2 \in \mathbf{KH}(\mathbf{c}_j, \mathbf{c}_k)$ and $c := (10^2 + 1)^{-1}$. In the case that an edge satisfies the condition (4.55), we shall call this edge *well-scaled*. The consideration made above enables us to restrict our concentration in the set (4.54) on those index sets $\mathbf{kante}_{P_i}(\mathbf{q})$, for which the associated edges are *well-scaled*. We obtain:

$$\mathbb{E}[K] \leq \lim_{\ell \rightarrow \infty} \mathbb{E} \left[\# \left(\left\{ \mathbf{kante}_{P_i}(\mathbf{q}) : \text{well-scaled}, \mathbf{q} \in \omega_2^{(\ell)}, i = 1, 2, 3 \right\} \right) \cdot \mathbf{1}[R_2] \right] + 1. \quad (4.56)$$

In addition it may happen that a well-scaled edge from the set in (4.56) is hit by several successive vectors $\mathbf{q}_r, \dots, \mathbf{q}_s$ from $\omega_2^{(\ell)}$. So it will be realized in the above set “several times”. In that case we keep only one \mathbf{q} . This one is selected by the criterion of having the largest angle from the set W_ℓ , which is known from definition 4.5.2. For this reason the angle between \mathbf{q} and the boundary of $\mathbf{Kante}_{P_i}(\mathbf{q})$ satisfies:

$$\mathbf{arc}(\mathbf{q}, \partial \mathbf{Kante}_{P_i}(\mathbf{q})) \leq \frac{2\pi}{\ell}.$$

Since the edge is well-scaled, the corresponding condition (4.55) permits the estimation:

$$\mathbf{dist}(\mathbf{q}_{P_i}, \partial \mathbf{Kante}_{P_i}(\mathbf{q})) \leq \frac{1}{c} \cdot \mathbf{arc}(\mathbf{q}, \partial \mathbf{Kante}_{P_i}(\mathbf{q})) \leq \frac{1}{c} \cdot \frac{2\pi}{\ell} = \frac{C_1}{\ell}. \quad (4.57)$$

Here \mathbf{q}_{P_i} denotes accordingly to the already known definition the intersection point $\mathbf{KK}(\mathbf{q}) \cap \mathbf{Kante}_{P_i}(\mathbf{q})$. From that insight we draw the following consequence: Instead of incorporating only well-scaled edges in our considerations, we count the edges

satisfying condition resp. property (4.57). Hence no well-scaled edge will remain unconsidered and uncounted. So we know:

$$\mathbb{E}[K] \leq \lim_{\ell \rightarrow \infty} \mathbb{E} \left[\# \left(\left\{ \mathbf{kante}_{P_i}(\mathbf{q}) : \mathbf{dist}(\mathbf{q}_{P_i}, \partial \mathbf{Kante}_{P_i}(\mathbf{q})) \leq \frac{C_1}{\ell}, \mathbf{q} \in \omega_2^{(\ell)}, i = 1, 2, 3 \right\} \right) \cdot \mathbf{1}[R_2] \right] + 1. \quad (4.58)$$

Now we make the following consideration

$$\begin{aligned} & \left\{ \mathbf{kante}_{P_i}(\mathbf{q}) : \mathbf{dist}(\mathbf{q}_{P_i}, \partial \mathbf{Kante}_{P_i}(\mathbf{q})) \leq \frac{C_1}{\ell}, \mathbf{q} \in \omega_2^{(\ell)}, i = 1, 2, 3 \right\} \\ &= \bigcup_{i=1,2,3} \left\{ \mathbf{kante}_{P_i}(\mathbf{q}) : \mathbf{dist}(\mathbf{q}_{P_i}, \partial \mathbf{Kante}_{P_i}(\mathbf{q})) \leq \frac{C_1}{\ell}, \mathbf{q} \in \omega_2^{(\ell)} \right\}. \end{aligned}$$

This leads to:

$$\begin{aligned} & \# \left(\left\{ \mathbf{kante}_{P_i}(\mathbf{q}) : \mathbf{dist}(\mathbf{q}_{P_i}, \partial \mathbf{Kante}_{P_i}(\mathbf{q})) \leq \frac{C_1}{\ell}, \mathbf{q} \in \omega_2^{(\ell)}, i = 1, 2, 3 \right\} \right) \\ &= \# \left(\bigcup_{i=1,2,3} \left\{ \mathbf{kante}_{P_i}(\mathbf{q}) : \mathbf{dist}(\mathbf{q}_{P_i}, \partial \mathbf{Kante}_{P_i}(\mathbf{q})) \leq \frac{C_1}{\ell}, \mathbf{q} \in \omega_2^{(\ell)} \right\} \right) \\ &\leq \sum_{i=1,2,3} \# \left(\left\{ \mathbf{kante}_{P_i}(\mathbf{q}) : \mathbf{dist}(\mathbf{q}_{P_i}, \partial \mathbf{Kante}_{P_i}(\mathbf{q})) \leq \frac{C_1}{\ell}, \mathbf{q} \in \omega_2^{(\ell)} \right\} \right) \\ &\leq 3 \cdot \max_{i=1,2,3} \# \left(\left\{ \mathbf{kante}_{P_i}(\mathbf{q}) : \mathbf{dist}(\mathbf{q}_{P_i}, \partial \mathbf{Kante}_{P_i}(\mathbf{q})) \leq \frac{C_1}{\ell}, \mathbf{q} \in \omega_2^{(\ell)} \right\} \right). \end{aligned}$$

So we get in place of the upper bound (4.58) a new term:

$$\mathbb{E}[K] \leq 3 \cdot \max_{i=1,2,3} \lim_{\ell \rightarrow \infty} \mathbb{E} \left[\# \left(\left\{ \mathbf{kante}_{P_i}(\mathbf{q}) : \mathbf{dist}(\mathbf{q}_{P_i}, \partial \mathbf{Kante}_{P_i}(\mathbf{q})) \leq \frac{C_1}{\ell}, \mathbf{q} \in \omega_2^{(\ell)} \right\} \right) \cdot \mathbf{1}[R_2] \right] + 1. \quad (4.59)$$

For enabling a further transformation we make some observations. As already known the vectors $\mathbf{a}_1, \dots, \mathbf{a}_m$ are distributed like that:

$$\mathbf{a}_h \sim \mathcal{N}_2(\bar{\mathbf{a}}_h, \sigma^2 \cdot \mathbf{E}_2)$$

with $\|\bar{\mathbf{a}}_h\| \leq 1$ for all $h = 1, \dots, m$ and $\sigma \leq \frac{1}{2\sqrt{\ln(m)}}$. Moreover we remember that for an arbitrary $i = 1, 2, 3$ we have:

$$P_i = \mathbf{K}\mathbf{H}(\mathbf{0}, -\mathbf{o}_i + \mathbf{a}_1, \dots, -\mathbf{o}_i + \mathbf{a}_m)$$

with $\|\mathbf{o}_1\| = \|\mathbf{o}_2\| = \|\mathbf{o}_3\| = 8$. For an arbitrary combination of i and h it results that

$$-\mathbf{o}_i + \mathbf{a}_h \sim \mathcal{N}_2(-\mathbf{o}_i + \bar{\mathbf{a}}_h, \sigma^2 \cdot \mathbf{E}_2)$$

and here

$$\|-\mathbf{o}_i + \bar{\mathbf{a}}_h\| \leq \|-\mathbf{o}_i\| + \|\bar{\mathbf{a}}_h\| \leq 8 + 1 = 9.$$

All this leads to a new upper bound :

$$\mathbb{E}[K] \leq 3 \cdot \sup_{\mathbf{b}_1, \dots, \mathbf{b}_m} \lim_{\ell \rightarrow \infty} \mathbb{E} \left[\# \left(\left\{ \mathbf{kante}_Z(\mathbf{q}) : \mathbf{dist}(\mathbf{q}_Z, \partial \mathbf{Kante}_Z(\mathbf{q})) \leq \frac{C_1}{\ell}, \mathbf{q} \in \omega_2^{(\ell)} \right\} \right) \cdot \mathbf{1}[R_{10}] \right] + 1.$$

Here $\mathbf{b}_i \sim \mathcal{N}_2(\bar{\mathbf{b}}_i, \sigma^2 \cdot \mathbf{E}_2)$ with $\|\bar{\mathbf{b}}_i\| \leq 9$ for all $i = 1, \dots, m$. Furthermore $Z = \mathbf{KH}(\mathbf{0}, \mathbf{b}_1, \dots, \mathbf{b}_m)$. In order to avoid concerning ourselves with the Supremum, let during the further course $\mathbf{b}_1, \dots, \mathbf{b}_m$ be arbitrary normally distributed vectors having the property just mentioned. Now the following insight is very important for an estimation of the expected value:

$$\begin{aligned} & \lim_{\ell \rightarrow \infty} \mathbb{E} \left[\# \left(\left\{ \mathbf{kante}_Z(\mathbf{q}) : \mathbf{dist}(\mathbf{q}_Z, \partial \mathbf{Kante}_Z(\mathbf{q})) \leq \frac{C_1}{\ell}, \mathbf{q} \in \omega_2^{(\ell)} \right\} \right) \cdot \mathbf{1}[R_{10}] \right] \\ & \leq \lim_{\ell \rightarrow \infty} \sum_{\mathbf{q} \in \omega_2^{(\ell)}} \sum_{\substack{\Delta \subset \{1, \dots, m\} \\ \#(\Delta)=2}} \mathbb{P} \left[\mathbf{kante}_Z(\mathbf{q}) = \Delta \text{ and} \right. \\ & \quad \left. \mathbf{dist}(\mathbf{q}_Z, \partial \mathbf{Kante}_Z(\mathbf{q})) \leq \frac{C_1}{\ell} \text{ and } R_{10} \right]. \end{aligned} \tag{4.60}$$

This estimation is deduced during the subsequent steps. We first note that:

$$\begin{aligned} & \left\{ \mathbf{kante}_Z(\mathbf{q}) : \mathbf{dist}(\mathbf{q}_Z, \partial \mathbf{Kante}_Z(\mathbf{q})) \leq \frac{C_1}{\ell}, \mathbf{q} \in \omega_2^{(\ell)} \right\} \\ & = \bigcup_{\mathbf{q} \in \omega_2^{(\ell)}} \left\{ \mathbf{kante}_Z(\mathbf{q}) : \mathbf{dist}(\mathbf{q}_Z, \partial \mathbf{Kante}_Z(\mathbf{q})) \leq \frac{C_1}{\ell} \right\}. \end{aligned}$$

So we obtain

$$\begin{aligned} & \# \left(\left\{ \mathbf{kante}_Z(\mathbf{q}) : \mathbf{dist}(\mathbf{q}_Z, \partial \mathbf{Kante}_Z(\mathbf{q})) \leq \frac{C_1}{\ell}, \mathbf{q} \in \omega_2^{(\ell)} \right\} \right) \\ & \leq \sum_{\mathbf{q} \in \omega_2^{(\ell)}} \underbrace{\# \left(\left\{ \mathbf{kante}_Z(\mathbf{q}) : \mathbf{dist}(\mathbf{q}_Z, \partial \mathbf{Kante}_Z(\mathbf{q})) \leq \frac{C_1}{\ell} \right\} \right)}_{(*)}. \end{aligned} \tag{4.61}$$

On closer examination of (*) in expression (4.61) we notice :

$$\begin{aligned} & \# \left(\left\{ \mathbf{kante}_Z(\mathbf{q}) : \mathbf{dist}(\mathbf{q}_Z, \partial \mathbf{Kante}_Z(\mathbf{q})) \leq \frac{C_1}{\ell} \right\} \right) \\ &= \sum_{\substack{\Delta \subset \{1, \dots, m\} \\ \#(\Delta)=2}} \mathbb{1} \left[\mathbf{kante}_Z(\mathbf{q}) = \Delta \text{ and } \mathbf{dist}(\mathbf{q}_Z, \partial \mathbf{Kante}_Z(\mathbf{q})) \leq \frac{C_1}{\ell} \right]. \end{aligned}$$

So we obtain:

$$\begin{aligned} & \# \left(\left\{ \mathbf{kante}_Z(\mathbf{q}) : \mathbf{dist}(\mathbf{q}_Z, \partial \mathbf{Kante}_Z(\mathbf{q})) \leq \frac{C_1}{\ell}, \mathbf{q} \in \omega_2^{(\ell)} \right\} \right) \\ &\leq \sum_{\mathbf{q} \in \omega_2^{(\ell)}} \sum_{\substack{\Delta \subset \{1, \dots, m\} \\ \#(\Delta)=2}} \mathbb{1} \left[\mathbf{kante}_Z(\mathbf{q}) = \Delta \text{ and } \mathbf{dist}(\mathbf{q}_Z, \partial \mathbf{Kante}_Z(\mathbf{q})) \leq \frac{C_1}{\ell} \right]. \end{aligned}$$

Now the monotony and the linearity of the expectation value yield:

$$\begin{aligned} & \lim_{\ell \rightarrow \infty} \mathbb{E} \left[\# \left(\left\{ \mathbf{kante}_Z(\mathbf{q}) : \mathbf{dist}(\mathbf{q}_Z, \partial \mathbf{Kante}_Z(\mathbf{q})) \leq \frac{C_1}{\ell}, \mathbf{q} \in \omega_2^{(\ell)} \right\} \right) \cdot \mathbb{1}[R_{10}] \right] \\ &\leq \lim_{\ell \rightarrow \infty} \mathbb{E} \left[\sum_{\mathbf{q} \in \omega_2^{(\ell)}} \sum_{\substack{\Delta \subset \{1, \dots, m\} \\ \#(\Delta)=2}} \mathbb{1} \left[\mathbf{kante}_Z(\mathbf{q}) = \Delta \text{ and} \right. \right. \\ &\quad \left. \left. \mathbf{dist}(\mathbf{q}_Z, \partial \mathbf{Kante}_Z(\mathbf{q})) \leq \frac{C_1}{\ell} \right] \cdot \mathbb{1}[R_{10}] \right] \\ &= \lim_{\ell \rightarrow \infty} \mathbb{E} \left[\sum_{\mathbf{q} \in \omega_2^{(\ell)}} \sum_{\substack{\Delta \subset \{1, \dots, m\} \\ \#(\Delta)=2}} \mathbb{1} \left[\mathbf{kante}_Z(\mathbf{q}) = \Delta \text{ and} \right. \right. \\ &\quad \left. \left. \mathbf{dist}(\mathbf{q}_Z, \partial \mathbf{Kante}_Z(\mathbf{q})) \leq \frac{C_1}{\ell} \text{ and } R_{10} \right] \right] \end{aligned}$$

$$\begin{aligned}
 &= \lim_{\ell \rightarrow \infty} \sum_{\mathbf{q} \in \omega_2^{(\ell)}} \sum_{\substack{\Delta \subset \{1, \dots, m\} \\ \#(\Delta)=2}} \mathbb{E} \left[\mathbb{1} \left[\mathbf{kante}_Z(\mathbf{q}) = \Delta \text{ and} \right. \right. \\
 &\quad \left. \left. \mathbf{dist}(\mathbf{q}_Z, \partial \mathbf{Kante}_Z(\mathbf{q})) \leq \frac{C_1}{\ell} \text{ and } R_{10} \right] \right] \\
 &= \lim_{\ell \rightarrow \infty} \sum_{\mathbf{q} \in \omega_2^{(\ell)}} \sum_{\substack{\Delta \subset \{1, \dots, m\} \\ \#(\Delta)=2}} \mathbb{P} \left[\mathbf{kante}_Z(\mathbf{q}) = \Delta \text{ and} \right. \\
 &\quad \left. \mathbf{dist}(\mathbf{q}_Z, \partial \mathbf{Kante}_Z(\mathbf{q})) \leq \frac{C_1}{\ell} \text{ and } R_{10} \right].
 \end{aligned}$$

So we have verified the validity of the inequality (4.60). Accordingly

$$\mathbb{E}[K] \leq 3 \cdot \sup_{\mathbf{b}_1, \dots, \mathbf{b}_m} \lim_{\ell \rightarrow \infty} \sum_{\mathbf{q} \in \omega_2^{(\ell)}} \sum_{\substack{\Delta \subset \{1, \dots, m\} \\ \#(\Delta)=2}} \mathbb{P} \left[\mathbf{kante}_Z(\mathbf{q}) = \Delta \text{ and} \right. \\
 \left. \mathbf{dist}(\mathbf{q}_Z, \partial \mathbf{Kante}_Z(\mathbf{q})) \leq \frac{C_1}{\ell} \text{ and } R_{10} \right] + 1.. \quad (4.62)$$

In the following we study the probability in the term (4.62) even more precisely:

$$\begin{aligned}
 &\lim_{\ell \rightarrow \infty} \sum_{\mathbf{q} \in \omega_2^{(\ell)}} \sum_{\substack{\Delta \subset \{1, \dots, m\} \\ \#(\Delta)=2}} \mathbb{P} \left[\mathbf{kante}_Z(\mathbf{q}) = \Delta \text{ and} \right. \\
 &\quad \left. \mathbf{dist}(\mathbf{q}_Z, \partial \mathbf{Kante}_Z(\mathbf{q})) \leq \frac{C_1}{\ell} \text{ and } R_{10} \right] \\
 &= \lim_{\ell \rightarrow \infty} \sum_{\mathbf{q} \in \omega_2^{(\ell)}} \sum_{\substack{\Delta \subset \{1, \dots, m\} \\ \#(\Delta)=2}} \mathbb{P} \left[\mathbf{dist}(\mathbf{q}_Z, \partial \mathbf{Kante}_Z(\mathbf{q})) \leq \frac{C_1}{\ell} \text{ and } R_{10} \mid \mathbf{kante}_Z(\mathbf{q}) = \Delta \right] \\
 &\quad \cdot \mathbb{P} [\mathbf{kante}_Z(\mathbf{q}) = \Delta] \\
 &\leq \lim_{\ell \rightarrow \infty} \sup_{\substack{\mathbf{q} \in \omega_2^{(\ell)} \\ \Delta \subset \{1, \dots, m\} \\ \#(\Delta)=2}} \mathbb{P} \left[\mathbf{dist}(\mathbf{q}_Z, \partial \mathbf{Kante}_Z(\mathbf{q})) \leq \frac{C_1}{\ell} \text{ and } R_{10} \mid \mathbf{kante}_Z(\mathbf{q}) = \Delta \right] \\
 &\quad \cdot \sum_{\mathbf{q} \in \omega_2^{(\ell)}} \sum_{\substack{\Delta \subset \{1, \dots, m\} \\ \#(\Delta)=2}} \mathbb{P} [\mathbf{kante}_Z(\mathbf{q}) = \Delta]. \quad (4.63)
 \end{aligned}$$

Further we recognize that

$$\sum_{\substack{\Delta \subset \{1, \dots, m\} \\ \#(\Delta)=2}} \mathbb{P}[\mathbf{kante}_Z(\mathbf{q}) = \Delta] \leq 1$$

is valid because

$$\sum_{\substack{\Delta \subset \{1, \dots, m\} \\ \#(\Delta)=2}} \mathbb{1}[\mathbf{kante}_Z(\mathbf{q}) = \Delta] \leq 1.$$

Hence

$$\sum_{\mathbf{q} \in \omega_2^{(\ell)}} \sum_{\substack{\Delta \subset \{1, \dots, m\} \\ \#(\Delta)=2}} \mathbb{P}[\mathbf{kante}_Z(\mathbf{q}) = \Delta] \leq \ell.$$

And this yields

$$\begin{aligned} \mathbb{E}[K] &\leq 3 \cdot \sup_{\mathbf{b}_1, \dots, \mathbf{b}_m} \lim_{\ell \rightarrow \infty} \ell \cdot \sup_{\substack{\mathbf{q} \in \omega_2^{(\ell)} \\ \Delta \subset \{1, \dots, m\} \\ \#(\Delta)=2}} \mathbb{P}\left[\mathbf{dist}(\mathbf{q}_Z, \partial \mathbf{Kante}_Z(\mathbf{q})) \leq \frac{C_1}{\ell}\right. \\ &\quad \left. \text{and } R_{10} \left| \mathbf{kante}_Z(\mathbf{q}) = \Delta \right. \right] + 1. \end{aligned} \quad (4.64)$$

The essential remaining challenge is to estimate the inner Supremum-term. For that purpose we put on record that:

$$\begin{aligned} &\sup_{\substack{\mathbf{q} \in \omega_2^{(\ell)} \\ \Delta \subset \{1, \dots, m\} \\ \#(\Delta)=2}} \mathbb{P}\left[\mathbf{dist}(\mathbf{q}_Z, \partial \mathbf{Kante}_Z(\mathbf{q})) \leq \frac{C_1}{\ell} \text{ and } R_{10} \left| \mathbf{kante}_Z(\mathbf{q}) = \Delta \right. \right] \\ &\leq \sup_{\substack{\mathbf{q} \in \omega_2 \\ \Delta \subset \{1, \dots, m\} \\ \#(\Delta)=2}} \mathbb{P}\left[\mathbf{dist}(\mathbf{q}_Z, \partial \mathbf{Kante}_Z(\mathbf{q})) \leq \frac{C_1}{\ell} \text{ and } R_{10} \left| \mathbf{kante}_Z(\mathbf{q}) = \Delta \right. \right]. \end{aligned}$$

For this reason let during the following considerations $\Delta \subset \{1, \dots, m\}$ with $\#(\Delta) = 2$ and $\mathbf{q} \in \omega_2$ be arbitrary. Moreover the following statement is important. The probability

$$\mathbb{P}\left[\mathbf{dist}(\mathbf{q}_Z, \partial \mathbf{Kante}_Z(\mathbf{q})) \leq \frac{C_1}{\ell} \text{ and } R_{10} \left| \mathbf{kante}_Z(\mathbf{q}) = \Delta \right. \right]$$

is based on the random vectors $\mathbf{b}_1, \dots, \mathbf{b}_m$ in correspondence with the polytope $Z = \mathbf{KH}(\mathbf{0}, \mathbf{b}_1, \dots, \mathbf{b}_m)$. Those vectors possess (as shown above) the distribution:

$$\mathbf{b}_i \sim \mathcal{N}_2(\bar{\mathbf{b}}_i, \sigma^2 \cdot \mathbf{E}_2).$$

Furthermore it holds that

$$\|\bar{\mathbf{b}}_i\| \leq 9 \quad (4.65)$$

for all $i = 1, \dots, m$. Since we see the property (4.65) with respect to the norm of the centers, we are at the moment not able to apply the most significant result from section 4.3, Lemma 4.3.4. For that we would need the guarantee that the norms of the centers of the basic random vectors are at most 1. Therefore we scale these vectors $\mathbf{b}_1, \dots, \mathbf{b}_m$ by the factor $\mu = \frac{1}{9}$ and so we receive the new random vectors $\mathbf{c}_1, \dots, \mathbf{c}_m$ with

$$\mathbf{c}_i \sim \mathcal{N}_2 \left(\bar{\mathbf{c}}_i, \left(\frac{\sigma}{9} \right)^2 \cdot \mathbf{E}_2 \right)$$

and $\|\bar{\mathbf{c}}_i\| = \|\frac{1}{9}\bar{\mathbf{b}}_i\| \leq 1$. They form the polytope $W = \mathbf{K}\mathbf{H}(\mathbf{0}, \mathbf{c}_1, \dots, \mathbf{c}_m)$. On basis of that scaling we have:¹⁰

$$\begin{aligned} & \mathbb{P}_{\mathbf{b}_1, \dots, \mathbf{b}_m} \left[\text{dist}(\mathbf{q}_Z, \partial Kante_Z(\mathbf{q})) \leq \frac{C_1}{\ell} \text{ and } R_{10} \middle| kante_Z(\mathbf{q}) = \Delta \right] \\ &= \mathbb{P}_{\mathbf{c}_1, \dots, \mathbf{c}_m} \left[\text{dist}(\mathbf{q}_W, \partial Kante_W(\mathbf{q})) \leq \frac{C_1}{9\ell} \text{ and } R_{\frac{10}{9}} \middle| kante_W(\mathbf{q}) = \Delta \right]. \end{aligned} \quad (4.66)$$

That equality can in more detailed form be calculated by means of the transformation theorem of the integration theory. But it becomes comprehensible in a simpler way if we take into regard that: For a fixed realization of $\mathbf{b}_1, \dots, \mathbf{b}_m$ and of the corresponding $\mathbf{c}_1, \dots, \mathbf{c}_m$ we have under our notation:

$$\begin{aligned} (\mathbf{b}_1, \dots, \mathbf{b}_m) \in R_{10} &\Leftrightarrow (\mathbf{c}_1, \dots, \mathbf{c}_m) \in R_{\frac{10}{9}} \\ kante_Z(\mathbf{q}) = \Delta &\Leftrightarrow kante_W(\mathbf{q}) = \Delta \end{aligned}$$

as well as

$$\text{dist}(\mathbf{q}_Z, \partial Kante_Z(\mathbf{q})) = 9 \cdot \text{dist}(\mathbf{q}_W, \partial Kante_W(\mathbf{q})).$$

For that reason we are interested in the estimation of the probability (4.66). And we observe the following fact:

$$\mathbb{P}_{\mathbf{c}_1, \dots, \mathbf{c}_m} \left[\text{dist}(\mathbf{q}_W, \partial Kante_W(\mathbf{q})) \leq \frac{C_1}{9\ell} \text{ and } R_{\frac{10}{9}} \middle| kante_W(\mathbf{q}) = \Delta \right] \quad (4.67)$$

$$\leq \mathbb{P}_{\mathbf{c}_1, \dots, \mathbf{c}_m} \left[\text{dist}(\mathbf{q}_W, \partial Kante_W(\mathbf{q})) \leq \frac{C_1}{9\ell} \text{ and } R_2 \middle| kante_W(\mathbf{q}) = \Delta \right]. \quad (4.68)$$

As already stated $\mathbf{c}_i \sim \mathcal{N}_2 \left(\bar{\mathbf{c}}_i, \left(\frac{\sigma}{9} \right)^2 \cdot \mathbf{E}_2 \right)$ with $\|\bar{\mathbf{c}}_i\| \leq 1$. For that reason we can apply Lemma 4.3.4 and so we obtain an upper bound for (4.68). We remind of that statement once more:

¹⁰To improve the perceptibility, we have associated at each probability which of the random vectors are involved.

Lemma (Small Distances).

Let $\mathbf{a}_1, \dots, \mathbf{a}_m \in \mathbb{R}^2$ be normally distributed random vectors with $\mathbf{a}_i \sim \mathcal{N}_2(\bar{\mathbf{a}}_i, \sigma^2 \cdot \mathbf{E}_2)$ and with density functions f_1, \dots, f_m . Moreover let $\|\bar{\mathbf{a}}_i\| \leq 1$ for all $i = 1, \dots, m$ and let $\sigma \leq \frac{1}{2\sqrt{\ln(m)}}$. Then

$$\mathbb{P}[(\mathbf{dist}(\mathbf{v}_Y, \partial \mathbf{Kante}_Y(\mathbf{v})) \leq \epsilon) \wedge R_2 | \mathbf{kante}_Y(\mathbf{v}) = \Delta] \leq 4e^5 \cdot \frac{\epsilon}{\sigma^2}$$

for an arbitrary index set $\Delta = \{j, k\} \subset \{1, \dots, m\}$, where the random vectors have the common density

$$\prod_{i=1}^m f_i(\mathbf{a}_i).$$

In consequence we obtain the identical upper bound for the probability (4.67):

$$\mathbb{P}_{\mathbf{c}_1, \dots, \mathbf{c}_m} \left[\mathbf{dist}(\mathbf{q}_W, \partial \mathbf{Kante}_W(\mathbf{q})) \leq \frac{C_1}{9\ell} \text{ and } R_{\frac{10}{9}} \middle| \mathbf{kante}_W(\mathbf{q}) = \Delta \right] \leq 4e^5 \cdot \frac{C_1}{9\ell} \cdot \left(\frac{9}{\sigma} \right)^2.$$

If we take the estimations carried out into regard, then we may insert that upper bound in the term (4.64). Finally we get to

$$\mathbb{E}[K] \leq 3 \cdot \sup_{\mathbf{b}_1, \dots, \mathbf{b}_m} \lim_{\ell \rightarrow \infty} \ell \cdot 4e^5 \cdot \frac{C_1}{9\ell} \cdot \left(\frac{9}{\sigma} \right)^2 + 1 \leq Const \cdot \frac{1}{\sigma^2}$$

for a suitable absolute constant $Const$. This concludes the proof. \square

In this section we have achieved our main goal, namely the derivation of an upper bound for the expected value of the number of edges of the polygon $P = \mathbf{KH}(\mathbf{a}_1, \dots, \mathbf{a}_m)$. We have summarized all the findings of that chapter and with additional ideas we came to the desired result. The consequences of those results (compare the introducing section 4.1), will be extremely valuable and useful in the Smoothed Analysis of the dimension-by-dimension-algorithm. .

5 Smoothed Analysis Of Complete Linear Optimization

The main topics of this chapter are the following two issues: First we introduce a deterministic algorithm for solving linear optimization problems. Then we carry out a smoothed analysis for that algorithm, which is based on the methods of Spielman, Teng and Vershynin described before.

5.1 Introduction And Main Results

In chapter 3 we have learned about the variants of the Simplex Method which have so far been investigated for the purpose of a smoothed analysis. Both procedures are randomized algorithms. This means that the realization of the algorithm is influenced by certain stochastic decisions. In contrast to that we explain a deterministic solution procedure and we evaluate its smoothed running time. This algorithm is capable to solve the same type of linear optimization problems as before, namely

$$\begin{aligned} & \text{maximize } \langle \mathbf{v}, \mathbf{x} \rangle \\ & \text{s.t. } \langle \mathbf{a}_1, \mathbf{x} \rangle \leq b^1 \\ & \quad \vdots \\ & \quad \langle \mathbf{a}_m, \mathbf{x} \rangle \leq b^m \end{aligned} \tag{LP}$$

with $\mathbf{v}, \mathbf{a}_1, \dots, \mathbf{a}_m \in \mathbb{R}^d$ and $\mathbf{b} := (b^1, \dots, b^m)^T \in \mathbb{R}^m$.

For constructing the solution procedure we combine concepts from [Bor99] as well as from [Ver09]. This delivers in a certain way an algorithmic synthesis of Average-Case-Analysis and Smoothed Analysis.

For the following smoothed analysis we assume that the restriction vectors and the upper bounds in the restrictions are not fixed, but that they vary according to the following perturbation-rule:

$$\mathbf{a}_i \sim \mathcal{N}_d(\bar{\mathbf{a}}_i, \sigma^2 \cdot \mathbf{E}_d)$$

and

$$b^i \sim \mathcal{N}(\bar{b}^i, \sigma^2)$$

for all $i = 1, \dots, m$. In addition we assume

$$\|(\bar{\mathbf{a}}_i, \bar{b}^i)\| \leq 1$$

for all i . This feature can be achieved by a suitable scaling of the data. Based on this principle of perturbation it is our goal to prove the following result :

Theorem 5.1.1 (Smoothed running time of algorithm 5.5.3).

The following problem is to be solved

$$\begin{aligned} & \text{maximize } \langle \mathbf{v}, \mathbf{x} \rangle \\ & \text{s.t. } \bar{\mathbf{A}}\mathbf{x} \leq \bar{\mathbf{b}} \end{aligned} \tag{LP}$$

in dimension $d \geq 2$ with $m > d$ restrictions. In addition we argue under an upper-bound condition for the single restrictions of the form $\max_{i=1, \dots, m} \|(\bar{\mathbf{a}}_i, \bar{b}^i)\| \leq 1$. Then the application of algorithm 5.5.3 requires on the average not more than

$$Const \cdot \left(\frac{1}{\sigma^2} + \frac{(d+1)^4}{\sigma^4} + (\ln m)^2 \cdot (d+1)^6 \right) + 4$$

pivot steps for the solution of the specific perturbed problem. Here $Const$ denotes an absolute constant value.

This result implies - as already mentioned - in contrast to available approaches - an upper bound for smoothed analysis of a purely deterministic realization of the Simplex Method.

The algorithm under consideration will be explained in detail at a later point. But already at this stage we should mention that the shadow vertex algorithm will be used to solve d auxiliary problems in d sequential stages. In order to make use of the necessary bounds on the number of visited or existing shadow vertices, we should restrict its application to problems with unit restrictions ($b^i = 1$). Therefore we are going to solve the original problem by solving certain substitution problems in unit form, i.e.

$$\begin{aligned} & \text{maximize } \langle \mathbf{v}, \mathbf{x} \rangle \\ & \text{s.t. } \langle \mathbf{a}_1, \mathbf{x} \rangle \leq 1 \\ & \quad \vdots \\ & \quad \langle \mathbf{a}_m, \mathbf{x} \rangle \leq 1 \end{aligned} \tag{EP}$$

For that reason we will think about the following question: How can we transform a linear optimization problem of general form into an equivalent unit problem?

But first we should clarify how a unit problem can be solved by means of the dimension-by-dimension algorithm. In that context we note that in a perturbed unit problem only the restriction vectors (not the right hand sides) are disturbed. That means that the unit-property is not destroyed under perturbations.

5.2 Fundamental Geometric Results

This section combines the hitherto known results on the investigation of perturbed polyhedra. We are going to make use of that for the purpose of smoothed analysis of the algorithm in 5.6.

In chapter 4 we have shown the following result:

Corollary 5.2.1 (Number of vertices in dimension $d = 2$).

Let $\mathbf{a}_1, \dots, \mathbf{a}_m$ be stochastically independent and normally distributed random vectors in \mathbb{R}^2 with centers $\bar{\mathbf{a}}_1, \dots, \bar{\mathbf{a}}_m$ whose norm is at most 1 and whose standard deviation is σ . Let the random variable V denote the number of vertices of the two-dimensional polyhedron $X = \{ \mathbf{x} : \langle \mathbf{a}_1, \mathbf{x} \rangle \leq 1, \dots, \langle \mathbf{a}_m, \mathbf{x} \rangle \leq 1 \}$. Then under the perturbation model under consideration it holds that

$$\mathbb{E}[V] \leq \text{Const} \cdot \left(\frac{1}{\sigma^2} + \ln(m) \right).$$

Here the expected value is calculated over the variation of the random vectors $\mathbf{a}_1, \dots, \mathbf{a}_m$ and Const means an absolute constant.

In addition we know from 3.2.1 the following estimation, which had been derived in [Ver09] for the number of shadow vertices of a perturbed polyhedron.

Corollary 5.2.2 (Number of shadow vertices in dimension $d \geq 3$).

Let $d \geq 3$ and let $\mathbf{a}_1, \dots, \mathbf{a}_m$ be independent, normally distributed random vectors in \mathbb{R}^d with centers of norm at most 1 and with standard deviation σ . Now consider a fixed, twodimensional plane E in \mathbb{R}^d and furthermore the perturbed polyhedron $X = \{ \mathbf{x} : \langle \mathbf{a}_1, \mathbf{x} \rangle \leq 1, \dots, \langle \mathbf{a}_m, \mathbf{x} \rangle \leq 1 \}$. Let the random variable S denote the number of shadow vertices of X with regard to the plane E . Then

$$\mathbb{E}[S] \leq \text{Const} \cdot \left(\frac{d^3}{\sigma^4} + d^5 \cdot (\ln m)^2 \right).$$

Again Const denotes an absolute constant.

These two results will play an important role in the following analysis of the algorithm.

5.3 An Algorithm For Solving Linear Unit Problems

This subsection deals with a procedure for the solution of unit problems. The so-called dimension-by-dimension algorithm had been introduced and used by Borgwardt for carrying out his Average-Case-Analysis of the Simplex Method [Bor82a]. It is in addition explained in [Bor87] and [Bor99]. First we are going to look at the principal mode of operation. After that we make a slight modification in order to handle problems with fixed objective function.

First we are in need of some notation.

Definition 5.3.1 (Π_k).

For $\mathbf{x} = (x^1, \dots, x^d)^T \in \mathbb{R}^d$ und $1 \leq k \leq d$ we denote

$$\Pi_k(\mathbf{x}) := \begin{pmatrix} x^1 \\ \vdots \\ x^k \end{pmatrix} \in \mathbb{R}^k.$$

The concrete meaning is that Π_k is an orthogonal projection from \mathbb{R}^d on \mathbb{R}^k , where the last $(d - k)$ components of the vector \mathbf{x} are truncated.

For $1 \leq k \leq d$ (EP_k) will mean the following linear optimization problem in k variables:

$$\begin{aligned} & \text{maximize } \langle \Pi_k(\mathbf{v}), \Pi_k(\mathbf{x}) \rangle \\ & \text{s.t. } \langle \Pi_k(\mathbf{a}_1), \Pi_k(\mathbf{x}) \rangle \leq 1 \\ & \quad \vdots \\ & \quad \langle \Pi_k(\mathbf{a}_m), \Pi_k(\mathbf{x}) \rangle \leq 1. \end{aligned} \tag{EP}_k$$

The feasibility region of (EP_k) will be called X_k . According to the condition of non-degeneracy 2.4.1, which holds in our case with probability 1, this is a k -dimensional polyhedron and it has vertices because of $m > d$. It is important to understand that (EP_d) is identical with the original problem (EP). To gain a solution for (EP), we may apply the following algorithm. It solves for increasing K the sequence of problems (EP_k):

Algorithm 5.3.2 (dimension-by-dimension-algorithm).

input: $\mathbf{A} = (\mathbf{a}_1, \dots, \mathbf{a}_m)^T$ und \mathbf{v}

procedure:

1. Set $k := 1$, $r := 0$ and find a vertex of X_1 .
2. If there is an optimal vertex, find it (\hat{x}^1) of (EP_1). Otherwise go to step 6.
3. If $k = d$ go to step 7. Else set $k := k + 1$ and proceed with the following stage.
4. For some $k \in \{2, \dots, d\}$ a solution of (EP_{k-1}) may be available . We denote it by

$$\begin{pmatrix} \hat{x}^1 \\ \vdots \\ \hat{x}^{k-1} \end{pmatrix}.$$

Then

$$\begin{pmatrix} \hat{x}^1 \\ \vdots \\ \hat{x}^{k-1} \\ 0 \end{pmatrix}$$

is feasible for (EP_k) and it is located on an edge of X_k . Determine

$$\begin{pmatrix} \tilde{x}^1 \\ \vdots \\ \tilde{x}^k \end{pmatrix},$$

this shall denote a vertex incident to the edge under consideration. This vertex is a shadow vertex under projection on the plane $\mathbf{LH}(\Pi_k(\mathbf{e}_k), \Pi_k(\mathbf{v}))$.

5. Use $\mathbf{LH}(\Pi_k(\mathbf{e}_k), \Pi_k(\mathbf{v}))$ as the projection plane and apply the shadow-vertex-algorithm in the point

$$\begin{pmatrix} \tilde{x}^1 \\ \vdots \\ \tilde{x}^k \end{pmatrix},$$

in order to find an optimal vertex

$$\hat{\mathbf{x}} := \begin{pmatrix} \hat{x}^1 \\ \vdots \\ \hat{x}^k \end{pmatrix}$$

for (EP_k) . Go to step 3, if $\hat{\mathbf{x}}$ exists, else go to step 6.

6. A solution for the original problem does not exist as a result of unboundedness. Set $r := 1$. STOP.

7. The vector $\hat{\mathbf{x}} \in \mathbb{R}^d$ is a solution for the original problem (EP_d) . STOP.

output:

In case of $r = 0$ we report the optimal vertex $\hat{\mathbf{x}}$ for (EP)

In case of $r = 1$ the output is “problem unbounded”.

The significant advantage of that procedure, which had also been used in the average-case-analysis, is the fact that for the stages $k = 2, \dots, d$ every time the shadow-vertex algorithm can be used for solving the unit problems (EP_k) . This effort dominates the effort for the complete method. Consequently summing up the effort for the $d - 1$ stages determines the complete effort.

In addition, we want to think about the following fact. For a fixed objective \mathbf{v} may have the following form:

$$\mathbf{v} = \begin{pmatrix} 0 \\ \vdots \\ 0 \\ \mathbf{v}' \end{pmatrix}.$$

Here we have $1 \leq \ell < d$ “zeros at the beginning” and the first component of \mathbf{v}' is different from zero. Then obviously $\Pi_k(\mathbf{v}) = \mathbf{0}$ for all $1 \leq k \leq \ell$, and therefore for the first ℓ iterations the projection plane $\mathbf{LH}(\Pi_k(\mathbf{e}_k), \Pi_k(\mathbf{v})) = \mathbf{LH}(\Pi_k(\mathbf{e}_k), \mathbf{0})$ does not have dimension two. This would make the use of the shadow-vertex algorithm impossible. But we can avoid that difficulty by simply re-ordering the components 1 und $(\ell + 1)$ in the whole problem. The problem after that re-ordering is harmless. Finally we give a short procedure for that action.

Algorithm 5.3.3 (Reordering the components).

input: $\mathbf{A} = (\mathbf{a}_1, \dots, \mathbf{a}_m)^T$ und \mathbf{v}

procedure:

1. Check \mathbf{v} for “beginning zeros”. If there are some, then go to step 2. Else go to step 3.
2. Determine the first component v^i von \mathbf{v} with $v^i \neq 0$. Interchange the components 1 and i of \mathbf{v} as well as $\mathbf{a}_1, \dots, \mathbf{a}_m$. Go to the next step.
3. Consider the matrix $\check{\mathbf{A}}$. formed from the available restriction vectors. Denote the objective vector by $\check{\mathbf{v}}$. STOP.

output:

Output: $\check{\mathbf{A}}$ and $\check{\mathbf{v}}$.

After use of that preprocessing, we can start the dimension-by dimension algorithm.

5.4 Transformation Rules For Linear Optimization Problems

Here we show how to transform an arbitrary canonical linear program into a program consisting almost only of unit restrictions. The demonstrated principle comes from [Ver09] and had been mentioned in 3.2.2. Sometimes we make use of slight modifications. A similar approach can be found in the paper of [Göh13]. The transformation principle under use is in as much important, as we are going to carry out a smoothed analysis of the algorithm and that unit problems can be studied much simpler.

We have a linear optimization of the form

$$\begin{aligned} & \text{maximize } \langle \mathbf{v}, \mathbf{x} \rangle \\ & \text{s.t. } \mathbf{Ax} \leq \mathbf{b}. \end{aligned} \tag{LP}$$

In order to transform (LP) into a problem with dominating ratio of unit restrictions , we interpolate between the restrictions

$$\mathbf{A}\mathbf{x} \leq \mathbf{b}$$

of the original problem and the corresponding unit restrictions

$$\mathbf{A}\mathbf{x} \leq \mathbf{1}.$$

For that purpose we introduce an interpolation variable. So the dimension increases by one. This interpolation variable, denoted by t , attains values in the interval $[0, 1]$. For $t = 1$ the new restrictions should behave like the original ones and for $t = 0$ they should simulate the introduced unit restrictions. So we obtain the modified form

$$\mathbf{A}\mathbf{x} \leq t \cdot \mathbf{b} + (1 - t) \cdot \mathbf{1}.$$

The objective is (at the moment) not modified. It keeps the form

$$\langle \mathbf{v}, \mathbf{x} \rangle + 0 \cdot t.$$

In total we have the new problem

$$\begin{aligned} & \text{maximize } \langle \mathbf{v}, \mathbf{x} \rangle \\ \text{s.t. } & \mathbf{A}\mathbf{x} \leq t \cdot \mathbf{b} + (1 - t) \cdot \mathbf{1} \\ & 0 \leq t \leq 1. \end{aligned}$$

The restrictions may be reformulated as follows:

$$\mathbf{A}\mathbf{x} \leq t \cdot \mathbf{b} + (1 - t) \cdot \mathbf{1} \Leftrightarrow \mathbf{A}\mathbf{x} + t \cdot (\mathbf{1} - \mathbf{b}) \leq \mathbf{1}.$$

So all original restrictions have been replaced by unit restrictions. In detail this means

$$\begin{aligned} & \text{maximize } \langle (\mathbf{v}, 0), (\mathbf{x}, t) \rangle \\ \text{s.t. } & \langle (\mathbf{a}_1, 1 - b^1), (\mathbf{x}, t) \rangle \leq 1 \\ & \vdots \\ & \langle (\mathbf{a}_m, 1 - b^m), (\mathbf{x}, t) \rangle \leq 1 \\ & \langle (0, \dots, 0, 1), (\mathbf{x}, t) \rangle \leq 1 \\ & \langle (0, \dots, 0, -1), (\mathbf{x}, t) \rangle \leq 0. \end{aligned} \tag{Int LP}$$

For simplification we denote the feasible region of (Int LP) by X_{IP} . In addition we mention that we plan to modify the objective in a suitable way to reach some goals. Each time we do that we shall give an hint.

5.5 A Solution Procedure For Arbitrary Linear Optimization Problems

On the basis of the dimension-by-dimension algorithm of 5.3, which can be applied to solve unit problems, and of the interpolation principle from 5.4 we develop a procedure for the solution of general linear optimization problems.¹

5.5.1 Preliminary Considerations

As already known we need an algorithm for problems of the form

$$\begin{aligned} & \text{maximize } \langle \mathbf{v}, \mathbf{x} \rangle \\ & \text{s.t. } \mathbf{A}\mathbf{x} \leq \mathbf{b}. \end{aligned} \tag{LP}$$

Therefore we start with studying the corresponding unit problem

$$\begin{aligned} & \text{maximize } \langle \mathbf{v}, \mathbf{x} \rangle \\ & \text{s.t. } \mathbf{A}\mathbf{x} \leq \mathbf{1}. \end{aligned} \tag{EP}$$

This problem can be treated with the dimension-by-dimension algorithm from section 5.3. If the algorithm announces that the objective of the unit problem is unbounded, then we can stop since the general problem cannot have an optimal point neither.

Proposition 5.5.1 (Unboundedness).

We have a general linear optimization problem (LP). If the corresponding unit problem (EP) is unbounded in the objective, then (LP) cannot have an optimal solution either.

Proof. At first we note that (EP) is always feasible, since the origin is feasible anyway. If (LP) is infeasible, this is trivial. Now let the problem be feasible. As a result of the unboundedness of the unit problem it is clear that there is a $\mathbf{w} \in \mathbb{R}^d$ with $\mathbf{Aw} \leq \mathbf{0}$ und $\langle \mathbf{v}, \mathbf{w} \rangle > 0$. Since (LP) is feasible there is a $\tilde{\mathbf{x}} \in \mathbb{R}^d$ such that $\mathbf{A}\tilde{\mathbf{x}} \leq \mathbf{b}$. Now look at $\tilde{\mathbf{x}} + \lambda\mathbf{w}$ für $\lambda \geq 0$. This point is feasible, since

$$\mathbf{A}(\tilde{\mathbf{x}} + \lambda\mathbf{w}) = \mathbf{A}\tilde{\mathbf{x}} + \lambda\mathbf{Aw} \leq \mathbf{A}\tilde{\mathbf{x}} \leq \mathbf{b}$$

because of $\mathbf{Aw} \leq \mathbf{0}$ and $\lambda \geq 0$. For $\lambda \rightarrow \infty$ we recognize the unboundedness as a result of $\langle \mathbf{v}, \mathbf{w} \rangle > 0$. \square

For the following we may assume that the unit problem is bounded and that an optimal point \mathbf{x}^* exists.² This point can be reached by the dimension-by-dimension algorithm. So we can construct the point $(\mathbf{x}^*, 0)$. On the basis of the results in 5.4 it becomes

¹We make use of the same partition into Phase 1 and Phase 2 as in [Ver09]. The solution of Phase 2 simulates the strategy of Vershynin as well.

²As we have nondegeneracy, 2.4.1 the optimal point is unique.

clear that this point is feasible in X_{IP} of the interpolation problem. As a reminder we list the system leading to X_{IP} once more

$$\begin{aligned} \langle (\mathbf{a}_1, 1 - b^1), (\mathbf{x}, t) \rangle &\leq 1 \\ &\vdots \\ \langle (\mathbf{a}_m, 1 - b^m), (\mathbf{x}, t) \rangle &\leq 1 \\ \langle (0, \dots, 0, 1), (\mathbf{x}, t) \rangle &\leq 1 \\ \langle (0, \dots, 0, -1), (\mathbf{x}, t) \rangle &\leq 0. \end{aligned}$$

Let $\Delta = \{\Delta^1, \dots, \Delta^d\}$ be the index set of the at \mathbf{x}^* tight restrictions of the (EP). Then the optimality of \mathbf{x}^* and the polar cone theorem 2.3.4 deliver :

$$\mathbf{v} \in \mathbf{KK}(\mathbf{a}_{\Delta^1}, \dots, \mathbf{a}_{\Delta^d}),$$

so there is a $\mathbf{y} \in \mathbb{R}^d$ such that a $\mathbf{y} \geq \mathbf{0}$ exists, which leads to

$$\mathbf{v} = \sum_{i=1}^d y^i \cdot \mathbf{a}_{\Delta^i}. \quad (5.1)$$

Take into regard the restrictions belonging to Δ of the interpolation problem (Int LP):

$$\begin{aligned} \langle (\mathbf{a}_{\Delta^1}, 1 - b^{\Delta^1}), (\mathbf{x}, t) \rangle &\leq 1 \\ &\vdots \\ \langle (\mathbf{a}_{\Delta^d}, 1 - b^{\Delta^d}), (\mathbf{x}, t) \rangle &\leq 1. \end{aligned}$$

As we easily see, these are tight for $(\mathbf{x}^*, 0)$. Also this holds for the restriction

$$\langle (0, \dots, 0, -1), (\mathbf{x}, t) \rangle \leq 0,$$

so $(\mathbf{x}^*, 0)$ delivers a vertex of X_{IP} . With \mathbf{y} from (5.1) we form the vector

$$\sum_{i=1}^d y^i \cdot \begin{pmatrix} \mathbf{a}_{\Delta^i} \\ 1 - b^{\Delta^i} \end{pmatrix} + \begin{pmatrix} \mathbf{0} \\ -1 \end{pmatrix} =: \begin{pmatrix} \mathbf{v} \\ v^+ \end{pmatrix} \quad (5.2)$$

and we notice, that on the basis of its construction it must be an element of the polar cone of $(\mathbf{x}^*, 0)$. So the vertex $(\mathbf{x}^*, 0)$ is optimal in X_{IP} with regard to the objective (\mathbf{v}, v^+) . v^+ does not have a specific meaning. It is a result of applying the coefficient vector \mathbf{y} from (5.1) no longer on the originals \mathbf{a}_{Δ^i} for $i = 1, \dots, d$ but now on the extended vectors $(\mathbf{a}_{\Delta^i}, 1 - b^{\Delta^i})$.

We summarize: We have constructed $(\mathbf{x}^*, 0)$ as a vertex of X_{IP} . This is optimal with respect to the objective direction (\mathbf{v}, v^+) . In addition, the interpolation variable has the value 0 at the moment.

Now it is our goal, to find a vertex of X_{IP} , which has the form $(\mathbf{x}^{**}, 1)$. Then \mathbf{x}^{**} would be a vertex for our original problem (LP). So it makes sense to optimize in direction $(0, \dots, 0, 1)^T$. For that purpose we are able to apply the shadow-vertex-algorithm. We start at the vertex $(\mathbf{x}^*, 0)$ and use the corresponding auxiliary vector (\mathbf{v}, v^+) . So $\mathbf{LH}((\mathbf{0}, 1), (\mathbf{v}, v^+))$ is the projection plane under use. By the way we obtain the output $(\mathbf{x}^{**}, t^{**})$.³ If $t^{**} < 1$, then the original problem is infeasible and we can stop. For $t^{**} = 1$ the original problem is feasible and \mathbf{x}^{**} is a vertex as desired. By some additional considerations we can even recognize that in that case \mathbf{x}^{**} is optimal for (LP).

Lemma 5.5.2 (Optimality of \mathbf{x}^{**}).

Let $(\mathbf{x}^{**}, t^{**})$ be the vector which has been calculated by means of the procedure described above. If $t^{**} = 1$, then \mathbf{x}^{**} is optimal for our original problem (LP).

Proof. We prove the lemma by contradiction. Under our precondition the point delivered by the algorithm is of the form $(\mathbf{x}^{**}, 1)$.

Assume that \mathbf{x}^{**} is not optimal for the original problem, i.e. for

$$\begin{aligned} &\text{maximize } \langle \mathbf{v}, \mathbf{x} \rangle \\ &\text{s.t. } \mathbf{A}\mathbf{x} \leq \mathbf{b}. \end{aligned} \tag{LP}$$

Instead let $\hat{\mathbf{x}}$ be an optimal vertex and better than \mathbf{x}^{**} . Then

$$\langle \mathbf{v}, \hat{\mathbf{x}} \rangle > \langle \mathbf{v}, \mathbf{x}^{**} \rangle. \tag{5.3}$$

Besides let Δ be the index set of the tight restrictions in $\hat{\mathbf{x}}$. Then the polar cone theorem 2.3.4 guarantees the existence of $\mathbf{z} \in \mathbb{R}^d$ with $\mathbf{z} \geq \mathbf{0}$ such that

$$\mathbf{v} = \sum_{i=1}^d z^i \cdot \mathbf{a}_{\Delta^i}.$$

Now look at the point $(\hat{\mathbf{x}}, 1)$, which is a vertex of X_{IP} and in addition optimal with respect to the objective direction $(0, \dots, 0, 1)$. We list the tight restrictions at $(\hat{\mathbf{x}}, 1)$:

$$\begin{aligned} &\langle (\mathbf{a}_{\Delta^1}, 1 - b^{\Delta^1}), (\mathbf{x}, t) \rangle \leq 1 \\ &\vdots \\ &\langle (\mathbf{a}_{\Delta^d}, 1 - b^{\Delta^d}), (\mathbf{x}, t) \rangle \leq 1 \\ &\langle (0, \dots, 0, 1), (\mathbf{x}, t) \rangle \leq 1. \end{aligned}$$

The theorem delivers the following insight: The vertex $(\hat{\mathbf{x}}, 1)$ is optimal with respect to the objective

$$\begin{pmatrix} \mathbf{v} \\ \hat{v} \end{pmatrix} := \sum_{i=1}^d z^i \cdot \begin{pmatrix} \mathbf{a}_{\Delta^i} \\ 1 - b^{\Delta^i} \end{pmatrix} + \begin{pmatrix} \mathbf{0} \\ 1 \end{pmatrix}$$

³Note that this problem cannot be unbounded because of $t \leq 1$.

and is in consequence a shadow vertex with respect to the projection plane under use $\mathbf{LH}((\mathbf{0}, 1), (\mathbf{v}, v^+))$. Observing the just constructed vector (\mathbf{v}, \hat{v}) (vertex $(\hat{\mathbf{x}}, 1)$ is optimal) and the auxiliary objective (\mathbf{v}, v^+) from (5.2) (vertex $(\mathbf{x}^*, 0)$ is optimal) we ensure in addition that $\hat{v} \geq v^+$. Hence the vector (\mathbf{v}, \hat{v}) is contained in the cone $\mathbf{KK}((\mathbf{0}, 1), (\mathbf{v}, v^+))$. Further we make use of both vectors and we define for $\lambda \in [0, 1]$ the convex combination

$$\begin{pmatrix} \mathbf{v} \\ v_\lambda \end{pmatrix} := \lambda \cdot \begin{pmatrix} \mathbf{v} \\ v^+ \end{pmatrix} + (1 - \lambda) \cdot \begin{pmatrix} \mathbf{v} \\ \hat{v} \end{pmatrix},$$

The two points $(\hat{\mathbf{x}}, 1)$ as well as $(\mathbf{x}^{**}, 1)$ will be evaluated with respect to that convex combination. So we obtain the bound

$$\langle (\mathbf{v}, v_\lambda), (\hat{\mathbf{x}}, 1) \rangle = \langle \mathbf{v}, \hat{\mathbf{x}} \rangle + v_\lambda \stackrel{(\diamond)}{>} \langle \mathbf{v}, \mathbf{x}^{**} \rangle + v_\lambda = \langle (\mathbf{v}, v_\lambda), (\mathbf{x}^{**}, 1) \rangle. \quad (5.4)$$

The strict inequality (\diamond) is a result of the optimality of $\hat{\mathbf{x}}$ for (LP) and the corresponding upper bound from (5.3). Let further $(\mathbf{x}_\lambda, t_\lambda)$ be an optimal point for X_{IP} in direction (\mathbf{v}, v_λ) .⁴ In combination with (5.4) we obtain

$$\langle (\mathbf{v}, v_\lambda), (\mathbf{x}_\lambda, t_\lambda) \rangle \geq \langle (\mathbf{v}, v_\lambda), (\hat{\mathbf{x}}, 1) \rangle > \langle (\mathbf{v}, v_\lambda), (\mathbf{x}^{**}, 1) \rangle.$$

So we note that for all objective directions from the (part-)cone

$$\mathbf{KK}\left(\begin{pmatrix} \mathbf{v} \\ v^+ \end{pmatrix}, \begin{pmatrix} \mathbf{v} \\ \hat{v} \end{pmatrix}\right) \subset \mathbf{KK}\left(\begin{pmatrix} \mathbf{v} \\ v^+ \end{pmatrix}, \begin{pmatrix} \mathbf{0} \\ 1 \end{pmatrix}\right)$$

the vertex $(\mathbf{x}^{**}, 1)$ cannot be optimal. Remember how the shadow-vertex algorithm works: the auxiliary vector \mathbf{r} (\mathbf{v}, v^+) is rotated in the direction $(\mathbf{0}, 1)$. So we can conclude that the vertex $(\hat{\mathbf{x}}, 1)$ is attained even before $(\mathbf{x}^{**}, 1)$ will be reached. Under that condition the algorithm would have to stop at $(\hat{\mathbf{x}}, 1)$ at the latest because of the obvious optimality in direction $(0, \dots, 0, 1)$. This contradicts the condition that $(\mathbf{x}^{**}, 1)$ had been calculated by the shadow-vertex algorithm. Hence there is no $\hat{\mathbf{x}}$ feasible for (LP) with $\langle \mathbf{v}, \hat{\mathbf{x}} \rangle > \langle \mathbf{v}, \mathbf{x}^{**} \rangle$. This ensures the optimality of \mathbf{x}^{**} . This proves the lemma. \square

5.5.2 Algorithmic Realization

Based on the considerations of the last section 5.5.1 we construct a procedure for solving linear optimization problems of the form

$$\begin{aligned} & \text{maximize } \langle \mathbf{v}, \mathbf{x} \rangle \\ & \text{s.t. } \mathbf{A}\mathbf{x} \leq \mathbf{b} \end{aligned} \quad (\text{LP})$$

⁴Such a point exists, since unboundedness is impossible

Our strategy is as follows: On the basis of (LP) we construct the corresponding unit problem (EP). This will then be treated by means of the dimension-by-dimension algorithm. We can stop if unboundedness is recognized. In that case the original problem is either infeasible or unbounded, too. If (EP) has an optimum, we can use that point in order to construct a vertex for the interpolation problem. Starting from that vertex we try in the following step to find a feasible point for the original problem. In case that we are successful, we have automatically obtained an optimal solution.

The algorithm for that realization runs as follows:

Algorithm 5.5.3 (Solution procedure for (LP)).

input: $\mathbf{A} = (\mathbf{a}_1, \dots, \mathbf{a}_m)^T$, \mathbf{b} und \mathbf{v}

procedure:

Phase 1 Solve (EP), the unit problem corresponding to (LP) with the help of the dimension-by-dimension algorithm from section 5.3. If this delivers a solution \mathbf{x}^* , then construct the feasible point $(\mathbf{x}^*, 0)$ for the interpolation problem (Int LP) and start Phase 2. If in contrast the algorithm reports unboundedness, then the original problem has no solution. STOP.

Phase 2 Solve the interpolation problem starting from the vertex $(\mathbf{x}^*, 0)$ and the corresponding auxiliary objective (\mathbf{v}, v^+) as defined in section 5.5.1. The actual optimization direction can be chosen as $(0, \dots, 0, 1)^T$. Let $(\mathbf{x}^{**}, t^{**})$ denote the solution calculated by means of the shadow-vertex algorithm. If $t^{**} < 1$, then our original problem is infeasible. If $t^{**} = 1$ then \mathbf{x}^{**} is an optimal solution for the original problem (LP). STOP.

output:

If we have an abort in phase 1 and as well in the case $t^{**} < 1$ the report should be “problem has no solution”. Else the output should be i \mathbf{x}^{**} .

The definition of that algorithm was the goal of this section. In the following we will study the smoothed behaviour of that algorithm.

5.6 Smoothed Analysis Of The Algorithm

In this section we want to derive an upper bound for the smoothed running time of the algorithm introduced in the last section 5.5.2 . According to our perturbation principle we have input data $\mathbf{A} = (\mathbf{a}_1, \dots, \mathbf{a}_m)^T$ und \mathbf{b} distributed as follows

$$\mathbf{a}_i \sim \mathcal{N}_d(\bar{\mathbf{a}}_i, \sigma^2 \cdot \mathbf{E}_d) \text{ sowie } b^i \sim \mathcal{N}(\bar{b}^i, \sigma^2)$$

and we assume that $\|(\bar{\mathbf{a}}_i, \bar{b}^i)\| \leq 1$ for $i = 1, \dots, m$. In addition we fix the objective vector \mathbf{v} .

We remark that the number of necessary pivot steps can be evaluated for Phase 1 and for Phase 2 separately.⁵

Now let us start with the investigation of both Phases.

5.6.1 The Number Of Pivot Steps In Phase 1

The aim of Phase 1 is the solution of (EP), which has the form

$$\begin{aligned} & \text{maximize } \langle \mathbf{v}, \mathbf{x} \rangle \\ & \text{s.t. } \langle \mathbf{a}_1, \mathbf{x} \rangle \leq 1 \\ & \quad \vdots \\ & \quad \langle \mathbf{a}_m, \mathbf{x} \rangle \leq 1. \end{aligned} \tag{EP}$$

As we know from 5.5.2 we make use of the dimension-by-dimension algorithm 5.3.2. For that reason we refer to the insights of section 5.3 and we make use of the fact that the total number of pivot steps is simply the sum of the numbers of pivot steps of the single stages.

The following definition will be helpful.

Definition 5.6.1 (S_k and s_k).

On the basis of the problem data $\mathbf{A} = (\mathbf{a}_1, \dots, \mathbf{a}_m)^T$, \mathbf{v} and referring to the notation introduced in 5.3 we define the following random variables for the stages $k = 2, \dots, d$ of the dimension-by-dimension algorithm:

1. Let S_k be the number of shadow vertices of X_k with respect to the two-dimensional plane $\mathbf{LH}(\Pi_k(\mathbf{e}_k), \Pi_k(\mathbf{v}))$. For $k = 2$ this is just the number of vertices of X_2 , now called S_2 .
2. Let s_k stand for the number of performed pivot steps for the solution of (EP_k) in stage k .

Since we apply the shadow-vertex algorithm in each stage, we have

$$s_k \leq S_k.$$

So as long as we are looking for upper bounds it is feasible to evaluate the expectation values of S_k . We remind that the feasible region X_k of (EP_k) is defined as follows:

$$X_k = \{ \mathbf{x} \in \mathbb{R}^k : \langle \Pi_k(\mathbf{a}_1), \mathbf{x} \rangle \leq 1, \dots, \langle \Pi_k(\mathbf{a}_m), \mathbf{x} \rangle \leq 1 \}. \tag{5.5}$$

⁵We use the considerations introduced in 5.4 for an interpolation and we follow in significant parts the procedure used in [Ver09]. For this reason one will find similar structures. But at some places the argumentation will differ.

The restriction vectors determining X_k are the result of truncations of the original vectors $\mathbf{a}_1, \dots, \mathbf{a}_m$, where the last $(d - k)$ components have been removed. In detail this is achieved formally by linear transformations :

$$\Pi_k(\mathbf{a}_i) = \underbrace{\begin{pmatrix} 1 & 0 & \cdots & 0 & 0 & \cdots & 0 \\ 0 & 1 & \cdots & 0 & 0 & \cdots & 0 \\ \ddots & & & \vdots & & & \vdots \\ 0 & 0 & \cdots & 1 & 0 & \cdots & 0 \end{pmatrix}}_{=: \mathbf{P}_k} \cdot \begin{pmatrix} a_i^1 \\ a_i^2 \\ \vdots \\ a_i^d \end{pmatrix}.$$

For arbitrary k the projection matrix $\mathbf{P}_k \in \mathbb{R}^{k \times d}$ has the following structure: In the first k columns we find the unit matrix $\mathbf{E}_k \in \mathbb{R}^{k \times k}$. The remaining $(d - k)$ columns are filled up with values 0. Based on that transformation and taking into regard that for the distribution of \mathbf{a}_i

$$\mathbf{a}_i \sim \mathcal{N}_d(\bar{\mathbf{a}}_i, \sigma^2 \cdot \mathbf{E}_d)$$

holds, we can apply Lemma 2.2.2 and conclude that $\Pi_k(\mathbf{a}_i)$ is distributed as follows

$$\Pi_k(\mathbf{a}_i) \sim \mathcal{N}_k(\mathbf{P}_k \cdot \bar{\mathbf{a}}_i, \mathbf{P}_k (\sigma^2 \cdot \mathbf{E}_d) \mathbf{P}_k^T).$$

Taking into regard that

$$\mathbf{P}_k \cdot \mathbf{E}_d \cdot \mathbf{P}_k^T = \mathbf{E}_k$$

and using the notation $\bar{\mathbf{a}}_i^{(k)} := \Pi_k(\bar{\mathbf{a}}_i)$ we obtain the simplified form:

$$\Pi_k(\mathbf{a}_i) \sim \mathcal{N}_k(\bar{\mathbf{a}}_i^{(k)}, \sigma^2 \cdot \mathbf{E}_k).$$

Here

$$\|\bar{\mathbf{a}}_i^{(k)}\| \leq \|(\bar{\mathbf{a}}_i, \bar{b}^i)\| \leq 1.$$

Exploiting these results in combination with the representation from (5.5) for X_k , we can apply Corollary 5.2.1 for stage $k = 2$:

$$\mathbb{E}[S_2] \leq C_1 \cdot \left(\frac{1}{\sigma^2} + \ln(m) \right).$$

Here C_1 is an absolute constant. Since $s_2 \leq S_2$, and based on the monotony of the expected value we obtain

$$\mathbb{E}[s_2] \leq C_1 \cdot \left(\frac{1}{\sigma^2} + \ln(m) \right). \quad (5.6)$$

For stages $k = 3, \dots, d$ we apply Corollary 5.2.2 and we obtain in combination with $s_k \leq S_k$

$$\mathbb{E}[s_k] \leq C_2 \cdot \left(\frac{k^3}{\sigma^4} + k^5 \cdot (\ln m)^2 \right), \quad (5.7)$$

Again C_2 is an absolute constant. For the number of pivot steps necessary to solve Phase 1 (explicitly)

$$\sum_{k=2}^d s_k$$

we observe (5.6) und (5.7) and we have the estimations

$$\mathbb{E} \left[\sum_{k=2}^d s_k \right] \leq C_1 \cdot \left(\frac{1}{\sigma^2} + \ln(m) \right) + C_2 \cdot \sum_{k=3}^d \left(\frac{k^3}{\sigma^4} + k^5 \cdot (\ln m)^2 \right).$$

This proves the following Lemma.

Lemma 5.6.2 (Number of necessary pivot steps in Phase 1).

The average number of pivot steps for the solution of Phase 1 under application of the dimension-by-dimension algorithm is not greater than

$$C_1 \cdot \left(\frac{1}{\sigma^2} + \ln(m) \right) + C_2 \cdot \sum_{k=3}^d \left(\frac{k^3}{\sigma^4} + k^5 \cdot (\ln m)^2 \right).$$

Again C_1 und C_2 are absolute constants..

Now the Smoothed Analysis for Phase 1 is complete..

5.6.2 The Number Of Pivot Steps In Phase 2

As known from 5.5.1 we start Phase 2 at the vertex $(\mathbf{x}^*, 0)$ of the interpolation problem (Int LP). Here \mathbf{x}^* denotes the optimal solution of the unit problem (EP). In addition we have seen that this vertex is optimal on the feasible region X_{IP} of the interpolation problems be in direction

$$\begin{pmatrix} \mathbf{v} \\ v^+ \end{pmatrix}$$

with

$$v^+ = \sum_{i=1}^d y^i \cdot (1 - b^{\Delta^i}) - 1.$$

$\Delta = \{\Delta^1, \dots, \Delta^d\}$ means the index set of the tight restrictions in \mathbf{x}^* of (EP). The actual optimization direction was $(0, \dots, 0, 1)^T$. So the shadow-vertex algorithm uses the projection plane

$$\mathcal{H} := \mathbf{LH} \left(\begin{pmatrix} \mathbf{v} \\ v^+ \end{pmatrix}, \begin{pmatrix} \mathbf{0} \\ 1 \end{pmatrix} \right).$$

A detailed consideration shows that the plane \mathcal{H} depends on the perturbed input data of (LP) since v^+ is involved. This causes a conflict with the rigorous conditions of the shadow-vertex-estimations in Corollary 5.2.2. But we are able to avoid and to clear away that conflict by taking into regard that

$$\mathbf{LH} \left(\begin{pmatrix} \mathbf{v} \\ v^+ \end{pmatrix}, \begin{pmatrix} \mathbf{0} \\ 1 \end{pmatrix} \right) = \mathbf{LH} \left(\begin{pmatrix} \mathbf{v} \\ 0 \end{pmatrix}, \begin{pmatrix} \mathbf{0} \\ 1 \end{pmatrix} \right).$$

However \mathcal{H} is a fixed two-dimensional plane which we use for application of the shadow-vertex algorithm. Before continuing with the analysis, we introduce a notation and make a remark.

Definition 5.6.3 (S_{d+1} und s_{d+1}).

On the basis of the input data $\mathbf{A} = (\mathbf{a}_1, \dots, \mathbf{a}_m)^T$, \mathbf{b} und \mathbf{v} we define the following random variables

1. Let S_{d+1} be the number of shadow vertices of X_{IP} with respect to the plane \mathcal{H} .
2. Furthermore let s_{d+1} stand for the number of pivot steps carried out for Phase 2.

Remark 5.6.4.

The number s_{d+1} of the pivot steps which will actually be carried out essentially equates the number of those shadow vertices of X_{IP} with respect to the plane \mathcal{H} belonging to the cone

$$\mathbf{KK} \left(\begin{pmatrix} \mathbf{v} \\ v^+ \end{pmatrix}, \begin{pmatrix} \mathbf{0} \\ 1 \end{pmatrix} \right). \quad (5.8)$$

This observation directly delivers $s_{d+1} \leq S_{d+1}$. A second look at the cone in question shows that it is not allowed to substitute the last component v^+ in the first vector by the value 0. So we conclude: The cone corresponding to the actual number of steps s_{d+1} for solving Phase 2 is highly correlated with the restriction vectors via the role of v^+ . Anyhow, as we have seen above, that correlation and dependence does not play any role when we are investigating the upper bound S_{d+1} . So, if the purpose is the derivation of the upper bound, we may ignore those difficulties and dependencies.

This remark justifies that in the following we may concentrate on the estimation of the mean value of S_{d+1} of shadow vertices. We remind that the feasible region X_{IP} of the interpolation problems is as follows:

$$\begin{aligned} \langle (\mathbf{a}_1, 1 - b^1), (\mathbf{x}, t) \rangle &\leq 1 \\ &\vdots \\ \langle (\mathbf{a}_m, 1 - b^m), (\mathbf{x}, t) \rangle &\leq 1 \\ \langle (0, \dots, 0, 1), (\mathbf{x}, t) \rangle &\leq 1 \\ \langle (0, \dots, 0, -1), (\mathbf{x}, t) \rangle &\leq 0. \end{aligned}$$

The last two restrictions are based on the fixed vectors $(0, \dots, 0, 1)^T$ and $(0, \dots, 0, -1)^T$. A precise look shows that both lie in the plane \mathcal{H} . Hence we conclude a very useful fact. First have a look at the orthogonal projection of X_{IP} on the plane \mathcal{H} . The last two restrictions should be ignored for the moment. An example for the resulting shadow can be found in 5.1.

After that let us take the two additional restrictions into regard. We make use of the fact that the corresponding restriction vectors lie in the plane \mathcal{H} . So we obtain the slightly modified projection polygon as shown in 5.2 .

A comparison of the two representations shows that adding the two restrictions delivers four new vertices, which are highlighted in the second representation. Besides a lot of former vertices will become infeasible. We are not able to make precise statements about their number. This allows to make the following general statement: With respect to the plane \mathcal{H} the number of shadow vertices S_{d+1} of X_{IP} is at most by four larger than the number of shadow vertices \widehat{S}_{d+1} of

$$\widehat{X}_{IP} := \{\mathbf{x} : \langle (\mathbf{a}_1, 1 - b^1), (\mathbf{x}, t) \rangle \leq 1, \dots, \langle (\mathbf{a}_m, 1 - b^m), (\mathbf{x}, t) \rangle \leq 1\}.$$

The polyhedron \widehat{X}_{IP} is totally defined by unit vectors which are on their part based on normally distributed random variables. In addition from condition $\|(\bar{\mathbf{a}}_i, \bar{b}^i)\| \leq 1$ for $i = 1, \dots, m$ we obtain the estimation

$$\max_{i=1, \dots, m} (\|(\bar{\mathbf{a}}_i, 1 - \bar{b}^i)\|) \leq 2.$$

When we want to apply Corollary 5.2.2 then the norms of the centers of the restriction vectors have to be one at most. In order to reach that goal, we must multiply all $(\mathbf{a}_1, 1 - b^1), \dots, (\mathbf{a}_m, 1 - b^m)$ by $\frac{1}{2}$. So we get for $i = 1, \dots, m$ the vectors

$$(\mathbf{p}_i, q^i) \sim \mathcal{N}_{d+1} \left((\bar{\mathbf{p}}_i, \bar{q}^i), \left(\frac{\sigma}{2}\right)^2 \cdot \mathbf{E}_{d+1} \right).$$

In the proof for Corollary 5.2.2 we had proceeded in a very similar way. There we have recognized that the mean value for the number of shadow vertices does not change under that scaling⁶. So we can apply the Corollary and we can conclude that

$$\mathbb{E} [\widehat{S}_{d+1}] \leq C_3 \cdot \left(\frac{(d+1)^3}{\sigma^4} \cdot 2^4 + (d+1)^5 \cdot (\ln m)^2 \right)$$

for an absolute constant C_3 . Taking into consideration that $s_{d+1} \leq S_{d+1} \leq \widehat{S}_{d+1} + 4$ and by use of $C_4 := 2^4 \cdot C_3$ we obtain

$$\mathbb{E} [s_{d+1}] \leq C_4 \cdot \left(\frac{(d+1)^3}{\sigma^4} + (d+1)^5 \cdot (\ln m)^2 \right) + 4.$$

So we have proven the following Lemma.

⁶Compare the proof to 3.2.3 in section 3.2.1.

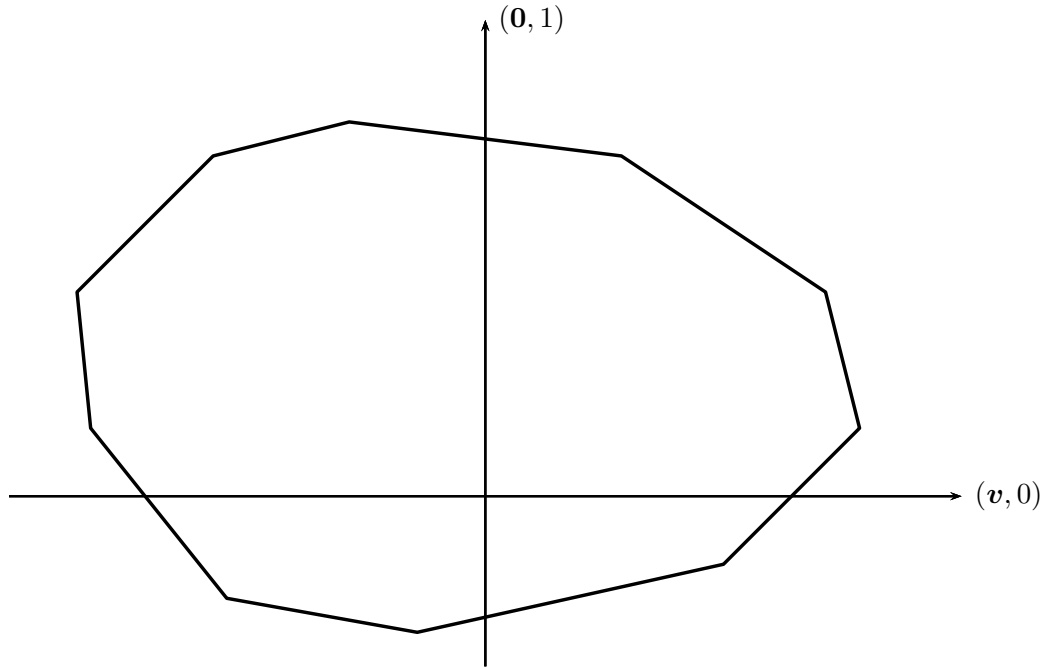


Figure 5.1: projection-polygon of X_{IP} under ignorance of the restrictions for the interpolation variable t

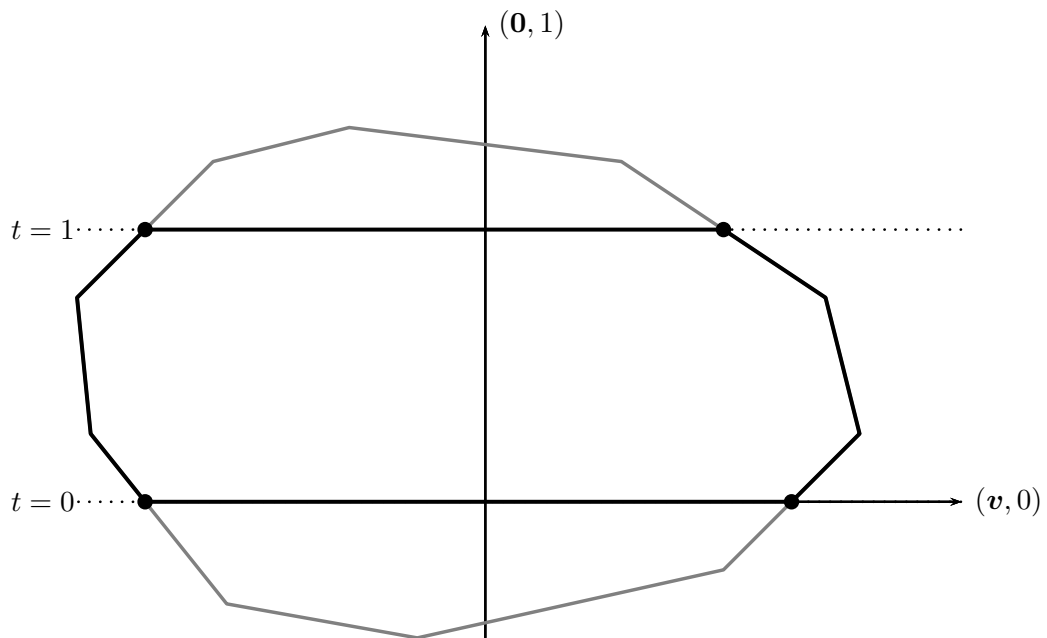


Figure 5.2: projection-polygon of X_{IP} with regard to the restrictions for the interpolation variable t

Lemma 5.6.5 (number of pivot steps in Phase 2).

For the application of the shadow-vertex algorithm the solution of Phase 2 in algorithm 5.5.3 requires on the average not more than

$$C_4 \cdot \left(\frac{(d+1)^3}{\sigma^4} + (d+1)^5 \cdot (\ln m)^2 \right) + 4$$

pivot steps. Here C_4 is an absolute constant..

5.6.3 Combination Of Results

Now we combine the two upper bounds for Phase 1 and Phase 2 in order to prove theorem 5.1.1 from section 5.1, which reads as follows:

Theorem 5.6.6 (Smoothed analysis of algorithm 5.5.3).

Consider the linear optimization problem

$$\begin{aligned} & \text{maximize } \langle \mathbf{v}, \mathbf{x} \rangle \\ & \text{s.t. } \bar{\mathbf{A}}\mathbf{x} \leq \bar{\mathbf{b}} \end{aligned} \tag{LP}$$

in dimension $d \geq 2$ with $m > d$ restrictions. Furthermore we make the assumption that $\max_{i=1,\dots,m} \|(\bar{\mathbf{a}}_i, \bar{b}^i)\| \leq 1$. Then application of algorithm 5.5.3 does on the average require not more than

$$Const \cdot \left(\frac{1}{\sigma^2} + \frac{(d+1)^4}{\sigma^4} + (\ln m)^2 \cdot (d+1)^6 \right) + 4$$

pivot steps for the solution of a corresponding perturbed problem. $Const$ is an absolute constant.

Proof. We combine the insights from Lemma 5.6.2 as well as from Lemma 5.6.5. So we obtain the upper bound for the average number of steps:

$$\begin{aligned} & C_1 \cdot \left(\frac{1}{\sigma^2} + \ln(m) \right) + C_2 \cdot \sum_{k=3}^d \left(\frac{k^3}{\sigma^4} + k^5 \cdot (\ln m)^2 \right) \\ & + C_4 \cdot \left(\frac{(d+1)^3}{\sigma^4} + (d+1)^5 \cdot (\ln m)^2 \right) + 4. \end{aligned}$$

Resorting delivers

$$\begin{aligned}
 & C_1 \cdot \frac{1}{\sigma^2} + C_2 \cdot \sum_{k=3}^d \frac{k^3}{\sigma^4} + C_4 \cdot \frac{(d+1)^3}{\sigma^4} \\
 & + C_1 \cdot \ln(m) + C_2 \cdot \sum_{k=3}^d (k^5 \cdot (\ln m)^2) + C_4 \cdot (d+1)^5 \cdot (\ln m)^2 + 4 \\
 & \leq \max \{C_1, C_2, C_4\} \cdot \left(\frac{1}{\sigma^2} + \frac{1}{\sigma^4} \cdot \sum_{k=3}^{d+1} k^3 \right) + \max \{C_1, C_2, C_4\} \cdot (\ln m)^2 \cdot \sum_{k=2}^{d+1} k^5 + 4 \\
 & \leq \max \{C_1, C_2, C_4\} \cdot \left(\frac{1}{\sigma^2} + \frac{(d+1)^4}{\sigma^4} + (\ln m)^2 \cdot (d+1)^6 \right) + 4 \\
 & \leq Const \cdot \left(\frac{1}{\sigma^2} + \frac{(d+1)^4}{\sigma^4} + (\ln m)^2 \cdot (d+1)^6 \right) + 4.
 \end{aligned}$$

This proves the proposition. □

Now we have reached the main goal of this section. For a conclusion we summarize the results and make some remarks.

5.7 Summary And Comments

The conception of a specific algorithm for the solution of general linear optimization problems and the calculation of its smoothed running time were the main intentions of this chapter.

Both aspects were motivated by the hitherto existing smoothed analysis of the Simplex Method by Spielman and Teng [ST04] and by Vershynin [Ver09]. Both investigations have been demonstrated in chapter 3. Spielman and Teng could derive a polynomial smoothed running time for the algorithm under their consideration. Ignoring logarithmic factors their upper bound has the order of $\mathcal{O}(m^{86}d^{55}\sigma^{-30})$. So this is rather a qualitative than a quantitative result. We have also seen that Vershynin could achieve a significantly decreased order by using a refined geometric analysis. Section 3.2.2 has demonstrated, that he employs a randomized form of Phase 1 for that purpose.. For achieving a success he can give a minimal probability. Hence he guarantees that on the average only a constant number of repetitions is necessary. But the following points should be kept in mind:

1. For a specific problem instance certain circumstances may enforce the algorithm to carry out a number of repetitions of Phase 1 which is significantly greater than the average value.

2. Furthermore the average running time will not only be influenced by the perturbation of input data but also be random decisions of the algorithm. This leads to the drawback that for a specific problem formulation we are not able to distinguish the impact of the data structure from the impact of random decisions on the running time.
3. The choice of an auxiliary vector \mathbf{u} causes an influence of the rotation symmetry model (which had been used for the Average-Case-Analysis [Bor87]). It is questionable if this is justified under the starting intention to replace average case results by something else which holds for each problem (Smoothed Analysis).

All these three drawbacks have been avoided in the approach used in our investigation. Algorithm 5.5.3 is a deterministic calculation procedure. And it solves each problem according to an exactly prescribed principle. As a consequence, the smoothed running time is a result of the disturbances of the input data only.

6 Computation Time Of Phase 2 In The Case Of Stochastic Dependency

In this chapter we perform an empirical study of the number of pivot steps in Phase 2 of the Simplex Method under various conditions for the generation of a start vertex. For the introduction we want to give a motivation in the background of the results obtained in this work so far. After that we will list the fundamentals of this analysis. And finally we shall draw the according conclusions. In addition we want to direct the focus on some interesting observations and to try to give some plausibility-explanations for these.

6.1 Introduction And Motivation

In chapter 5 we have dealt with the construction and analysis of the dimension-by-dimension algorithm for the solution of linear optimization problems. The motivation for the study of that procedure lies in the possibility of a rigorous theoretical analysis (and in the avoidance of randomization). But this algorithmic approach is not used in and is not recommended for practical calculations because of its higher arithmetical effort. This results from the dimension-wise application of the shadow-vertex algorithm in d stages in order to get to a specific start vertex for the next stage. This is different in the usual practical approach consisting of only two Phases. There the first Phase has only the task to find any vertex of the polyhedron. And this is then used as start vertex for Phase 2.

In the following we shall go away from that somehow artificial procedure and we will focus on the classical two-Phase approach for the Simplex Method. The essential task of Phase 1 is to clarify the question whether the problem is feasible and if it is to calculate any vertex. Starting from that vertex we initiate a real optimization process for finding the best resp. optimal vertex for the problem. If we plan to apply the shadow vertex in Phase 2, we need as known an additional auxiliary objective function for which our starting vertex for Phase 2 would be optimal. In general it is not possible to fix such an auxiliary objective a priori, i.e. before our calculations. Instead we must pick the according objective vector from the polar cone of the available start vertex. The effect of that limitation is the dependency of this chosen direction from the original restriction vectors, i.e. the data of the problem. But the theoretical results on the (expected) numbers of shadow vertices rely on the independency of (\mathbf{u}) from

those data. So that method used in practical applications does not admit a rigorous theoretical analysis..

As already mentioned, we know a solution method, namely the dimension-by-dimension method ensuring the desired stochastic independence and guaranteeing theoretical upper bounds. But that method is somehow circumstantial as it requires d Phases instead of two. But the cost of avoidance of d -Phases would be the loss of stochastic independence.

If one is very sceptical one would suspect that the stochastic dependence in the practical method has fatal impacts on the running time resp. number of pivot steps in Phase 2. That means that this would yield prolongations of Phase 2. Therefore we dedicate this to the following central question:

Has the loss of guarantee for stochastic independence in practical applications a significant increasing impact on the average number of pivot steps in Phase 2? And do the theoretical bounds still hold although the condition of independence is neglected?

The described fear accompanies the investigations at all times. It constitutes the starting point for the subsequent investigation. For clarification of that question we will carry out an empirical average-case-analysis. For that empirical analysis we make use of the so-called rotation-symmetry-distribution in the sense of the definition in chapter 1 for having a stochastic distribution model.¹ The rotation-symmetry-model has been valuable for the successful average-case-analysis of the Simplex Method [Bor87] of Borgwardt. Before starting the investigation, we want to present some fundamentals about rotation-symmetric distributions.

6.2 Rotational-Symmetric Distributions

In this section we give a short survey over the class of rotation symmetric distributions. The information stems from [Bor87] and from [Bor07], where further interesting aspects can be found. One of the most famous representatives of that class is the multivariate normal or Gaussian distribution. This distribution features for a d -dimensional, real-valued random vector \mathbf{U} the density function

$$f_{\mathbf{U}}(\mathbf{u}) = \left(\frac{1}{\sqrt{2\pi}} \right)^d \cdot e^{-\frac{\|\mathbf{u}\|^2}{2}}.$$

If we consider two possible realizations \mathbf{u}_1 and \mathbf{u}_2 of those random variables, then assuming the condition $\|\mathbf{u}_1\| = \|\mathbf{u}_2\|$ yields under insertion in the density function

$$f_{\mathbf{U}}(\mathbf{u}_1) = f_{\mathbf{U}}(\mathbf{u}_2). \quad (6.1)$$

¹The definiton of smoothed running time from chapter 1 would not admit to study that question in the context of a smoothed analysis.

This is the essential property characterizing rotation symmetric distributions. To simplify the following considerations, we want to concentrate on those rotation symmetric distributions, that feature a density function.² So we are going to call a d -dimensional random vector \mathbf{U} rotation-symmetrically distributed, if for any two arbitrary realizations \mathbf{u}_1 and \mathbf{u}_2 with $\|\mathbf{u}_1\| = \|\mathbf{u}_2\|$ just the equality of the corresponding density function values $f_{\mathbf{U}}$ as in (6.1) holds. Based on that property we can introduce for $r \geq 0$ a so-called radial density $g_{\mathbf{U}}(r)$ which is a cumulated density over all points with radius r . Formally this means:

$$g_{\mathbf{U}}(r) := \int_{\omega_d(r)} f_{\mathbf{U}}(\mathbf{u}) d\mathbf{u} = \lambda_{d-1}(\omega_d(r)) \cdot f_{\mathbf{U}}(\bar{\mathbf{u}}),$$

where for $\bar{\mathbf{u}}$ just $\|\bar{\mathbf{u}}\| = r$ holds. Furthermore one is able (as Borgwardt remarks) to characterize a rotation symmetric distribution uniquely by its so-called *radial distribution function*. This is for $0 \leq r < \infty$ just

$$F_{\mathbf{U}}(r) := \mathbb{P}[\|\mathbf{U}\| \leq r] = \int_0^r g_{\mathbf{U}}(r) dr.$$

It describes the probability that a random realization of \mathbf{U} has a distance to the origin of at most r .

After that look on rotation-symmetrical distributions from a very general point of view, we are going to focus on a special class of rotation-symmetrical distributions. They have played an important role in the average-case-analysis of convex-hull-algorithms.³ The following definition and characterization of that subclass stems from the paper [Bor07] of Borgwardt. That subclass is parametrized by a parameter $\kappa > -1$. For the according radial distribution function we have :

$$F_{\kappa}(r) = \begin{cases} \frac{\int_0^r (1-\tau^2)^{\kappa} \tau^{d-1} d\tau}{\int_0^1 (1-\tau^2)^{\kappa} \tau^{d-1} d\tau} & \text{für } 0 \leq r \leq 1, \\ 1 & \text{für } r > 1. \end{cases} \quad (6.2)$$

So we obtain for the corresponding radial density function:

$$g_{\kappa}(r) := \begin{cases} \frac{(1-r^2)^{\kappa} r^{d-1} d\tau}{\int_0^1 (1-\tau^2)^{\kappa} \tau^{d-1} d\tau} & \text{für } 0 \leq r \leq 1, \\ 0 & \text{für } r > 1. \end{cases} \quad (6.3)$$

²For the desired empirical investigation this is no essential restriction.

³Compare the papers [Bor07], [Bor97] and [Wör11].

Two essential points attract attention at this place. The support for that family of distributions is in any case the unit ball Ω_d , and we can use the parameter κ to weight certain radii between 0 and 1 in a desired way. For $\kappa \rightarrow -1$ the weight lies on the boundary of the ball. For $\kappa \rightarrow \infty$ the weight accumulates near the center of the ball and the outer region is devaluated. There are some prominent special cases. They are listed in the following table:

κ	consequence	Remark
$\kappa = 0$	g_κ constant on Ω_d	uniform distribution on Ω_d
$\kappa \rightarrow -1$	total dominance at $r = 1$	uniform distribution on ω_d
$\kappa \rightarrow \infty$	total dominance at $r = 0$	complete centralization
$\kappa = \frac{d-1}{2}$	symmetry of the distribution about $r = \frac{1}{2}$	

Table 6.1: Interesting special cases in the rotation-symmetric distribution family

For the following investigation we want to concentrate on the special case $\kappa \rightarrow -1$, i.e. the uniform distribution on the unit sphere. This distribution can be simulated numerically in a very efficient way. And it seems to be plausible that the insights obtained by the way will be transferable to the whole class of distributions.

For the generation of uniform distributions on the unit sphere we would like to avoid the use of the mentioned radial density- and distribution- function. This has the reason that the numerical integral evaluations turn out to be computationally rather intensive and often very instable. But we have a much simpler way to generate the simulation data. Remember the beginning of this section, where we have got to know the multivariate standard normal distribution as one prominent element from the class of rotationally symmetrical distributions. There is a close relationship between this distribution and the uniform distribution on the unit sphere. This will be clarified in the following Lemma.

Lemma 6.2.1.

Let \mathbf{W} be a random vector distributed according to the multivariate standard normal distribution in dimension d , i.e. $\mathbf{W} \sim \mathcal{N}_d(\mathbf{0}, \mathbf{E}_d)$. Then the normalized random vector

$$\mathbf{U} := \frac{\mathbf{W}}{\|\mathbf{W}\|}$$

is uniformly distributed on the unit sphere ω_d in \mathbb{R}^d .

Proof. The Lemma is a direct consequence of the definition of the random variable \mathbf{U} combined with the rotation symmetry of the multivariate standard normal distribution. \square

In view of our goal to generate uniformly distributed random vectors on ω_d we first generate a d -dimensional, normally distributed random vector \mathbf{W} . Afterwards we normalize this vector to give it length 1. This discloses a further essential advantage of our method: For the generation of one random vector \mathbf{W} we need only d independent, standard normally distributed random variables W_1, \dots, W_d . From these we are able to calculate the random vector $\mathbf{W} := (W_1, \dots, W_d)^T$. For the generation of the single values W_i there are efficient numerical standard methods as for instance the Polarmethod [MB64], which we are going to use.

In the next section we discuss in detail the algorithmic aspects of the empirical study, which will turn out to be important.

6.3 The Algorithmic Principle Of The Investigation

The content of this section is subdivided in two main subjects. In the first part we will explain how Phase 1 in our investigation is organized. In the second part we shall discuss the two variants for Phase 2 and we are going to compare their efficiency. Besides we shall develop a geometrical interpretation of the method used in Phase 1. This will at a later point be helpful, when we try to explain and to interpret the quantitative effects observed in our empirical studies.

6.3.1 The Phase 1 And Its Geometrical Interpretation

The following investigation is based on the classical Two-Phase-Approach⁴ of the Simplex Method for the solution of problems in the form

$$\begin{aligned} & \text{maximize } \langle \mathbf{v}, \mathbf{x} \rangle \\ & \text{s.t. } \mathbf{Ax} \leq \mathbf{1}. \end{aligned} \tag{EP}$$

For $\mathbf{A} = (\mathbf{a}_1, \dots, \mathbf{a}_m)^T$ and \mathbf{v} we stick to the introduced dimensions and again X will denote the feasible region. For our problem class the origin is always feasible due to the positive right hand sides. So the two stages have the following goals :

Phase 1 Find a vertex \mathbf{x}_s of X .⁵

Phase 2 Now try to optimize starting from \mathbf{x}_s in \mathbf{v} -direction, until either an optimal \mathbf{x}_* is available or it becomes obvious that the optimization problem cannot be completed, because of unboundedness of the objective.

Figure 6.1 shows an example of a polyhedron given by restriction vectors all of length 1.

⁴Compare section 2.3.1.

⁵Since all right hand sides of the restrictions are positive, the standard procedure used in this section is suited for Phase 1. Compare for instance [Bor01].

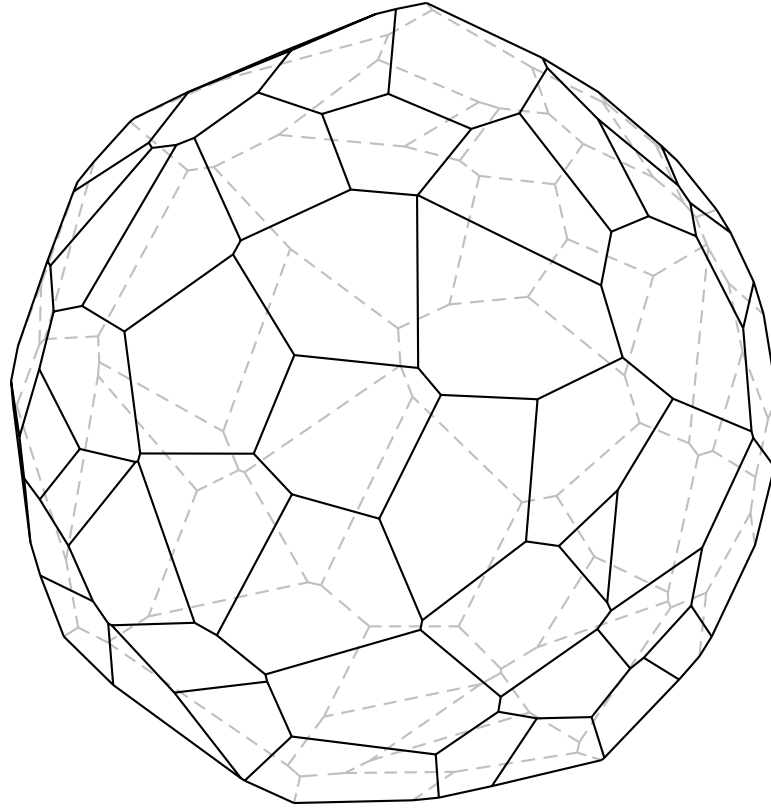


Figure 6.1: A polyhedron defined by unit constraints

For easier notation in further considerations the following definition will be helpful.

Definition 6.3.1 ($X^{(i)}$).

For $i = 1, \dots, d$ we define the constructed feasible regions

$$X^{(i)} := \{ \mathbf{x} : \mathbf{Ax} \leq \mathbf{1}, x^i \geq 0, \dots, x^d \geq 0 \}.$$

In addition we set $X^{(d+1)} := X$.

For the start of Phase 1 we establish the property of being a vertex in an artificial way. This is done by introduction of sign-restrictions $\mathbf{x} \geq \mathbf{0}$ on the feasible region $X^{(1)}$. So we are able to set up the feasible Tableau for our objective direction \mathbf{v} on $X^{(1)}$ directly for starting the Simplex Method:

	\mathbf{a}_1	\mathbf{a}_2	\cdots	\mathbf{a}_m	$-\mathbf{e}_1$	\cdots	$-\mathbf{e}_d$	\mathbf{v}
$-\mathbf{e}_1$								
\vdots								
$-\mathbf{e}_d$								
	1	1	\cdots	1	0	\cdots	0	0

Tableau 6.1: A potential Start-Tableau for solving a unit problem

The restriction vectors $-\mathbf{e}_1, \dots, -\mathbf{e}_d$ result from the sign conditions

$$\mathbf{x} \geq \mathbf{0} \Leftrightarrow -x^1 \leq 0, \dots, -x^d \leq 0.$$

In the first Phase we start from $\mathbf{0}$ and search for a Tableau corresponding to a feasible vertex of X . This is achieved in d pivot steps by successive pivot steps removing those vectors from the basis which correspond to the auxiliary restrictions. This is explained in detail in the following algorithm.

Algorithm 6.3.2 (Phase 1/Search for a vertex of X).

Input: A und v

Initialization:

Set up the start Tableau using the original data 6.1. After that set $i := 1$ for the iteration variable i and set the current iteration point on $\mathbf{w}_1 := \mathbf{0}$. This is a vertex of $X^{(1)}$.

Iteration (while $i \leq d$):

1. Check whether the vector $-\mathbf{e}_i$ can be removed from the basis. This would correspond to a slackening of the restriction $-x^i \leq 0$. If this is impossible because of unboundedness, then go to step 2. Else go to step 3.
2. Transform the restriction $-x^i \leq 0$ into $x^i \leq 0$. Numerically this is done by multiplication of the corresponding Tableau-row by -1 . The resulting restriction vector \mathbf{e}_i can be removed from the basis.⁶ After that go to step 3.
3. Execute the according pivot step. So one moves from \mathbf{w}_i to the next iteration point \mathbf{w}_{i+1} . This is feasible for X and it is a vertex of $X^{(i+1)}$. The Tableau has the structure demonstrated in 6.2.
4. Mark complementary to step 3 the Tableau-column to $-\mathbf{e}_i$, such that this column will be disregarded in future selections of pivot columns. Finally set $i := i + 1$.

Output:

The point \mathbf{w}_{d+1} is a vertex of $X^{(d+1)} = X$. Report this point resp. the corresponding Tableau and stop.

Before proceeding, it pays to consider the role of the sign restrictions: As stated in the algorithm, after removal of $\pm \mathbf{e}_i$ from the basis the corresponding sign restriction loses its validity and it will therefore be disregarded in future steps for the pivot selection. This procedure means a successive extension of the feasible region in the form

⁶If one uses the stochastic model introduced in section 6.2 for the generation of problem instances, then these instances satisfy the condition of nondegeneracy 2.4.1 almost surely. For that reason we can without loss of generality assume, that no line space exists. This can only appear in the case of degeneracy. Hence the removal of the new restriction vector \mathbf{e}_i is surely possible.

	a_1	a_2	\cdots	a_m	$-e_1$	\cdots	$-e_i$	$-e_{i+1}$	\cdots	$-e_d$	v
a_{j_1}	*	*		*	*		*	0		0	*
\vdots	\vdots	\vdots	\ddots	\vdots	\vdots	\ddots	\vdots	\vdots	\ddots	\vdots	\vdots
a_{j_i}	*	*		*	*		*	0		0	*
$-e_{i+1}$	*	*		*	*		*	1		0	*
\vdots	\vdots	\vdots	\ddots	\vdots	\vdots	\ddots	\vdots		\ddots	\vdots	\vdots
$-e_d$	*	*		*	*		*	0		1	*
	*	*	\cdots	*	w_{i+1}^1	\cdots	w_{i+1}^i	0	\cdots	0	*

 Tableau 6.2: Tableau-structure after removal of the i th sign restriction

$$X^{(1)} \rightsquigarrow X^{(2)} \rightsquigarrow \dots \rightsquigarrow X^{(d)} \rightsquigarrow X^{(d+1)} = X.$$

For execution of Phase 2 we can directly use the Tableau, that has been calculated by the algorithm described above. Here is its structure:

	a_1	a_2	\cdots	a_m	$-e_1$	\cdots	$-e_d$	v
a_{j_1}	*	*		*	*		*	*
\vdots	\vdots	\vdots	\ddots	\vdots	\vdots	\ddots	\vdots	\vdots
a_{j_d}	*	*		*	*		*	*
	*	*	\cdots	*	w_{d+1}^1	\cdots	w_{d+1}^d	*

Tableau 6.3: Tableau-Structure after the end of Phase 1

The $-e_i$ -columns should be regarded separately from the block of genuine restrictions. Their future role is only for statistical purposes. So the Tableau has exactly the form as mentioned in section 2.3.2.

After having discussed the algorithmic procedure in Phase 1, we profit from an attempt to interpret what happens, geometrically. For that demonstration let the polyhedron from figure 6.1 serve as the starting point. The introduction of sign restrictions $\mathbf{x} \geq 0$ diminishes that to the polyhedron shown in figure 6.2. As remarked, the origin will be a feasible vertex for that latter polyhedron. It is marked as a grey point in the illustration.

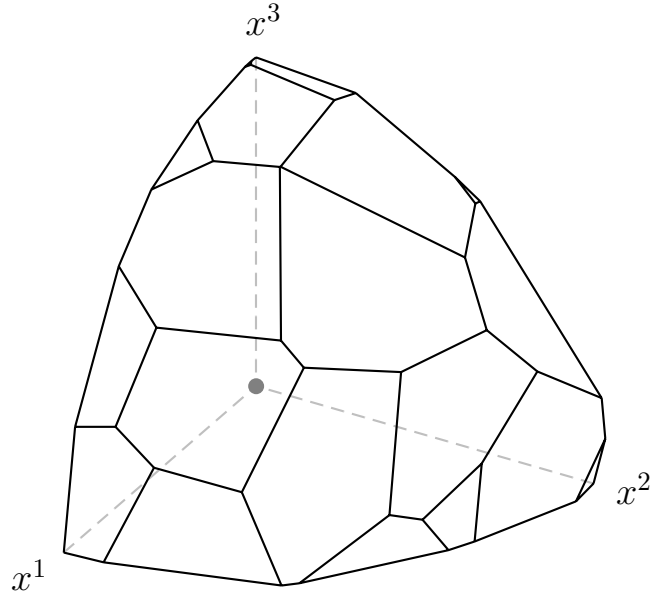


Figure 6.2: The polyhedron diminished by the sign restrictions $x^1, x^2, x^3 \geq 0$ from figure 6.1

Caused by the removal of $-\mathbf{e}_1$ from the basis we walk from the origin on that edge having just the direction \mathbf{e}_1 . We stop that movement in the moment when we arrive at an adjacent vertex. Now the loss of the first sign restriction enlarges our polyhedron by the set of all points in the original polyhedron, whose first component is negative while all its other components are still nonnegative. So we arrive at the configuration illustrated in figure 6.3. The current vertex is marked as a black point.

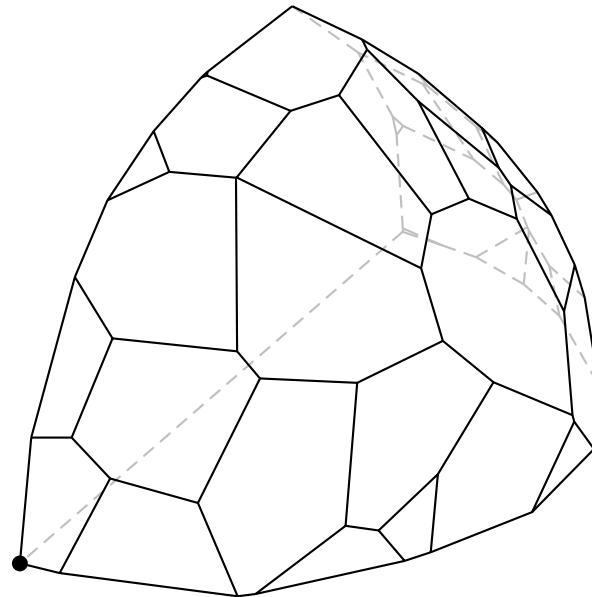


Figure 6.3: The polyhedron diminished by the sign restrictions $x^2, x^3 \geq 0$ from figure 6.1

Remark 6.3.3.

As already taken into account in algorithm 6.3.2, it may happen that during the i -th step the restriction $x_i \geq 0$ cannot be slackened, because the according movement direction \mathbf{d}_i is not stopped at the boundary. Then we are also unable to find a successor vertex \mathbf{w}_{i+1} von $X^{(i+1)}$. The reason is that \mathbf{d}_i is an unlimited direction in $X^{(i+1)}$ respectively in X . In that case we react by “flipping” the restriction. Consequently the successor point resp. vertex will be seeked in direction $-\mathbf{d}_i$. For the essential procedure this does not make a difference.

In our example $\mathbf{d}_1 = \mathbf{e}_1$ has turned out to be a possible movement direction. Else we had chosen the direction $-\mathbf{d}_1 = -\mathbf{e}_1$ and we had carried out the analogous movement. The second iteration step leads to the configuration illustrated in figure 6.4. The current iteration point is again emphasized.

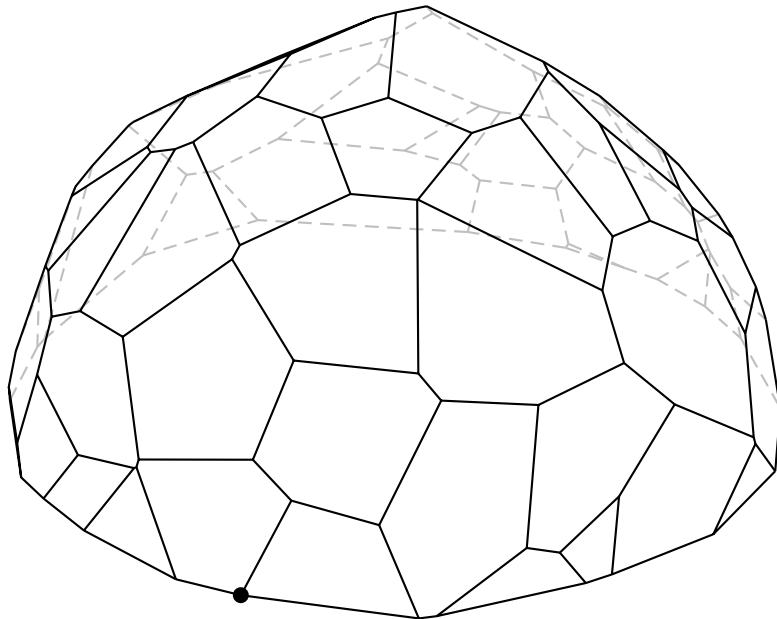


Figure 6.4: The polyhedron diminished by the sign restriction $x^3 \geq 0$ from figure 6.1

In the final step the temporary feasible region extends to the complete original polyhedron and we can see the marked vertex of X in figure 6.5. Now we are going to start the second Phase at that vertex.

After the study of the procedure in Phase 1 and with the knowledge of its geometrical meaning, we come to another consideration. This will be helpful for the argumentation in section 6.6. As known, in the first Phase an iteration sequence is constructed:

$$\mathbf{w}_1 \rightsquigarrow \mathbf{w}_2 \rightsquigarrow \dots \rightsquigarrow \mathbf{w}_{d+1}$$

This sequence leads to a vertex of the feasible X . We emphasize that there is a significant difference between the first and the remaining $(d-1)$ steps: In the transition from

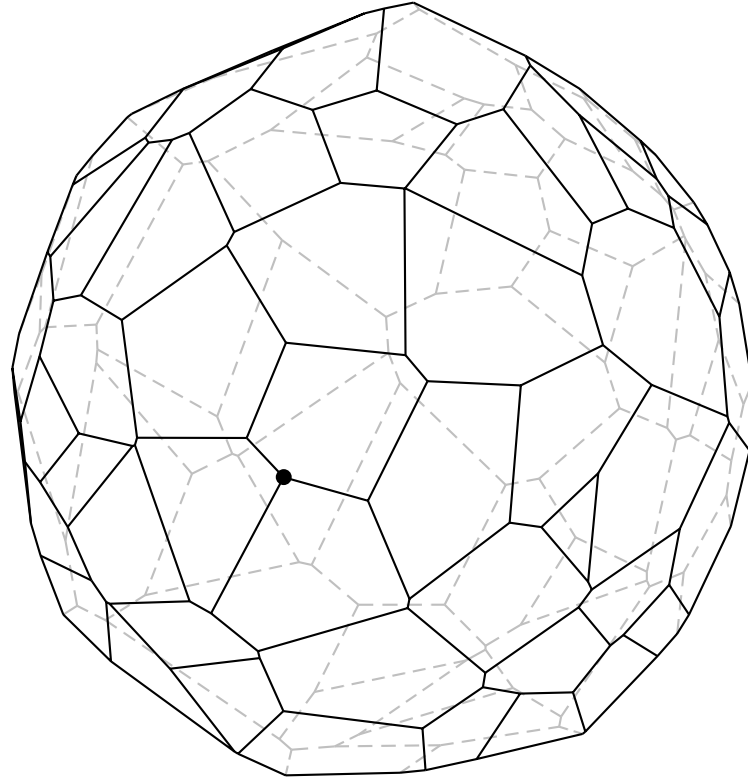


Figure 6.5: The polyhedron from figure 6.1 with the vertex determined in Phase 1

\mathbf{w}_1 to \mathbf{w}_2 we walk from an interior point of the feasible region X to a boundary point. This second point is located in a facet, denoted by F . In all the subsequent steps we will never leave that facet F . For graphical illustration the iteration sequence in our example is shown in figure 6.6 once more.

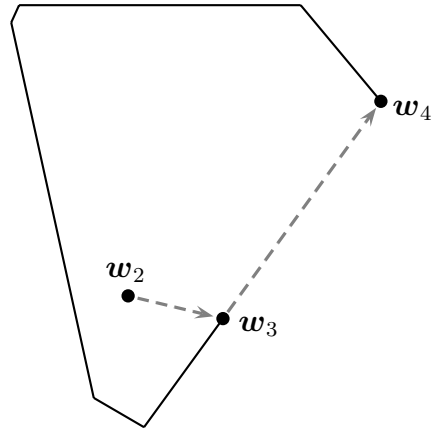


Figure 6.6: Iteration-process in the facet F towards a vertex of X

The course of the iterations can even be described more precisely. Therefore have a look at the Tableau (Tableau 6.2) for step 3 in algorithm 6.3.2. After removal of $-\mathbf{e}_i$ from the basis there are exactly i original restrictions tight at the current iteration

point. Hence it is located in a $(d - i)$ -dimensional face of X . As the facet reached in the first step will never be left again, we can make the statement, that \mathbf{w}_{i+1} lies in a $(d - i)$ -dimensional face of F . Geometrically interpreted the procedure works according to the following principle: Search starting from the current point \mathbf{w}_i , located in the face F_i , the next iteration point \mathbf{w}_{i+1} in a face F_{i+1} , which bounds F_i and whose dimension is 1 less than the dimension of F_i .

Having understood the functionality of Phase 1 we are well prepared for the argumentation in section 6.6.

6.3.2 The Variants Of Phase 2 Under Investigation

In the previous subsection we explained the algorithmic principle of the Phase 1 method under application. Afterwards we discussed essential properties. Based on that we develop in this subsection two possible versions of the shadow vertex algorithm for Phase 2. One of them is theoretically secured, and the other is a usually faster method used in practical applications. For these two versions we calculate the empirical and experimental results given in the following section. In the version motivated from practice we start the second Phase directly from the vertex calculated in Phase 1, namely \mathbf{w}_{d+1} , which resulted from application of the principle described in section 6.3.1. Contrary to that the start of the theoretically secured Phase 2 requires an additional correction ensuring the stochastic independence between the projection plane of the shadow vertex algorithm and the restriction vectors of the problems. The goal of this subsection is to present the functionality of both versions and to discuss relevant aspects with regard to their practical realization.

Practically motivated variant for Phase 2:

After execution of the first Phase a vertex \mathbf{w}_{d+1} of X and a corresponding Tableau for the objective direction \mathbf{v} are at hand. Emanating from that start position we want to apply the shadow vertex algorithm for the search for an optimal point. For that reason we need an additional auxiliary objective direction \mathbf{u}_b , for which the vertex \mathbf{w}_{d+1} is optimal (compare section 2.4.1). Suitable for that is any arbitrary vector from the polar cone⁷ of \mathbf{w}_{d+1} . Since we have nondegeneracy⁸, exactly d restrictions are tight at the vertex \mathbf{w}_{d+1} . The corresponding vectors will be denoted by $\mathbf{a}_{j_1}, \dots, \mathbf{a}_{j_d}$. Using this notation we may for example choose for \mathbf{u}_b the vector

$$\mathbf{u}_b := 1 \cdot \mathbf{a}_{j_1} + \dots + 1 \cdot \mathbf{a}_{j_d}.$$

We extend our Tableau of Phase 1 by one according column for the auxiliary objective direction \mathbf{u}_b , then we obtain

⁷Compare Theorem 2.3.4.

⁸Compare assumption 2.4.1.

	\mathbf{a}_1	\mathbf{a}_2	\cdots	\mathbf{a}_m	$-\mathbf{e}_1$	\cdots	$-\mathbf{e}_d$	\mathbf{v}	\mathbf{u}_b
\mathbf{a}_{j_1}	*	*		*	*		*	*	1
\vdots	\vdots	\vdots	\ddots	\vdots	\vdots	\ddots	\vdots	\vdots	\vdots
\mathbf{a}_{j_d}	*	*		*	*		*	*	1
	*	*	\cdots	*	\mathbf{w}_{d+1}^1	\cdots	\mathbf{w}_{d+1}^d	*	*

Tableau 6.4: Tableau-Structure at the beginning of the practical Phase 2

On that fundamentum we can carry out the shadow vertex algorithm in Tableau-form (compare section 2.4.3). The number of executed pivot steps should be noted in an additional variable.

Now we are prepared to perform Phase 2 for the optimization in direction \mathbf{v} . So the numerical realization is clarified. Let us formulate this procedure in an algorithmic terminology:

Algorithm 6.3.4 (Practical variant for Phase 2).

Input: \mathbf{A} , \mathbf{v} as well as a vertex \mathbf{x}_s of the feasible region X

Procedure:

1. Determine the indices j_1, \dots, j_d for the restrictions tight at \mathbf{x}_s .
2. Choose $\mathbf{u}_b := \mathbf{a}_{j_1} + \dots + \mathbf{a}_{j_d}$ from the polar cone at the vertex \mathbf{x}_s and start the shadow vertex algorithm with auxiliary objective \mathbf{u}_b and with the effective objective direction \mathbf{v} . Save in addition the number of performed pivot steps.
3. After termination or the algorithm fix the $S_{\mathbf{u}_b, \mathbf{v}}$ of totally performed pivot steps. Here it is not essential, whether the problem was unbounded or whether it features an optimum. $S_{\mathbf{u}_b, \mathbf{v}}$ is just one less than the number of shadow vertices of X , which belong to the cone $\mathbf{KK}(\mathbf{u}_b, \mathbf{v})$ ⁹.

Output: $S_{\mathbf{u}_b, \mathbf{v}}$ (Number of performed pivot steps)

As already mentioned, the aim of this chapter is an investigation of the impact of a tolerated stochastic dependency on the running time of Phase 2. So far we have not exactly specified what is meant by stochastic dependency. Having studied the functionality of the practical Phase-2-variant, we can now specify where this dependency comes from. In order to start directly from the vertex \mathbf{x}_s using the shadow vertex algorithm, we are forced to select the auxiliary objective direction out of the polar cone $\mathbf{KK}(\mathbf{a}_{j_1}, \dots, \mathbf{a}_{j_d})$ of that vertex. Hence \mathbf{u}_b does in fact depend on the input data of the problem. And this holds in consequence for the projection plane $\mathbf{LH}(\mathbf{u}_b, \mathbf{v})$, too.

⁹This means here and in the future just the following set of shadow vertices:

$\{\mathbf{x} : \mathbf{x} \text{ vertex of } X \text{ and } \exists \mathbf{z} \in \mathbf{KK}(\mathbf{u}_b, \mathbf{v}), \text{ such that } \mathbf{x} \text{ optimal on } X \text{ resp. } \mathbf{z}\}.$

This is needed for the execution of the shadow vertex algorithm. This fact contradicts the conditions for the theoretical results, but it is usual in practical realizations.

In the following we want to give the details of the theoretically approved variant. Some aspects should be taken into regard.

Theoretically safe variant for Phase 2:

Phase 1 delivers a vertex \mathbf{w}_{d+1} of the feasible region X . In order to start Phase 2 from that vertex, we must select the auxiliary objective out of the polar cone of that vertex. In our theoretically approved version we desire to avoid any potential stochastic dependency, which may occur with that selection. Therefore we change the concept of our algorithmic procedure. We make use of the following principle: First determine a fixed vector $\mathbf{u}_a \in \omega_d$ and try to find an optimal point for that direction with start from the vertex found in Phase 1. From there we can afterwards carry out the shadow vertex algorithm with auxiliary objective vector \mathbf{u}_a for finding the true optimum. Since \mathbf{u}_a is now fixed and was separately chosen, it is stochastically independent from the problem data. So this procedure confirms the conditions for the secure variant in Phase 2. However, it remains to clarify two further questions:

1. How can we estimate the length of the path of shadow vertices between the vertex \mathbf{w}_{d+1} in direction \mathbf{u}_a ? Here we meet the same problems as in the practical Phase 2.
2. What should we do, if we cannot find an optimal point in direction \mathbf{u}_a , but identify unboundedness? Here we are at the moment not ready to start the Phase 2.

The first point is not difficult at all. This comes, because the intermediate optimization process in direction \mathbf{u}_a is only to generate the configuration which ensures the independency of the auxiliary objective from the problem data. So it is absolutely unimportant how many pivot steps will be carried out in that intermediate process.

For handling the second point we will develop a procedure, which is consistent with the secure variant. Using the algorithmic principle of the practical Phase 2 we count (with a difference of 1) the number of shadow vertices traversed in the cone $\mathbf{KK}(\mathbf{u}_b, \mathbf{v})$.¹⁰ For that reason we are in this case mainly interested in the number of shadow vertices traversed in the cone $\mathbf{KK}(\mathbf{u}_a, \mathbf{v})$. Before proceeding, we want to remark, that the algorithm has the only purpose to make our investigation possible and correct. It is not designed to solve problems in the most effective way.

Since we do not want to gain further information about the optimization process, and since we do only want to know the number of shadow vertices resp. of pivot steps, the following procedure works: Starting from the vertex \mathbf{w}_{d+1} we first clarify the question for the existence of a solution in direction \mathbf{u}_a . In the positive case we then start to carry out the shadow vertex algorithm with \mathbf{u}_a in the role of the auxiliary

¹⁰Compare again step 3 in algorithm 6.3.4.

objective vector and with optimization direction \mathbf{v} . And we count the number of pivot steps. In the negative case the process aborts at a vertex $\tilde{\mathbf{w}}$, where unboundedness becomes obvious. But this does not yet admit the conclusion that there are no shadow vertices belonging to the cone $\mathbf{KK}(\mathbf{u}_a, \mathbf{v})$. This would be true only if for any possible objective direction from $\mathbf{KK}(\mathbf{u}_a, \mathbf{v})$ the problem would be unbounded. But exploiting the information available at the vertex $\tilde{\mathbf{w}}$ we are able to restrict the set of directions from $\mathbf{KK}(\mathbf{u}_a, \mathbf{v})$, featuring shadow vertices. Stated more precisely, we can determine a direction $\tilde{\mathbf{u}} \in \mathbf{KK}(\mathbf{u}_a, \mathbf{v})$, for which we know the following: For all possible directions in $\mathbf{KK}(\mathbf{u}_a, \tilde{\mathbf{u}})$ unboundedness holds. Hence there are no shadow vertices in that region. On the basis of that knowledge we optimize in direction $\tilde{\mathbf{u}}$. If we find an optimal point, then we use this vertex as a starting point for the shadow vertex algorithm with auxiliary objective $\tilde{\mathbf{u}}$ and with actual optimization direction \mathbf{v} . By the way we count the number of pivot steps. If in direction $\tilde{\mathbf{u}}$ unboundedness should appear again, then we determine analogously as above a new vector $\hat{\mathbf{u}}$. This will afterwards be used as we would do with $\tilde{\mathbf{u}}$. This process can be continued until either a vertex is reached, from which we can start the shadow vertex algorithm in optimization-direction \mathbf{v} , or until we get to know that there are no such shadow vertices. This principle shall be formulated in algorithmic notation.

Algorithm 6.3.5 (Safe variant for Phase 2).

Input: \mathbf{A} , \mathbf{v} , \mathbf{u}_a and a vertex \mathbf{x}_s of the feasible region X

Prozedur:

1. Optimize starting from \mathbf{x}_s in direction \mathbf{u}_a . If an optimal solution \mathbf{x}_{u_a} can be found, go to step 3. Else unboundedness is true. Then go to step 2.
2. The optimization process has stopped at a vertex $\tilde{\mathbf{w}}$, where unboundedness in direction \mathbf{u}_a could be observed. One could identify an unbounded edge $\tilde{\mathbf{w}} + \mathbf{KK}(\mathbf{d})$ with $\langle \mathbf{u}_a, \mathbf{d} \rangle > 0$. Consider now the objective parametrized by

$$\mathbf{u}_a + \lambda \cdot \mathbf{v}$$

and try to increase λ in order to achieve $\langle \mathbf{u}_a + \lambda \cdot \mathbf{v}, \mathbf{d} \rangle = 0$. For $\langle \mathbf{v}, \mathbf{d} \rangle \geq 0$ this is not possible. In that case go to step 4. For $\langle \mathbf{v}, \mathbf{d} \rangle < 0$ choose

$$\lambda := -\frac{\langle \mathbf{u}_a, \mathbf{d} \rangle}{\langle \mathbf{v}, \mathbf{d} \rangle}$$

and set $\mathbf{u}_a := \mathbf{u}_a + \lambda \cdot \mathbf{v}$. After that go back to step 1.

3. Start the shadow vertex algorithm at the vertex \mathbf{x}_{u_a} . Use \mathbf{u}_a as the vector for the auxiliary objective and optimize in direction \mathbf{v} . Save in the variable $S_{\mathbf{u}_a, \mathbf{v}}$ the number of pivot steps carried out. STOP.
4. For all $\mathbf{z} \in \mathbf{KK}(\mathbf{u}_a, \mathbf{v})$ we observe unboundedness. In that case there are no shadow vertices belonging to the cone $\mathbf{KK}(\mathbf{u}_a, \mathbf{v})$. Hence there are no pivot steps either. For that reason set $S_{\mathbf{u}_a, \mathbf{v}} := 0$. STOP.

Output: $S_{\mathbf{u}_a, \mathbf{v}}$ (number of pivot steps carried out)

Remark 6.3.6.

The parametrization of the objective function used in step 2 in the algorithm above dates back to the introduction of the parametric Simplex variant by Gass and Saaty [GS55]. In our context this procedure is a tool for a correction and modification of the objective in the case of unboundedness. In addition, as we shall see, it delivers information about the practical realization.

Now we want to clarify, how this algorithm can be realized numerically. But before we shall discuss two justified objections.

1. Is it ensured that the procedure always terminates?
2. This algorithm is not very efficient for saving computation time.

For the second point we explain the following: It is not necessary to start the optimization path again from the start vertex x_s after modification of the objective in step 2. Instead one can proceed directly at the vertex $\tilde{\mathbf{w}}$. The algorithmic formulation above is made this way only for simplification of understanding and implementation.

The second point is clarified with the help of the next Lemma. It ensures the finiteness of the procedure.

Lemma 6.3.7.

Algorithm 6.3.5 terminates after finitely many steps in all cases of nondegenerate problems.

Proof. To begin with we state the following: The finiteness of the procedure could only be in danger by an endless repetition of the following process:

- (i) In step 1 we observe unboundedness.
- (ii) For that reason we determine a correction factor λ in step 2.
- (iii) We go back to the first step with the modified auxiliary objective direction $\mathbf{u}_a + \lambda \mathbf{v}$.

But this situation cannot happen, as the following consideration shows. Look at the hypothetical “infinite cycle” in detail. So let in step 1 the problem be unbounded in direction \mathbf{u}_a . This will be observed (compare step 2) at the vertex $\tilde{\mathbf{w}}$ detecting an emanating unbounded edge $\tilde{\mathbf{w}} + \mathbf{K}\mathbf{K}(\mathbf{d})$ featuring $\langle \mathbf{u}_a, \mathbf{d} \rangle > 0$. For that reason we rotate the new objective vector $\mathbf{u}_a + \lambda \mathbf{v}$ by choice of

$$\lambda := -\frac{\langle \mathbf{u}_a, \mathbf{d} \rangle}{\langle \mathbf{v}, \mathbf{d} \rangle}$$

so far in direction \mathbf{v} , that $\langle \mathbf{u}_a + \lambda \mathbf{v}, \mathbf{d} \rangle = 0$ holds. By the way at the vertex $\tilde{\mathbf{w}}$ the edge $\tilde{\mathbf{w}} + \mathbf{K}\mathbf{K}(\mathbf{d})$ will not be regarded during the pivot choice for optimization in direction $\mathbf{u}_a + \lambda \mathbf{v}$. Any further corrections of the objective vector will not change that fact.

Afterwards we start the optimization process with the modified objective $\mathbf{u}_a + \lambda \mathbf{v}$ again from \mathbf{x}_s . If we had an “endless cycle” then we would obtain unboundedness again, either at $\tilde{\mathbf{w}}$ or at another vertex.

Let us discuss that configuration more generally and assume nondegeneracy. Now any vertex \mathbf{x} of X has exactly d emanating edges. Hence for that vertex at most d corrections can be carried out. Afterwards the algorithm cannot stop at \mathbf{x} because of unboundedness anymore.

Summarizing our considerations, we realize: At any one of the finitely many vertices it is not possible to make more than d corrections. This allows only finitely many modifications of the objective. An “infinite cycle”, as assumed, cannot occur for that reason. This ensures the finiteness. \square

Finally we care about the practical realization.

Numerical Realization of Algorithm 6.3.5:

To setup the Tableau in step 1 and in step 3 the following consideration is helpful: As known from 2.3.2, in the statistical part of the Tableau reflects the matrix $(-\mathbf{A}_\Delta^{-1})^T$, where Δ denotes the temporary actual basis index set. If we want to record a further vector $\mathbf{z} \in \mathbb{R}^d$ in the Tableau, then we have to calculate $(\mathbf{A}_\Delta^{-1})^T \mathbf{z}$ from the Tableau data. So these values can be inserted in an additional column.

In combination with the considerations from the practical applied variant we are able obtain the Tableau by means of a simple matrix-vector-multiplication:

	\mathbf{a}_1	\mathbf{a}_2	\cdots	\mathbf{a}_m	$-\mathbf{e}_1$	\cdots	$-\mathbf{e}_d$	\mathbf{u}_a	$\bar{\mathbf{u}}$
\mathbf{a}_{j_1}	*	*		*	*		*	*	1
\vdots	\vdots	\vdots	\ddots	\vdots	\vdots	\ddots	\vdots	\vdots	\vdots
\mathbf{a}_{j_d}	*	*		*	*		*	*	1
	*	*	\cdots	*	\mathbf{x}_s^1	\cdots	\mathbf{x}_s^d	*	*

Tableau 6.5: Tableau at the start of step 1

So we have a start for step 1. In the same way the Tableau

	\mathbf{a}_1	\mathbf{a}_2	\cdots	\mathbf{a}_m	$-\mathbf{e}_1$	\cdots	$-\mathbf{e}_d$	\mathbf{v}	\mathbf{u}_a
\mathbf{a}_{k_1}	*	*		*	*		*	*	*
\vdots	\vdots	\vdots	\ddots	\vdots	\vdots	\ddots	\vdots	\vdots	\vdots
\mathbf{a}_{k_d}	*	*		*	*		*	*	*
	*	*	\cdots	*	$\mathbf{x}_{u_a}^1$	\cdots	$\mathbf{x}_{u_a}^d$	*	*

Tableau 6.6: Tableau for starting step 3

for step 3 can be calculated. The execution of the shadow vertex algorithm runs as described in section 2.4.3.

One important point should still be clarified. How can the correction factor λ in step 2 using the data available at the vertex $\tilde{\mathbf{w}}$ be determined? Therefore we need information from the actual Tableau. In addition we determine the representation of the objective direction \mathbf{v} in terms of the actual basis. For simplification these data are already integrated in the following Tableau and the column for $\bar{\mathbf{u}}$ -Spalte is removed, as it is unnecessary.

	\mathbf{a}_1	\mathbf{a}_2	\cdots	\mathbf{a}_m	$-\mathbf{e}_1$	\cdots	$-\mathbf{e}_d$	\mathbf{u}_a	\mathbf{v}
\mathbf{a}_{j_1}	*	*	\cdots	*	————	\mathbf{d}_1^T	————	ξ^1	ν^1
\vdots	\vdots	\vdots				\vdots		\vdots	\vdots
\mathbf{a}_{j_k}	*	*	\cdots	*	————	\mathbf{d}_k^T	————	ξ^k	ν^k
\vdots	\vdots	\vdots				\vdots		\vdots	\vdots
\mathbf{a}_{j_d}	*	*	\cdots	*	————	\mathbf{d}_d^T	————	ξ^d	ν^d
	*	*	\cdots	*	\tilde{w}^1	\cdots	\tilde{w}^d	*	*

Tableau 6.7: Useful information in the statistical part of the Tableau

In that Tableau the rows of the statistical part have been denoted by $\mathbf{d}_1^T, \dots, \mathbf{d}_d^T$. This reflects the following fact (which will be useful in the following): On the basis of our condition of nondegeneracy we know that at the vertex $\tilde{\mathbf{w}}$ exactly those restrictions are tight that belong to the index set $\Delta = \{j_1, \dots, j_d\}$. So we can set up the basis matrix $\mathbf{A}_\Delta = (\mathbf{a}_{j_1}, \dots, \mathbf{a}_{j_d})^T$. Using these information we can describe the edge-directions emanating from $\tilde{\mathbf{w}}$ as follows:

$$\mathbf{d}_i = -\mathbf{A}_\Delta^{-1} \mathbf{e}_i, \quad i = 1, \dots, d.$$

Here we have just the rows in the statistical part of the Tableau. Irrespective of a potential scaling factor we can find for the edge $\tilde{\mathbf{w}} + \mathbf{K}\mathbf{K}(\mathbf{d})$ the direction in the Tableau. That edge had been detected in the second step of algorithm 6.3.5 disclosing the unboundedness. Assume that this is \mathbf{d}_k . In addition we are going to denote the basis representations in the \mathbf{u}_a - and in the \mathbf{v} -column by $\boldsymbol{\xi}$ and $\boldsymbol{\nu}$. That means:

$$\mathbf{u}_a = \mathbf{A}_\Delta^T \boldsymbol{\xi} \quad \text{and} \quad \mathbf{v} = \mathbf{A}_\Delta^T \boldsymbol{\nu}.$$

Hence it is possible to calculate the correction factor λ in the following way:

$$\begin{aligned}
 \lambda &= -\frac{\langle \mathbf{u}_a, \mathbf{d}_k \rangle}{\langle \mathbf{v}, \mathbf{d}_k \rangle} \\
 &= -\frac{\langle \mathbf{A}_\Delta^T \boldsymbol{\xi}, -\mathbf{A}_\Delta^{-1} \mathbf{e}_k \rangle}{\langle \mathbf{A}_\Delta^T \boldsymbol{\nu}, -\mathbf{A}_\Delta^{-1} \mathbf{e}_k \rangle} \\
 &= -\frac{\langle \mathbf{A}_\Delta^T \boldsymbol{\xi}, \mathbf{A}_\Delta^{-1} \mathbf{e}_k \rangle}{\langle \mathbf{A}_\Delta^T \boldsymbol{\nu}, \mathbf{A}_\Delta^{-1} \mathbf{e}_k \rangle} \\
 &= -\frac{\langle \boldsymbol{\xi}, \mathbf{A}_\Delta \mathbf{A}_\Delta^{-1} \mathbf{e}_k \rangle}{\langle \boldsymbol{\nu}, \mathbf{A}_\Delta \mathbf{A}_\Delta^{-1} \mathbf{e}_k \rangle} \\
 &= -\frac{\langle \boldsymbol{\xi}, \mathbf{e}_k \rangle}{\langle \boldsymbol{\nu}, \mathbf{e}_k \rangle} \\
 &= -\frac{\xi^k}{\nu^k}.
 \end{aligned}$$

So it suffices to know the two entries in the \mathbf{u}_a - and in the \mathbf{v} -column.

In this section we have presented the two algorithms, which form the basis of the empirical investigation. Moreover we have dealt with further aspects as the termination after a finite number of pivot steps and with the numerical realization.

6.4 Empirical Results For The Number Of Pivot Steps

In this section we present the empirical results for the running time of the algorithms introduced in section 6.3.2. So we will be able to clarify, whether the fear formulated in section 6.1, that the non-analyzed practical variant could significantly suffer from the neglection of independency in comparison to the stochastically and theoretically safe variant. First we list some technical details.

1. Average numbers of pivot steps were obtained in the course of $k = 50000$ randomly generated problem instances.
2. The data obtained that way are separated according to different values of the dimensions d and presented in distinct graphics for each dimension. For a fixed value of d always the number of restrictions m varies and this is illustrated in the diagrams.
3. The stochastic principle for generation of the restriction vectors $\mathbf{a}_1, \dots, \mathbf{a}_m$ as well of the objective vector \mathbf{v} is the unit distribution on the unit sphere ω_d . This had been presented in section 6.2.
4. For the auxiliary objective vector \mathbf{u} we always choose the fixed vector \mathbf{e}_1 . This specific choice has due to rotation symmetry no impact on the results.

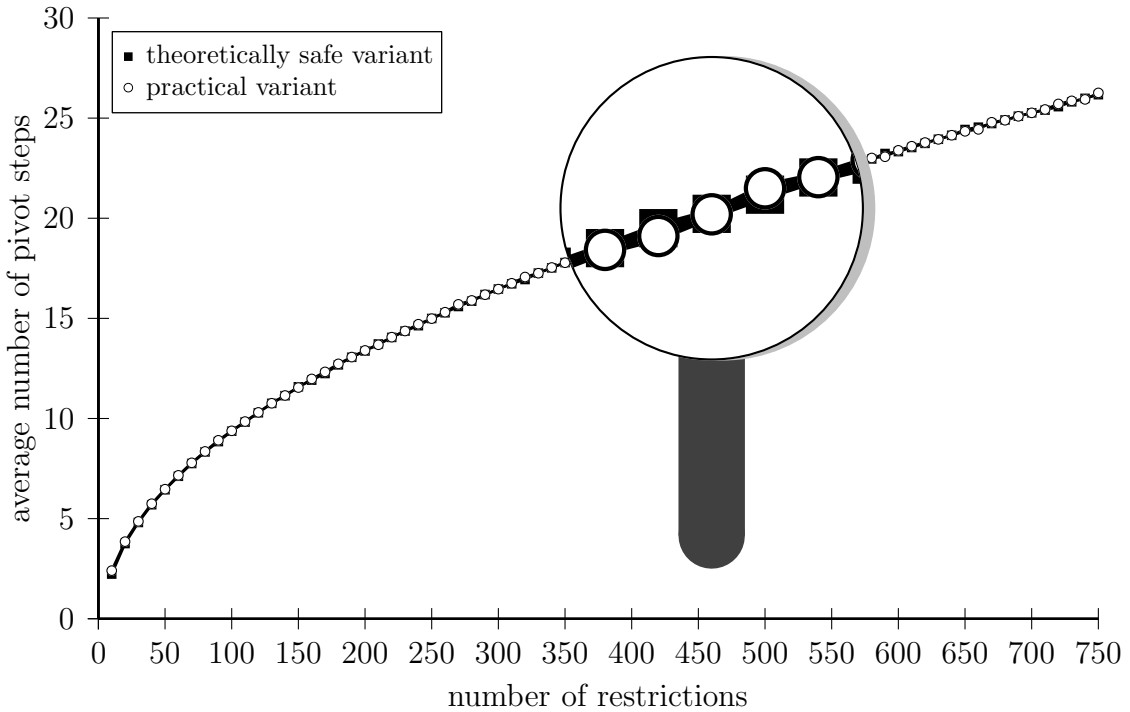


Figure 6.7: Average number of pivot steps of the Phase-2-variants for dimension 3

So we can start presenting results. In figure 6.7 we find the average numbers of pivot steps for $d = 3$. It is obvious that for that dimension the average numbers under the theoretically secure and for the practically applied variant are almost identical. Under magnification one recognizes the the values for the applied variant sometimes are greater and sometimes smaller than for the secure variant. Consequently we regard both alternative variants as equivalent with respect to their arithmetical effort. So for this dimension $d = 3$ the stochastic dependency of \mathbf{u} from the restriction vectors has no significant impact on the running time of the shadow vertex algorithm in Phase 2.

Besides we make an interesting observation also valid for the results in higher dimensions. For the average number of pivot steps as illustrated the curve starts with a somehow steeper ascent and it becomes more and more flat for higher values of m . This is true for both variants. If one compares the first diagram with that in figure 6.8 for dimension 4, then a slightly different behaviour becomes apparent. In principle the behaviour is identical for $d = 4$, nevertheless there is one difference: The curve increases at the beginning for small values of m somehow steeper than for $d = 3$, but it flattens stronger in the sequel. A look at the results for the other dimension in (figure 6.9 up to figure 6.24) shows this effect becomes even stronger for increasing d : For small numbers of restrictions m the average number of pivot steps increases steeply, i.e. a slight variation of m has a strong impact on the average number of steps. This effect weakens for higher restriction numbers more and more.

We go back to the individual results. For $d = 4, \dots, 8$, look at figures 6.8 up to 6.12. It is affirmed that the fear of longer running times caused by stochastic dependency is baseless. Still the calculated average number are very similar for both variants. A precise examination shows that the applied variant is often even faster than the theoretically secure variant.

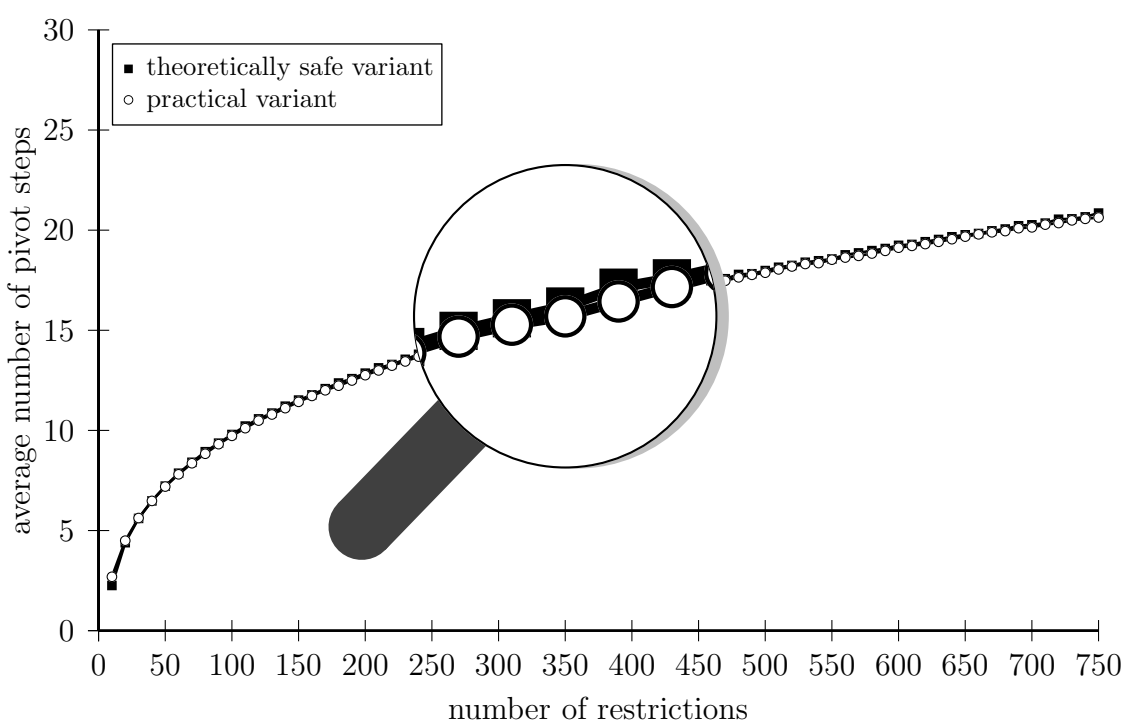


Figure 6.8: Average number of pivot steps of the Phase-2-variants for dimension 4

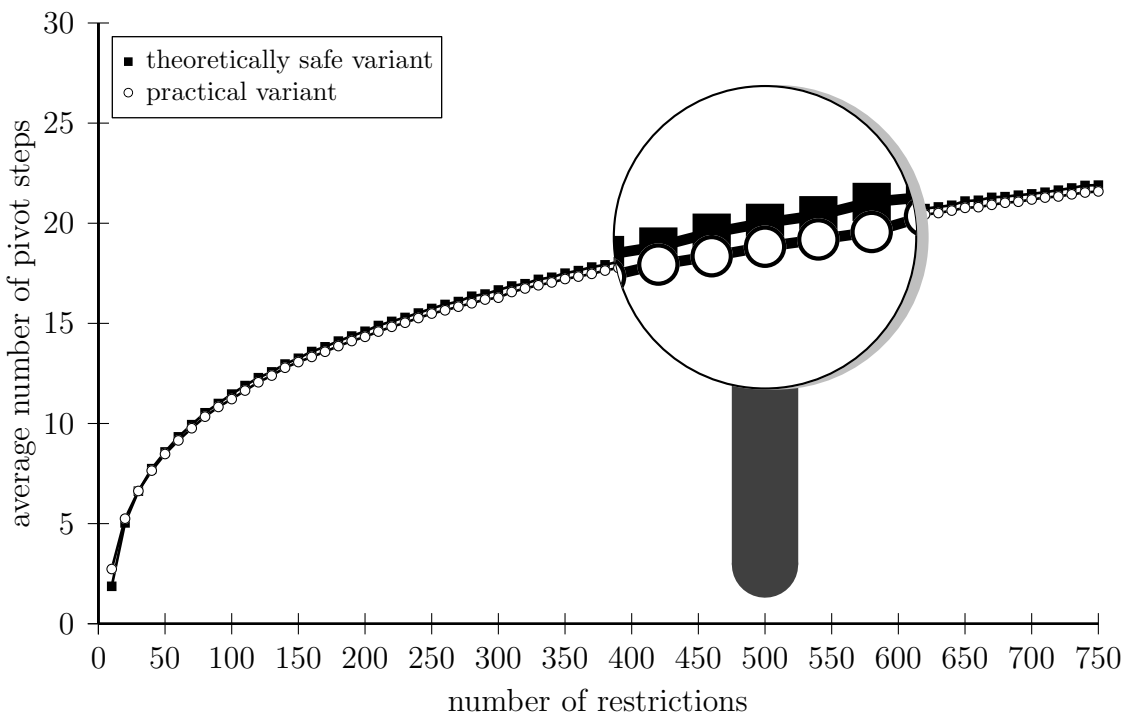


Figure 6.9: Average number of pivot steps of the Phase-2-variants for dimension 5

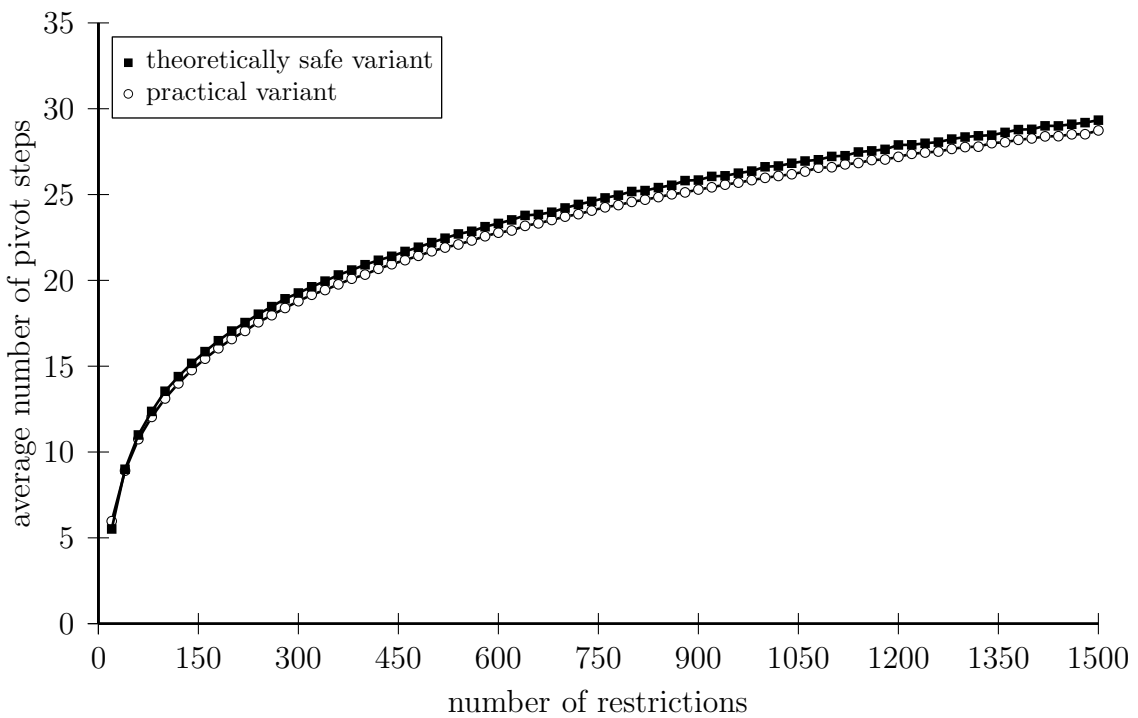


Figure 6.10: Average number of pivot steps of the Phase-2-variants for dimension 6

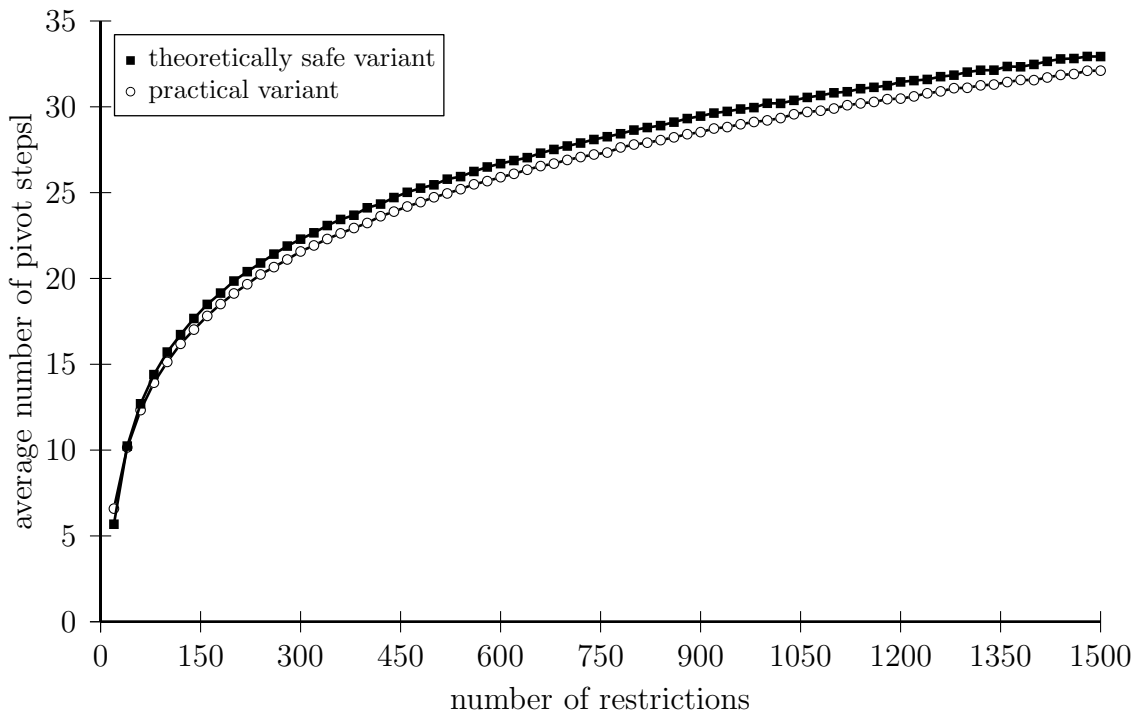


Figure 6.11: Average number of pivot steps of the Phase-2-variants for dimension 7

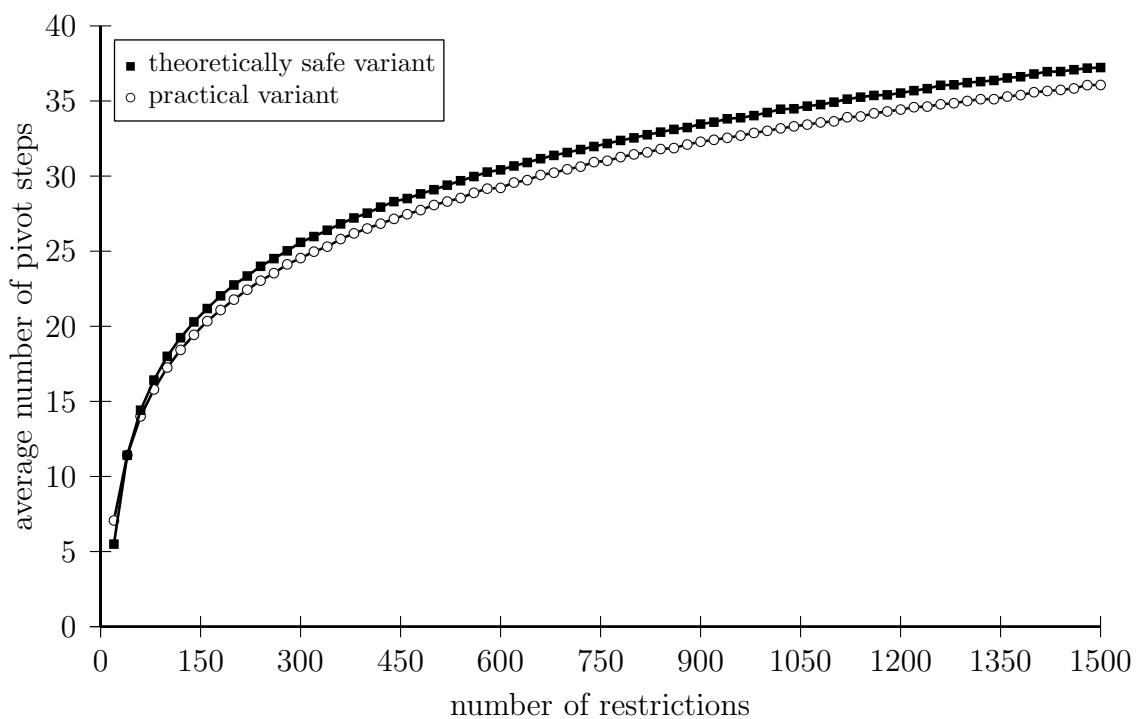


Figure 6.12: Average number of pivot steps of the Phase-2-variants for dimension 8

The presented data suggest that the fear of an impact of the nonobservance of stochastic independence, that would increase the average number of pivot steps, is not justified. In fact, there are slight differences in the charts of both variants, but these are not at all significant. Anymore we observe even the effect, that the practical method mostly performs a little bit better (less pivot steps) than the theoretically secure method. Of course the question for the reason for these little deviations arises. A very naive approach would expect significant differences or some kind of accordance. From a practical point of view it is interesting to know, why both variants differ in their average behaviour at all. The choice of the auxiliary objective vector from the polar cone of the start vertex may be a fatal intervention in the concept of the rotation symmetry model. But is there a systematic compensation through the practical choice? The little quantitative advantage of the practical method is not in the focus of our interest. However we do not like to ignore it and we want to know why it appears and to do something like a cause analysis. This is done in section 6.6.

For the dimensions $d = 9, \dots, 13$, whose diagrams are given in figures 6.13 till 6.17 the observed trend sustains. The average running times of the practical methods still do not show any increasing impact of the loss of independence. This is all we can do to dispel the fear of a bad impact on the running time of Phase 2, as long as our arguments are only empirical.

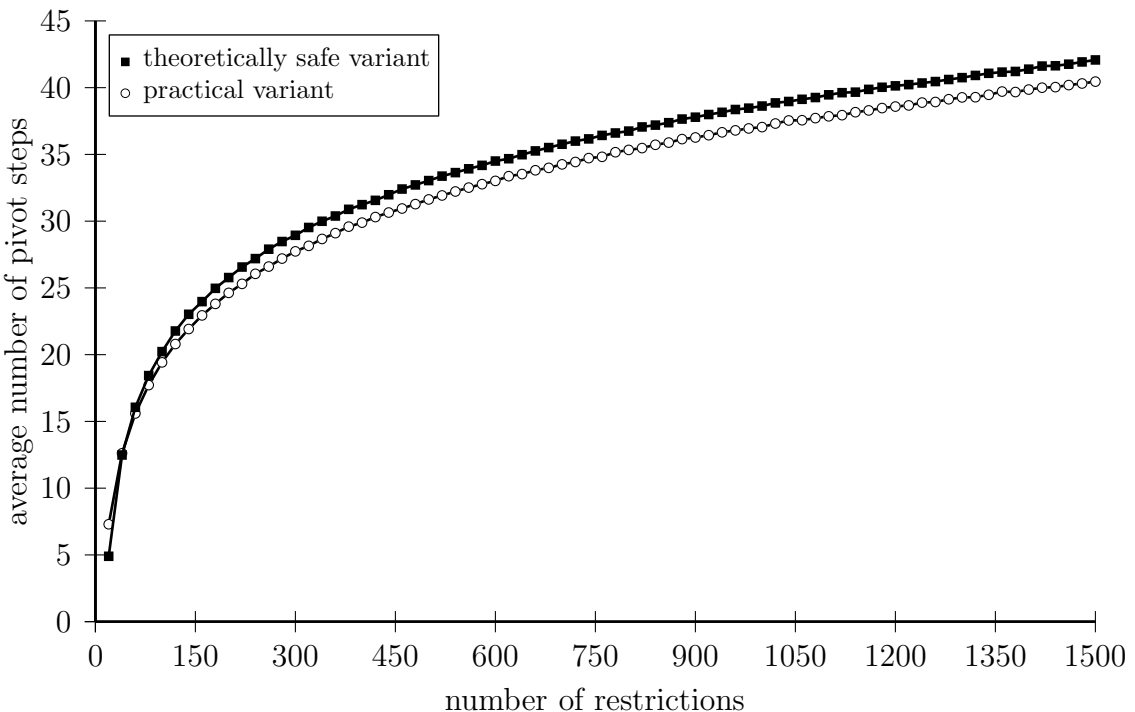


Figure 6.13: Average number of pivot steps of the Phase-2-variants for dimension 9

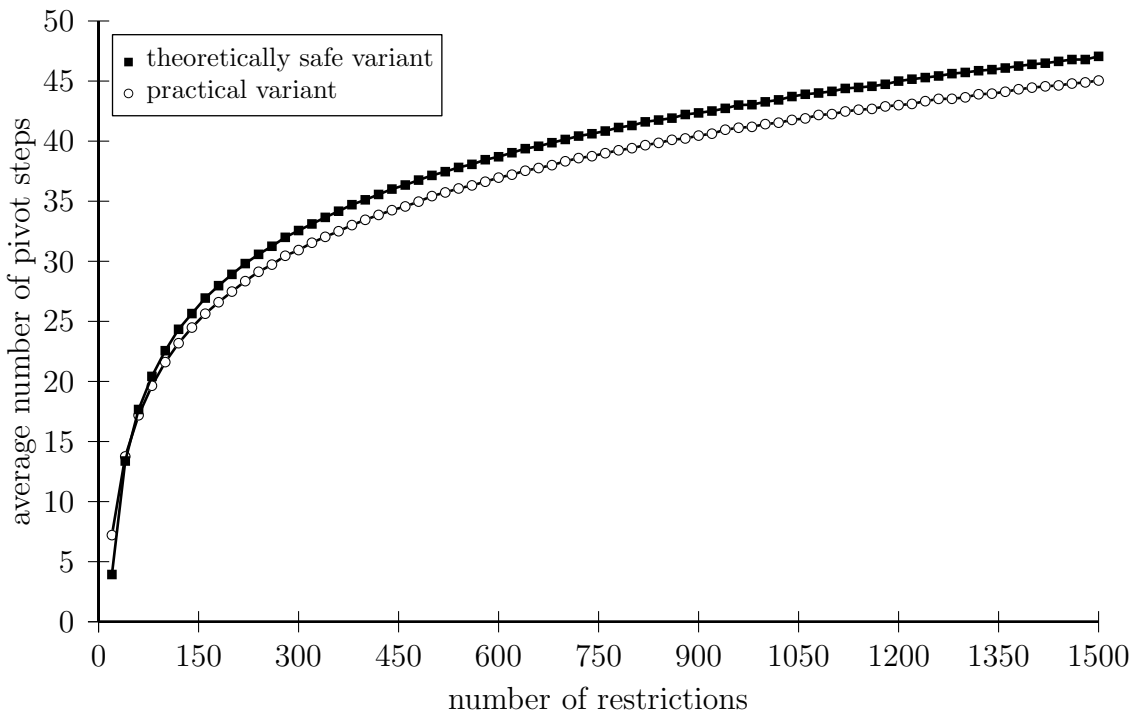


Figure 6.14: Average number of pivot steps of the Phase-2-variants for dimension 10

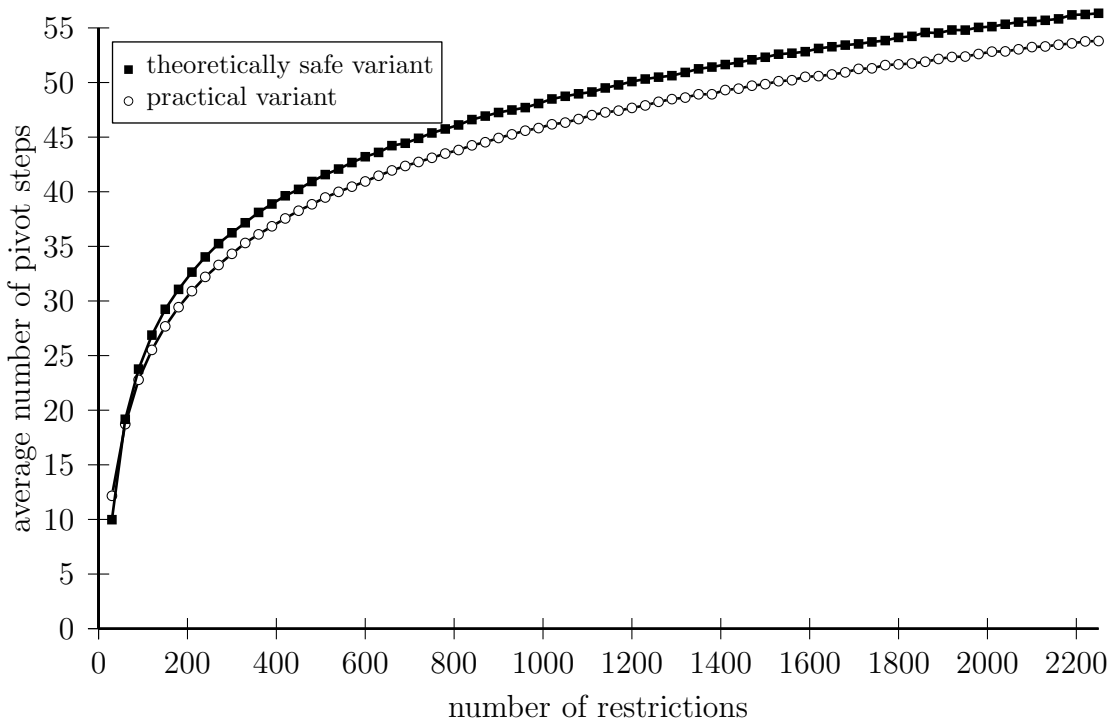


Figure 6.15: Average number of pivot steps of the Phase-2-variants for dimension 11

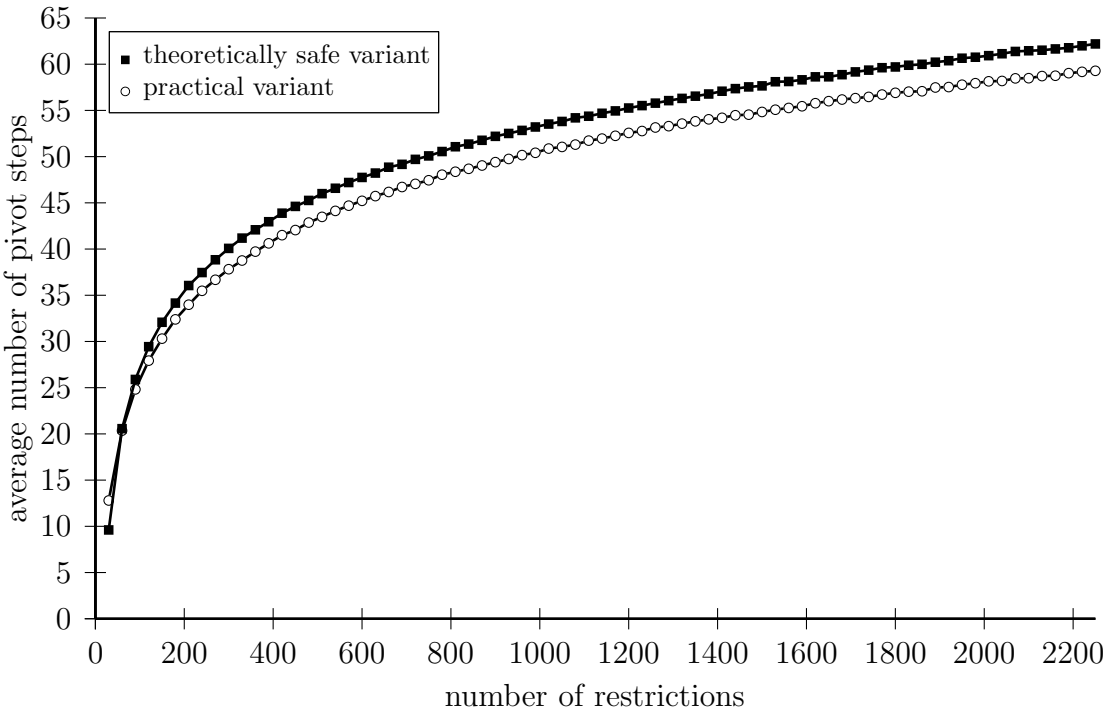


Figure 6.16: Average number of pivot steps of the Phase-2-variants for dimension 12

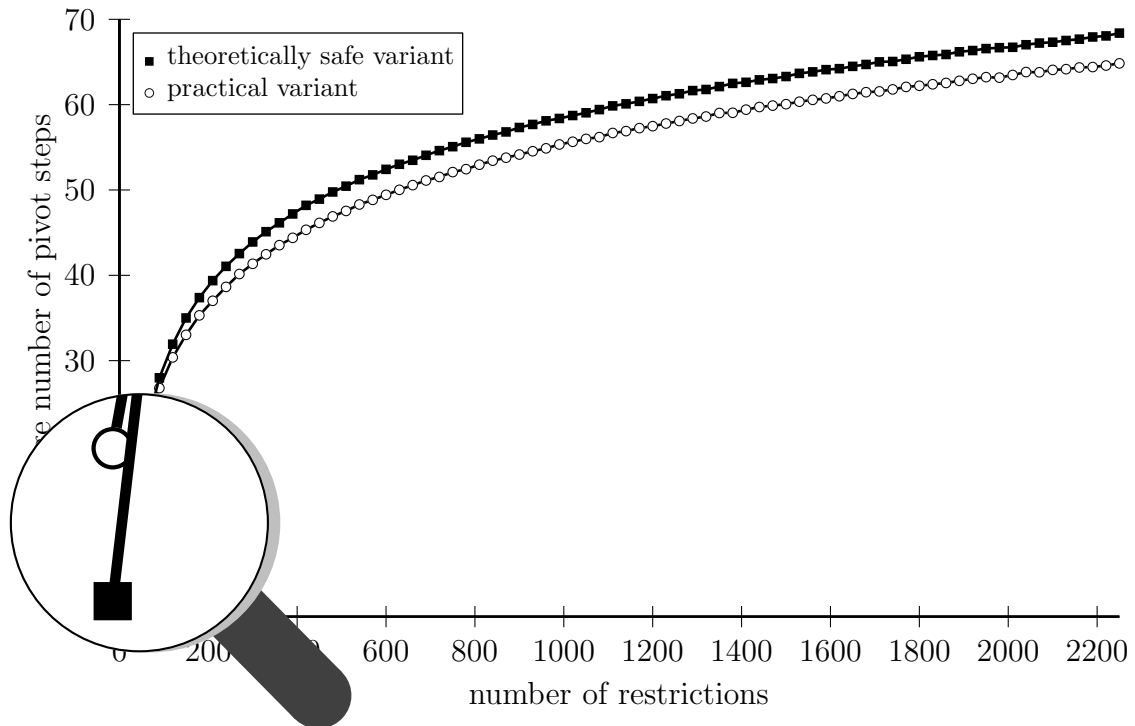


Figure 6.17: Average number of pivot steps of the Phase-2-variants for dimension 13

As mentioned several times before, the practical method mostly exhibits a slight advance in the running time. This effect is notably stronger when the number of restric-

tions m is significantly greater than the corresponding value d for the dimension. For moderate restriction numbers, - i.e. m slightly larger than d - the comparison turns out in the contrary way. Here the advantage of shorter running times lies on the side of the theoretically secure variant. As an example regard the magnified extract in figure 6.17. Of course it would be nice to know the reason for that effect as well. In this case it is rather simple and plausible. So we want to explain it directly.

Roughly spoken the reason lies in the concept of the algorithms 6.3.4 and 6.3.5, which have been used to calculate the results. In the stochastically safe variant we cannot use an available vertex found in Phase 1 directly, in order to start the optimization process in direction \mathbf{v} . Instead we first try to reach the optimal point for the direction of \mathbf{e}_1 . Whether this will be successful or whether this ends up with the cognition of unboundedness, is unknown at the beginning. In the latter case it is impossible to determine the number of shadow vertices corresponding to the cone $\mathbf{KK}(\mathbf{e}_1, \mathbf{v})$ by measuring the Simplex Path from the optimal point to \mathbf{e}_1 to the final point for direction of \mathbf{v} . However we want to make a statement about the number of shadow vertices also in this case generated by our random data-generator. So we manage this with an alternative procedure: We try to rotate the auxiliary objective vector \mathbf{e}_1 in direction \mathbf{v} as far as we reach a direction that does not feature the unboundedness. By the way we reach a (first) shadow vertex, from which we can start the optimization process and measure the length of the path. We remark that it may occur, as incorporated in algorithm 6.3.5, that “all” directions from the cone $\mathbf{KK}(\mathbf{e}_1, \mathbf{v})$ feature unboundedness. On that basis we can conclude that there are no shadow vertices corresponding to that cone. For that reason one cannot carry out pivot steps. Besides that extremal case (more often) the case may occur that the entry in Phase 2 becomes possible after a specific rotation from direction of \mathbf{e}_1 in direction of \mathbf{v} . Then only a reduced “partial rotation” in direction \mathbf{v} , which should for plausible reasons lead due to rotation symmetry. Both mentioned configurations cause a decrement of the mean value. And these cases can only occur in unbounded feasible regions. Here it is important to know that a problem setting according to our stochastic model of rotation symmetry has a probability for unboundednes of

$$p(d, m) = 2^{-m+1} \sum_{k=0}^{d-1} \binom{m-1}{k}$$

according to an important result in a paper of Wendel [Wen62]. This probability decreases very fast to increasing values of m . And this is the reason why the two mentioned more difficult- configurations have an impact only for moderate restriction numbers, i.e. m still in the size of d .

For further clarification we look at the practical method in more detail and compare it again with the safe method. In contrast to the theoretical variant the practical method will not cause configurations that urge to rotate the auxiliary objective direction before being able to start Phase 2. The generated problem instances do all have some vertices because of $m > d$ and of the validity of the condition of nondegeneracy 2.4.1. The first Phase has lead us to one of those vertices. From there we can start Phase 2 using \mathbf{u}_b

as auxiliary objective. Hence the number of shadow vertices resp. the number of pivot steps is defined always over the total cone $\mathbf{KK}(\mathbf{u}_b, \mathbf{v})$. A decrement according to an initial correction of \mathbf{u}_b in direction \mathbf{v} is not necessary and not possible (in contrast to the safe method).

Combining both considerations leads to the conclusion that the system of counting under use does privilege the safe variant for moderate restriction numbers with respect to d , the dimension, i.e. m in the size of d . So the results on the effort will for that variant be somehow understating for moderate dimension relations. So this explanation matches the observations.

Let us come back to the presentation of the results about empirical running times. The remaining figures for dimensions $d = 14, \dots, 20$ confirm all our hitherto existing observations. We suppose that this is a well-grounded empirical basis for the following conclusion. The tolerated stochastic dependency between the vector \mathbf{u}_b and the remaining problem-data in the practical method for Phase 2 has no significant and no unfavorable impact on the computation time. This will be stated in a formulation of an empirically motivated result in the following section.

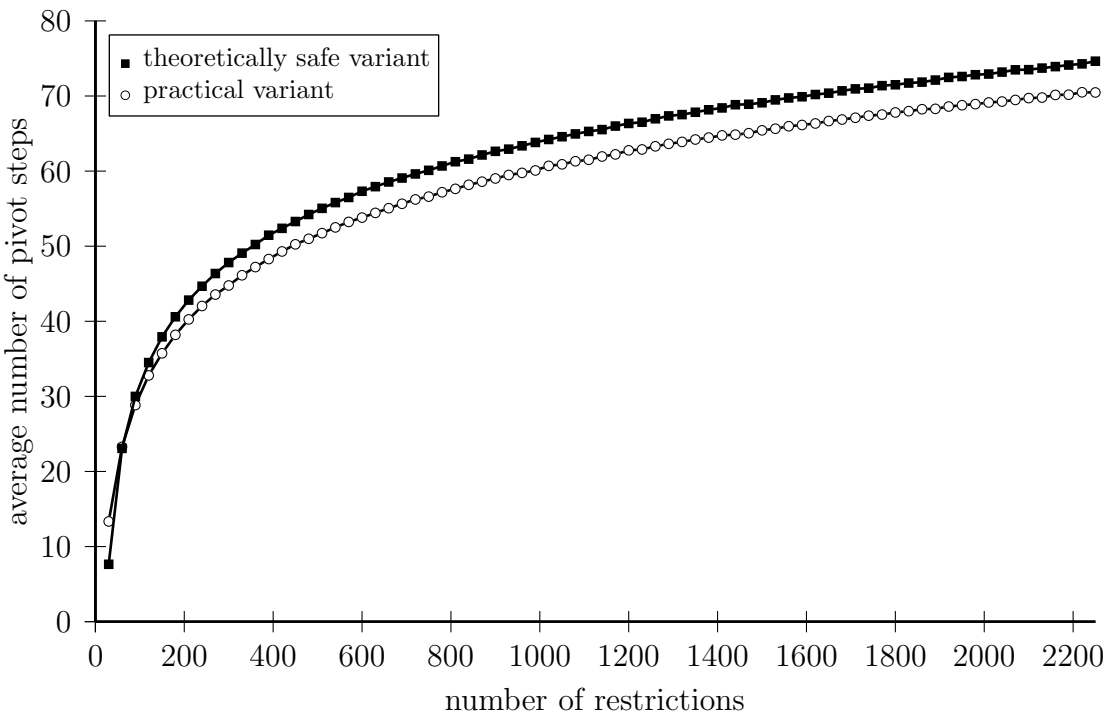


Figure 6.18: Average number of pivot steps of the Phase-2-variants for dimension 14

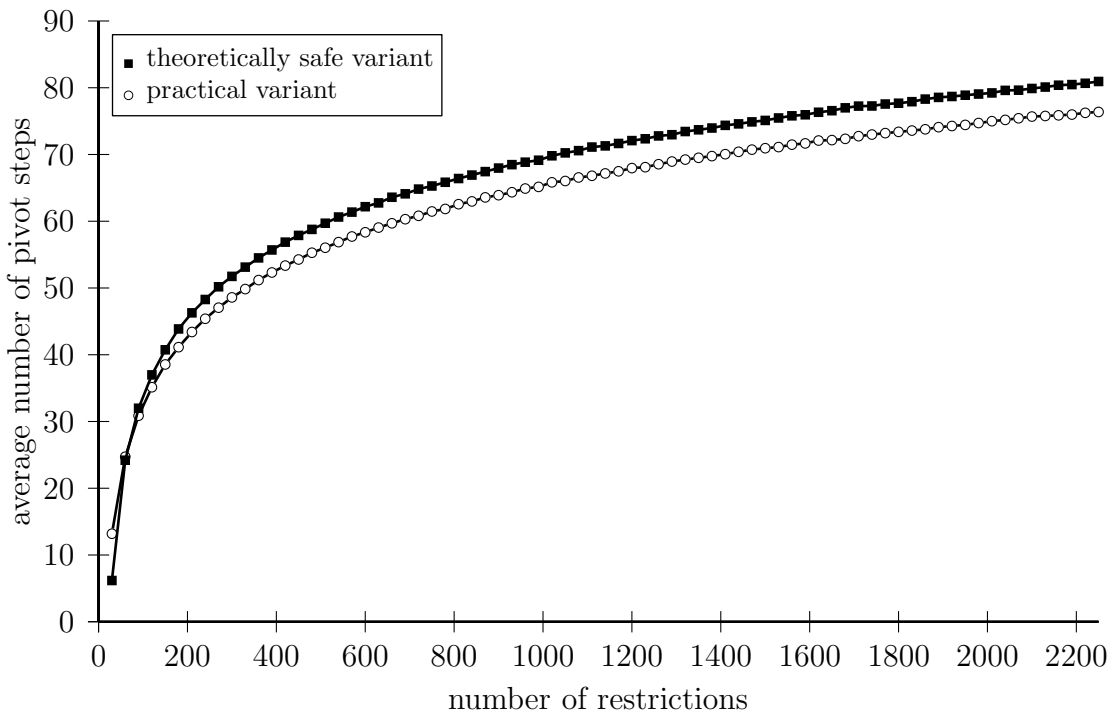


Figure 6.19: Average number of pivot steps of the Phase-2-variants for dimension 15

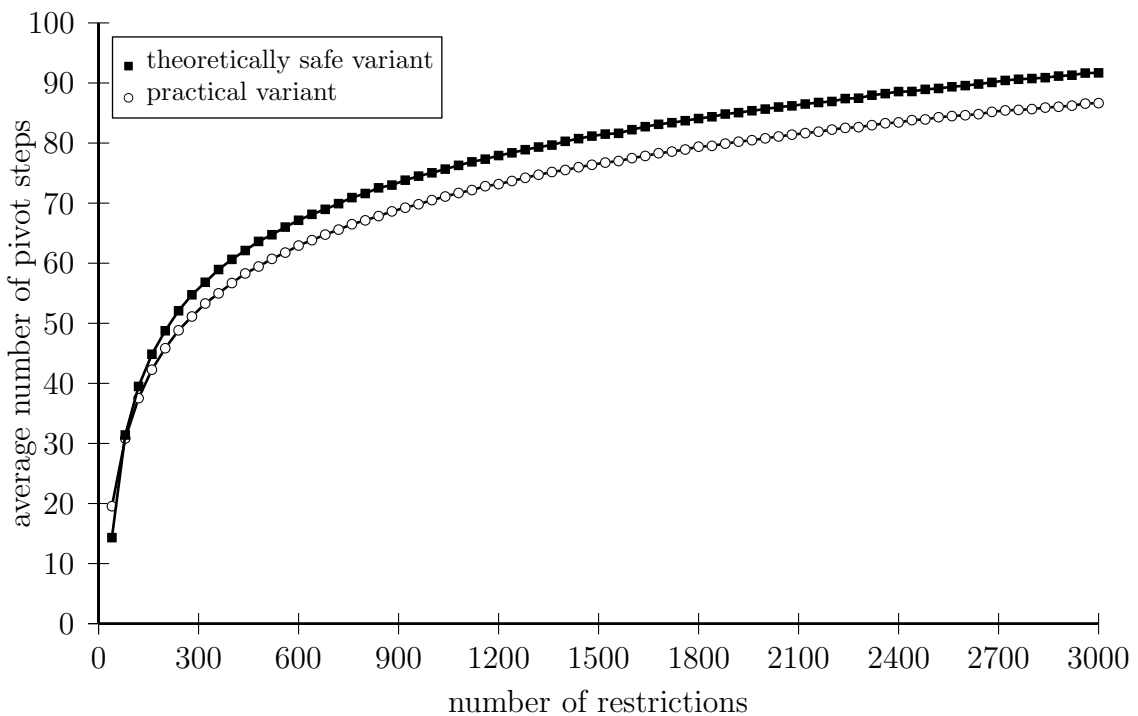


Figure 6.20: Average number of pivot steps of the Phase-2-variants for dimension 16

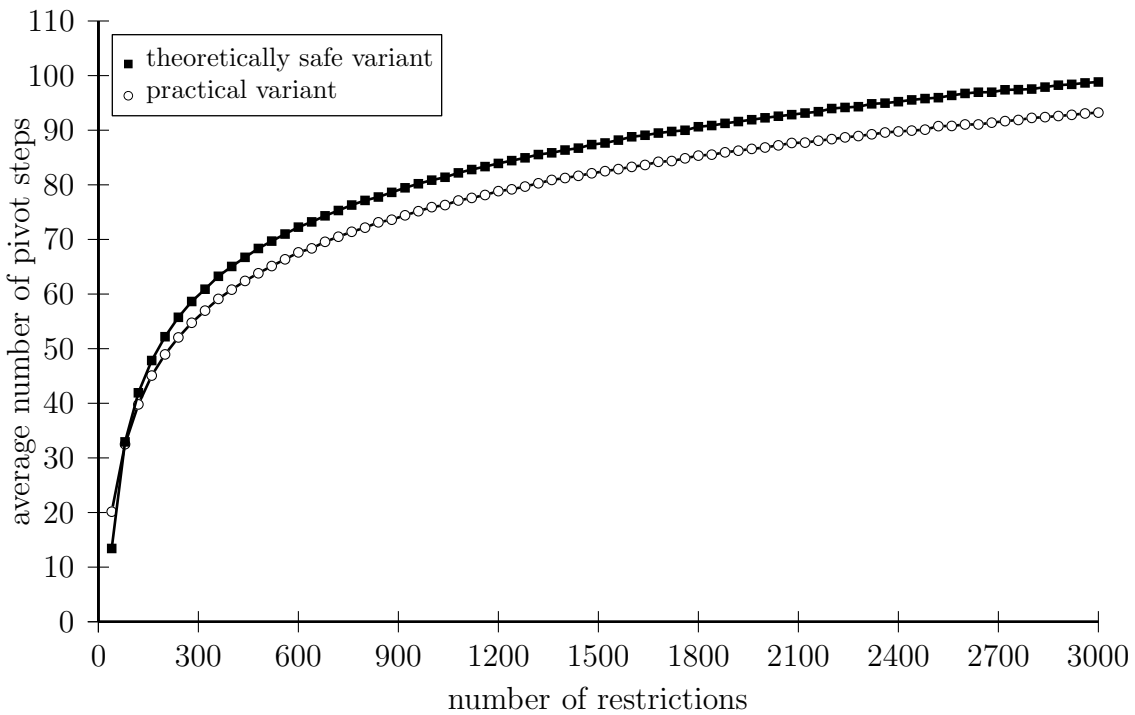


Figure 6.21: Average number of pivot steps of the Phase-2-variants for dimension 17

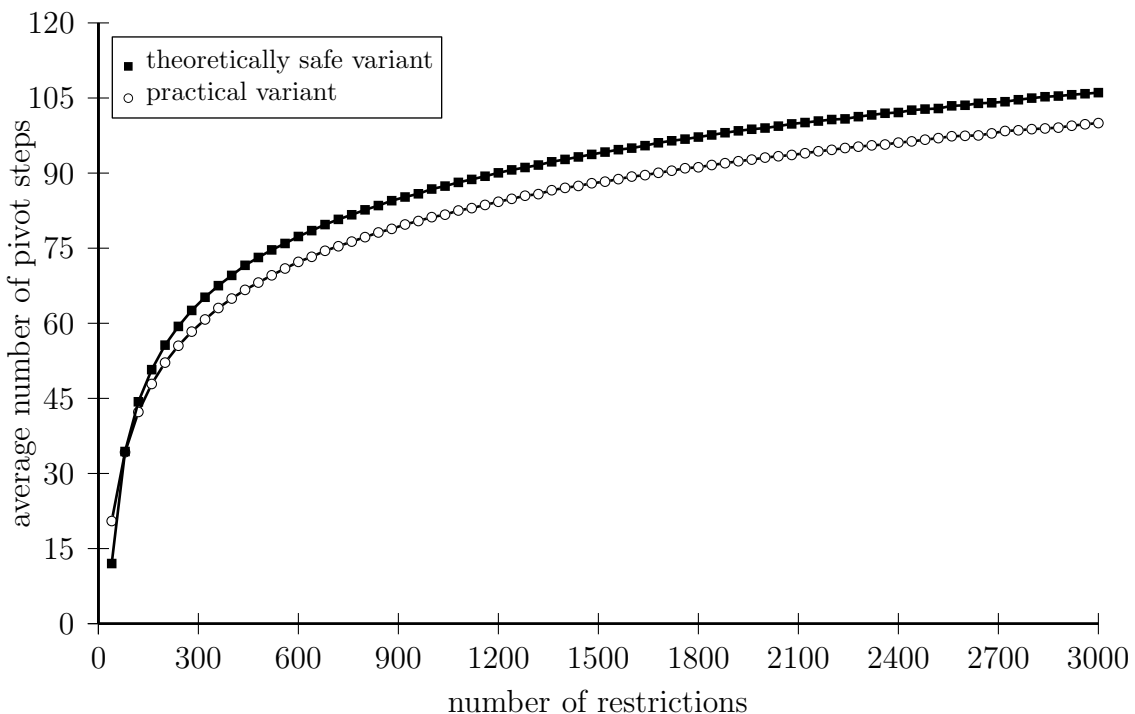


Figure 6.22: Average number of pivot steps of the Phase-2-variants for dimension 18

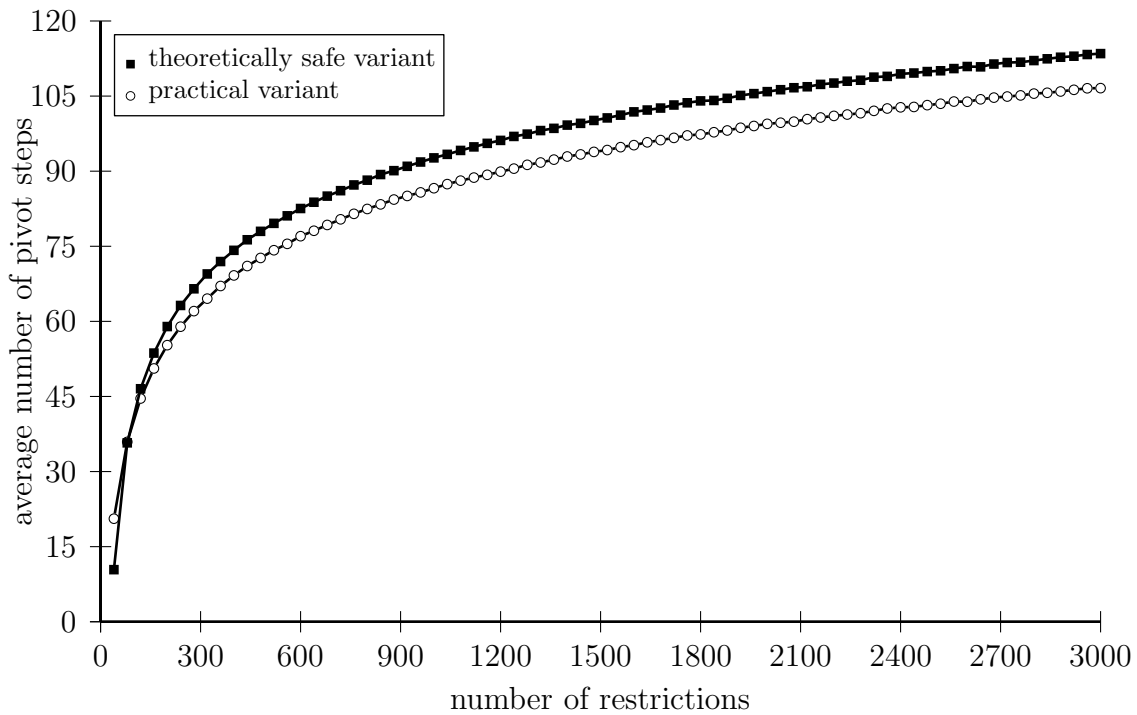


Figure 6.23: Average number of pivot steps of the Phase-2-variants for dimension 19

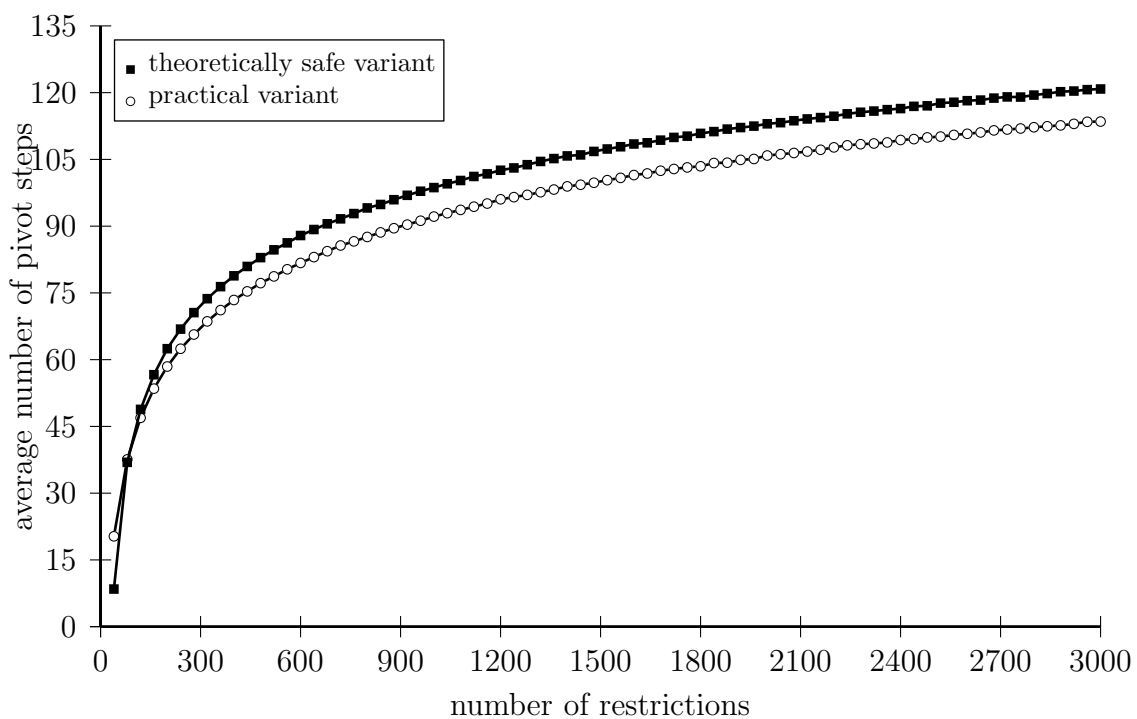


Figure 6.24: Average number of pivot steps of the Phase-2-variants for dimension 20

6.5 Consequences Of The Calculated Results

Here we formulate an empirically motivated statement on the average case complexity even for the practical method. We rely on the calculated and in the previous section presented results about empirical numbers of pivot steps.

Conjecture 6.5.1 (Average Case).

Consider a linear optimization problem of the form

$$\begin{aligned} & \text{maximize } \langle \mathbf{v}, \mathbf{x} \rangle \\ & \text{s.t. } \mathbf{Ax} \leq \mathbf{1} \end{aligned}$$

with $\mathbf{A} = (\mathbf{a}_1, \dots, \mathbf{a}_m)^T \in \mathbb{R}^{m \times d}$, $\mathbf{v} \in \mathbb{R}^d$ und $m \geq d \geq 2$. If the restriction vectors $\mathbf{a}_1, \dots, \mathbf{a}_m$ and the objective vector \mathbf{v} are distributed according to the Rotation-Symmetry-Model, then the shadow-vertex-algorithm requires on the average less than

$$\text{Const} \cdot m^{\frac{1}{d-1}} \cdot d^2 + d$$

pivot steps for the solution. Here Const is an absolute constant.

Reasoning for the Conjecture. The d pivot steps fall upon Phase 1 for the removal of the auxiliary restrictions. The second summand results from the execution of Phase 2 according to the practical method. Since the empirical results do not exhibit a significantly worse behaviour than in the case of the theoretically safe variant, we may use the theoretical estimation for the average number of shadow vertices from [Bor99]. \square

6.6 Complimentary Considerations On The Computation Time Of Phase 2

In this section we will investigate the deviations between the computation time in the practical method and in the theoretically safe method. Our aim is to find the reasons for these (little) differences. As already observed and stated, the practical algorithm requires (in particular when m is much larger than d) less pivot steps in Phase 2 than the safe variant does. An obvious cause is not at hand, so we deal with the details of that phenomenon. Since the main target of this chapter is already met -the crucial question was answered in 6.4 -, we have separated the following argumentation about the deviation from the presentation of the similarity of the results.

In a very naive approach to the comparison of the two versions one would assume that one of two cases applies: Either the stochastic dependence has no relevant impact and the running times are almost identical. Or the behaviour should differ significantly. But it is surprising that there is a slight deviation always in one direction (better for the practical variant). Let us discuss the reasons.

Now the geometrical interpretation of our procedure in Phase 1 as given in section 6.3.1 becomes important and enlightening.

One conjecture about the deviation could possibly lead to numerical aspects. For the simulations we have used an implementation of the restriction-oriented Simplex Method based on Tableaus. The limited precision of the numerical realization may cause numerical effects and instabilities, which could influence our calculations. But the realization of both variants is numerically equivalent and based on the same numerical concept. For that reason it seems to be comprehensible that all effects based on such numerical issues would be reflected in both variants in the same way. The absolute number of steps may be influenced. But the impact should be neutralized under the comparison. .

In fact another reason seems to be relevant. This reason or effect will be called *Greenland-Effect*. We shall explain the choice of this name later. As several times stated before, we start the safe variant from the optimal vertex for the direction of \mathbf{e}_1 ¹¹. So \mathbf{e}_1 is used in the role of the auxiliary objective vector. In contrast to that we cannot give such a global statement about the direction of the auxiliary objective \mathbf{u}_b , as used for the execution of the practical method in Phase 2. So it pays to generate a certain number of problem instances and to study the generated auxiliary objective directions \mathbf{u}_b , in particular their distribution. For that purpose we present the figures 6.25 and 6.26. Here we see the direction of auxiliary objective directions \mathbf{u}_b as generated in 5000 problem instances. Both figures base on $d = 3$, so the difference of both is caused by the value of m . Our direction of view is always orthogonal to the x_2 - x_3 -plane, i.e. alongside $-\mathbf{e}_1$. So the vector \mathbf{e}_1 , which always serves as auxiliary objective for the safe variant of Phase 2, is always exactly in the middle of the graphic. What we call Greenland-effect, consists of the following characteristics, which can be recognized in both figures.

1. The auxiliary objective directions \mathbf{u}_b go under a certain variance.
2. They cumulate near the north-pole \mathbf{e}_1 .
3. The distribution of the points \mathbf{u}_b is not symmetrical about the north-pole, but systematically unidirectional with a concentration on the first octant.

As we shall see, these three characteristics are mainly caused by the kind how Phase 1 worked. This has been the motivation to discuss the basic geometrical interpretation in detail in section 6.3.1. Now let us give explanations.

Characteristic 1:

Phase 1 iterates as known in the first step in direction of \mathbf{e}_1 (only in some unbounded cases one uses $-\mathbf{e}_1$ and we should disregard these cases here) until a facet of the feasible region is reached. After that one makes corrections according to the remaining coordinate directions, till one reaches one of the vertices. For the upcoming execution

¹¹Here we deal mainly with $m \gg d$, so we disregard the appearance of unboundedness.

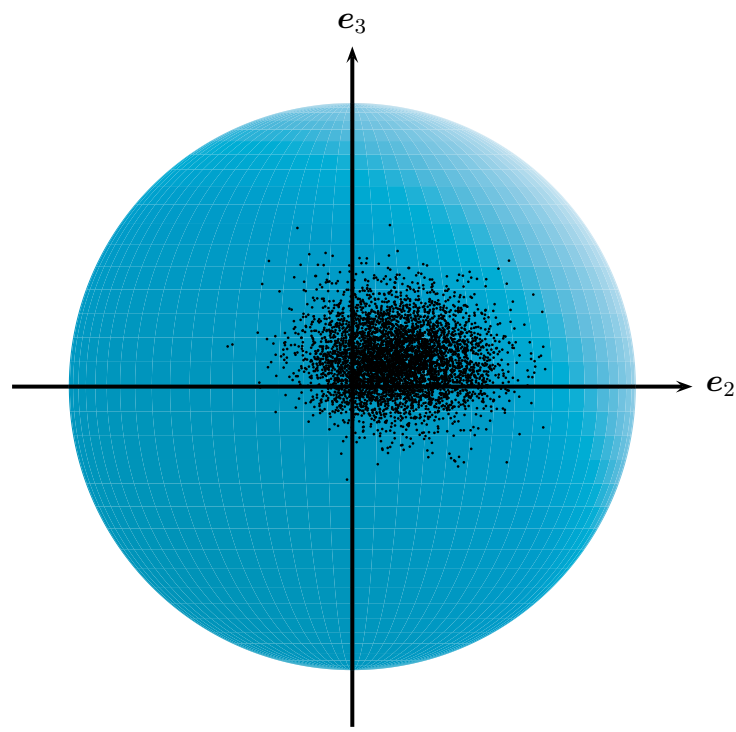


Figure 6.25: 5000 realized vectors \mathbf{u}_b for starting the practical Phase 2 in case of $m = 100$ and $d = 3$

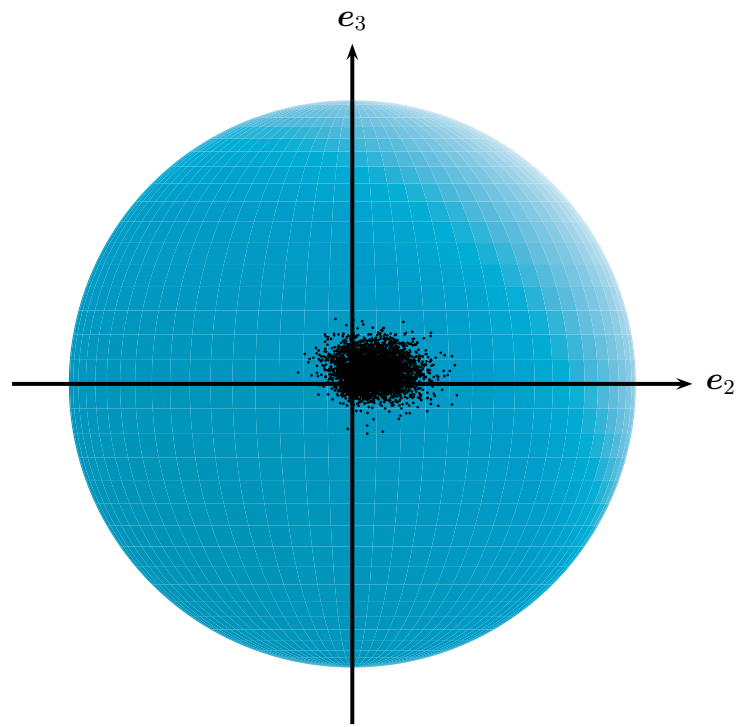


Figure 6.26: 5000 realized vectors \mathbf{u}_b for starting the practical Phase 2 in case of $m = 500$ and $d = 3$

of the practical Phase 2 one chooses the required auxiliary objective direction \mathbf{u}_b as the barycenter of the polar cone of the vertex at hand. It is obvious that this procedure reflects the specification of the respective problem instance. So it is clear that we observe a certain variation in the large set of experiments.

Characteristic 2:

Also the second property can be explained by the systematic of Phase 1. As mentioned before the first iteration in direction \mathbf{e}_1 determines and fixes a facet F . All remaining iterations remain in that facet, until a vertex of that facet is reached. After arrival we choose an auxiliary objective direction \mathbf{u}_b from the barycenter of the corresponding polar cone. So we have a strong dependence of the final vertex on the direction \mathbf{e}_1 via the facet F , which contains that vertex.¹² Besides the vertex, also the orientation of \mathbf{u}_b is influenced by the first iteration direction \mathbf{e}_1 . This fact delivers a fundamental explanation for the cumulation of the vectors \mathbf{u}_b near \mathbf{e}_1 .

Characteristic 3:

We have seen that the first step in Phase 1 explains the second characteristic. Moreover the remaining iterations $2, \dots, d$ are responsible for the systematically one-sided deviations of the vectors \mathbf{u}_b relative to the pole \mathbf{e}_1 . During these iterations (roughly spoken) some corrections according to the coordinate directions $\mathbf{e}_2, \dots, \mathbf{e}_d$ will be carried out till a vertex is reached. This follows two principles: On one side the fixed sequence of corrections causes that the deviation with respect to the direction \mathbf{e}_i is by trend stronger than with respect to \mathbf{e}_{i+1} . On the other side the i -th step prefers a movement in the (positive) direction \mathbf{e}_i against a movement in the (negative) direction $-\mathbf{e}_i$. This comes from the specific functionality of Phase 1. If one combines both principles (which hold for arbitrary dimensions), then one obtains in case of $d = 3$ and under rotation-symmetry the concentration of the auxiliary objective directions \mathbf{u}_b in the first octant as shown in figures 6.25 and 6.26.

Now having listed and introduced the three essential properties characterizing the Greenland-effect, we want to explain the nomenclature. For understanding this it is worthwhile to look again at figures 6.25 and 6.26. These show exemplarily the variation of the auxiliary objective vectors \mathbf{u}_b in the practical variant of Phase 2. Irrespective of the size of the distribution region we perceive the slightly shifted position of that region relative to the north pole. With some imagination we observe a certain similarity to the size, the form of Greenland and its relative position to the north pole. In contrast to the theoretical variant, which will always have the start at the north pole with the auxiliary objective, the practical method starts in our imagination “somewhere in Greenland”. For this reason we call the observed variation Greenland-effect. Moreover we want to state the conjecture, that this disturbance of the ideal location at the north pole, is responsible for the deviation of the average numbers between both variants.

So far we have discussed the theoretical reasons for the occurrence of the Greenland-effect in Phase 1. Complementary we want to illustrate its origination graphically at

¹²The facet F was determined just by the walk from the origin in direction \mathbf{e}_1 .

an example. In section 6.3.1 we have introduced the Phase 1 under use and we have illustrated it at such an example. Let us get back to that example. The vertex found in that example and the corresponding feasible region are presented in figure 6.27. There are two highlighted vertices. Look at that one which lies more in the right and higher. This vertex is used for the entry in the practical Phase 2 and we choose the barycenter \mathbf{u}_b from the corresponding polar cone as auxiliary objective vector. Moreover the facet F , which has been reached in the first step of Phase 1, is drawn in dashed lines. As we have seen, it is a significant property of Phase 1 that the final vertex always will be located on that facet F . In addition we recognize the second vertex, which is highlighted more in the left and lower. This vertex belongs to the same facet. And this is the optimal point for the objective direction \mathbf{e}_1 . As we know this is the point where the stochastically safe Phase 2 under use of the fixed auxiliary objective \mathbf{e}_1 will start.

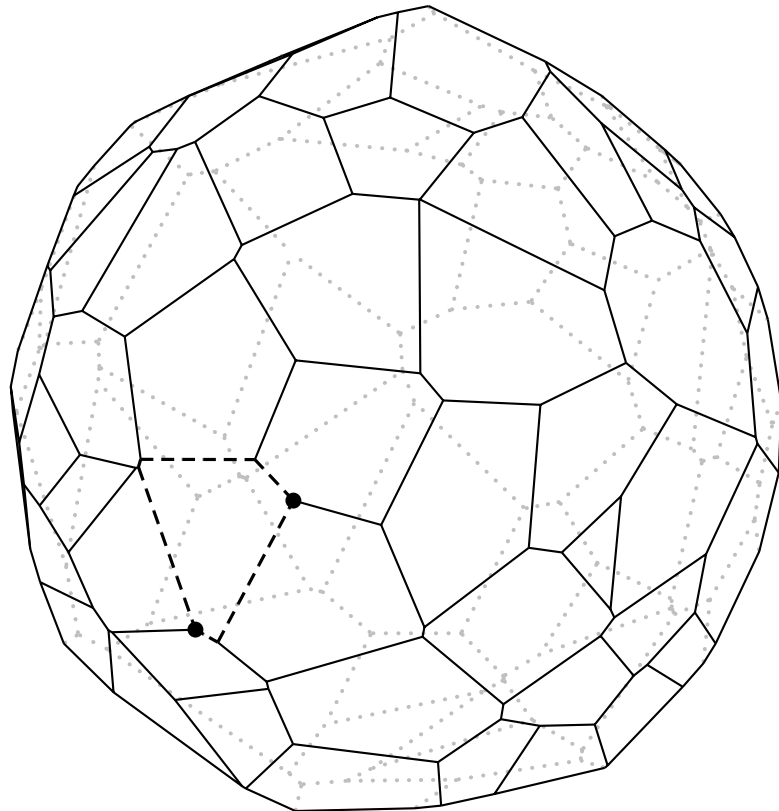


Figure 6.27: Result of Phase 1 versus optimum with respect to \mathbf{e}_1

As we see in our example, the two vertices lie close to each other, resp. the angle between both vertices is rather small.¹³ On the basis of the rotation symmetry model the following fact essentially holds: The angle between a vertex (interpreted as a vector) and any direction from its polar cone is rather small. Consequently the angle between \mathbf{e}_1 and \mathbf{u}_b should be small as well.

¹³Here we interpret the vertices as vectors emanating from the origin.

For both variants of Phase 2 we obtain shadow vertex pathes with slightly differing and shifted start positions. This is illustrated in figure 6.28. For better comprehension we have rotated the graphic in a way, such that the vector e_1 is directed upwards.

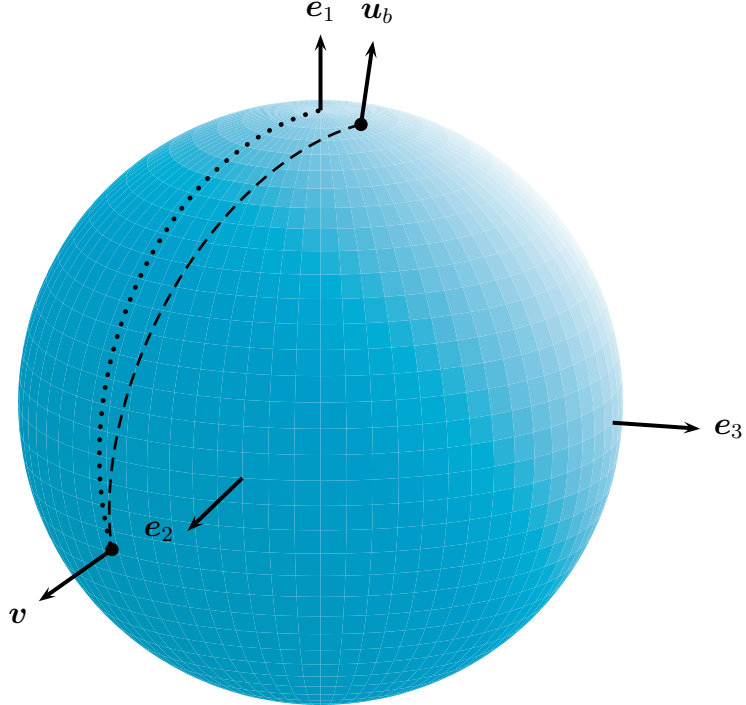


Figure 6.28: Illustration of start positions for the two variants of Phase 2

Repeating these observations for a very large number of concrete problem instances yields the behaviour that is shown in figure 6.25 and figure 6.26. We detect a systematic one-sided deviation u_b from e_1 . This is what we call Greenland-Effect.

At this point we want to mention an additional item, that can be recognized in both figures. But we have not paid attention to this so far. It is obvious that for $m = 100$ the variation or deviation is rather strong and that for $m = 500$ the variation decreases significantly. Under a detailed consideration we should not be surprised by that effect. This is caused by the fact that for increasing values of m the polyhedron will have in trend more vertices and more facets. And that gives the surface a much finer structure. For that reason the facet hit in Phase 1 will in trend be smaller as well. The remaining correction steps, which do not leave the facet, can consequently lead to very small deviations only.

Further one can observe (compare in particular figure 6.25), that large deviations appear more seldom and that the set of points shown in the figure exhibits some structure. In particular the latter observation reveals that it would be extremely difficult to find a theoretical distribution model for the deviation in question. Hence it will be nearly impossible to describe the Greenland-effect theoretically and rigorously.

In the course of the introduction of the Greenland-effect we have dealt with the slightly

reduced running time of the practical Phase 2 in a rather general way. Let us now have a closer look at some aspects. There are some factors having an impact on the deviation-behaviour. Besides the concept of the Phase 1 under use, for example the precise choice of the auxiliary objective vector should be considered. If we look at this choice separately, then we recognize that already the choice of the barycenter from the polar cone for \mathbf{u}_b yields a reduction of the average number of pivot steps. This is clarified in figures 6.29, 6.30 and 6.31, whose empirical results are based on a modification of the theoretical variant.

To clarify the question for the impact of the barycentralization we discuss the theoretical Phase 2 once more and we modify it slightly. Still we try to reach the optimal point for \mathbf{e}_1 and then – in the positive case – we start the optimization process in direction \mathbf{v} . But this time we do not use \mathbf{e}_1 as auxiliary objective vector for the shadow vertex algorithm. Instead – analogously to the practical method – we replace it by the barycenter in the polar cone of the vertex. By the way we produce a similar configuration as we know from the practically applied procedure. For the possible case of unboundedness in direction \mathbf{e}_1 , where we first have to make corrections with the help of \mathbf{v} , we do not perform that barycentralization at the start vertex. And the result is: This slight modification yields slightly reduced numbers of pivot steps. In figures 6.29, 6.30 and 6.31 we see results for dimensions $d = 6, 11, 18$.

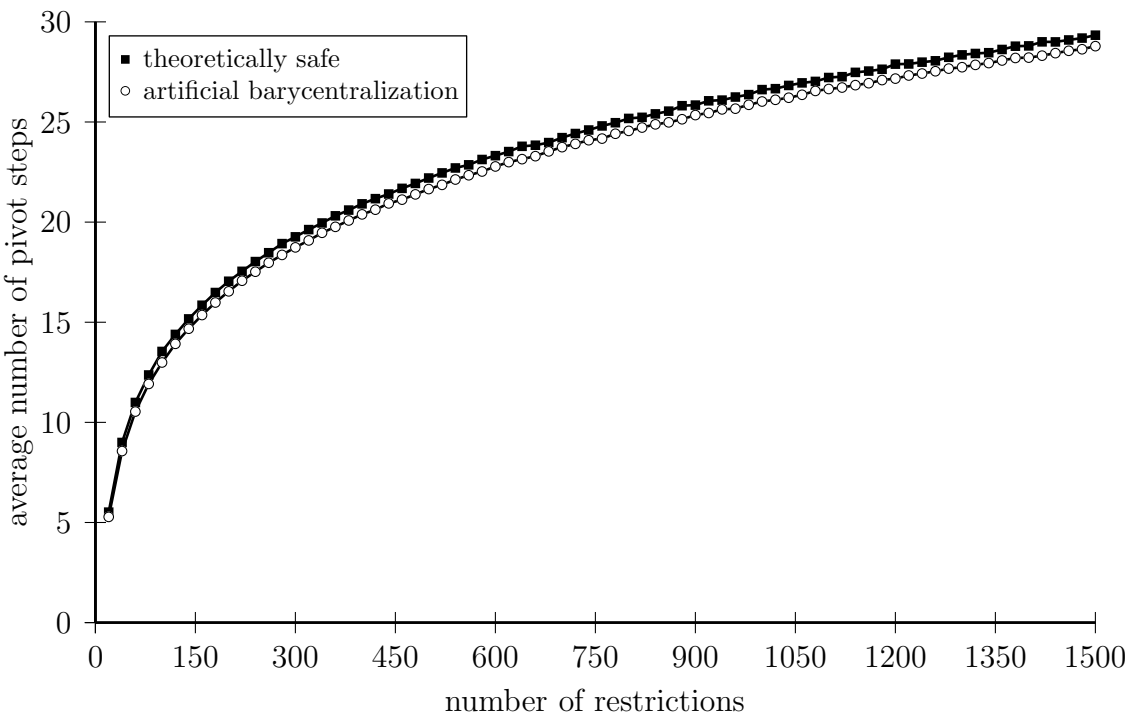


Figure 6.29: Average step-numbers of the safe Phase 2 and the variant with artificial barycentralizatiion of the auxiliary objective direction in dimension 6

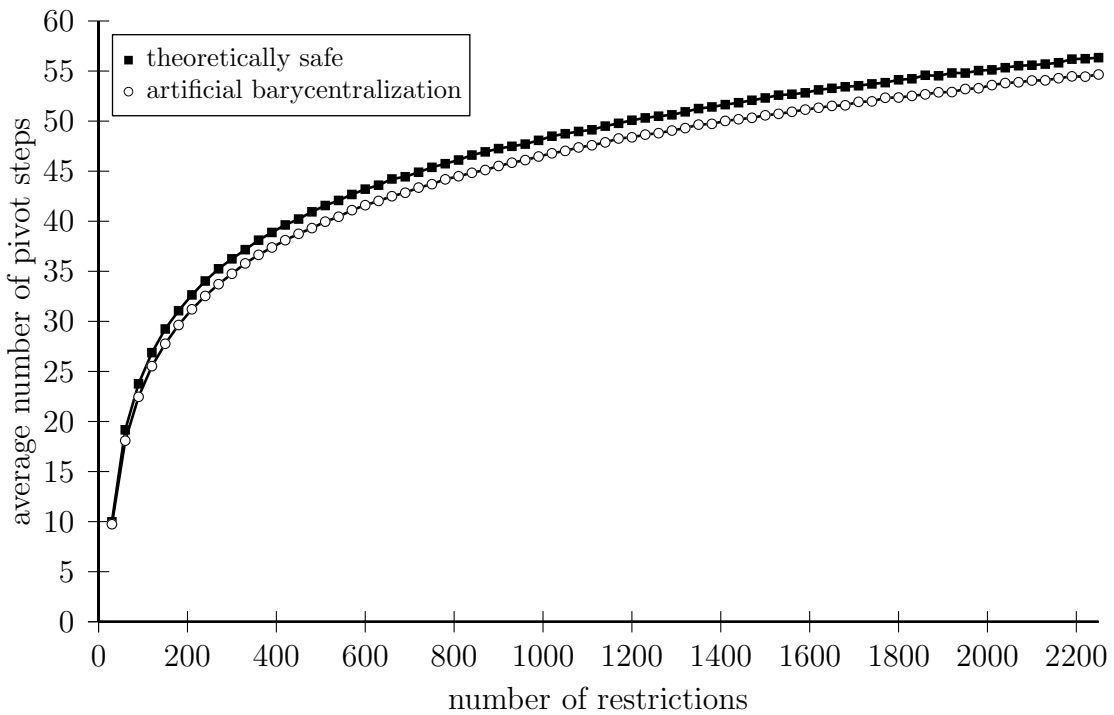


Figure 6.30: Average step-numbers of the safe Phase 2 and the variant with artificial barycentralizatiion of the auxiliary objective direction in dimension 11

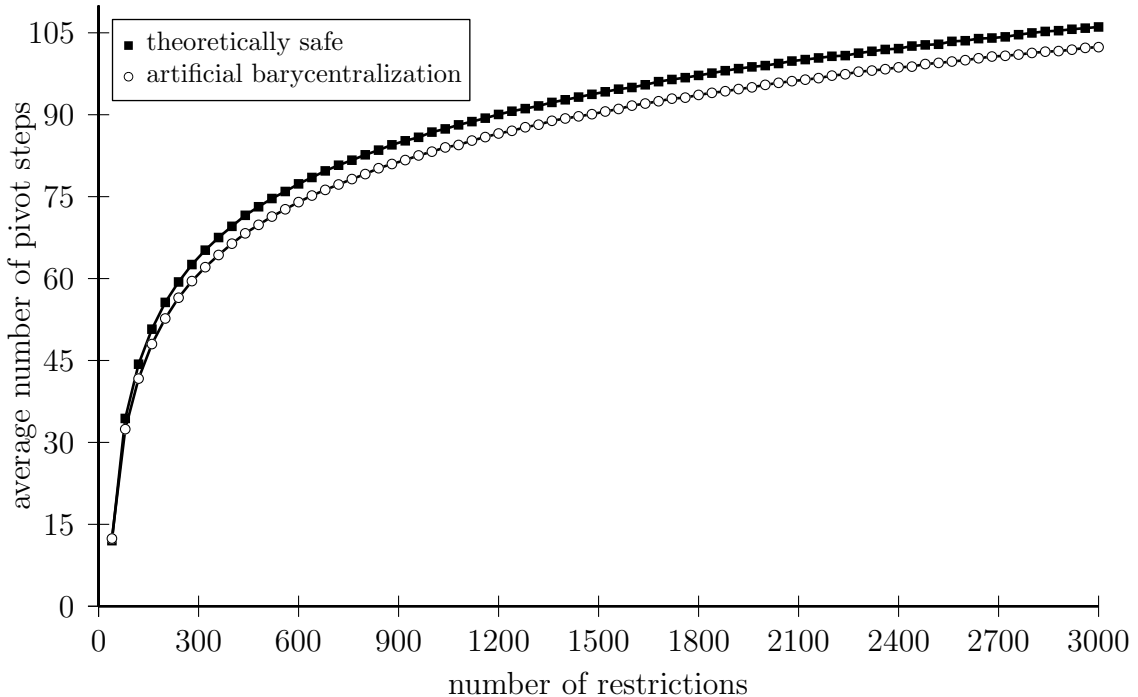


Figure 6.31: Average step-numbers of the safe Phase 2 and the variant with artificial barycentralizatiion of the auxiliary objective direction in dimension 18

So we comprehend that even the isolated modification of barycentralization in the choice of the auxiliary objective yields a reduction of the average number of pivot steps.

From a quantitative point of view the question is justified, which portion of the deviation between the theoretically safe and the practical method can be explained by barycentralization. An empirical answer is given in the graphics of figures 6.32, 6.33 and 6.34. Supplementary to those three illustrations we see for $d = 6, 11, 18$ how the average numbers of the secure method and of the variant with artificial barycentralization exceed the values for the practical method in Phase 2. More precisely: For the calculated numbers of pivot steps the following differences are illustrated graphically:

$$\begin{aligned} & \text{safe Phase 2} - \text{practical Phase 2} \\ & \text{artificial barycentral Phase 2} - \text{practical Phase 2}. \end{aligned}$$

For better clarity the “Zero-Line” is highlighted. A curve progression below that line indicates smaller average numbers than in the practical Phase 2 and a progression above indicates greater numbers in comparison with the practical behaviour. The strikingly ragged course of the curves is due to the refinement of the scaling (in comparison with the graphics seen so far).

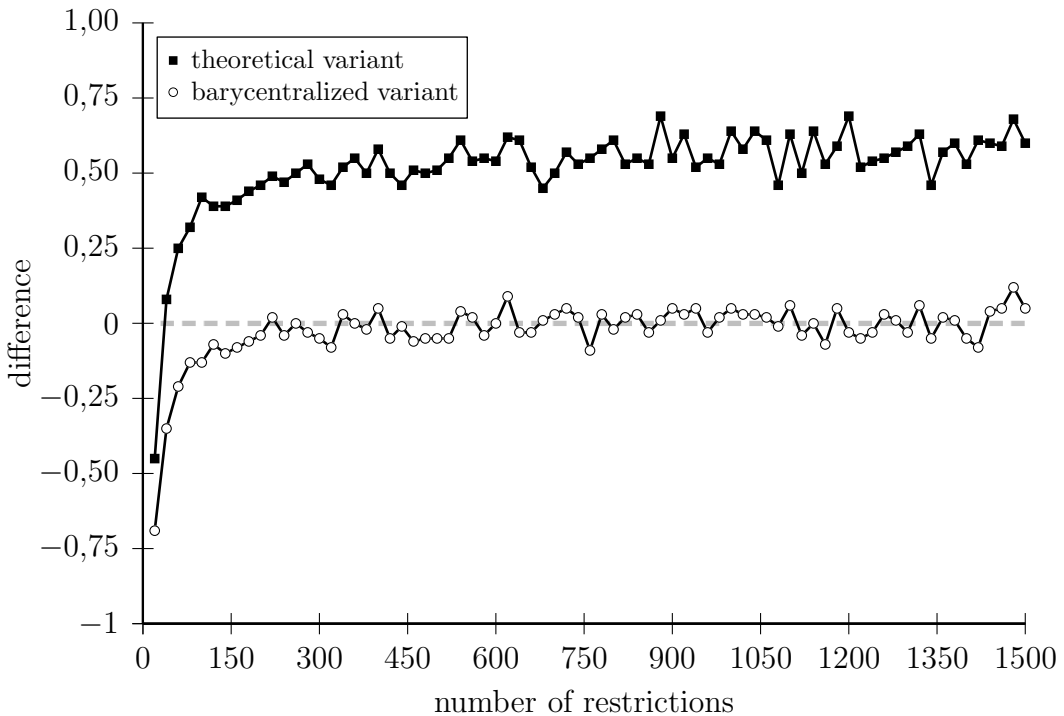


Figure 6.32: Differences between average step-numbers in dimension 6

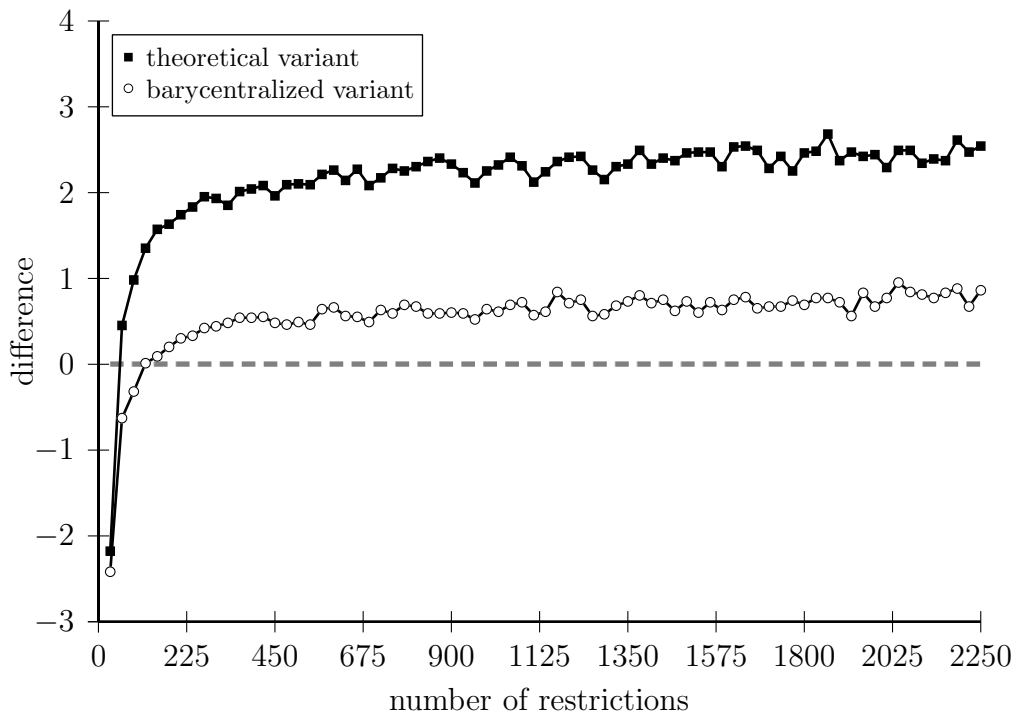


Figure 6.33: Difference between the average step-numbers in dimension 11

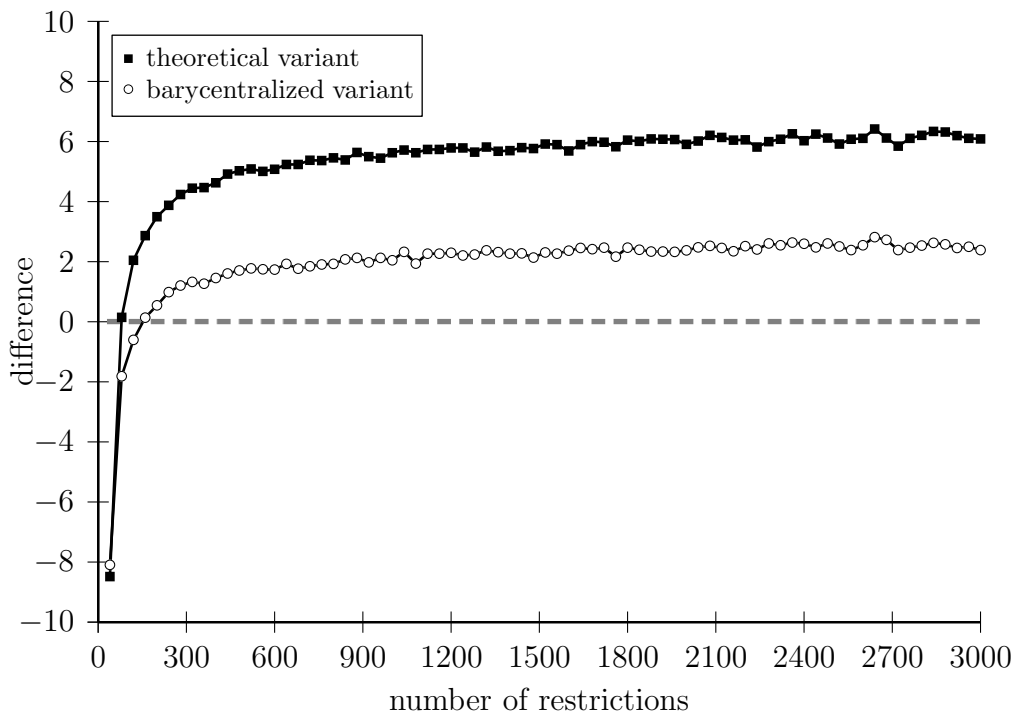


Figure 6.34: Difference between the average step-numbers in dimension 18

In all three plots we see that for small restriction numbers the curves run below the Zero-Line. This is, as explained in section 6.4, caused by the fact that for moderate relations between m and d the practical method in Phase 2 delivers a bit larger values than the theoretical variant. This perception holds as well for the barycentered form and for the safe method. For $d = 6$ the values for the average numbers of the barycentered Phase 2 are almost on zero-level. Hence we suspect that barycentralization can almost alone be hold responsible for reduced numbers of pivot steps in dimension 6. In case of $d = 11$ the zero-level will not be reached by barycentralization completely, but we see a drastic approximation. Here a great portion of the difference can be explained by that way. Similar is the situation with dimension 18.

As mentioned, one may recognize that for higher dimensions also other effects contribute to the reduction of the running time. But for the remaining difference we cannot fix the direct causes. These reasons lie, as we suppose, more deeply in the concept of Phase 1 and in the hereby produced Greenland-effect. Finally we want to discuss a property of the first Phase. And we want to contrast it with the situation in the secure case. This comparison, which is not really founded by concrete facts, however gives a plausible reason for the yet unexplained deviation.

In general, without explicitly regarding the possibility of unboundedness, we find the following situation for both variants:

Safe Phase 2:

Before we start the actual Phase 2 one determines the optimal point for direction e_1 . Starting from there one starts the optimization process in objective direction v . Here it is essential to remember that both vectors e_1 and v are stochastically independent of the restriction vectors, that define the feasibility region. For this reason we are not able to make statements about the surface structure of the polyhedron in the region close to the optimal point in direction e_1 , i.e. the start vertex.

In contrast to that the practical Phase 2 orients itself somehow at the surface structure of the actual and specific feasible regions. This will now be elaborated.

Practical Phase 2:

As a dominating factor influencing the running time of the Phase 2 is –as seen before – the barycentralization of the auxiliary objective vector. At this point we want to mention further properties. These are not directly induced by the concept of Phase 2, but they are caused by the principles of Phase 1. For further observations we will in particular look at these properties of Phases 1 as we have already done before in section 6.3.1.

Let us concentrate on the first step in Phase 1: Starting from the origin we walk in direction e_1 , until we reach the boundary of the feasible region X , i.e. we reach a facet F . This iteration step corresponds to the naïve attempt to obtain an optimal point on X with respect to the objective direction e_1 . From that we can conclude that the hit facet F has a tendency to a larger extension, as it has been hit. For the sequel in the

first Phase we want to emphasize two facts:

- In the remaining $(d - 1)$ iteration steps the facet will never be left. The vertex \mathbf{x}_s , which will be handed over to Phase 2, and from which the optimization process in direction \mathbf{v} is started, is also an element of F .
- As stated for the first step, the faces reached in the subsequent iterations (in according lower dimension) have a similar tendency to a larger extension. This suggests that the case, where we arrive at a vertex incident to a relatively long edge of F , seems to have a strong preference.

When we optimize starting from that vertex in direction \mathbf{v} , then we can – as discussed in the following – often profit from that configuration. To understand that, we consider three alternative cases for the Simplex Path emanating from \mathbf{x}_s :

Fall 1: It is completely contained in the facet F .

Fall 2: The path runs partially on the facet F .

Fall 3: In the first step F is left and never visited again.

For further considerations we suppose that the first two cases are mainly caused by the location of the start vertex \mathbf{x}_s on F . For the start vertex of the Simplex Path in the secure variant we cannot make such a position statement¹⁴. So the first two cases do not occur systematically, but this happens rather randomly. In total their portion should be somehow smaller. Stated in other words: The cases 1 and 2 appear less often in the theoretically secure variant. Therefore the third case will have a higher weight in the secure method in contrast to the practical method of Phase 2, where its weight is smaller.

For case 3 we do not have additional information and for that reason we suggest that we meet the average number of steps. For the first two cases we formulate theses or assumptions. The first thesis summarizes our hitherto considerations. The second thesis delivers in addition one new aspect. This will be justified afterwards. And then we will think about the profit of both theses in connection with cases 1 and 2.

Thesis I:

In the first step of Phase 1 we choose the direction \mathbf{e}_1 , for moving to a facet F of the feasible region. With regard to the structure of the polyhedron that direction may be seen as random. Therefore, i.e. because the specific facet is hit, it must have a tendency to large extension (otherwise the chance of being hit would have been small). Along movements in F it is possible to traverse large distances on the surface of the basic polyhedron X . And F has a tendency to cover a greater portion of the surface of X than other facets do.

Thesis II:

¹⁴We assume its existence without loss of generality.

For movements in the facet F we can expect a somehow reduced computational effort in comparison with the general situation.

Before we discuss the consequences, we want to specify the reasons for that reduced effort. That means we want to justify the second thesis. As long as we remain on the facet F , the corresponding restriction vector \mathbf{a}_i stays in the basis and it is never replaced. In technical words: We move in the hyperplane corresponding the i -th restriction $\langle \mathbf{a}_i, \mathbf{x} \rangle = 1$, i.e. in a $(d - 1)$ -dimensional affine space. Moreover the i -th restriction – as it determines that space – never loses its role as a basis restriction. The movement in facet F shall for that reason be interpreted a movement for the solution of a problem in dimension $(d - 1)$ with $(m - 1)$ restrictions. The consequence is that for the distance covered in facet F the number of pivot steps should be a bit less than in the general situation.

These Theses deliver together with the two yet undiscussed cases the following insight: For cases 1 and 2 we know, that the optimization process runs at least partially on the facet F . The significance of that information is that on this partial path in F a large distance on the surface of X can be traversed in rather few pivot steps. Since both cases should occur more often for the practical Phase 2, this variant profits from the given situation to a larger extent than the theoretical secure variant does. This argument makes a further reduction of the number of pivots plausible in addition to the previously mentioned reduction by barycentralization.

It cannot be excluded, that there are still other characteristics of the Phase 1 under use have an impact on the average number of pivot steps in the practical Phase 2. But since none of these properties can be proven rigorously and since we suppose that we have discovered the main geometrical reasons, we want to finish the discussion at this point.

The aim of this section was to work out the reasons, why the practical variant in Phase 2 slightly outperforms the secure variant in Phase 2.

6.7 Summary

In this last chapter we have dealt with the question, whether the application of the shadow vertex algorithm causes a significantly larger computational effort, if the used twodimensional plane is not chosen independently from the data of the linear optimization problem. The clarification of this question concerns in particular the application of the shadow vertex algorithm in Phase 2. A choice of the auxiliary objective direction for the start of Phase 2 from the polar cone of the discovered vertex, as it is usual in practical applications, yields an interdependency between projection plane and problem data. Hence the very moderate theoretical results for the running time cannot be proven rigorously. Being extremely sceptical, one would fear a significantly higher effort.

This complication and this fear have been settled by an empirical average-case-analysis. For the random generation of our problem instances we made use of the rotation-symmetry-model. After the presentation of the algorithmic principles we have reported on the measured results and have illustrated them in many diagrams. This assured us that the tolerated dependency of start and data does not deteriorate the computation time on the average.

In addition to that positive insight we could even observe that the practical Phase 2 runs a little bit faster than the theoretically secured method. This effect was not the goal of our investigation, but it is an interesting observation. We have detected some impact factors which are responsible for that effect. It may be possible to clarify these effects to a larger extent even from a quantitative point of view. But this should be done in future investigations.

7 Final Remarks

Now we are at the end of this work. It pays to summarize once more what we have achieved in the previous chapters and to list the questions that are still open.

After the introduction of the subject and after presenting the necessary fundamentals we have demonstrated how the hitherto existing smoothed analysis investigations of the Simplex Method by Spielman and Teng and by Vershynin worked in chapter 3. Spielman and Teng investigated a randomized variant of the Simplex Method, which is capable to solve problems in the form

$$\begin{aligned} & \text{maximize } \langle \mathbf{v}, \mathbf{x} \rangle \\ & \text{s.t. } \langle \mathbf{a}_1, \mathbf{x} \rangle \leq b^1 \\ & \quad \vdots \\ & \quad \langle \mathbf{a}_m, \mathbf{x} \rangle \leq b^m. \end{aligned}$$

If one disregards logarithmic factors, then the upper bound for the smoothed running time is of order $\mathcal{O}(m^{86}d^{55}\sigma^{-30})$. So the result of Spielman und Teng is rather of a qualitative than of a quantitative nature. In contrast to that Vershynin can make some improvements by modifying the analysis and the algorithm under consideration for solving such problems. So he achieves an upper bound of order

$$\mathcal{O}(\max\{d^5(\ln m)^2, d^9(\ln d)^4, d^3\sigma^{-4}\}).$$

¹ For the derivation of that result he also employs a randomized variant of the Simplex Method. For a single execution of that Simplex Method he can only give a positive probability that the problem will be solved. Else the attempt must be repeated.

In contrast to that we have employed the dimension-by-dimension algorithm. And for that version of the Simplex Method we could calculate and bound its smoothed running time based on a smoothed analysis. Using the terminology of Vershynin our upper bound for the smoothed running time is (roughly spoken) of order

$$\mathcal{O}(\max\{d^6(\ln m)^2, d^4\sigma^{-4}\}).$$

Since we have investigated a similar algorithmic principle as Vershynin did, and since we base our analysis on his upper bound for the number of shadow vertices, it is worth while to compare the obtained upper bounds. It strikes that the term $d^9(\ln d)^4$ does not appear in the bound derived in our work. This results from the fact that in contrast to

¹This formula is from [Ver06].

Vershynin's approach we do not generate d artificial and additional restrictions. This had been done in Vershynin's paper to construct an artificial vertex of the modified feasible region, from which the optimization process could be started. The comparison of the two remaining terms shows that in our result the power of d is by 1 higher. The plausible reason for that is that in the application of the dimension-by-dimension algorithm we have to run through d stages instead of the usual 2. And this factor can consequently be found in the result on the number of pivot steps.

So we can state that we have achieved a smoothed analysis result on the running time of a deterministic Simplex variant. In order to derive that goal it was necessary to estimate the expectation value for the number of vertices of twodimensional polyhedra. This has been done in chapter 4.

In addition we have in chapter 6 dealt with the question, what is the impact on the expected running time in Phase 2, if the first Phase is not constructed in a way that ensures the stochastic independence between the projection plane in the shadow vertex algorithm and the restriction vectors. Since this obviously cannot be clarified through a theoretical analysis, we have studied this empirically by a huge number of numerical experiments. These experiments confirmed the plausible conjecture (at least empirically) that the average number of pivot steps for solving optimization problems of the form

$$\begin{aligned} & \text{maximize } \langle \mathbf{v}, \mathbf{x} \rangle \\ & \text{s.t. } \langle \mathbf{a}_1, \mathbf{x} \rangle \leq 1 \\ & \quad \vdots \\ & \quad \langle \mathbf{a}_m, \mathbf{x} \rangle \leq 1 \end{aligned}$$

under the conditions of the rotation symmetry model is bounded from above by

$$Const \cdot m^{\frac{1}{d-1}} \cdot d^2 + d.$$

Again this is another example of the mathematical experience, that things may be true, even if they are still unproven.

Now the question arises, whether there are still other deterministic and even more efficient versions of the Simplex Method, that permit an average case analysis and a smoothed analysis. Still there is a lot to do.

List of Figures

1.1	Graphical illustration of the actual computation time	8
1.2	Graphical illustration of the average computation time	9
1.3	Graphical illustration of the smoothed computation time	10
1.4	Graphical illustration of an alternative actual computation time distribution	11
2.1	Graphical illustration of the functionality of the primal shadow-vertex-algorithm	33
2.2	Graphical illustration of the dual interpretation of the shadow-vertex-algorithm	36
3.1	Graphical illustration of the number of shadow vertices in the dual perspective	40
3.2	Discretization of the shadow plane	42
3.3	Graphical illustration of the ball containing all further configurations .	43
3.4	Graphical illustration of the cone about the vector \mathbf{q}	46
3.5	The basic solution in red is not feasible as long as the orange restriction is not relaxed	48
3.6	The basic solution in red - which had been infeasible before - becomes an edge after relaxation of the orange restriction	48
3.7	An example for an intersection $V \cap E$	56
3.8	Calculation of the number of edges according to Spielman and Teng .	56
3.9	The Three-Viewpoints-Principle	57
3.10	Graphical illustration of the distance-probability	60
3.11	Augmentation of an additional facet to Y	63
3.12	Graphical illustration of the <i>numb set</i> under boundedness	67
3.13	Graphical illustration of a subset of the <i>numb set</i> in case of unboundedness	67
4.1	Original polygon with 60 edges and polygon generated through perturbation	72
4.2	Graphical illustration of the change of coordinates	76
4.3	Graphical illustration of definition 4.3.2	80
4.4	Useful illustration for the replacement of original by perturbed vectors	83
4.5	Useful illustration for the replacement of original by perturbed vectors	92
4.6	Graphical illustration of the Three-Viewpoints-Principle	125
4.7	Distance of the vertices in the triangle to the straight line \mathcal{G}	125
4.8	Illustration for the proof of 4.4.1	126

4.9	Angle between \mathbf{x}_1 and \mathbf{x}_2	127
4.10	Discretization $\omega_2^{(20)}$ of the unit circle	131
4.11	edge is not hit under discretization with $k = 10$	132
4.12	edge is hit under discretization with $k = 20$	132
5.1	projection-polygon of X_{IP} under ignorance of the restrictions for the interpolation variable t	158
5.2	projection-polygon of X_{IP} with regard to the restrictions for the interpolation variable t	158
6.1	A polyhedron defined by unit constraints	168
6.2	The polyhedron diminished by the sign restrictions $x^1, x^2, x^3 \geq 0$ from figure 6.1	171
6.3	The polyhedron diminished by the sign restrictions $x^2, x^3 \geq 0$ from figure 6.1	171
6.4	The polyhedron diminished by the sign restriction $x^3 \geq 0$ from figure 6.1	172
6.5	The polyhedron from figure 6.1 with the vertex determined in Phase 1 .	173
6.6	Iteration-process in the facet F towards a vertex of X	173
6.7	Average number of pivot steps of the Phase-2-variants for dimension 3 .	182
6.8	Average number of pivot steps of the Phase-2-variants for dimension 4 .	183
6.9	Average number of pivot steps of the Phase-2-variants for dimension 5 .	184
6.10	Average number of pivot steps of the Phase-2-variants for dimension 6 .	184
6.11	Average number of pivot steps of the Phase-2-variants for dimension 7 .	185
6.12	Average number of pivot steps of the Phase-2-variants for dimension 8 .	185
6.13	Average number of pivot steps of the Phase-2-variants for dimension 9 .	186
6.14	Average number of pivot steps of the Phase-2-variants for dimension 10	187
6.15	Average number of pivot steps of the Phase-2-variants for dimension 11	187
6.16	Average number of pivot steps of the Phase-2-variants for dimension 12	188
6.17	Average number of pivot steps of the Phase-2-variants for dimension 13	188
6.18	Average number of pivot steps of the Phase-2-variants for dimension 14	190
6.19	Average number of pivot steps of the Phase-2-variants for dimension 15	191
6.20	Average number of pivot steps of the Phase-2-variants for dimension 16	191
6.21	Average number of pivot steps of the Phase-2-variants for dimension 17	192
6.22	Average number of pivot steps of the Phase-2-variants for dimension 18	192
6.23	Average number of pivot steps of the Phase-2-variants for dimension 19	193
6.24	Average number of pivot steps of the Phase-2-variants for dimension 20	193
6.25	5000 realized vectors \mathbf{u}_b for starting the practical Phase 2 in case of $m = 100$ and $d = 3$	196
6.26	5000 realized vectors \mathbf{u}_b for starting the practical Phase 2 in case of $m = 500$ and $d = 3$	196
6.27	Result of Phase 1 versus optimum with respect to \mathbf{e}_1	198
6.28	Illustration of start positions for the two variants of Phase 2	199
6.29	Average step-numbers of the safe Phase 2 and the variant with artificial barycentralizatiion of the auxiliary objective direction in dimension 6 .	200

6.30	Average step-numbers of the safe Phase 2 and the variant with artificial barycentralizatiion of the auxiliary objective direction in dimension 11 .	201
6.31	Average step-numbers of the safe Phase 2 and the variant with artificial barycentralizatiion of the auxiliary objective direction in dimension 18 .	201
6.32	Differences between average step-numbers in dimension 6	202
6.33	Difference between the average step-numbers in dimension 11	203
6.34	Difference between the average step-numbers in dimension 18	203

List of Tableaus

2.1	General Tableau-Structure in componentwise illustration	27
2.2	General Tableau-representation in matrix-notation	28
2.3	Tableau with pivot element for the execution of a pivot step	29
2.4	Tableau for execution of the shadow vertex algorithm	37
6.1	A potential Start-Tableau for solving a unit problem	168
6.2	Tableau-structure after removal of the i th sign restriction	170
6.3	Tableau-Structure after the end of Phase 1	170
6.4	Tableau-Structure at the beginning of the practical Phase 2	175
6.5	Tableau at the start of step 1	179
6.6	Tableau for starting step 3	179
6.7	Useful information in the statistical part of the Tableau	180

Bibliography

- [AKS87] ADLER, Ilan ; KARP, Richard ; SHAMIR, Ron: A Simplex Variant Solving an $m \times d$ Linear Program in $O(\min(m^2, d^2))$ Expected Number of Pivot Steps. In: *Journal of Complexity* 3 (1987), Nr. 4, S. 372–387
- [AMR11] ARTHUR, David ; MANTHEY, Bodo ; RÖGLIN, Heiko: Smoothed Analysis of the k-Means Method. In: *Journal of the ACM* 58 (2011), Nr. 5, S. 1–31
- [BA12] BÜRGISSE, Peter ; AMELUNXEN, Dennis: Robust Smoothed Analysis of a Condition Number for Linear Programming. In: *Mathematical Programming* 131 (2012), Nr. 1-2, S. 221–251
- [Bor77] BORGWARDT, Karl H.: *Untersuchungen zur Asymptotik der mittleren Schrittzahl von Simplexverfahren in der linearen Optimierung*, Universität Kaiserslautern, Diss., 1977
- [Bor82a] BORGWARDT, Karl H.: The Average Number of Pivot Steps Required by the Simplex-Method is Polynomial. In: *Zeitschrift für Operations Research* 26 (1982), Nr. 1, S. 157–177
- [Bor82b] BORGWARDT, Karl H.: Some Distribution-Independent Results About the Asymptotic Order of the Average Number of Pivot Steps of the Simplex Method. In: *Mathematics of Operations Research* 7 (1982), Nr. 3, S. 441–462
- [Bor87] BORGWARDT, Karl H.: *The Simplex Method: A Probabilistic Analysis*. Berlin : Springer, 1987
- [Bor97] BORGWARDT, Karl H.: Average Complexity of a Gift-Wrapping Algorithm for Determining the Convex Hull of Randomly Given Points. In: *Discrete and Computational Geometry* 17 (1997), Nr. 1, S. 79–109
- [Bor99] BORGWARDT, Karl H.: A Sharp Upper Bound for the Expected Number of Shadow Vertices in LP-Polyhedra Under Orthogonal Projection on Two-Dimensional Planes. In: *Mathematics of Operations Research* 24 (1999), Nr. 3, S. 544–603
- [Bor01] BORGWARDT, Karl H.: *Optimierung, Operations Research, Spieltheorie*. Basel : Birkhäuser, 2001

Bibliography

- [Bor07] BORGWARDT, Karl H.: Average-Case Analysis of the Double Description Method and the Beneath-Beyond Algorithm. In: *Discrete and Computational Geometry* 37 (2007), Nr. 2, S. 175–204
- [Dam06] DAMEROW, Valentina: *Average and Smoothed Complexity of Geometric Structures*, Universität Paderborn, Diss., 2006
- [Dan51] DANTZIG, George: Maximization of a Linear Function of Variables Subject to Linear Inequalities. In: *Activity Analysis of Production and Allocation*. New York, N. Y. : John Wiley & Sons Inc., 1951 (Cowles Commission Monograph No. 13), S. 339–347
- [Dan02] DANTZIG, George: Linear Programming. In: *Operations Research* 50 (2002), Nr. 1, S. 42–47
- [DGG13] DEVILLERS, Olivier ; GLISSE, Marc ; GOAOC, Xavier: Complexity Analysis of Random Geometric Structures Made Simpler. In: *Proceedings of the Twenty-ninth Annual Symposium on Computational Geometry*, 2013 (SoCG '13), S. 167–176
- [DST11] DUNAGAN, John ; SPIELMAN, Daniel ; TENG, Shang-Hua: Smoothed Analysis of Condition Numbers and Complexity Implications for Linear Programming. In: *Mathematical Programming* 126 (2011), Nr. 2, S. 315–350
- [FKPT07] FAHRMEIR, Ludwig ; KÜNSTLER, Rita ; PIGEOT, Iris ; TUTZ, Gerhard: *Statistik*. London : Springer, 2007
- [Geo04] GEORGII, Hans-Otto: *Stochastik: Einführung in die Wahrscheinlichkeitstheorie und Statistik*. Berlin : Walter de Gruyter, 2004
- [Göh13] GÖHL, Markus: *Der durchschnittliche Rechenaufwand des Simplexverfahrens unter einem verallgemeinerten Rotationssymmetriemodell*, Universität Augsburg, Diss., 2013
- [GS55] GASS, Saul ; SAATY, Thomas: The Computational Algorithm for the Parametric Objective Function. In: *Naval Research Logistics Quarterly* 2 (1955), Nr. 1-2, S. 39–45
- [Hai83] HAIMOVICH, Mordecai: The Simplex Algorithm is Very Good! – On The Expected Number of Pivot Steps and Related Properties of Random Linear Programs / 415 Uris Hall, Columbia University, New York. 1983. – Forschungsbericht
- [Kar84] KARMAKAR, Narendra: A New Polynomial-Time Algorithm for Linear Programming. In: *Combinatorica* 4 (1984), Nr. 4, S. 373–395
- [Kha79] KHACHIYAN, Leonid: A Polynomial Algorithm in Linear Programming. In: *Doklady Akademii Nauk SSSR* 244 (1979), S. 1093–1096. – Translated in Soviet Mathematics Doklady 20 (1979), S. 191–194

- [Kle08] KLENKE, Achim: *Wahrscheinlichkeitstheorie*. London : Springer, 2008
- [KM72] KLEE, Victor ; MINTY, George: How Good is the Simplex Algorithm? In: SHISHA, O. (Hrsg.): *Inequalities III*. New York : Academic Press, 1972, S. 159–175
- [MB64] MARSAGLIA, George ; BRAY, Thomas: A Convenient Method for Generating Normal Variables. In: *SIAM Review* 6 (1964), S. 260–264
- [Meg84] MEGIDDO, Nimrod: Linear Programming in Linear Time When the Dimension is Fixed. In: *Journal of the ACM* 31 (1984), Nr. 1, S. 114–127
- [MR07] MANTHEY, Bodo ; REISCHUK, Rüdiger: Smoothed Analysis of Binary Search Trees. In: *Theoretical Computer Science* 378 (2007), Nr. 3, S. 292–315
- [RV07] RÖGLIN, Heiko ; VÖCKING, Berthold: Smoothed Analysis of Integer Programming. In: *Mathematical Programming* 110 (2007), Nr. 1, S. 21–56
- [Sch98] SCHRIJVER, Alexander: *Theory of Linear and Integer Programming*. Chichester : John Wiley & Sons, 1998
- [Sch12] SCHNALZGER, Emanuel: *The Handling of Phase I in the Smoothed Analysis of Linear Optimization*, Universität Augsburg, Master's Thesis, 2012
- [Sma83] SMALE, Steve: On the Average Number of Steps of the Simplex Method of Linear Programming. In: *Mathematical Programming* 27 (1983), Nr. 3, S. 241–262
- [SST06] SANKAR, Arvind ; SPIELMAN, Daniel ; TENG, Shang-Hua: Smoothed Analysis of the Condition Numbers and Growth Factors of Matrices. In: *SIAM Journal on Matrix Analysis and Applications* 28 (2006), Nr. 2, S. 446–476
- [ST01] SPIELMAN, Daniel ; TENG, Shang-Hua: Smoothed Analysis of Algorithms: Why the Simplex Algorithm Usually Takes Polynomial Time. In: *Proceedings of the Thirty-Third Annual ACM Symposium on Theory of Computing*, 2001, S. 296–305
- [ST04] SPIELMAN, Daniel ; TENG, Shang-Hua: Smoothed Analysis of Algorithms: Why the Simplex Algorithm Usually Takes Polynomial Time. In: *Journal of the ACM* 51 (2004), Nr. 3, S. 385–463
- [ST09] SPIELMAN, Daniel ; TENG, Shang-Hua: Smoothed Analysis: An Attempt to Explain the Behavior of Algorithms in Practice. In: *Communications of the ACM* 52 (2009), Nr. 10, S. 76–84
- [Tod86] TODD, Michael J.: Polynomial Expected Behavior of a Pivoting Algorithm for Linear Complementarity and Linear Programming Problems. In: *Mathematical Programming* 35 (1986), Nr. 2, S. 173–192

Bibliography

- [Tod02] TODD, Michael J.: The Many Facets of Linear Programming. In: *Mathematical Programming* 91 (2002), Nr. 3, S. 417–436
- [Ver06] VERSHYNIN, Roman: Beyond Hirsch Conjecture: Walks on Random Polytopes and Smoothed Complexity of the Simplex Method. In: *Proceedings of the 47th Annual IEEE Symposium on Foundations of Computer Science*, 2006, S. 133–142
- [Ver09] VERSHYNIN, Roman: Beyond Hirsch Conjecture: Walks on Random Polytopes and Smoothed Complexity of the Simplex Method. In: *SIAM Journal on Computing* 39 (2009), Nr. 2, S. 646–678
- [Wen62] WENDEL, James G.: A Problem in Geometric Probability. In: *Mathematica Scandinavica* 11 (1962), S. 109–111
- [Wör11] WÖRLE, Thomas: *Algorithmen zur Bestimmung der Struktur konvexer Hüllen und der Eckenmenge von Polyedern: Eine vergleichende probabilistische Analyse*, Universität Augsburg, Diss., 2011

Lebenslauf

Persönliche Daten

Vorname: Emanuel
Nachname: Schnalzger
Geburtsdatum: 12.10.1986
Geburtsort: Augsburg
Staatsangehörigkeit: deutsch

Schulbildung

1993 - 1997: Grundschule in Dinkelscherben
1997 - 2006: Justus-von-Liebig-Gymnasium in Neusäß
2006: Allgemeine Hochschulreife

Akademische Ausbildung

2007 - 2009: Bachelorstudium Wirtschaftsmathematik an der Universität Augsburg
2009 - 2010: Bachelorstudium Mathematik im Studiengang „TopMath - Angewandte Mathematik mit Promotion“ an der TU München und der Universität Augsburg
2010: Abschluss als Bachelor of Science
2010 - 2012: Masterstudium Wirtschaftsmathematik an der Universität Augsburg
2012: Abschluss als Master of Science
seit 2010: Promotionsstudium mit parallelem Honours Master im Studiengang TopMath an der TU München und der Universität Augsburg
2012: Abschluss als Master of Science with Honours